Function, phenotype and development of human CD161+ CD8 T cells

Dr Lucy Walker
Wolfson College and Nuffield Department of Medicine, University of Oxford
2012

This thesis is submitted for the degree of Doctor of Philosophy

Dedication

I dedicate this thesis to Rowan, for his love, support and the many lifts home after late nights in the lab.

Contents

Thesis abstract……1

Acknowledgements……2

List of abreviations……3

Chapter 1- Introduction……..4

1.1 Type 17 Immunity……..4

Human type 17 immunity and immunopathology.

Th17 cells

Tc17 cells

Mucosal associated invariant T cells

1.2 CD8αα T cells…….…….22

CD8αβ and CD8αα molecules

CD8αα cells

1.3 The role of CD161++CD8+ T cells in the immune response to hepatitis C……...28

The liver immune environment

Immunity to hepatitis C virus

CD161++CD8+ T cells and chronic viral hepatitis

1.4 Key questions to be addressed in the thesis……..41

Chapter 2 - Methods and reagents……...42

2.1 Study subjects……42

2.2 Sample preparation……42

Peripheral blood mononuclear cell and cord blood

mononuclear cell separation

Cell freezing and thawing protocol

Liver derived lymphocyte extraction

Lamina propria mononuclear ell extraction

2.3 Fluorescent antibody staining for flow cytometry ……..45

Surface staining of separated lymphocytes

Whole blood surface staining

Intracellular cytokine staining

Intracellular staining for transcription factors and

proliferation markers

Controls, flow cytometry and analysis

2.4 Cell sorting……47

CD8 enrichment

Positive selection

MoFlo cell sorting
2.5 Cell culture……49
2.6 RNA extraction……...49
2.7 Microarray……50
cDNA amplification
Quality control of amplified cDNA product
cDNA fragmentation and labelling
Array hybridization
Microarray data processing
2.8 Real-time PCR……..…56
First strand cDNA synthesis
RT PCR
2.9 Immunofluorescent staining……..……57
2.10 Antibody conjugation……..……..57
2.11 Statistical analysis……58
2.12 Reagents……58
Antibodies
Media recipes
Commercial kits

Chapter 3 - Programming and differentiation of CD161++CD8+ T-cells……....62
3.1 Introduction……...62
3.2 Hypothesis and Aims……..63
3.2 Methods……....63
Study subjects
Lymphocyte recovery
Antibody staining for flow cytometry
Cell sorting for microarray
RNA extraction
Microarray
Real-time PCR
Statistical analysis
Gene set enrichment analysis
3.4 Results……69
CD161++CD8α+ T cells are present in cord and infant blood
CD161++CD8α+ T cells have a naïve phenotype in cord blood
CD161++CD8α+ T cells in cord blood are pre-determined type-17 subset
MAIT/ CD161++CD8α+ T cell co-receptor expression
T cell receptor usage of CD161++ CD8α+ T cells
3.5 Discussion……87

3.6 Conclusions……91

Chapter 4 - Human CD8αα cells……93

4.1 Introduction……...93
4.2 Hypothesis and Aims……..94
4.3 Methods……95
Study subjects
Lymphocyte recovery and sample preparation
Fluorescent antibody staining for flow cytometry
Cell sorting for microarray
RNA extraction
Microarray
Cell culture
Statistical analysis
4.4 Results……..99
Human CD8αα cells are exclusive to the CD161++CD8+ T cell subset
Human CD8αα cells are present at diverse tissue sites
Human CD161++CD8αα cells share Tc17 phenotype, function and gene expression profiles with CD161++CD8αβ cells
Human CD8αα cells share a common differentiation pathway with CD161++CD8αβ cells
4.5 Discussion……....111
4.6 Conclusions……...113

Chapter 5 - Activation of CD8 T cell subsets and regulation of CD8β expression in chronic viral hepatitis

5.1 Introduction……115
5.2 Hypothesis and aims……119
5.3 Methods……..120
Study subjects
Lymphocyte recovery and sample preparation
Fluorescent antibody staining for flow cytometry
Cell culture
Statistical analysis
5.4 Results……122
CD161++CD8+ T cell subset redistribution in chronic HBV and HCV infection.
Expression of activation and exhaustion markers on CD161++/CD161+ and CD161- subsets in chronic HBV and HCV compared to healthy controls

Patients with chronic HBV have a prominent CD161-CD8β^{low} population
CD161-CD8β^{low} cells in chronic HBV produce greater amounts of IFN-γ than CD161-CD8β^{high} cells
CD8β down-regulation does not correlate with e-antigen status, ALT or viral load
CD8β is readily down regulated on CD161-CD8+ T cells in culture
5.5 Discussion……..149
5.6 Conclusions……155

Chapter 6 Conclusions and further work ……157
6.1 CD161++CD8$\alpha\alpha$ and CD8$\alpha\beta$ cells cell development and their role in health and disease……157
Conclusions
Overall model for CD161++CD8α+ T cell development and role in immunity
Further work

6.2 Bulk CD8+ T cell effects in chronic Hepatitis B infection……164
Conclusions
Overall model for generation and role of CD161-CD8β^{low}CD28^{low}HLADR^{high} T cells in chronic HBV infection.
Further work

6.3 Final thesis conclusions……167

Chapter 7 References……170

Appendix 1 ……**193**
Billerbeck, Kang et al (2010): Analysis of the role of CD161 expression on human CD8+ T cells defines a distinct functional subset with tissue homing properties.

Appendix 2……213
Microarray data comparing up and down regulated genes between CD161+ and CD161- CD8+ T cell subsets in cord blood.

Appendix 3……230
CD161++CD8α+ vs CD161-CD8α+: Geneset enrichment analysis

Appendix 4……259
CD161+CD8α+ vs CD161-CD8α+: Geneset enrichment analysis

Appendix 5 ……278
CD161+CD8α+ vs CD161-CD8α+: Geneset enrichment analysis

Appendix 6 ……289
Microarray data comparing up and down regulated genes between CD161++CD8αβ and CD161++CD8αα T cells from adult healthy donors.

Abstract

Tc17 cells and the semi-invariant human mucosal associated invariant T (MAIT) cells are important CD8+ tissue-homing cell populations. Both are characterized by high expression of CD161 (++) and type-17 differentiation, yet their origins and relationships remain poorly defined. By transcriptional and functional analyses it is demonstrated that a pool of polyclonal, pre-committed type-17 CD161++CD8αβ+ T cells exists in cord blood, from which a prominent MAIT cell (TCR Vα7.2+/Vβ2 or 13.2) population emerges post-natally. During this expansion, CD8αα T-cells appear exclusively within CD161++CD8+/MAIT subset, sharing cytokine production (IL17, IL-22 and IFN-γ), chemokine-receptor expression (CCR2, CCR6 and CXCR6), TCR-usage and transcriptional profiles with their CD161++CD8αβ+ counterparts. These data demonstrate the origin and differentiation pathway of MAIT cells from a naïve type-17 pre-committed CD161++CD8+ T cell pool and the distinct phenotype and function of CD8αα cells in man. The CD161++CD8αβ and CD8αα T cell subsets are reduced in the peripheral circulation in chronic hepatitis B and C and are enriched in the liver in chronic hepatitis C. Their potential role in immunity to chronic viral hepatitis B and C is demonstrated by their expression of activation/exhaustion markers CD69, CD25, HLA-DR and PD-1. In addition a substantial distinct CD161-CD8β^{low} population is demonstrated in chronic hepatitis B, co-characterised by a CD28^{low}, HLA-DR^{high} phenotype and high expression of IFN-γ, with important implications for the development of immunotherapy and vaccination.

Acknowledgements

I would like to thank first and foremost my supervisors Paul Klenerman and Eleanor Barnes who have provided great guidance, support and mentorship throughout my time at Oxford. The members of the Klenerman group, whom are too numerous to name, have also all helped to shape my project, providing both practical support and critique throughout. I would like to thank our collaborators in Oxford, around the UK and the rest of the world for their contributions of thoughts, expertise, time, lab space, reagents and samples; including Natasha Saghal (University of Oxford, UK), Andrew Worth (University of Oxford, UK), David Adams (University of Birmingham, UK), Georg Lauer (Harvard, USA), Thomas Schriba (University of Cape Town, SA) and Olivier Lantz (Institut Currie, France). I also must mention Professor David Jones (Newcastle University), whose enthusiasm persuaded me into all of this in the first place. Lastly, I express my gratitude to the MRC for their generous funding.

List of abbreviations

CDR3	Complementary determining region 3

EAE	Experimental autoimmune encephalitis
ES	Enrichment score
G-CSF	Granulocyte colony-stimulating factor
HC	Healthy control
HCV	Hepatitis C virus
HBV	Hepatitis B virus
HLA	Human leukocyte antigen
IELs	Intraepithelial lymphocytes
IFN	Interferon
Ig	immunoglobulin
IL-	interleukin
KIR	Killer inhibitory receptor
LAT	Linker of activated T cells
LCMV	Lymphocytic choriomeningitis virus
LLT-1	Lectin-like transcript-1
MAIT	Mucosal-associated invariant T cells
MHC	Major histocompatibility
MR1	Major histocompatibility complex, class 1-related
NK	Natural killer
NKRP1	Natural killer receptor p-1
PBMC	Peripheral blood mononucleocytes
PCR	Polymerase chain reaction
PD-1	Programmed death -1
PILAR	Proliferation induced lymphocyte associated receptor
PMA	Phorbol 12-myristate 13-acetate
R	Receptor
RNA	Ribonucleic acid
RORγt	Retinoid-related orphan receptor gamma-t
STAT	Signal transducer and activator of transcription
TAP	Transporter associated with antigen processing
Tc17	Type 17 CD8+ T cells
TCR	T cell receptor
Th	T helper
TL	Thymic leukemia antigen
TLR	Toll like receptor
TNF-α	Tumour necrosis factor alpha
Tregs	Regulatory T cells
ZBTB16	Zinc finger and BTB domain containing protein 16

1 Introduction

1.1 Type 17 immunity

1.1.1 Human type 17 immunity and immunopathology

Adaptive cellular immune responses are broadly categorised into 4 sub-types (type 1, type 2, type 17 and regulatory), based on the type of immune help their CD4+ T helper (Th) cells provide (**Figure 1.1**) (Zhu, Yamane et al. 2010). Type 17 responses have been implicated in both protective immunity and inflammatory pathology in human and murine disease. The major type 17 cytokines interleukin- (IL-) -17A, IL-17F and IL-22 are produced either together or independently by a variety of immune cell subsets. These range from innate lymphoid cells (Spits and Di Santo 2011) to CD4+(Korn, Bettelli et al. 2009) and CD8+ T cells (Billerbeck, Kang et al. 2010) (**Appendix 1**) of the adaptive immune system. These populations share other common features including expression of the transcription factor retinoid-related orphan receptor (ROR) gamma t; such evolutionary conservation and redundancy is testament to their pervasive importance in the immune system.

Data on the role of type 17 cells in host immunity in both mice and humans have demonstrated that they are required for protection against a range of extracellular bacteria and fungi, particularly at mucosal surfaces. Type 17 cells mediate their effects via the cytokines they produce, notably IL-17A, IL-17F and IL-22, but also IL-21, IL-26, interferon (IFN) gamma and tumour necrosis factor alpha (TNF-α). IL-23 is not a direct effector cytokine, but has

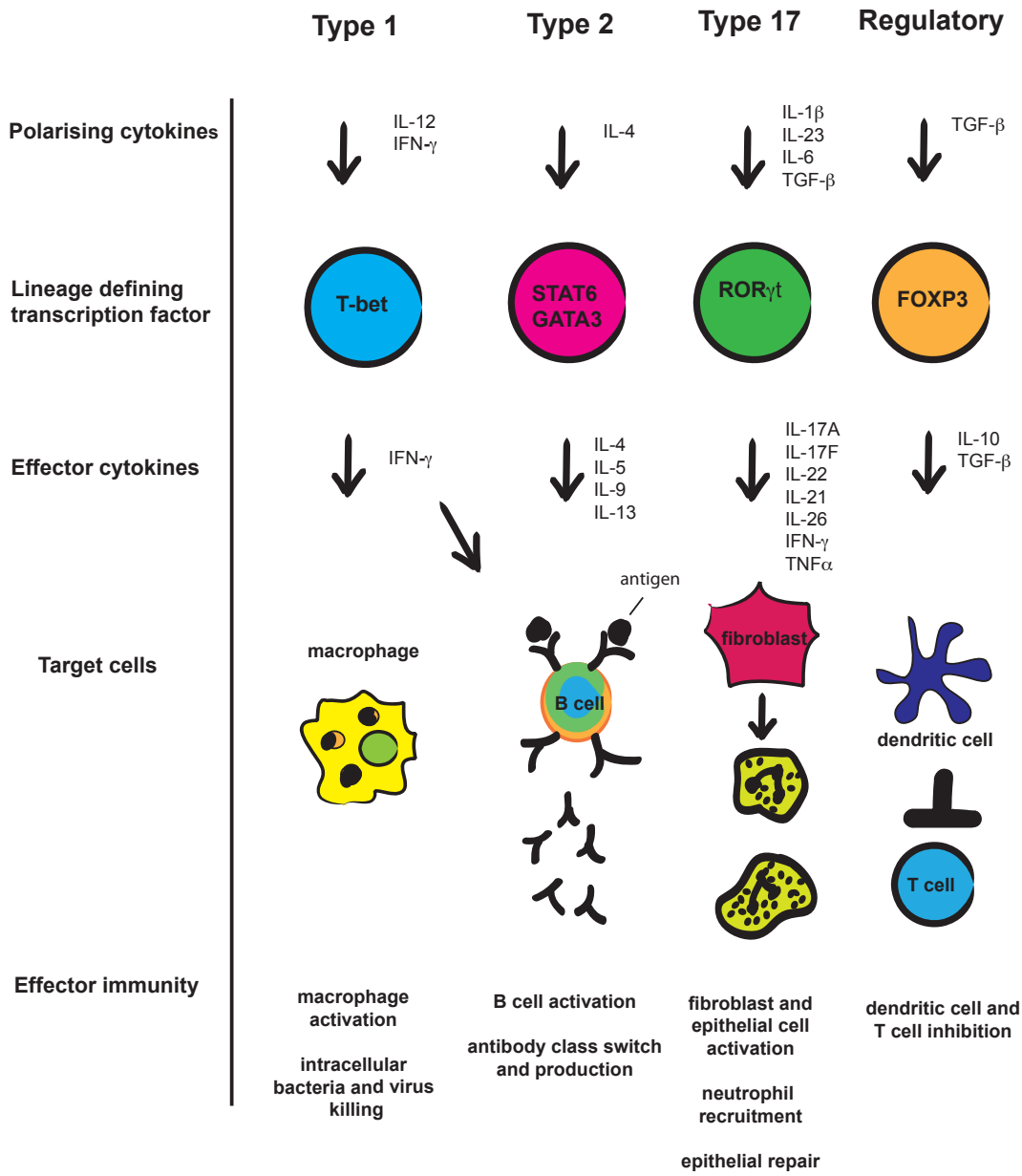


Figure 1.1. Type 1, 2, 17 and regulatory immune responses.

Th1 cells produce cytokines that activate macrophages helping them to destroy intracellular pathogens. They also activate B cells to produce complement fixing and neutralising IgG antibodies. Th2 cells activate B cells to produce IgE antibodies to help fight parasitic infection and opsonising IgG antibodies. Th17 cells induce cytokines that activate epithelial and stromal cells and drive recruitment of neutrophils to kill extracellular bacteria and fungi. T regulatory cells help to suppress T cell activity and prevent uncontrolled immune responses and autoimmunity.

important role in differentiation and augmentation of type 17 cells (Sallusto and Lanzavecchia, 2009). IL-17A and IL-17F form part of the structurally related, 6 -member IL-17 cytokine family, IL-17 A-F. IL-17A and IL-17F have an important role in driving neutrophil granulopoiesis and chemotaxis via granulocyte colony-stimulating factor (G-CSF) and induction of CXC chemokine expression (CXCL1, CXCL8, CXCL10) by fibroblasts, vascular endothelium and airway epithelial cells (Korn, Bettelli et al. 2009). Studies of IL-17RA knock-out mice have shown IL-17A to be important in defense against *Klebsiella* (Happel, Dubin et al. 2005) and *Candida* (Huang, Na et al. 2004), where pathogen clearance is reliant on neutrophils. However, in other infections, such as *Pseudomonas aeruginosa* (Dubin and Kolls 2007) and *Aspergillus fumigatus* (Romani, Fallarino et al. 2008), although IL-17 is induced neutrophils are not sufficient for clearance and IL-17 driven inflammation mediates severe immunopathology.

IL-22 is a member of the IL-10 family of cytokines. Its receptor, the IL-22 receptor (R)/IL10R2 heterodimer, is widely expressed on epithelial and endothelial cells, but not cells of the immune system (Kotenko, Izotova et al. 2001). IL-22 is needed to maintain barrier function at a variety of mucosal surfaces including the gut and the lung. IL-22 knock-out mice are more susceptible to the intestinal infection *Citrobacter Rodentium* (Zheng, Valdez et al. 2008) and to *Klebsiella pneumoniae* pneumonia after anti-IL-22 antibody treatment (Aujla, Chan et al. 2008). It promotes immunity by maintenance of epithelial barrier function via a variety of mechanisms. It has been shown to induce secretion of anti-microbial peptides (Liang, Tan et al. 2006), promote

epithelial cell (Brand, Beigel et al. 2006) and keratinocyte (Boniface, Bernard et al. 2005) migration *in vitro* and enhance mucus production and goblet cell replacement in the colon *in vivo* (Sugimoto, Ogawa et al. 2008). IL-22 also has a role in limiting inflammation induced tissue damage, as demonstrated in the liver (Zenewicz, Yancopoulos et al. 2007), gut (Sugimoto, Ogawa et al. 2008) and myocardium (Chang, Hanawa et al. 2006). This is likely mediated through signal transducer and activator of transcription (STAT)-3 dependent up-regulation of anti-apoptotic genes and those involved in cell cycle progression (Radaeva, Sun et al. 2004).

Type 17 cells are implicated in the pathogenesis of a number of autoimmune and inflammatory disorders. Genetic susceptibility to immune dysregulation in the context of an environmental factor or triggering microorganism is a long held hypothesis as to the genesis of such disease. The cells and cytokines found at the scene of the crime are numerous and often difficult to interpret in terms of implicating any one factor in particular. However, some interesting data with regard to type 17 immunity are emerging. For example, in psoriasis a mixture of type 1 and type 17 cytokines can be isolated from skin lesions and the serum of patients (Tesmer, Lundy et al. 2008). Injection of IL-23 into the skin of the ears of mice induces epidermal hyperplasia and a type 17 inflammatory cellular-infiltration similar to psoriasis (Zheng, Danilenko et al. 2007). IL-22 has been shown to induce proliferation and differentiation of keratinocytes and levels in plasma correlate with disease severity in patients (Wolk, Witte et al. 2006). Treatment with an antibody against the shared IL-12/IL-23 p40 subunit has had promising results (Krueger, Langley et al. 2007),

as has anti-TNF-α treatment (Zaba, Cardinale et al. 2007), where notable reductions in type 17 and not type 1 cytokines are observed in skin lesions. A further example is inflammatory bowel disease, where in mouse models IL-23 has been shown to be an essential cytokine mediating intestinal inflammation (Yen, Cheung et al. 2006) and, like in psoriasis, clinical remission is induced in patients by treatment with antibodies to the IL-12/IL-23 p40 subunit (Mannon, Fuss et al. 2004). Further to this, single nucleotide polymorphisms in the IL-23 receptor have been significantly associated with both ulcerative colitis and Crohn's disease in a genome-wide association study (Duerr, Taylor et al. 2006) and T cells isolated from the lamina propria of patients with inflammatory bowel disease produce high levels of IL-17 on *ex vivo* re-stimulation compared to healthy controls (Fujino, Andoh et al. 2003).

An important role has therefore been established for the main type 17 cytokines IL-17A/F and IL-22 in both immunity and immunopathology. The cellular sources of these cytokines have been widely studied, with CD4+ Th17 cells being the first and most extensively described.

1.1.2 Th17 cells

Although IL17A had been previously described (Yao, Fanslow et al. 1995), and its importance in mediating immunity to infection known (as discussed above) (Luzza, Parrello et al. 2000), IL-17A producing T cells were first identified through work on the mouse models of autoimmunity, such as experimental autoimmune encephalolmyelitis (EAE). IFN-γ producing Th1

clones had previously been believed to be the mediators of pathology through experiments using adoptive transfer of antigen specific Th1 cells. This idea was questioned when it was shown that IFN-γ, IFN-γ receptor and IL-12p35, IL-12- receptor-β2 knock-out mice were not protected from EAE and developed a more severe phenotype of the disease (Krakowski and Owens 1996), (Tran, Prince et al. 2000), (Gran, Zhang et al. 2002), (Zhang, Gran et al. 2003). IL-23 was discovered after the identification of the p19 cytokine chain (Oppmann, Lesley et al. 2000). This was shown to form a heterodimer with the p40 chain to make IL-23, which is shared with IL-12. Previous experiments targeting the p40 chain would have knocked out both IL-12 and IL-23. It was subsequently shown that it was IL-23, and not IL-12, which was responsible for EAE (Cua, Sherlock et al. 2003) and that the disease was mediated through IL-17 producing T cells which expanded in the presence of IL-23 in culture (Langrish, Chen et al. 2005).

Initial studies identified human IL-17 producing cells to be CD4+ 'Th17 cells', distinct from Th1 and Th2 CD4+ lineages (Harrington, Hatton et al. 2005) (**Figure 1.1**). A CD4+CD45RO+CCR7-CCR6+ population was described (Liu and Rohowsky-Kochan 2008) in which IL-17 production was induced on exposure to IL-23 following up-regulation of the IL23R and the transcription factor RORγt (Chen, Tato et al. 2007). The cytokine cocktails required for *in vitro* polarisation of human Th17 cells from naïve uncommitted CD4+ precursors have been elucidated to be IL-23 and IL-1β, +/- IL-6 and TGF-β which acts indirectly via suppression of Th1 development (**Figure 1.2**) (Crome, Wang et al. 2009), although there is evidence that Th17 cells can

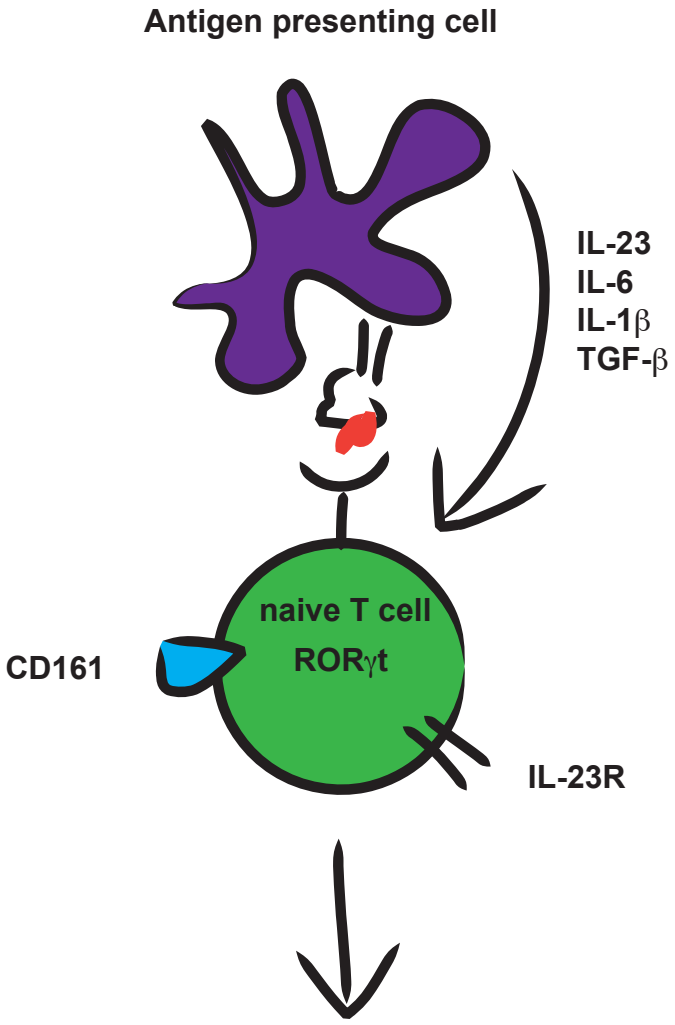


Figure 1.2. Differentiation of human Th17 cells. CD161+CD4+ naive precursors are polarised to become Th17 cells on exposure to type 17 polarising cytokines IL-23, IL-6, IL-1b and TGF-β.

only be derived from a subset of CD4+ naïve cells that express CD161, suggesting these cells arise from a lineage pre-committed precursor (see below) (Cosmi, De Palma et al. 2008).

A number of transcription factors have been identified in murine studies to be important for Th17 development including IFN-regulatory factor-4 (Brustle, Heink et al. 2007), STAT3 (Yang, Panopoulos et al. 2007), the aryl-hydrocarbon receptor (Quintana, Basso et al. 2008), ROR-α (Yang, Pappu et al. 2008) and RORγt (Ivanov, McKenzie et al. 2006) , of which RORγt seems to be the most specific and is seen to be the lineage defining transcription factor. RORγt over-expression promotes Th17 development; deficient mice have significantly reduced numbers of Th17 cells in the gut and are protected from EAE (Ivanov, McKenzie et al. 2006). RORC2 is the human orthologue of RORγt, although the terms are often used interchangeably in the literature, and its over-expression in adult CD4+ T cells induces a Th17 cell phenotype and cytokine profile (Crome, Wang et al. 2009). In this study, only 20% of the transduced T cells were able to produce IL-17 however, suggesting that other transcription factors, such as those described in mice, might be required for full Th17 development in humans. These have been poorly characterised, but of note patients with hyper-IgE syndrome who carry an autosomal dominant mutation in STAT3, required for RORC2 expression, fail to develop Th17 cells (Ma, Chew et al. 2008).

CD161 was first identified as a potential lineage identifier for human Th17 cells when it was found to be the most differentially up-regulated gene on

microarray comparison of gene expression between Th1, Th2 and Th17 clones. It was also shown in the same study that all circulating Th17 cells were contained within the CCR6+CD161+CD4+ population and that IL-17 producing cells, including IL-17/IFN-γ co-producers, could only be derived from the naïve CD161+CD4+ (and not the CD161-CD4+) T cell population of cord blood and the thymus after culture in a combination of serum containing medium (and so TGF-β), IL-1β and IL-23 (Cosmi, De Palma et al. 2008). Further to this, it has been shown that CD161 is highly expressed by peripheral and gut-resident human Th17 cells (Kleinschek, Boniface et al. 2009). Cord blood CD161+ CD4+CD8-, CD8+CD4- and CD4-CD8- T cell receptor (TCR) αβ+ and TCRγδ+ cells have been shown to already express IL-23R and RORγt mRNA and to produce IL-17 on phorbol 12-myristate 13-acetate (PMA)/ ionomycin stimulation after 7 days in culture with anti-CD3/CD28 beads and IL1-β/ IL-23, unlike their CD161- counterparts. The transcription factor RORγt has been defined as the driver for the hallmark features of these cells, as CD161, IL-23R and IL-17 expression could be directly induced by RORC2 transduction of CD161- cord cells (Maggi, Santarlasci et al. 2010).

The role played by CD161 beyond being a potent marker for type 17 cells is the subject of current research. CD161 is a member of the natural killer receptor p-1 (NKR-P1) family of C-type lectin-like molecules. In humans CD161/NKR-P1A is the only member of the family found, encoded by the *KLRB1* gene. In mice there are six NKR-P1 molecules, of which NKR-P1A is the most homologous to human CD161. CD161 is, importantly, not homologous to the mouse NK1.1 expressed on natural killer (NK) and NK-T

cells which is homologous to NKR-P1C (Lanier, Chang et al. 1994). CD161 is expressed by a wide variety of human immune cells; NK cells, NK-T cells, CD4+ T-cells, CD8+ T cells and γδ T cells. Lectin-like transcript-1 (LLT1) has been identified to be a natural ligand for CD161 (Aldemir, Prod'homme et al. 2005), (Rosen, Bettadapura et al. 2005). It is has been shown to be expressed on B cell lines, activated primary B cells, toll-like receptor (TLR)-activated plamacytoid dendritic cells and TLR-activated monocyte-derived dendritic cells (Rosen, Cao et al. 2008). Studies have shown that interactions between CD161+ NK cells and LLT1 on target cells inhibit NK cell-mediated cytotoxicity and cytokine production (Aldemir, Prod'homme et al. 2005), (Rosen, Bettadapura et al. 2005). Its effects on conventional T cells have shown that whilst there was no effect on TCR-activated CD4+ T cell production of IFN-γ or TNF-α, reduced production of TNF-α from CD8+ T cells was shown in some donors, demonstrating a possible inhibitory role (Rosen, Cao et al. 2008). Other reports have identified proliferation induced lymphocyte associated receptor (PILAR) to also be a CD161 ligand and to modulate T cell proliferation by the up-regulation of the anti-apoptotic factor Bcl-xL (Huarte, Cubillos-Ruiz et al. 2008).

1.1.3 Tc17 cells

Human IL-17 producing CD8+ T-cells (Tc17) were first described to be a predominantly CD28+CD45RA- memory subset that expressed high levels of CCR6 and CCR5 and to be IL-17/IFN-γ co-producers (Kondo, Takata et al. 2009). In conjunction with this, a Tc17 subset was also identified in murine lungs following primary challenge with influenza A (Hamada, Garcia-

Hernandez Mde et al. 2009). Subsequent work on CD8+ T cells by the Klenerman group (University of Oxford) using a discriminating CD161 antibody clone enabled the identification of two CD8+CD161+ populations, one expressing very high levels of CD161 (CD161++) and the other expressing an intermediate amount (CD161+) (**Figure 1.3**). CD161++CD8+ T cells were shown to be the exclusive producers of IL-17 amongst CD8s co-characterised by the expression of RORγt, IL23R, IL-18R, CCR2, CCR6, CXCR6, and production of IL-22 and IFN-γ (**Figure 1.4**) (Billerbeck, Kang et al. 2010) (**Appendix 1**). Consistent with their expression of CXCR6, associated with liver homing (Heydtmann, Lalor et al. 2005) via its ligand CXCL16 which is constitutively expressed on liver sinusoids, CD161++CD8+ T cells were found to be enriched in the liver in patients with chronic HCV. Although their presence is not limited to the liver, as they were also described in tissue in a range of pathological conditions (liver in Hepatitis C; synovial fluid in rheumatoid arthritis and skin in psoriasis) (Billerbeck, Kang et al. 2010).

A further human CD8+ T cell subset called mucosal associated invariant T cells (MAITs) has been described and has many parallels to the CD161++ Tc17 subset. MAITs also express high levels of CD161 and IL-18R and have recently been demonstrated to have 'type 17' phenotype and function (Dusseaux, Martin et al. 2011). Such a parallel description is intriguing and may be instrumental in opening up this field of immunology to greater research and scrutiny.

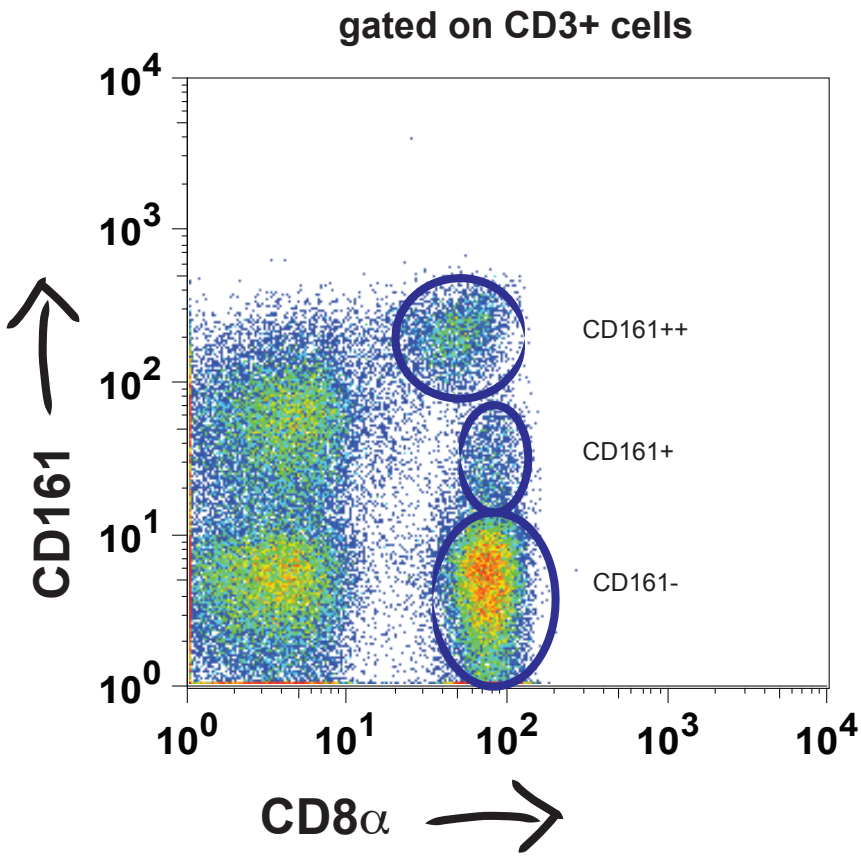


Figure 1.3. CD161++, CD161+ and CD161- CD8+ T cell subsets. Representative FACS plot demonstrating the three distinct CD161 CD8+ T cell subsets.

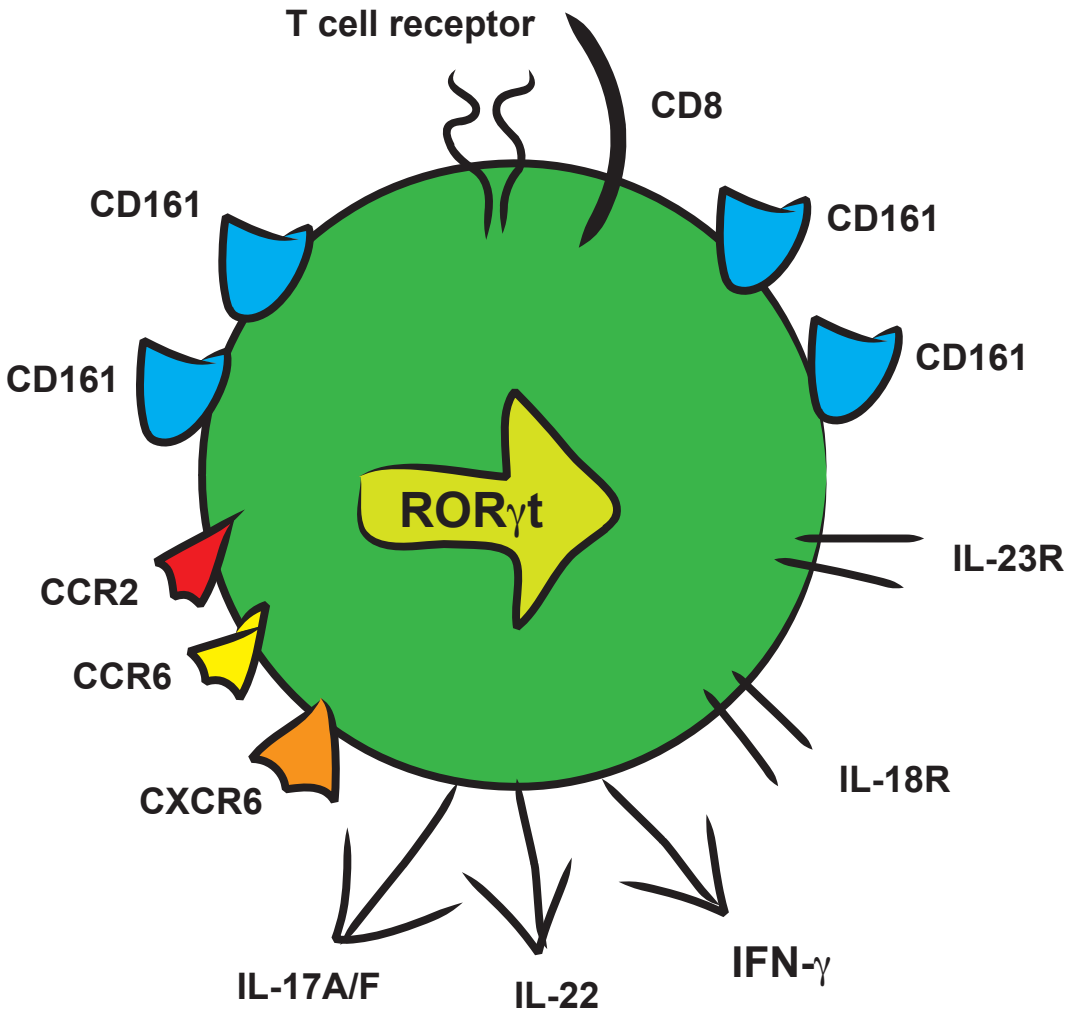


Figure 1.4. CD161++CD8+ Tc17 cells.

Phenotype and cytokine expression profile of CD161++CD8+ T cells.

1.1.4 Mucosal associated invariant T cells

MAIT cells are a prominent human semi-invariant T cell subset, the study of which has largely been the focus of just one research group under Olivier Lantz in Paris, France. Their discovery was based on the observation of an abundance of a canonical T cell receptor (TCR) α chain, made up of rearranged hAV7S2AJ33 elements with a complementary determining region 3 (CDR3) of constant length but some variability in the two junctional codons, amongst sorted human double negative (CD4-CD8α-) and CD8$\alpha\alpha$+ T cells. Based on single cell nested polymerase chain reaction (PCR) of sorted double negative cells from three individuals, Vα7.2-Jα33+ cells were shown to have a heavy bias towards Vβ 2 and 13.2 usage. However, there were no restrictions in Jβ usage or in β chain CDR3 length observed. Homologous murine and bovine TCRα chain transcripts (AV19AJ33) were also identified amongst sorted double negative T cells, with predominant Vβ 6 and 8 usage and no Jβ restriction, although the population is much less numerous in these species (Tilloy, Treiner et al. 1999). These data have been supported by a study of Vα19 transgenic mice (Kawachi, Maldonado et al. 2006).

MAIT cells earned their description as ‘mucosal-associated’ on the basis of there being an enrichment of Vα7.2-Jα33 transcripts in both human gut-homing TCR$\alpha\beta$+ CD4-CD8-α4β7+ T-cells sorted from peripheral blood and gut biopsy samples (compared to skin). On comparison between different gut biopsies containing variable amounts of gut-tissue layers and Vα7.2-Jα33+ transcripts, the authors suggest restriction of this subset to the lamina propria.

This is supported by data from transporter associated with antigen processing- (TAP) and invariant chain-deficient mice (that have a more abundant population of Vα19-Jα33+ T cells than wild type mice), which demonstrate an abundant Vα19-Jα33+ population in the lamina propria compared to mesenteric lymph nodes (Treiner, Duban et al. 2003). Further data on the phenoype and function of these cells at this site is limited however, as they have never been isolated from the gut for more extensive analysis by flow cytometry.

Work with knockout mice initially identified the selecting ligand of MAIT cells to be a CD8 independent, β2m-dependent, and TAP-independent molecule distinct from CD1 (Tilloy, Treiner et al. 1999). Mixed chimeras were used to identify β2m+ B cells to be the cell type responsible for selecting MAIT cells. Major histocompatibility complex, class 1-related (MR1) was targeted as a candidate major histocompatibility (MHC) class-I like molecule. MR1 transfected cell lines were able to stimulate IL-2 production from mouse Vα19-Ja33+ T-T hybridomas, which could be blocked with an anti-TCR antibody. Few T cells with the canonical Vα19-Jα33 sequences could be detected in MR1 deficient or germ-free mice, indicating a role for MR1 and commensal gut-bacteria in either the selection or expansion of this population (Treiner, Duban et al. 2003).

MR1 is an MHC class 1b molecule, which by comparison with the classical MHC class 1a molecules, exhibits very limited polymorphism between individuals (Parra-Cuadrado, Navarro et al. 2000). In fact there is very striking

conservation of the MR1 sequence across a number of species (Goldfinch, Reinink et al. 2010), and human MAIT cells can be activated by mouse MR1 and vice-versa (Le Bourhis, Martin et al. 2010). MHC class 1b molecules typically have specialised functions presenting specific types of antigens to lymphocytes with very restricted receptor repertoires, of which lipid antigen presentation by CD1d to NK-T cells is a good example.

Evidence suggests that MR1 activation of MAIT cells is ligand dependent. Targeted mutations to the MR1 gene demonstrates that MAIT cell activation requires a folded MR1 molecule and that MR1 folding and MAIT cell activation is peptide dependent (Huang, Gilfillan et al. 2005). Although MR1 encoding mRNA is widely expressed, the MR1 molecule has been difficult to detect at the cell surface, with the molecule remaining largely intracellular (Miley, Truscott et al. 2003) and the exact nature of the ligand has yet to be defined. MR1 antigen processing is thought to occur independently of conventional pathways of antigen presentation via MHC class I and II. This is demonstrated by the activation of MAIT cells by bone marrow derived dendritic cells from TAP- and invariant chain- knock out mice (Le Bourhis, Martin et al. 2010). MR1 localises in multivesicular endosomes and traffics through endocytic compartments – allowing sampling of both endocytosed and endogenous antigens (Huang, Gilfillan et al. 2008). Presentation of phagocytosed exogenous antigen to and activation of MAIT cells has been demonstrated by culture overnight with bone marrow derived dendritic cells that have been infected with *E.coli*. This effect is abrogated on the addition of inhibitors of endocytosis (Le Bourhis, Martin et al. 2010).

NK-T cells and MAIT cells are similar in that they are the only lymphocyte populations to have a restricted TCR repertoire and restricting MHC molecule that is conserved between species. NK-T cells are more abundant in mice, whereas MAIT cells are more numerous in man. Their developmental pathways however would appear to be distinct, in that NK-T cells are selected, expand and develop their innate-like phenotype and function prior to exit from the thymus. On leaving the thymus they already express the transcription factor zinc finger and BTB domain-containing protein 16 (ZBTB16), which is crucial for the ready innate/effector functions of NK-T cells (Kovalovsky, Uche et al. 2008). MAIT cells are found in the thymus, but are naïve at this stage and low in number (Martin, Treiner et al. 2009). Very small amounts of the TCR Vα7.2-J33 transcript are found in cord blood (Tilloy, Treiner et al. 1999), yet MAIT cells are abundant in adults and have acquired an effector memory phenotype. Mouse studies demonstrate that MAIT cells require MR1 expression on a non-hematopoietic cell in the thymus for selection. Their subsequent peripheral expansion requires B cells and mucosal commensal flora. MAIT cells also express the transcription factor ZBTB16, but this has only been described to date in the effector memory population found in adults (Martin, Treiner et al. 2009).

MAIT cells have been demonstrated to play a possible role in immunity. Human MAIT cells respond *in vitro* to dendritic cells infected with a diverse range of bacteria, including *Mycobacterium tuberculosis, Escherichia coli, Salmonella typhimurium and Staphlococcus aureus* in an MR1 dependent

manner (Gold, Cerri et al. 2010), which has been replicated using murine *i*Vα19-transgenic cells (Le Bourhis, Martin et al. 2010). Interestingly *Enterococcus facalis* and *Streptococcus* failed to induce activation, indicating that maybe they don't possess an MR1 restricted antigen or stimulate an intermediate pattern recognition receptor required for surface expression of MR1. MAIT cells are also activated by yeast infected dendritic cells, but not those exposed to number of unrelated viruses (Le Bourhis, Martin et al. 2010). *In vivo* experiments using *i*Vα19-transgenic mice on MR1+/+, compared to MR1-/-, backgrounds demonstrated lower bacterial loads in the spleen at day 15-post infection with the mycobacterium *M abscessus.* MAIT cells are numerous in peripheral blood and at diverse tissue sites in humans, including the gut, lung, liver and peritoneal cavity (Le Bourhis, Martin et al. 2010), (Dusseaux, Martin et al. 2011) and are likely to play an important role in bridging innate and adaptive immunity at these sites of pathogen entry.

MAIT cells are a striking human T cell subset that are likely to be encompassed by the population described to be CD161++ Tc17 cells, on the basis of shared phenotypic and functional features. Cross-over in terms of TCR usage is yet to be explored, however further evidence of parallels between these subsets comes from the fact that CD161++CD8+ T cells have lower expression of CD8β (Billerbeck, Kang et al. 2010 ; Takahashi, Dejbakhsh-Jones et al. 2006) and preliminary flow cytometry data from the Klenerman group (unpublished) would suggest that this population contains a further subset of cells that are CD8β negative, or CD8$\alpha\alpha$ cells. Human MAIT cells are also described to contain a prominent CD8$\alpha\alpha$ population. CD8$\alpha\alpha$ T

cells have been extensively described in mice, but remain poorly studied in man.

1.2 CD8αα T cells

1.2.1 CD8αβ and CD8αα molecules

CD8 was first discovered as a cell surface marker for cytotoxic T cells, distinguishing them from the T helper cells that express CD4 (Cantor and Boyse 1975; Cantor and Boyse 1977). The CD8 molecule is a disulphide-linked dimer of CD8α and CD8β molecules, stably expressed on the cell surface as either a CD8αβ heterodimer or a CD8αα homodimer. The CD8 molecules are trans-membrane proteins containing N-terminal immunoglobulin (Ig) domains, extended and glycosylated hinge and stalk regions, and trans-membrane and cytoplasmic portions (Weber G 1998). CD8αβ and CD8αα are found expressed independently or together on mature TCRαβ+ cells and are also co-expressed with CD4. CD8αα expression has also been described on murine TCRγδ+ T cells (Cheroutre and Lambolez 2008). CD8αβ and CD8αα molecules are not functionally homologous and play quite different roles in CD8 T cell function.

The CD8αβ molecule is important for T cell activation. Despite extremely low affinity binding, it stabilizes the interaction between the T and antigen-presenting cell by binding to an invariant region of the MHC class I molecule. Analysis of the crystal structure of CD8αα molecules has demonstrated an asymmetric interaction with MHC class I. The Ig domain of one CD8α chain

predominantly binds to an invariant site in the α3 domain of MHC class I, with more minor binding to the α2 domain and β2-microglobulin. The second CD8α molecule provides some contact points with the α3 domain only (Gao, Tormo et al. 1997; Kern, Teng et al. 1998). There is no equivalent structural data for the CD8αβ heterodimer, however BIAcore experiments demonstrate that soluble CD8αα and CD8αβ bind to MHC class I with similar affinities (Garcia, Scott et al. 1996), (Kern, Hussey et al. 1999), although when expressed at the cell surface CD8αβ is a much better co-receptor compared to CD8 (Witte, Spoeri et al. 1999). This suggests an important role for CD8β in enhancing the quality of the interaction between CD8 and MHC class I, despite it being the CD8α molecule that associates with the TCR-CD3 signaling components p56lck and linker of activated T cells (LAT) (Bosselut, Zhang et al. 1999). Experiments using β chimeric constructs demonstrate the ectodomain of CD8β to enhance the interaction of CD8 with MHC class I, whereas the cytoplasmic tail increases association of the CD8α chain with intracellular signaling molecules (Bosselut, Kubo et al. 2000). The enhanced MHCI ligation is likely due to modifications in the β stalk glycosylation that improve the stoichiometry of CD8αβ compared to CD8αα binding (Wong, Wang et al. 2003). CD8β also actively recruits the TCR to lipid rafts and aids the association of p56lck and LAT to the CD8α tail in a mechanism reliant on CD8β palmitoylation (Arcaro, Gregoire et al. 2000).

Unlike the CD8αβ heterodimer, the molecule CD8αα is believed to act as a co-repressor rather than a co-receptor (Cheroutre and Lambolez 2008). Co-

expression decreases the functional avidity of the TCR$\alpha\beta$;MHC-peptide activation complex (Cawthon and Alexander-Miller 2002), failing to support activation of CD8$\alpha\beta$ dependent TCRs on CD8$\alpha\alpha$ cells (McNicol, Bendle et al. 2007). The exact mechanisms of the co-repressor function are not fully elucidated, however CD8$\alpha\alpha$ is excluded from the lipid rafts of the activation complex (Pang, Hayday et al. 2007), suggesting that its inhibitory effects are mediated via invariant components of the signaling cascade downstream of the CD3-TCR complex and might sequester non-raft associated p56lck and LAT from the activatory signaling cascade. In fact, CD8$\alpha\alpha$ disrupts the integrity of the lipid raft CD3-TCR complex (Cawthon and Alexander-Miller 2002). CD8$\alpha\alpha$ cells also express high levels of LAT2, a negative regulator of LAT, although direct binding to the CD8α cytoplasmic tail has not been demonstrated (Denning, Granger et al. 2007) (**Figure 1.5**).

Thymic leukemia antigen (TL) is an MHC class 1b molecule in mice that has been found to bind to CD8$\alpha\alpha$ with very high affinity (Leishman, Naidenko et al. 2001). It is constitutively expressed by mouse intestinal epithelium (Hershberg, Eghtesady et al. 1990), where it is believed to regulate homeostatic proliferation (Yamamoto, Fujihashi et al. 1998) of CD8$\alpha\alpha$ cells and stabilise CD8$\alpha\alpha$ expression. It is not thought to act as an antigen presenting molecule in this context, as binding to CD8$\alpha\alpha$ leads to structural changes to the antigen binding groove that make it impossible for antigen to

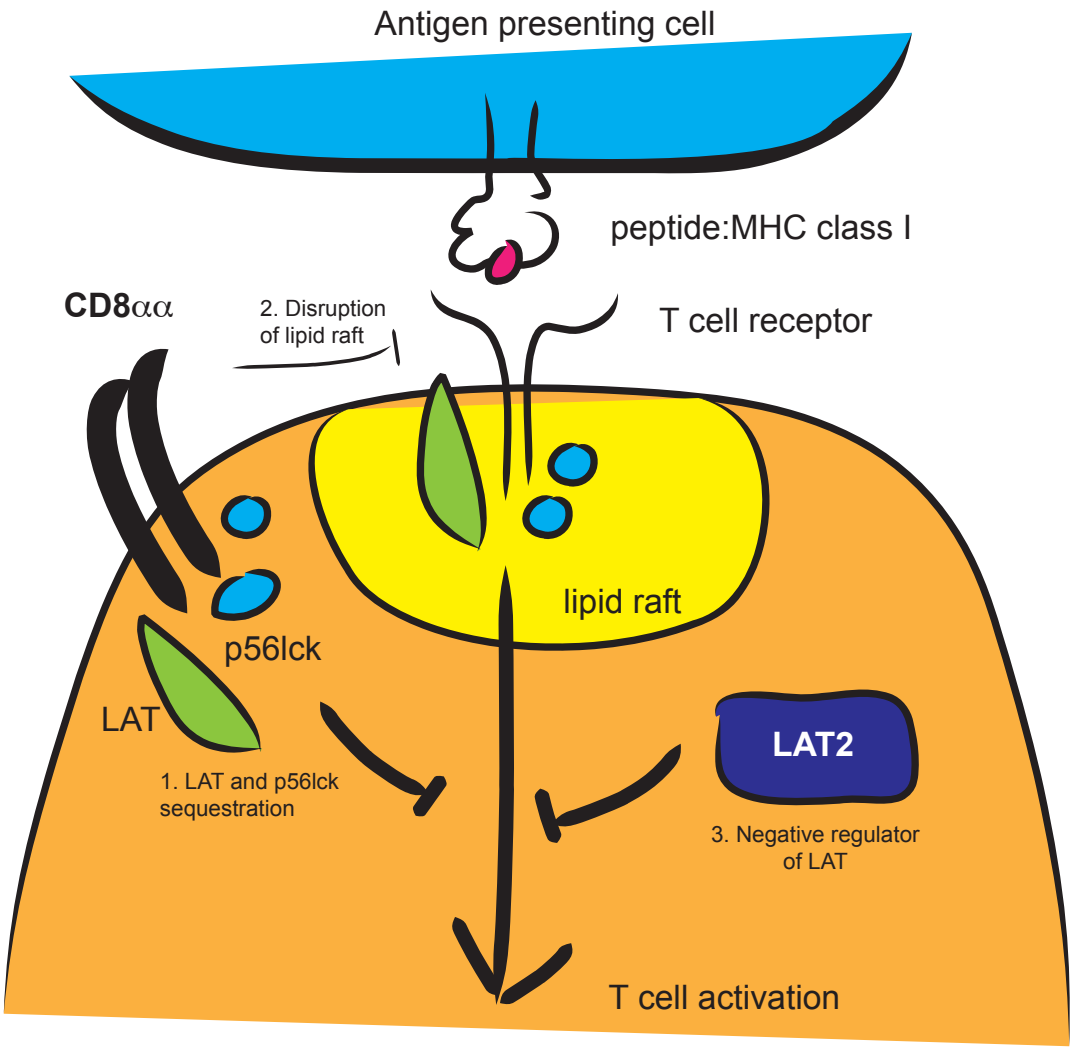


Figure 1.5. Potential mechanisms of CD8aa co-repressor function.

The co-repressor function of CD8αα may act via a number of mechanisms. 1. Sequestration of LT and p56lck from the activatory cascade outside the lipid raft. 2. Disruption of the lipid raft CD3-TCR complex. 3. High LAT2 expression by CD8αα cells, a negative regulator or LAT2. bind (Liu, Xiong et al. 2003). A homologue has not been identified in humans to date.

1.2.2 CD8αα cells

CD8αα expressing cells have been most extensively described to be an intraepithelial cell population of the small intestine in mice. Murine models suggest two pathways of differentiation of this CD8αα subset. The first model is of a subset of single positive CD8αα cells that undergo agonist selection in the thymus, where they co-express CD8αα, CD8αβ and CD4. The expression of CD8αα allows survival of cells with self-reactive TCRs that would otherwise be negatively selected under conventional thymic selection. Such cells are observed to migrate preferentially to the gut mucosa as CD8-CD4- cells, and re-express CD8αα due to antigen stimulation and exposure to IL-15. The second pathway describes conventionally selected activated CD4 and CD8αβ cells that express CD8αα on migration to the gut (Cheroutre and Lambolez 2008). In addition, in a murine lymphocytic choriomeningitis virus (LCMV) model, high avidity CD8αβ cells transiently expressed CD8αα during early antigen-induced activation and these cells were thought to show a preferential ability to differentiate to memory cells on adoptive transfer (Madakamutil, Christen et al. 2004).

Expression of CD8αα is believed to play an immuno-modulatory role, its co-repressor functions allowing the persistence of a diverse repertoire of high-risk effector cells to reside at sites with high-risk of pathogen entry without causing overt immunopathology. Murine CD8αα cells have been shown to protect against EAE (Tang, Maricic et al. 2007) and colitis (Poussier, Ning et al. 2002) in adoptive transfer models. In fact, mice that lack the CD8αα ligand TL, which is constitutively expressed in the murine gut, develop a more severe phenotype of colitis in experimental models (Olivares-Villagomez, Mendez-Fernandez et al. 2008).

In humans, CD8αα/CD8α+β^{low} cells are found within the memory cell population of adult peripheral blood and the overall proportion of these cells increases with age (Konno, Okada et al. 2002). The TCR repertoire of intraepithelial lymphocytes (IELs) in mice (Regnault, Cumano et al. 1994), (Regnault, Kourilsky et al. 1995), rats (Helgeland, Johansen et al. 1999) and humans (Gross, Schwartz et al. 1994) is notably oligoclonal. However, in germ free rats, both SP CD8αα and CD8αβ IELs have a broad and non-overlapping TCR diversity that becomes randomly polarised on subsequent exposure to gut antigen on microbial colonization (Helgeland, Dissen et al. 2004). In rats there is an increase from early life in the proportion of CD8αα cells compared to CD8αβ cells (Helgeland, Brandtzaeg et al. 1997), a phenomenon also observed in mice (Podd, Aberg et al. 2004). Narrow TCR usage has been described for CD8αα cells of human adult peripheral blood (Konno, Okada et al. 2002), with matching polarised clones present in the CD8αβ and CD8α+/β^{low} populations. The expansion in number and the narrowing of the TCR repertoire of the CD8αα subset with age across species would suggest an antigen driven process, in keeping with the requirement of MR1 expression and mucosal commensal flora for the development of MAIT cells, already described to express CD8αα.

1.3 The role of CD161++CD8+ T cells in the immune response to hepatitis C virus

The immune response to chronic hepatitis C virus (HCV) infection is much studied in an attempt to understand why immune failure occurs, the virus

persists and how such failure might be overcome by vaccination or immunotherapy. Work on the CD161++ Tc17 cells by the Klenerman group started with the identification of CD161 as a marker for hepatitis B and C specific T cells (Northfield, Kasprowicz et al. 2008). Although the CD161++CD8+ T cell subset is not thought to contain these antigen specific T cells, which are thought to be CD161+, there is good evidence that this subset are present in the liver and enriched there in the context of chronic HCV, where they may play a role in determining disease progression (Billerbeck, Kang et al. 2010) (**Appendix 1**).

1.3.1 The liver immune environment

The liver is exposed to a heavy burden of antigen of microbial products and food absorbed through the intestine via the portal circulation. These are recognised and taken up by elements of both the innate and adaptive immune system of the liver, but the predominant response is of tolerance and not inflammation. This makes physiological sense, yet does create a vulnerable setting of which certain pathogens, such as malaria and chronic viral hepatitis, take clear advantage.

Arterial systemic and portal venous blood mixes in the liver along its thin walled vessels called sinusoids (**Figure 1.6**). The sinusoid is host to a number of cells with immune activity including resident Kupffer cells, dendritic cells liver sinusoidal epithelial cells and hepatic stellate cells, in addition to the circulating lymphocyte populations. Large populations of NK, NK-T and CD8 T cells are observed, with a relative paucity of CD4+ T cells.

The innate immune system responds to its environment via a constellation of intra- and extracellular pattern recognition receptors that recognise conserved elements of pathogens. When engaged by their ligands on cells of the innate immune system, these activate shared, intracellular, signalling cascades and typically leads to the production of cytokines and chemokines involved in providing first line immunity and in augmenting the immune response. In the liver however instead of producing pro-inflammatory factors, such as IL-1, IL-6, TNF-α, IL-12 and IL-8 in response to various bacterial products, there is marked production of the anti-inflammatory cytokine IL-10 (Crispe 2009).

The resident innate lymphocytes of the liver, NK and NK-T cells, are prominent populations and present at higher frequencies than found in other tissues. Evidence would suggest they have a greater role in mediating liver immunity as opposed to tolerance. However, there is scope for potentially dichotomous functions, likely controlled by the nature of the reaction of their immune partners in the liver to pathogens and antigen encountered. Hepatic NK cells are activated by both cytokines and interaction with an excess of

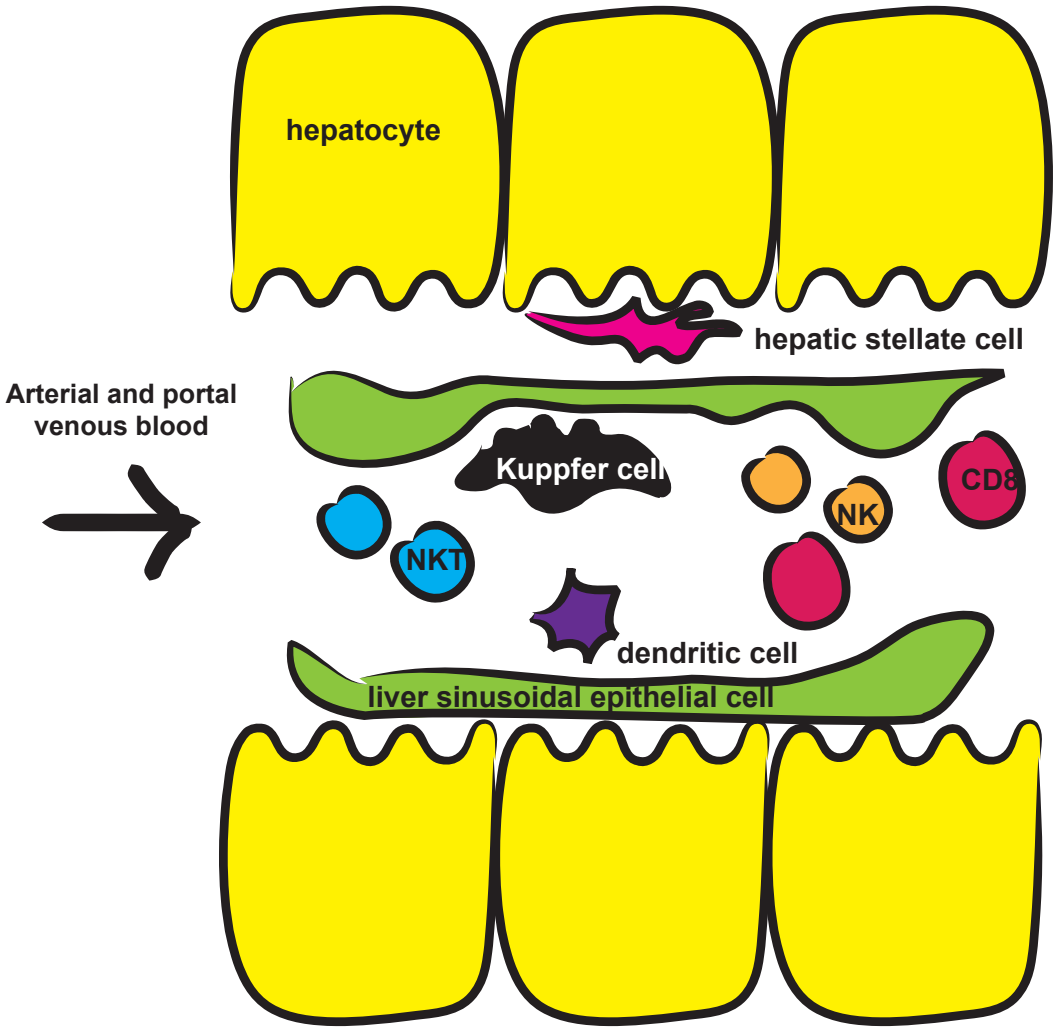


Figure 1.6. The hepatic sinusoid and resident antigen presenenting cells.

Systemic arterial and portal blood mix closely with the cells of the hepatic sinusoid. Kuppfer cells, liver sinusoidal epithelial cells, hepatic stellate cells, dendritic cells and heptocytes all act as antigen presenting cells for the circulating T and NKT cells.

activatory over inhibitory ligands. They make IFN-γ in response to IL-12 (Nguyen, Salazar-Mather et al. 2002), and display cytotoxicity in response Kuppfer cell derived IL-18 (Dao, Mehal et al. 1998). Depletion in mouse models suggest a role for NK cells in immunity to hepatotrophic viruses (Salazar-Mather, Orange et al. 1998) and human studies show they may be involved in liver transplant rejection (Hanvesakul, Spencer et al. 2008). NK-T cells are classically defined by their expression of an invariant TCR that binds CD1d, although a non-classical subset also exists that is not restricted by this ligand. They have been shown to have a role in anti-tumour immunity (Shin, Nakayama et al. 2001) and to promote inflammation and fibrosis following xenobiotic-induced liver injury (Ishikawa, Ikejima et al. 2010).

Evidence suggests that primary T cell activation and induction of adaptive immunity does occur within the liver (Klein and Crispe 2006). However CD8 T cells primed here appear to undergo activation followed by apoptosis (Qian, Lu et al. 1997), (Lee, Lu et al. 1999). This could be explained by the concept of 'death by neglect', where T cells are primed on non-professional antigen presenting cells (APCs) in the absence of co-stimulation, e.g by hepatocytes. However, a number of different cell types in the liver do have the capacity to act as professional APCs, including dendritic cells, Kupffer cells, liver sinusoidal endothelial cells and stellate cells through expression of co-stimulatory molecules although they appear to promote tolerance by secreting IL-10 in response to TLR ligation as opposed to pro-inflammatory cytokines and express inhibitory and apoptosis inducing receptors, such as Fas ligand and PD-1 (programmed death-1) ligand (Crispe 2009). These phenomenon

help explain the ease of liver transplantation between MHC mismatched individuals and relative tolerance to the covert operations of chronic hepatotrophic viruses such as HCV. In circumstances where tolerance is broken a greater strength of or different immune signal may be required explaining why some pathogens, such as hepatitis A, are predictably cleared following an acute hepatitis. In keeping with this Kuppfer cells are shown to produce IL-10 in response to bacterial components (via the Myd-88 pathway) yet are also producers of NK activating IL-18. The effects of IL-18 are potentiated when Kupffer cells are activated by viral components via the alternative IFN regulatory factor 3 pathway to produce IFN-β and the amount of IL-10 produced is reduced (Tu, Bozorgzadeh et al. 2008).

As well as being an inducer of tolerance locally the liver also plays a role in systemic tolerance to antigen elsewhere. The classic experiments to demonstrate this were those looking at rejection of renal transplants between unrelated pigs. In the absence of immunosuppression non-HLA matched renal transplants were rapidly rejected whereas where a kidney and liver where transplanted together survival of the donor kidney was better (Calne, Sells et al. 1969). The process by which this occurs, where the antigens concerned are present in both grafts, is in the context of tolerance induction to antigens encountered in the liver not hard to understand with antigen specific T cells likely undergoing activation/ apoptosis as described above. However, the liver may also be involved in control of the immune response to antigens not encountered in the liver. Antigen-specific CD8 T cells are found sequestered in the liver in influenza, despite the viral ribonucleic acid (RNA) and antigen

being restricted to the respiratory system (Polakos, Klein et al. 2007). Given the persistence of influenza T cell memory amongst intrahepatic lymphocytes on adoptive transfer (Bertolino, Bowen et al. 2007), it is unlikely that such sequestration leads to wholesale CD8 deletion. Activated lymphoblasts that accumulate in liver sinusoids may be preferentially phagocytosed by Kupffer cells, unlike resting memory cells that may not have the same fate.

Further mediators of hepatic tolerance are regulatory T cells (Tregs). Tregs cells constitute a mixed population of naturally occurring thymically derived CD4+CD25+FoxP3+ regulatory cells, which provide bystander suppression, and antigen specific Th3 and Tr1 regulatory cells, which can be derived from naïve uncommitted CD4+ precursors. They function by secretion of the anti-inflammatory cytokines TGF-β and IL-10 and are implicated in the pathogenesis of a number of liver diseases. In chronic HCV infection (Rushbrook, Hoare et al. 2007) and hepatocellular carcinoma (Unitt, Rushbrook et al. 2005) there is an enrichment of Tregs, whereas in autoimmune liver disease a relative reduction is observed (Lan, Cheng et al. 2006), (Longhi, Hussain et al. 2006). They are actively recruited to the liver in the context of hepatic inflammation (Oo, Weston et al. 2010). Whether Tregs are involved in exporting tolerance to antigen expressed elsewhere has not been established, although antigen-specific regulatory cells could be detected in the spleens of mice infected with a liver-targeting adeno-associated virus (Breous, Somanathan et al. 2009).

1.3.2 Immunity to hepatitis C virus

HCV is a small, enveloped, single stranded RNA virus of the *Flavivirdae* family. It is primarily transmitted through infected blood products, either through contaminated medical equipment, blood products or unsafe injection of recreational drugs. It represents a global health threat with an estimated 200 million people infected worldwide, leading to a high burden of liver failure and cancer (Lauer and Walker 2001). About 80% of people who become infected go on to develop chronic infection and the difference in immunity between those who clear the virus and those who don't has raised real hope in terms of the eventual possibility of successful prophylactic vaccine design.

The role of the immune response to HCV has been the subject of much study in trying to establish the determinants of viral clearance during the acute phase of infection. T cells, antibodies and NK cells have all been implicated to play an important role, clearing the virus before it has a chance to mutate and escape immune control. In chronic HCV infection the immune system appears to have become ineffectual and exhausted, with the virus evolved beyond the immune system's reach.

Chimpanzee models and human correlative studies would suggest that both CD4+ and CD8+ T cells are key to viral control and clearance (Bowen and Walker 2005). In self-limiting acute disease, a broad and sustained CD4+ T cell response is observed from early infection (Aberle, Formann et al. 2006). Antigen-specific CD8 T cells are observed at 4-8 weeks post-infection, although have a stunned phenotype and do not secrete INF-γ. At a later stage

they do become able to secrete INF-γ and a corresponding rapid drop in viral load and clearance is seen (Thimme, Oldach et al. 2001). In chimpanzees, intra-hepatic antigen-specific CD4+ and CD8+ T cells accumulate from weeks 8-14 post infection, which corresponds to liver inflammation and viral clearance (Thimme, Bukh et al. 2002). These cells persist for decades post-infection (Takaki, Wiese et al. 2000) and may play a role in protective immunity to re-infection where shorter disease course and lower viral loads are observed upon re-challenge with the virus (Major, Mihalik et al. 2002). Further evidence that both CD4+ and CD8+ T cells are important in viral clearance in HCV is supported its association of spontaneous clearance with certain human leukocyte antigen (HLA) class I and II alleles. In a cohort of Irish women who were infected with HCV from a single source, the HLA alleles A3, B27, Cw*01, DRB1*01, DQB1*15 and DRB1*0401 were found to be protective, of which HLA-B27 had the strongest association with 80% of the women carrying the allele clearing their HCV spontaneously (McKiernan, Hagan et al. 2004).

The role of antibodies in viral clearance has also been explored. In acute infection antibodies are detectable against a variety of structural and non-structural proteins in most individuals. Many of these have no anti-viral activity, but some do have the capacity to block viral binding, entry and uncoating and target epitopes encoded within the envelope region in and adjacent to hypervariable region 1 which undergoes rapid mutation in the evolution of viral quasi-species, indicating such antibodies exert immune selection pressure. (Thimme, Neumann-Haefelin et al. 2008). Evidence for

the potential protective effect of neutralising antibodies comes from a study of a cohort of women infected from a single source with contaminated anti-D immunoglobulin where the contaminating strain was known. This has shown there to be a strong association between an early neutralising antibody response and clearance (Pestka, Zeisel et al. 2007).

NK cells are also implicated in successful clearance of HCV. They are a numerous cell population within the liver and capable of exerting anti-viral effects via production of cytotoxic granules, induction of apoptosis and secretion of the anti-viral cytokines IFN-γ and TNF-α. In contrast to T and B lymphocytes they act independently of antigen-specific priming to recognise and kill virus specific cells and so have the capacity to act early in infection, prior to the development of adaptive responses. In acute infection it has been reported that there is an increase in $CD56^{bright}$ NK cells compared to healthy controls, and that these cells are activated, indicating an active role in the immune response. They show increased expression of the activating receptor NKG2D, higher levels of IFN-γ production and cytotoxicity in those who go on to clear the virus (Amadei, Urbani et al. 2010). In further support of a role for NK cells in HCV viral clearance, genetic studies looking at the role of killer-inhibitory receptor (KIR) diversity and their HLA ligands in determining outcome to infection, have found that the combination of KIR2DL3 and its group 1 HLA-C ligand is protective against infection (Khakoo, Thio et al. 2004).

Where there is no clearance seen in the acute phase of HCV infection and patients develop chronic disease, immune failure is observed at many levels. There is a lack of a detectable CD4+ response, even in patients who have had detectible CD4+ responses in acute disease and transiently controlled the virus – these disappear as the virus persists. Antigen-specific CD8 T cells are few in number, have a stunned phenotype, produce little IFN-γ, are poorly cytotoxic and fail to proliferate (Rehermann 2009). Why this occurs is not clear, but maybe due to a number of causes; being primed in the tolerogenic environment of the liver, lack of CD4+ T cell help, immune exhaustion in the context of persistent antigen or induction of regulatory responses.

Neutralising antibodies are detected in chronic disease in most individuals, however a number of viral mechanisms may contribute to their failure to help control the infection at this stage. The targeting of epitopes in the hypervariable region 1 of the viral envelope genome leads to rapid loss of any effect as the virus mutates, evolves and escapes. In addition, the association of HCV with lipid particles enables viral uptake into cells via lipid receptors, so avoiding the neutralising effects of antibodies that inhibit direct HCV binding to hepatocytes.

NK cells are much reduced in number in peripheral blood from patients with chronic HCV compared to healthy controls (Morishima, Paschal et al. 2006), and whether this is a cause or a consequence of persistent infection is not known. NK cell numbers return to normal following successful anti-viral treatment (Dessouki, Kamiya et al. 2010). Deficiency in IL-15 during chronic

HCV infection may explain the reduction in numbers seen, which is required for NK cell development, proliferation and function (Meier, Owen et al. 2005). Further to this, changes in NK cell phenotype and function may also contribute to viral persistence. They fail to produce anti-viral IFN-γ yet increase production of immunoregulatory IL-10 and TGF-β, helping to skew the adaptive immune response and creating an advantageous environment for the persistence of the virus. Increased expression of the inhibitory receptor NKG2A alongside increased expression of its ligand, HLA-E, on HCV infected hepatocytes also acts to suppress NK cell function (Cheent and Khakoo, 2011).

In addition to the role of the cellular and humoral immune response in HCV clearance, recent data from genome-wide enrichment studies shows very significant advantage of certain variants within the IL28B gene region in achieving spontaneous clearance and clearance on treatment of HCV (Ge, Fellay et al. 2009), (Thomas, Thio et al. 2009). The IL-28B gene forms a gene cluster with IL-28A and IL-29 on the human chromosome 19. These genes encode the type III interferons IFN-λ 1, 2 and 3, which all have high sequence homology. They have antiviral activities similar to type I interferons (IFNα/β) and their expression depends on similar stimuli. The mechanism by which IFN-λ, from patients with a favourable genotype, exerts its differential effect are not yet fully elucidated, but the subject of intense on-going research.

1.3.3 CD161++CD8+ T cells and chronic viral hepatitis

Previous work by the Klenerman group at the University of Oxford identified the NK receptor CD161 to be expressed on HCV specific CD8+ T cells in humans, compared to those of other viral infections which did not (Northfield, Kasprowicz et al. 2008). The hypothesis driving this work was that NK receptors expressed on HCV-specific CD8+ T cells might be acting to modify T cells and explain the poor functionality observed (Spangenberg, Viazov et al. 2005). Subsequent to this CD161 was found to be a surface and differentiation marker for human type 17 CD4+ T cells (Cosmi, De Palma et al. 2008), which led to the investigation of the link between CD161 expression on CD8+ T cells and type 17 differentiation, phenotype and function as described above.

The role of CD161+CD8+ T cells and IL-17 producing cells in the liver in HCV has subsequently been further explored. A more discriminating antibody clone against CD161 allowed two CD161+CD8+ T cell populations to be identified, one expressing high levels (CD161++) and one expressing a lower level (CD161+) (**figure 1.3**). The CD161+CD8+ T cells are have now been shown by tetramer analysis to contain the HCV antigen-specific cells (personal communication, Georg Lauer) described previously (Northfield, Kasprowicz et al. 2008). The CD161+CD8+ T cell subset does not have type-17 phenotype and function by FACS analysis, although IL-17 production was demonstrated from intra-hepatic antigen-specific cells on ELISPOT (Billerbeck, Kang et al. 2010) (**Appendix 1**). However, the intra-hepatic IL-17 producers were shown by FACS analysis to be CD161++ after stimulation with phorbol 12-myristate

13-acetate (PMA) and ionomycin and, in keeping with their expression of CXCR6, were enriched in the liver compared to peripheral blood in HCV. Intra-hepatic IL-17 producing CD8+ T cells were shown to co-produce IL-22 and IFN-γ, with the frequency of IL-17/IFN- γ co-producers inversely correlated to hepatic fibrosis although no relationship was seen to viral load or liver inflammation. IL-17 itself has not been demonstrated to have a direct antiviral role (un-published data, Klenerman group).

Data from the MAIT cell literature enforces the idea that the CD161++CD8+ T cells are a distinct T cell lineage, which may play a niche role in immunity at tissue sites, such as the liver, and there is much scope for further research into the role of the CD161++CD8+ T cell subset in health and disease overall. Analysis of their role in chronic HCV forms an interesting frame for their further exploration in this thesis.

1.4 Key questions to be addressed in the thesis

1. **Do CD161++CD8+ T cells develop from a pre-committed naïve CD161+ precursor?**

2. **To what extent are CD161++CD8+ T cells related to MAIT cells?**
3. **What is its relationship of the human CD8αα T cell population to the CD161++CD8+ T cell subset?**

4. **What is the phenotype, function and tissue distribution of the human CD8αα T cell subset?**

5. **Are CD161++CD8+ T cells playing an active role in the immune response to chronic hepatitis C?**

2 Methods and Reagents

2.1 Study subjects

Details of the study subjects used for individual experiments are detailed in the methods section of each results chapter.

2.2 Sample preparation

2.2.1 Peripheral blood mononuclear cell and cord blood mononuclear cell separation

Mononuclear cells were isolated from fresh EDTA peripheral blood and cord blood samples stored for less than 12 hours at ambient temperature by Ficoll-Histopaque density gradient centrifugation (Axis Sheild). Whole blood or cord blood samples were carefully layered onto 15mls of Lymphoprep (Axis Sheild) in 50ml falcon tubes and spun in a refrigerated centrifuge, with a swinging bucket rotor at 20^0C, 2200 revolutions per minute (rpm) for 24mins with the brake setting off. The buffy layer was then removed using a sterile pastette from immediately above the lymphoprep layer and placed in a second 50ml falcon tube. R10 media (see section 1.12.2 below for recipe) was then added to a volume of 50mls and spun down at 1800 rpm for 10 minutes at 20^0C. The supernatant was poured off and the cell pellet re-suspended in a further 50mls of R10 media and re-spun at 1600 rpm for 7 minutes at 20^0C. The supernatant was again poured off and the cells re-suspended in 10mls of R10 prior to counting using a haemocytometer. All steps other than centrifugations were performed in a biological safety cabinet.

2.2.2 Cell freezing and thawing protocols

Cells not required for immediate experimental use were frozen by the following method. Cells were spun down after counting at 1600rpm for 7 min at 20˚C. The cell pellet was then re-suspended in 1ml of fetal calf serum (FCS), followed by a solution of FCS and chilled freezing mix (see section 1.12.2 below for recipe) at a ratio of 1:1 resulting a cell concentration of 10-12 x 10^6 cells/ml. 1ml of cell suspension was then placed in a chilled freezing vial and vials placed in a 5100 Cryo 1˚C freezing container (Nalgene) and stored at -80˚C for up to 3 days prior to transfer to a liquid nitrogen storage container.

Thawing of samples was performed by the following method. 10mls per vial of cells to be defrosted of thawing media (see section 1.12.2 below for recipe) was prepared and pre-warmed to 37˚C in a water bath. Frozen vials of cells were removed from liquid nitrogen storage and placed on dry ice. The vials were then placed in a 37˚C water bath and gently agitated. The thawed cell suspension was then transferred into a 15ml falcon tube and re-suspended in the pre-warmed thawing mix on a drop-wise basis whilst swirling the tubes gently until a full 10mls had been added. The thawed samples were then centrifuged at 1600rpm for 10mins at 20˚C. The cell pellet was then re-suspended in the desired volume of media or phosphate buffered saline (PBS) depending on the subsequent experimental protocol.

2.2.3 Liver infiltrating lymphocyte extraction

Liver infiltrating lymphocytes (LILs) were extracted by collaborative partners in Birmingham University, UK and Harvard, USA using the following method. LILs were freshly isolated from explanted liver tissue from chronic liver

diseases including alcoholic cirrhosis, primary biliary cirrhosis and HCV from Queen Elizabeth Hospital (Birmingham, UK) and Massachusetts General Hospital (Boston, USA) transplantation programs. Explanted human liver tissue was diced into 5 mm^3 cubes and washed in PBS/10% (v/v) 2%FCS to remove any peripheral blood and re-suspended in RPMI-1640/10% (v/v) FCS. This suspension was then homogenized for 6 minutes at 260 rpm in a Stomacher-400 circulator (Seward, Norfolk, UK) before being filtered through a fine (60 μm) nylon mesh. The resulting heterogeneous cell population was washed several times in RPMI-1640/10% FCS, layered onto Lympholyte (VH Bio) and density gradient centrifugation was applied at 720 g for 25 minutes. Separated liver derived lymphocytes at the interface were removed, washed and cell viability assessed by trypan blue exclusion. Cells were then frozen and stored in liquid nitrogen tanks for later analysis.

2.2.4 Lamina propria mononuclear cell extraction

Lamina propria mononuclear cells (LPMCs) we isolated from endoscopic biopsy samples from human colon and small bowel after overnight storage in RPMI-1640/5% FCS at 4^0C. Biopsies were put in a 1mM DDT solution in Hanks Buffered saline solution (HBSS) (Invitrogen) and put in a shaking incubator at room temperature for 15 mins. The samples were then washed 3 times in HBSS. Biopsies were then placed in a gentleMACS tube (Miltenyi biotech) with 5ml of collagenase A (1.5mg/ml)/ DNAse (1:200) solution and shaken on a gentle gentleMACS dissociator (Miltenyi biotech) brain01 setting. Samples were then shaken at 37^0C for 1 hour, before being placed on an

energetic gentleMACS brain01 programme. Cells were then washed in HBSS and stained for FACS analysis.

2.3 Fluorescent antibody staining for flow cytometry

Antibodies and concentrations used are detailed in section 1.12.1 below.

2.3.1 Surface staining of separated lymphocytes

PBMCs, cord blood mononuclear cells, LPMCs and LILs in 100μl of PBS were incubated with anti-surface antigen directed antibodies and a live/dead marker at 4^0C for 20mins. All cells were then washed in phosphate buffered saline (PBS) and fixed with 1% formaldehyde in PBS prior to analysis by flow cytometry.

2.3.2 Whole blood surface staining

200μl of whole blood was incubated with anti-surface antigen directed antibodies at 4˚C for 20mins. The red blood cells were then lysed with 10% FACS-lysis buffer (BD Pharminogen, Heidelberg, Germany) in sterile de-ionized water. The cell lysate solution was then washed in PBS and fixed with 1% formaldehyde in PBS prior to analysis by flow cytometry.

2.3.3 Intracellular cytokine staining

Intracellular cytokine staining was performed on freshly isolated PBMCs. 4 x 10^6 cells in 1ml of R10 medium were stimulated with 2μl of leukocyte activation cocktail (BD Pharminogen) and incubated (37^oC, 5% CO_2) for 4 hours. Cells were then washed in PBS and stained with anti-surface antigen

directed antibodies and a live/dead marker and incubated at 4^{o}C for 20 minutes. After fixation/permeabilisation (FoxP3 staining kit, BD Pharminogen), cells were stained with antibodies against intracellular antigens and incubated at 4^{o}C for 20 minutes and then washed in 10% PermWash buffer (BD Pharminogen) in sterile de-ionised water prior to analysis by flow cytometry.

2.3.4 Intracellular staining for transcription factors and proliferation markers

Intracellular staining for RORγt, ZBTB16 and Ki-67 was performed on separated mononuclear cells. 1 x 10^{6} cells were fixed/permeabilsed (FoxP3 staining kit, BD Pharminogen), then washed X3 in 10% PermWash buffer (BD Pharminogen). Cells were then stained with intracellular antigen-specific antibodies and incubated at 4^{o}C for 20mins. Cells were subsequently stained with antibodies against surface antigens and a live/dead marker, washed in 10% PermWash buffer (BD pharminogen) and fixed in a 1% formaldehyde solution in PBS prior to analysis by flow cytometry.

2.3.5 Controls, flow cytometry and analysis

Samples prepared as outlined above were analysed by flow cytometry, either using a FACSCaliber or LSRII cytometer (BD). For the FACSCaliber, samples were single stained with antibody and compensation was set manually. For the LSRII each experiment was individually compensated using FACSDiva software (BD) and single antibody stained compensation beads (BD) for the specific antibodies and fluorochromes used in any particular experiment along with a negative bead control. Compensation was also verified using ‘fullstain

minus one' (FMO) panels for anchor antibody panels used (CD3, CD4, CD8, CD161). Test antibodies against non-anchor panel antigens were titrated to find the optimum concentration and then stained along with parallel isotype and negative controls to ensure accurate subsequent gating of positive and negative populations. All analysis of flow cytometry data was performed using FLowJo software (Tree star, Ashland, OR, USA).

2.4 Cell sorting

2.4.1 CD8 enrichment

Cell suspensions were placed in a 5ml polystyrene FACS tube (BD) and prepared at a concentration of $5x10^7$ cells/ml in the EASYSep recommended medium (see section 1.12.2 below for recipe). EasySep negative selection human CD8 T cell enrichment cocktail (STEMCELL Technologies) was added at 50μl/ml cells, mixed well and incubated at room temperature for 10 mins. Then EasySep magnetic nanoparticles (STEMCELL Technologies) were added at 50μl/ml cells, mixed well and incubated at room temperature for 10mins. The cell suspension was then brought up to a total volume of 2.5ml by adding the recommended medium and mixed by pipetting. The 5ml FACS tube was then placed into the EasySep magnet (STEMCELL Technologies) and set aside for 5 mins. After this time the magnet was picked up, inverted and the CD8 enriched contents of the FACS tube poured into a second 5ml FACS tube. This second tube was then placed into the magnet, set aside for 5 mins, inverted and the contents poured into a third FACS tube. The CD8 enriched sample was then spun down at 1700rpm for 7 minutes and the pellet re-suspended in either R10 media or PBS for subsequent use.

2.4.2 Positive selection

Cell suspensions were placed in a 5ml polystyrene FACS tube (BD) and prepared at a concentration of 2 x 10^8 cells/ml in EasySep recommended medium (see section 1.12.2 below for recipe). Samples containing 10^7 cells or fewer were re-suspended in 100μl of recommended medium. Species-specific FcR blocking antibody (STEMCELL Technologies) was added at 100μl/ml cells and mixed by pipetting. A PE-conjugated antibody against the desired antigen to be selected was then added at a concentration of 3μg/ml cells, mixed well and incubated at room temperature for 15 mins. EasySep PE selection cocktail (STEMCELL Technologies) was then added at 100 μl/ml cells and incubated for a further 15 mins at room temperature. EasySep magnetic nanoparticles (STEMCELL Technologies) were then added at 50μl/ml cells, mixed well and incubated at room temperature for 10 mins. The total volume of the cell suspension was then brought up to 2.5mls with recommended medium, mixed well and the 5ml FACS tube placed in the EasySep magnet (STEMCELL Technologies) for 5 mins. The magnet was then inverted and the contents poured into a second 5ml FACS tube. This sample was then either discarded or saved for further experiments. 2.5mls of recommended medium was then added to the first 5ml FACS tube containing the positively selected cell population and placed back in the magnet for a second and then third round of purification. At the end of this process the positively selected population was re-suspended in either PBS or R10 media prior to use in subsequent experiments.

2.4.3 MoFlo cell sorting

1 x 10^7 PBMCs or cord blood mononuclear cells were initially CD8 enriched as described above, and stained with CD3-FITC, CD8α-PECy7, CD8β–PE and CD161-APC. The desired populations were then gated and sorted using a MoFlo high-speed cell sorter (Beckman Coulter) in collaboration with Andrew Worth from the Jenner Institute, University of Oxford. Sorted cell populations were snap frozen and stored at -80^0C prior to RNA extraction.

2.5 Cell culture

PBMCs were CD8 enriched and subsequently PE-positively selected using a CD8β–PE antibody to obtain a >95% pure CD8$\alpha\beta$ cell population, depleted of CD8$\alpha\alpha$ cells. 2 x10^5 cells were then placed in 96 well culture plates at a concentration of 1 x 10^6 cells/ml in an incubator (5% CO_2, 37^0C). Cells were incubated in either R10 culture media alone or with anti-CD3/CD28 beads (Dyna beads, Invitrogen) at a bead to cell ratio of 1:1 and with or without cytokines in different combinations as described under specific experiments; IL-1β (10ng/ml), IL-2 (25ng/ml), IL-15 (10ng/ml) and IL-18 (40ng/ml). Media was changed and cytokines added on days 3 and 6. Cultures containing anti-CD3/CD28 beads were placed in an EasySep magnet for 1 min to remove the beads. Cells were washed in PBS and prior to analysis by flow cytometry.

2.6 RNA extraction

Total RNA was extracted from snap frozen sorted cell samples using the RNeasy mini kit and an adapted protocol from the manufacturer's instructions. (Qiagen). Frozen samples were defrosted on ice and 350μl of RTL buffer

added. Samples were then homogenized by placing the samples on QIAShedder columns (Qiagen) and spun for 2 mins at full speed. 350μl of freshly prepared 70% ethanol was then added to the homogenized sample, which were then loaded onto the Qiagen spin columns and spun at 10,000 x g for 15 secs. The flow-through was then discarded. 700μl of RW1 buffer was added to each column and inverted several times. The columns were then spun again at 10,000 x g for 15 secs and the flow-through dicarded. 500μl of RPE was added to the columns and again spun at 10,000 x g for 15 secs and the flow-through discarded. This step was repeated before a further 500μl was added to the columns, which were then spun at 10g for 2 mins. The collection tube was changed and to dry the columns were spun at full speed with the lid closed for 1 min. 30μl of RNAse free water was then added to the column membrane and incubated for 5 mins. Columns were then spun at 10,000 x g for 1 min. The eluted RNA was then stored at -80^{0}C prior to further use. 1μl of each sample was retained for quantitative and qualitative analysis using the Nanodrop 2000 spectrophotometer (Thermo Scientific).

2.7 Microarray

2.7.1 cDNA amplification

The Pico Ovation WTA kit (NuGEN) was used for amplification of RNA according to the manufacturer's instructions. First strand cDNA synthesis was performed as follows. First strand buffer mix (A2), first Strand enzyme mix (A3), RNase-free water (Green D1) and the first strand primer mix (A1) were thawed on ice, flicked to mix, spun down for 2 secs and placed on ice. 2uL of A1 was added to each assigned well of a 0.2mL PCR strip (Star Lab) on ice

and 5uL of total RNA sample was added to the primer in the appropriate well and pipetted to mix, spun for 2 secs then returned to ice. PCR tubes were then placed in a thermal cycler (BioRad) on the following programme; 65^0C- 2 min, hold at 4^0C. Samples were removed, spun down briefly and placed on ice. Master mix I was then prepared on ice; A2 2.5 μl/ sample, A3 0.5 μl/ sample. 3μl of the master mix I was added to each sample, mixed well and spun down for 2 secs prior to transfer to the thermal cycler and run on the following programme; 4^0C – 1 min, 25^0C – 10 min, 42^0C – 10 min, 70^0C – 15 min, hold at 4^0C. Samples were then removed, spun down briefly and placed on ice.

Second strand cDNA synthesis was then performed as follows. RNAClean purification beads (Agencourt Bioscience) were incubated at room temperature for 15 mins prior to use. Second strand buffer mix (B1) and second strand enzyme mix (B2) were thawed, spun down and placed on ice. Master mix 2 was prepared with 2^{nd} strand buffer mix B1 9.75μl/ sample and 2^{nd} strand enzyme mix B2 0.25μl/ sample, mixed by pipetting, spun down and placed on ice. 10μl of master mix 2 was added to each reaction and mixed well by pipetting, spun down and placed on ice prior to transfer to the thermal cycler and run on the following programme; 4^0C – 1 min, 25^0C – 10 min, 50^0C – 30 mins, 70^0C – 5 mins, hold at 4^0C. Samples were then removed, spun down briefly and placed on ice.

The cDNA was then purified using the RNAClean beads that had been incubated at room temperature for 15 mins. 32μl of the bead suspension was

added to each reaction, mixed by pipetting and incubated at room temperature for 10 mins. The PCR strip was then transferred to the SPRIPlate 96R magnet plate (Agencourt) and left to stand for 5 mins to clear the solution of beads. With the PCR strip still on the magnetic plate 45μl of the binding buffer was carefully removed and discarded. With the PCR tubes still on the magnet 200μl of freshly prepared 80% ethanol was added to each reaction, allowed to stand for 30 secs and then removed. This step was repeated twice before the remaining beads were allowed to air dry for 20 mins.

For the cDNA SPIA amplification SPIA primer mix (C1), SPIA buffer mix (C2) and SPIA enzyme mix (C3) were thawed, mixed by vortexing, spun down and placed on ice. Master mix 3 was then made by adding together in the following order; SPIA buffer mix C2 80μl/ sample, SPIA primer mix C1 40μl/ sample, SPIA enzyme mix (C3) 40μl/ sample. 160μl of master mix 3 was then added to each reaction and mixed well, carefully washing the sides of the tubes to mix the beads. The reactions were then split and half the reaction volume (80μl) placed in a second PCR tube. The reactions were placed on ice prior to transfer to the thermal cycler which was run on the following programme; 4^0C - 1 min, 47^0C - 60 min, 95^0C - 5 min, hold at 4^0C. Samples were then removed, spun down briefly and placed on ice. The PCR strip placed on the magnetic plate and set aside for 5 mins to clear the solution of beads. The cleared supernatant was then carefully removed and transferred to a fresh tube prior to purification.

Amplified cDNA was then purified using MinElute spin columns (Qiagen) following a protocol that differs from the manufacturers instructions. 300μl of ERC buffer was added to two labeled 1.5ml tubes for each amplification reaction. 100μl of each sub-amplification reaction was then added to the ERC buffer, vortexed for 5 secs and spun down briefly. Each 400μl sample was then loaded on the a MinElute spin column placed in a collection tube and spun for 1 min at >10,000 x g in a microcentrifuge. The flow-through was discarded and the column replaced in the same collection tube. The columns were then washed by adding 500μl of PE buffer (with added ethanol) and spun for 1 min at >10,000 x g in a microcentrifuge. The flow-through was then discarded and 500μl of freshly prepared 80% ethanol added to the columns, spun for 1 min at >10,000 x g and the flow-through discarded. The columns were then placed back in the same collection tube and spun for a further 2 mins at >10,000 x g. The bottom of the columns were then blotted on paper and transferred to a clean 1.5ml microcentrifuge tube. 15μl of room temperature nuclease-free water (D1) was then added to the centre of each column and left to stand for 5 mins before being spun for 1 min at >10,000 x g. The sub-reactions were then pooled, mixed by vortexing and spun at full speed for 2 secs. The cDNA yield was then measured using the Nanodrop 2000 spectrophotometer (Thermo Scientific). Samples were then stored at -20 ^{o}C prior to quality control, labelling and fragmentation steps.

2.7.2 Quality control of amplified cDNA product

Quality control of the amplified cDNA product was performed using an Aligent bioanalyser and the RNA 6000 Nano kit (Aligent) according to the

manufacturers instructions. Samples that failed to meet the quality required were discarded and samples re-amplified from total RNA.

2.7.3 cDNA fragmentation and labelling

Using the Encore Biotin Module (NuGEN) amplified SPIA cDNA was fragmented as follows. Fragmentation buffer mix (FL1) and fragmentation enzyme mix (FL2) were thawed, spun and placed on ice. 25μl of each sample SPIA cDNA was placed into a 0.2ml PCR tube. The fragmentation master mix was then prepared with fragmentation buffer mix FL1 5μl per sample and fragmentation enzyme mix FL2 2μl per sample. 7μl of fragmentation master mix was added to each tube, mixed, spun briefly and placed on ice. The PCR tubes were then transferred to the thermal cycler and run on the following programme; 37 ^{o}C - 30 mins, 95 ^{o}C - 2 mins, 4 ^{o}C – hold. Samples were then removed, spun down briefly and placed on ice.

Biotin labelling was performed as follows. The labelling reagents were thawed, spun down briefly and placed on ice. The labelling master mix was prepared using labelling buffer mix (FL3) 15μl per sample, biotin reagen (FL4) 1.5μl per sample and labelling enzyme mix (FL5) 1.5μl per sample. 18μl of the labelling master mix was then added to each fragmented cDNA sample, mixed and spun prior to placing on the thermal cycler on the following programme; 37 ^{o}C – 60 mins, 70 ^{o}C – 10 mins, 4 ^{o}C – hold. The samples were then removed and stored at -20 ^{o}C prior to array hybridization.

2.7.4 Array Hybridization

Sample array hybridization was performed by an external third party (Imperial College Genomics Laboratory, London, UK) using the Genechip hybridization wash and stain kit (Affymetrix), Genechip hybridization oven (Affymetrix), Genechip fluidics station 450/250 (Affymetrix), Genechip scanner 3000 7G with autoloader (Affymetrix) and Human Genome U133 Plus 2.0 arrays, according to the manufacturers instructions.

2.7.5 Microarray data processing

Gene expression output CEL data files were received from Imperial College Genomics Laboratory and passed onto the Bioinformatics Group, Welcome Trust Centre for Human Genetics, Oxford, UK who analysed the data as outlined below.

The output CEL files were processed and analysed using the R statistical software (v 2.11) (R Development Core Team, R: A language and environment for statistical computing, R Foundation for Statistical Computing, Vienna Austria, 2010 (http://www.R-project.org). and BioConductor packages(Gentleman, Carey et al. 2004). Signal data were background corrected and normalised using the robust multichip average (RMA) method (Irizarry, Bolstad et al. 2003), which is implemented in the affy BioConductor package. Quality control analyses did not reveal any outlier samples.

Statistical testing was performed using the Linear Models for Microarray Analysis (limma) package (SMYTH 2005). Raw *p*-values were corrected for

multiple testing using the false discovery rate controlling procedure of Benjamini and Hochberg (BENJAMINI and HOCHBERG 1995), adjusted p-values below 0.05 were considered significant. Gene annotation was added to the final probe list from the NetAffx™ Analysis Center via the Affymetrix website (http://www.affymetrix.com).

2.8 Real-time PCR

2.8.1 First strand cDNA synthesis

cDNA synthesis was performed in 0.2ml PCR tubes. Per sample, RNA (10μg/ml) was added to a mix of 0.1μl random primers (Invitrogen), 1μl oligo (dT) primers (50μM) (Invitrogen), 0.5μl dNTPs (10mM) (Invitrogen) and sterile distilled water to make the reaction up to 13μl. The reactions were then transferred to a thermal cycler (BioRad) and heated to 65^{o}C for 10 mins. After this the Superscript III reverse transcriptase kit (Invitrogen) was used to make the following mix per reaction; 4μl 5X first strand buffer, 1μl 0.1M DTT, 1μl RNAseOUT recombinant RNAse inhibitor (40 units/μl). This was added to each reaction and transferred to the thermal cycler set at 50^{o}C for one hour.

2.8.2 Real-Time PCR

Quantitative real-time PCR reactions were carried out using a LightCycler 480 (Roche Diagnostics) and cDNA generated as described above**.** The following was added to each reaction; 6.7μl sterile, distilled water, 1.0 μl forward primer, 1.0μl reverse primer, 0.3μl of the appropriate probe from the Roche universal probe library, 10 μl of Faststart universal probe master (Roche) and 1.0 μl cDNA. Samples were loaded onto a 96-well LIghtcycler 480 multiwell plate

(Roche) and run on the LIghtcycler 480 96-well block (Roche) on the following cycle; 95^0C for 15 min and 55 cycles of 94^0C for 15s, 54^0C for 30s and 72^0C for 30s. Lightcycler 480 software (Roche), version 1.5, was used for setup, running and analysis of the real-time PCR quantification. Fold change in expression between samples was determined in relation to the GADPH house-keeping gene expression by the 2-ΔΔCT method (Livak and Schmittgen 2001).

2.9 Immunofluorescent staining

CD8+T cells were isolated using an EasySep CD8 negative selection kit and positive PE selection beads (Stem Cell Technologies) following anti-CD161 staining. Cells were plated in eight-chamber slides coated with CC2 (Nunc), fixed with methanol/acetone, air dried, blocked with 1% BSA, and washed with PBS/Tween 1% solution before staining.

2.10 Antibody Conjugation

The lightening link ATTO 488 kit (INNOVA Biosciences) was used to conjugate ZBTB16 and RORγt antibodies for immunofluorescence experiments. 1μl of LL-modifier reagent was added to 20μg of antibody in a volume of 10μl and mixed gently. This mixture was then added to the lyophilized lightening-link mix and pipetted up and down. The vial was then incubated for 3 hours at room temperature before the addition of 1μl of LL-quencher. The conjugated antibodies were then ready for use.

2.11 Statistical analysis

Statistical analysis, unless otherwise stated, was performed using GraftPad PRISM (GraphPad software) version 4 and appropriate statistical tests were chosen for each individual analysis. A *p* value of <0.05 was considered significant.

2.12 Reagents

2.12.1 Antibodies

ANTIGEN	CONJUGATED FLUOROCHROME	ANTIBODY CLONE	ISOTYPE	DILUTION	SUPPLIER
CD3	AmCyan	SK7	mouse IgG1	1/100	BD
CD3	Pacific Orange	UCHT1	mouse IgG1	1/100	Invitrogen
CD3	FITC	UCHT1	mouse IgG1	1/50	R and D
CD8α	PERCP	SK1		1/100	BD
CD8α	Alexa Fluor 700	RPA-T8	mouse IgG1	1/100	BD
CD8α	FITC	SK1		1/100	BD
CD8α	PE-Cy7	RPA-T8	mouse IgG1	1/200	BD
CD4	Alexa Fluor 700	RPA-T4	mouse IgG1	1/100	BD
CD8β	PE	2ST8.5HT	mouse IgG2a	1/100	Beckman Coulter
CD8β	APC	2ST8.5HT	mouse IgG2a	1/100	BD
CD161	APC	191B8	mouse IgG2a	1/100	Miltenyi Biotech
CD161	FITC	191B8	mouse IgG2a	1/100	Miltenyi Biotech
CD161	PE	191B8	mouse IgG2a	1/100	Beckman coulter
CCR1	PE	53504	mouse IgG2B	1/10	R and D
CCR2	APC	48607	mouse IgG2b	1/10	R and D
CCR5	APC	CTC5	mouse IgG2b	1/10	R and D
CCR6	FITC	53103	mouse IgG2b	1/10	R and D

CCR7	FITC	150503	mouse IgG2a	1/10	R and D
CXCR6	Alexa Fluor 647	TG3	mouse IgG2b	1/10	Biolegend
CXCR6	PE	56811	mouse IgG2b	1/10	R and D
IL-18R	PE	H44	mouse IgG1	1/10	eBioscience
CD26	PE	L272	mouse IgG2a	1/10	BD
CD45RA	PE	HI100	mouse IgG2b	1/10	BD
CD45RO	PE	UCHL1	mouse IgG2a	1/10	BD
CD62L	APC	Dreg 56	mouse IgG1	1/10	BD
CD69	FITC	FN50	mouse IgG1	1/10	eBioscience
CD25	PeCy7	BC96	mouse IgG1	1/10	eBioscience
PD-1	FITC	MIH4	mouse IgG1	1/10	eBioscience
HLA-DR	PeCy7	L243	Mouse IgG2a	1/10	eBioscience
CD28	FITC	CD28.2	mouse IgG1	1/10	BD
CD38	FITC	HIT2	mouse IgG1	1/10	BD
RORγτ	PE	AFKJS-9	rat IgG2a	1/10	eBioscience
RORγτ	Unconjugated	AFKJS-9	rat igG2a		eBioscience
ZBTB16	Unconjugated	D-9	mouse IgG1		Santacruz Biotech
Granzyme B	APC	GB12	mouse IgG1	1/10	Invitrogen
Perforin	PE	δG9	mouse IgG2b	1/10	BD
Ki-67	FITC	20Raj1	mouse IgG1	1/10	eBiosciences
TGF beta RIII	PE		Goat IgG	1/10	R and D
IL-15Rα	PE	JM7A4	mouse IgG2b	1/10	eBioscience
IL-17	PE	eBio64DEC17	mouse, IgG1	1/10	eBioscience
IFN-γ	FITC	4S.B3	mouse IgG1	1/10	BD
IL-22	PE	142928	mouse IgG1	1/10	R and D

2.12.2 Media recipes

R-10

RPMI medium 1640 (GibcoBRL)

10% heat inactivated (56°C, 60 min.) fetal calf serum (FCS)

200mM L-glutamine (GibcoBRL), diluted 1:100

100X penicillin-streptomicin solution (GibcoBRL), diluted 1:100

Freezing mix

Per vial to freeze down:

250μl RPMI medium 1640 (GibcoBRL)

250μl DMSO (Sigma)

500μl FCS

Thawing media

For stock solution:

RPMI medium 1640 (GibcoBRL)

200mM L-glutamine (GibcoBRL), diluted 1:100

100X penicillin-streptomicin solution (GibcoBRL), diluted 1:100

For immediate use to 9 mls of above stock solution add -

1 ml CTL wash supplement (CTL Ltd).

100μl DNase 1 (Roche) of 30U/ml stock.

EasySep recommended media

PBS containing 2% FCS and 1mM EDTA (Sigma).

2.12.3 Commercial kits

KIT NAME	SUPPLIER
EasySep Human CD8 enrichment kit	STEMCELL Technologies
EasySep PE-Positive selection kit	STEMCELL Technologies
Pico Ovation WTA kit	NuGEN
Encore Biotin module	NuGEN
RNeasy Mini kit	QIAgen
MinElute kit	QIAgen
FOXP3 staining kit	eBioscience
Lightening link ATTO488 antibody conjugation kit	Innova Bioscience
Live/Dead fixable dead cell stain kit	Invitrogen

3 Programming and differentiation of CD161++CD8α+ T cells

3.1 Introduction

CD161++CD8α+ T cells are a type 17 human T cell subset, sharing key differentiation factors with Th17 cells, including cytokine expression (IL-17A and IL-22), transcription factors (RORγt and RUNX2), chemokine receptors (CCR6 and CCR2), cytokine receptors (IL23R and IL18R) and expression of CD161 (Billerbeck, Kang et al. 2010) (**Appendix 1**) (Cosmi, De Palma et al. 2008). Such features are under the overall control of the transcription factor RORγt and co-expression of RORγt/CD161 in cord blood defines those cell populations which are able to produce IL-17 following stimulation with PMA and ionomycin (Maggi, Santarlasci et al. 2010). This would suggest that these cells exist in pre-determined populations as naïve cells in cord blood and not merely polarized on exposure to certain cytokines on activation and expansion.

A number of parallels have been drawn between CD161++CD8α+ T cells and the innate-like MAIT cells, including high expression of CD161 and type-17 characteristics. They have been described in humans to be CD8αβ, CD8αα and double negative and to have semi-invariant TCR usage (Vα7.2-Jα33 with predominant usage of Vβ chains Vβ2 and 13.2). MAIT cells have been identified in both the thymus and cord blood and their expansion in the periphery in mouse models is reliant on both expression of MR1, peripheral B cells and commensal gut flora (Martin, Treiner et al. 2009). In the literature the definition of MAIT cells is restricted to those CD161++ cells that are Vα7.2+.

How these relate to the other CD161++ populations described is not clear from current published data.

3.2 Hypothesis and Aims

I hypothesise that CD161++CD8+ T cells are a pre-determined T cell subset with a distinct differentiation pathway to conventional CD8+ T cells. In addition, I predict a close relationship to the MAIT cell population already described.

The aims of this chapter are:

1. To identify a CD161++CD8α+ T cell population in cord blood.

2. To further define the CD161++CD8α+ T cell population of cord blood.

3. To establish the relationship of CD161++CD8α+ T cells of cord blood to those found in adults.

4. To establish the relationship of CD161++CD8α+ T cells to MAIT cells.

3.3 Methods

3.3.1 Study subjects

20 adult healthy donors were enrolled after informed consent. 22 umbilical cord blood samples were obtained from Stem Cell Services, NHS Blood and Transplant, Oxford, UK. PBMCs from 20 healthy 10 week-old infants were obtained from the South African TB Vaccine Initiative field site in Worcester, near Cape Town, South Africa. All subjects were recruited in agreement with local ethics committees.

3.3.2 Lymphocyte recovery

Mononuclear cells from from EDTA peripheral blood and cord blood samples were isolated as detailed in chapter 2 section 2.2.1. Cryopreserved samples from 10 week old infants were thawed as per the protocol detailed in chapter 2.2.2 section.

3.3.4 Antibody staining for flow-cytometry

Surface staining of separated lymphocytes, whole blood staining and intracellular staining for transcription factors was performed as outlined in chapter 2 sections 2.3.1, 2.3.2 and 2.3.4 respectively.

For staining using the Vα7.2 (3C10) biotinylated antibody (obtained from Olivier Lantz), samples were incubated initially with the primary biotinylated antibody at 4^{o}C for 20mins, washed in PBS and subsequently stained with the streptavidin-conjugated secondary antibody. This was incubated at 4^{o}C for a further 20mins and washed in PBS. The sample was then incubated with the rest of the anti-surface antigen antibodies at 4^{o}C for 20mins, before further washing in PBS and fixation with 1% formaldehyde in PBS prior to FACS analysis.

Samples were acquired on either a FACSCaliber or LSRII cytometer (BD) using FACSDiva software (BD). FACS data was analysed using FloJo software (Treestar ltd). Gates were set using isotype and unstained control samples to identify positive populations following panel set up using a ‘full minus one’ strategy.

3.3.4 Cell sorting for microarray

Cell sorting of cord blood for micro-array analysis was performed by initial Ficoll-Histopaque density gradient centrifugation (Lymphoprep, Axis Sheild), of fresh cord blood samples (see chapter 2, section 2.2.1 for full protocol) followed by magnetic-bead CD8 enrichment (Easy-sep human CD8 enrichment kit, STEMCELL Technologies, Grenoble, France) (see chapter 2 section 2.4.1 for full protocol). Cells were labeled with fluorescent conjugated antibodies and sorted using a MoFlo MLS cell sorter (Dako), in collarboration with Andrew Worth, Jenner Institute, University of Oxford. Sorted cell populations were snap frozen and stored at -80^{0}C prior to RNA extraction.

3.3.5 RNA extraction

Total RNA was extracted from snap frozen sorted cell samples. These were lysed and homogenized using a QIAshredder spin column (Qiagen). Total RNA was extracted using an RNeasy mini kit (Qiagen) according to the manufacturer's instructions (see chapter 2 section 2.6 for full protocol).

3.3.6 Microarray

cDNA was amplified from total RNA using the Ovation Pico WTA System (NuGEN). Amplified cDNA was then fragmented and labeled using the Encore Biotin Module kit (NuGEN) (see chapter 2 section 2.7 for full protocol). Samples were then passed on to the Imperial College Genomics Laboratory for hybridization to GeneChip Human Genome U133 Plus 2.0 arrays (Affymetrix) using a hybridization, wash and stain kit (Affymetrix) and scanning with the GeneChip scanner 3000 7G (Affymetrix). Data analysis was performed in collaboration with the Natasha Sahgal, Wellcome Trust centre for human genetics, Oxford, UK as outlined in chapter 2 section 2.7.5.

3.3.7 Real-time PCR

First strand cDNA synthesis was performed with RNA (10ug/ml) according to the protocol detailed in chapter 2 section 2.8.1. Quantitative real-time PCR reactions were carried out using a LightCycler 480 (Roche Diagnostics) using cDNA from the above reaction and primers (IL23R_F ccatctctacagggcaccttac, IL23R_R cgatcattcccaataaaagtcc; IL18RAP_F cagatattctggatcctgtcgag, IL18RAP_R tgctttgcagctaatagttaaagg; RORC_F cagcgctccaacatcttct, RORC_R ccacatctcccacatggact; ZBTB16_F gcacagttttcgaagga, ZBTB16_R cagaagacggccatgtca; GAPDG_F agccacatcgctcagacac, GAPDH_R gcccaatacgaccaaatcc, obtained from Eurofins, mwg Operon). For the full protocol see chapter 2 section 2.8.2. Fold change in expression was determined by the 2-ΔΔCT method (Livak and Schmittgen 2001).

3.3.8 Statistical analysis

Statistical analysis, other than that for the microarray data, was performed using GraftPad PRISM (GraphPad software) version 4. A *p* value of <0.05 was considered significant.

3.3.9 Gene set enrichment analysis

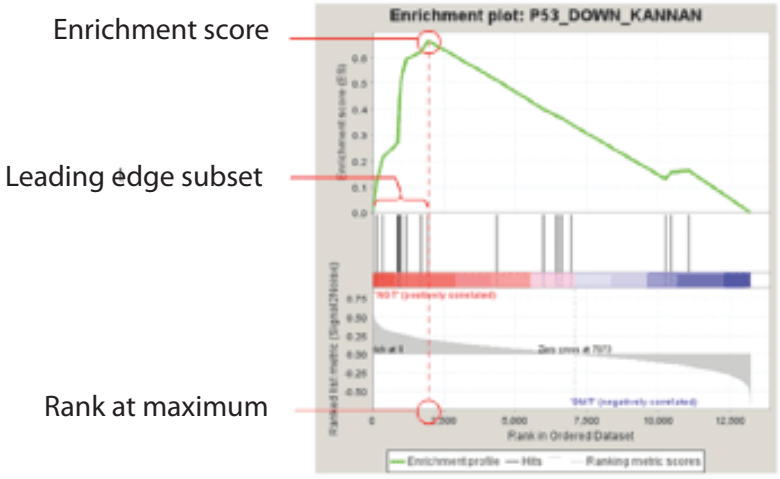
Gene set enrichment analysis was performed using the GSEA software, developed at the Broad Institute of MIT and Harvard (Mootha, Lindgren et al. 2003; Subramanian, Tamayo et al. 2005), which can be downloaded from this site: http://www.broadinstitute.org/gsea/index.jsp. The interpretation of geneset enrichment plots is explained in **Box 1**.

The **enrichment score (ES)** is the primary result of the geneset enrichment analysis.
The ES

- describes whether a gene set is overrepresented at the top or bottom of a ranked list of genes.
- is calculated by walking down the ranked list of genes, increasing a running-sum statistic when a gene is in the gene set and decreasing it when it is not. The magnitude of the increment in the running-sum statistic depends on the correlation of the gene with the phenotype.
- is the maximum deviation from zero encountered in walking the list.
- a positive ES indicates gene set enrichment at the top of the ranked list.
- a negative ES indicates gene set enrichment at the bottom of the ranked list.

The **leading edge subset** of a gene set is the subset of members that contribute most to the ES. For a positive ES, the leading edge subset is the set of members that appear in the ranked list prior to the peak score. For a negative ES, it is the set of members that appear subsequent to the peak score.

The enrichment plot below provides a graphical view of the enrichment score for a gene set analysis:



- The top of the plot shows the running ES for the gene set as the analysis walks down the ranked list. The ES is the score at the peak of the plot (the score furthest from 0.0).
- The middle of the plot shows where the members of the gene set appear in the ranked list of genes.
- The bottom of the plot shows the value of the ranking metric as you move down the list of ranked genes. This measures a gene's correlation with a phenotype. The value of the ranking metric goes from positive to negative as you move down the ranked list. A positive value indicates correlation with the first phenotype and a negative value indicates correlation with the second phenotype.

Box 1: Interpretation of geneset enrichment analysis

3.4 Results

3.4.1 CD161++CD8α+ T cells are present in cord and infant blood.

The CD161++CD8α+ T cell subset represents a mean of 11% of CD8α+ T cells in adult blood. CD161++CD8α+ T cell populations can also be identified in infant and cord blood, representing a mean of 0.9% and 4.4% of CD8α+ cells respectively (**Figure 3.1a**). The proportion of CD161++CD8α+ T cells in infant and cord blood is significantly less than that found in adult blood (**Figure 3.1b**) indicating that there is expansion of the existing subset seen in cord blood with age. (N.B. The CD161++CD8α+ T cell population have been

observed to be particularly sensitive to the effects of freezing and thawing, which would explain the discrepancy in the proportions seen between infant and cord samples, as infant samples were cryopreserved, whereas the cord samples were stained fresh).

3.4.2 CD161++CD8α+ T cells have a naïve phenotype in cord blood.

CD161++CD8α+ T cells are CD45RA+, CD45RO-, $CCR7^{low}$ and $CD62L^{low}$ in cord blood (**Figure 3.2a and 3.2b**). They express significantly less CCR7 and CD62L compared to the CD161+ and CD161-CD8α+ subsets. This indicates that even as naïve cells they may have an alternative homing pattern, with a reduced propensity to circulate to lymph nodes. In adults these CD161++CD8α+ T cells have already been described to have an effector memory phenotype (CD45RA-, CD45RO+, $CCR7^{low}$ and $CD62L^{low}$) (Billerbeck, Kang et al. 2010)(**Appendix 1**) as demonstrated here for

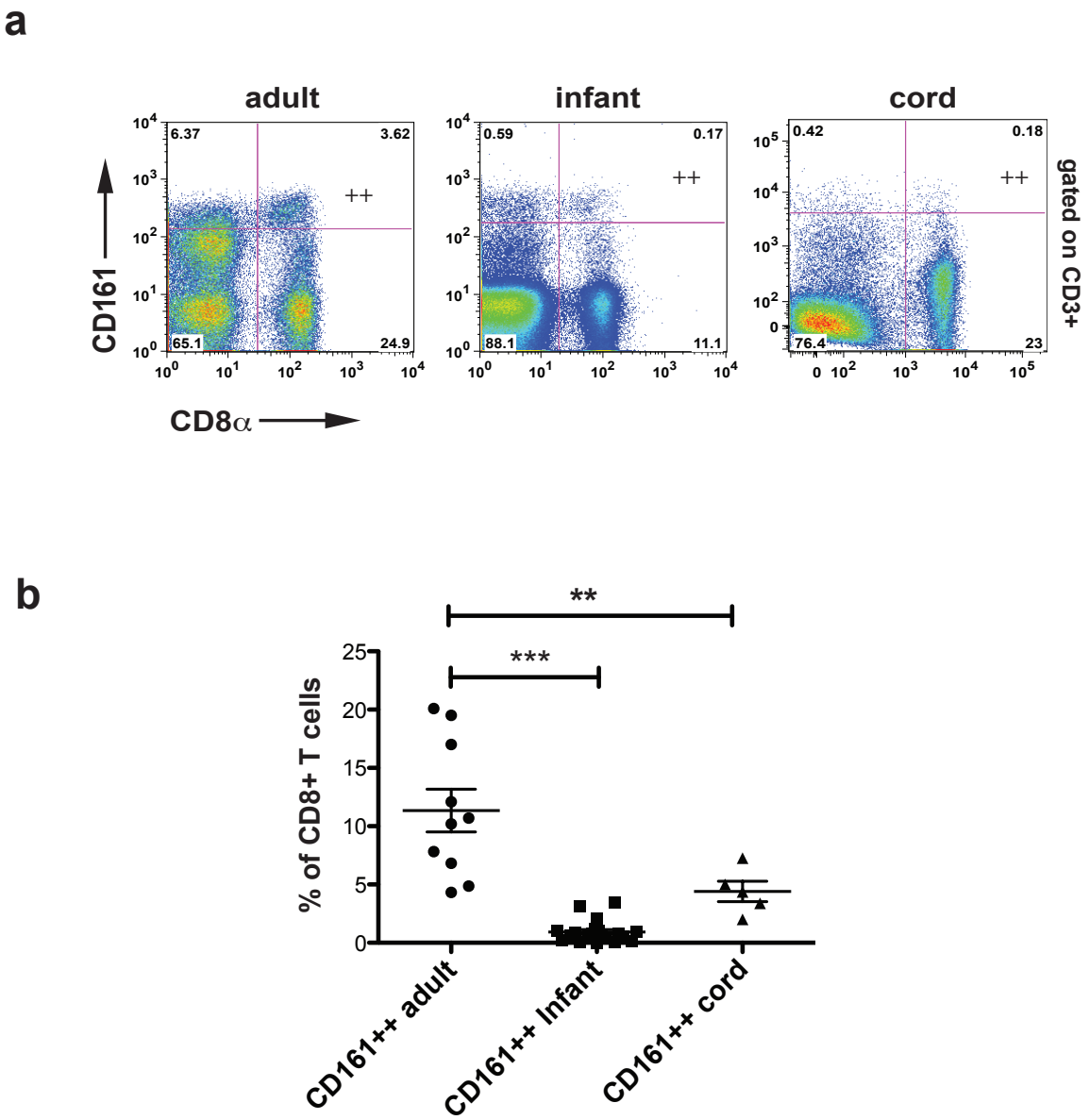


Figure 3.1. CD161++CD8α+ T cells are found in cord and infant blood.

(a) Representative FACS plots show a prominent CD161++ CD8α+ T cell population in adult peripheral blood. CD161++CD8α+ T cell populations also identified in infant and cord blood. (b) Cumulative data comparing CD161++CD8α+ T cell populations in adult (n=10), infant (n=20) and cord blood (n=5) as a proportion of CD8a+ T cells. *** $p < 0.0001$, ** $p < 0.001$ (one-way ANOVA).

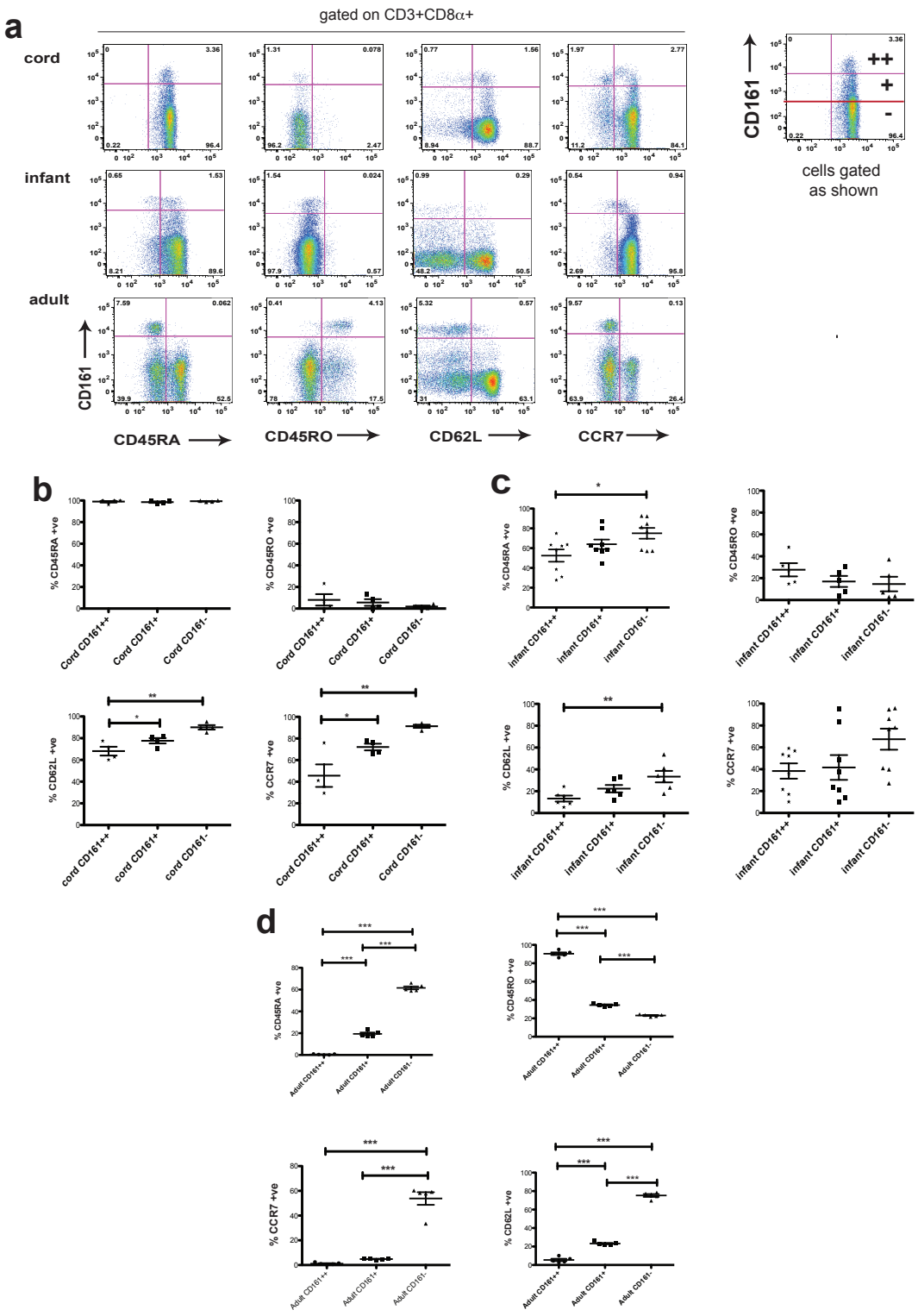


Figure 3.2. Memory phenotype of CD161++CD8a+ T cells in cord, infant and adult blood.

(a) Representative FACS plots showing the memory phenotype of CD161++/+/- CD8a+ subsets in cord (n=4) infant (n=8) and adult blood (n=5). Cumulative data for memory phenotype of cord (b), infant (c) and adult (d) CD8a+ CD161 subsets. * p<0.05, **p<0.001 (one way ANOVA).

comparison (**Figure 3.2a and d**). In infants CD161++CD8α+ T cells appear to be in a state of transition, where a proportion of cells are already CD45RA- and CD45RA expression is significantly lower in the CD161++CD8α+ T cell subset compared to the CD161+ and CD161-CD8α+ subsets (**Figure 3.2c**). This is in keeping with the hypothesis that the CD161++CD8α+ T cell population seen in adults expands from the smaller CD161++CD8α+ naïve T cell subset identified in cord blood.

3.4.3 CD161++CD8α+ T cells in cord blood are a pre-determined type-17 subset.

To examine the relationship of the CD161++CD8α+ T cell population in cord blood to that identified in adult peripheral blood in more detail I performed a microarray analysis of the gene expression profiles of the CD161++, CD161+ and CD161-CD8α+ subsets in cord blood. The data obtained provides lists of up and down regulated genes on comparison between the subsets studied (i.e. CD161++ vs CD161+, CD161++ vs CD161- and CD161+ vs CD161) (Tables of genes with >2 fold change in expression between subsets detailed in **Table 1, Table 2 and Appendix 2**; for full dataset see Gene Expression Omnibus (GEO) under accession number GSE33425). Using the Broad institute geneset enrichment software I was able to compare the gene expression profiles of these subsets to data obtained from an identical analysis on lymphocytes from adult donors, as previously published (Billerbeck, Kang et al. 2010) (**Appendix 1**). This demonstrated that in cord blood the CD161++CD8α+ population already bares the strong hallmark of the type-17 CD161++CD8α+ population described in adults (**Figure 3.3a**). I demonstrated a highly significant correlation on gene set enrichment analysis

comparing both up- regulated and down-regulated gene sets between the cord and adult CD161++ CD8α+ vs CD161- CD8α+ data sets (**Figure 3.3b; Table 1; Table 2; Appendix 3**). This demonstrates that these are highly comparable populations and that CD161++CD8α+ T cells in cord blood are a pre-programmed type-17 subset, supporting the hypothesis that naive CD161++CD8α+ T cells expand to form the more prominent population seen in adults. Such a correlation was also between on comparison between up- and down-regulated genes of the CD161+CD8α+ vs CD161-CD8α+ datasets in cord and adult blood, suggesting that the CD161+CD8α+ subset may also be a pre-determined subset in cord blood (**Appendix 4**). Interestingly there was no such preservation of gene expression on comparison between CD161++CD8α+ vs CD161+CD8α+ in cord and adult blood (**Appendix 5**).

In order to clarify the gene-expression data, FACS analysis was performed to look at surface expression of a number of markers of interest that were significantly up-regulated on the CD161++ vs CD161-CD8α+ dataset on microarray (**Figure 3.4a**). This confirmed CCR6, IL-18R and CD26 to be expressed at significantly greater levels compared to the CD161+ and CD161-CD8α+ subsets.

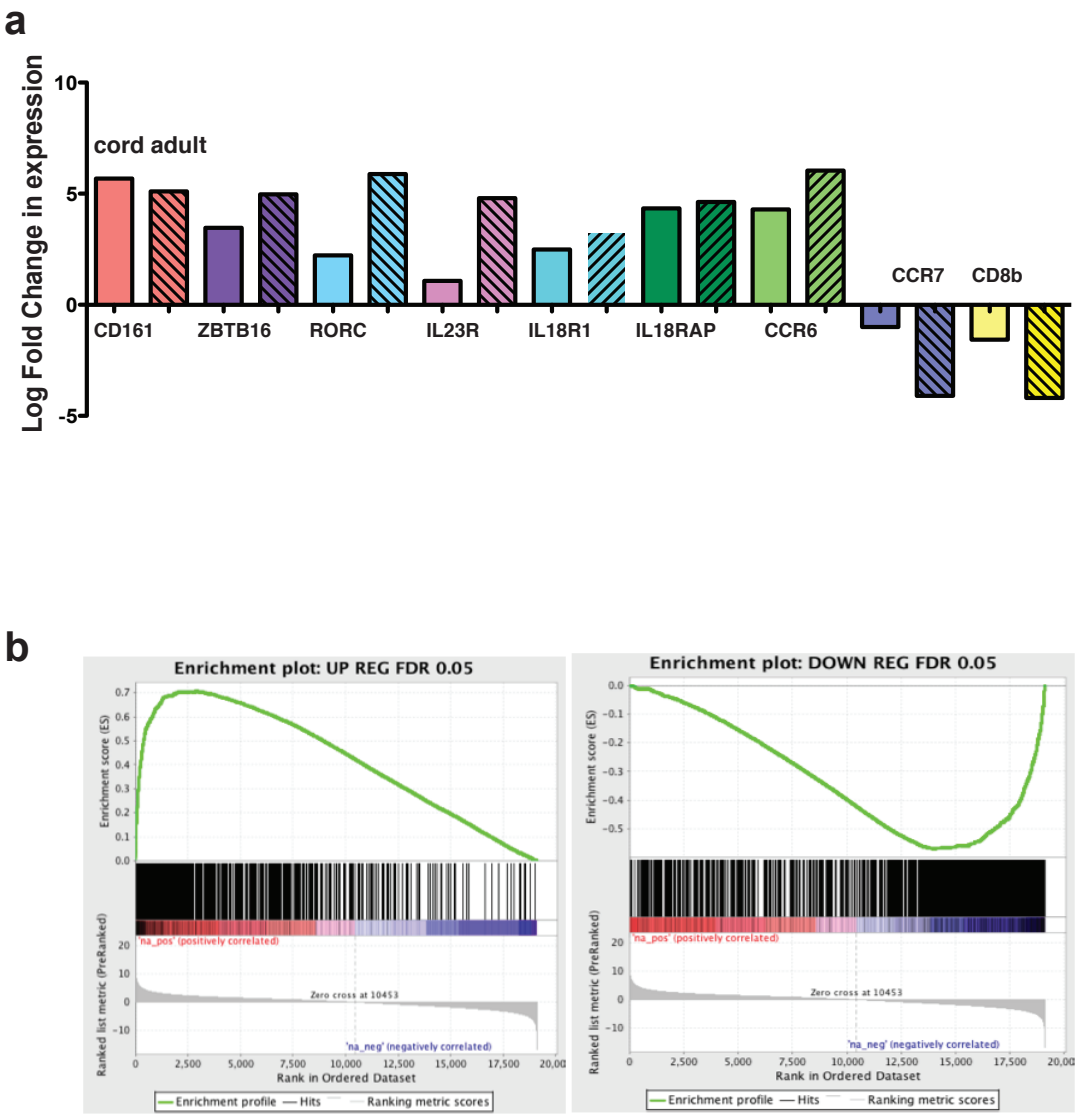


Figure 3.3. CD161++CD8α+ T cells in cord blood are a pre-programmed type-17 subset.

(a) Comparison of log fold change in gene expression for selected genes between CD161++CD8α+ vs CD161-CD8α+ T cells in adult and cord blood (n=3). (b) Gene set enrichment summary plots comparing gene expression on microarray analysis between CD161++CD8α+ vs CD161-CD8α+ subsets from adult and cord blood. Left panel shows the plot for up regulated genes, right hand panel shows plot for down-regulated genes. Normalised enrichment score (NES), up-regulated genes, = 4.21, p <0.00001. NES, down regulated genes, = -3.25, p <0.0001.

Gene.Symbol	Gene ID	logFC	P.Value	adj.P.Val

CCR6	206983_at	6.037506096	3.80288E-08	0.000415845
KLRB1	214470_at	5.684114733	9.08461E-09	0.000373938
---	228854_at	5.116841851	1.08128E-07	0.000591191
---	228858_at	5.11679723	2.06062E-08	0.000375548
IL18RAP	207072_at	4.338796842	5.53734E-07	0.001882719
---	227762_at	4.108904262	1.03835E-07	0.000591191
FAM43A	227410_at	4.015665945	2.86946E-08	0.000392219
MAF	206363_at	3.794064659	1.74335E-06	0.003286807
CEBPD	213006_at	3.672946516	8.33286E-07	0.002040156
---	229327_s_at	3.578528114	1.18595E-05	0.007032549
FEZ1	203562_at	3.462241656	2.30976E-05	0.010184374
ZBTB16	205883_at	3.4618117	1.36786E-08	0.000373938
C10orf128	228372_at	3.456548016	3.51348E-06	0.004278154
LOC619207	1569212_at	3.229929555	1.17302E-05	0.007032549
S1PR5	230464_at	3.212449969	0.000256936	0.024632037
KIT	205051_s_at	3.146806812	5.8539E-07	0.001882719
MAF	209348_s_at	3.14077685	3.17206E-06	0.004230063
NCR3	210763_x_at	3.134811413	4.59127E-07	0.001693637
CEBPD	203973_s_at	3.105434743	0.00014358	0.019271388
LATS2	227013_at	3.093731102	2.99457E-06	0.004131554
NCR3	211583_x_at	3.089643137	2.93822E-06	0.004131554
CXCR6	206974_at	3.08603321	1.77113E-05	0.008884082
PLXND1	38671_at	3.074962542	6.83769E-08	0.000534072
---	231262_at	3.073544309	4.85152E-08	0.000442094
KLRF1	220646_s_at	3.035060972	6.94283E-06	0.006122564
ADAM12	213790_at	3.03130028	5.88382E-05	0.013866281
CFH /// CFHR1	215388_s_at	2.975028849	7.33644E-05	0.014905979
SH2D1B	1553177_at	2.890998315	0.000543276	0.033374866
NCR3	211010_s_at	2.825058301	6.89078E-06	0.006122564
GYG1	201554_x_at	2.811374514	1.07365E-05	0.0069006
PDE4D	1554717_a_at	2.733129028	4.52669E-05	0.012454981
CCL20	205476_at	2.673487508	0.000270783	0.024906393
KIAA0146	228325_at	2.654769811	6.19363E-05	0.01389494
KIF5C	203130_s_at	2.650960788	3.35692E-06	0.004278154
---	227755_at	2.562975499	8.58228E-07	0.002040156
ZNF462	226575_at	2.558788236	4.64647E-07	0.001693637
MYBL1	213906_at	2.529854639	0.000685316	0.037346725
---	244697_at	2.523207173	1.38361E-06	0.002909569
ERN1	207061_at	2.519406937	4.41844E-06	0.004930163
IL18R1	206618_at	2.492177799	3.45812E-06	0.004278154
P2RY14	206637_at	2.472576557	0.000338179	0.027569043
CEBPD	213003_s_at	2.451518841	6.91601E-05	0.014656305
LATS2	223380_s_at	2.44478252	6.7354E-06	0.006122564
KIF5C	203129_s_at	2.424442747	2.91529E-05	0.011069005
CYTH3	225147_at	2.421773993	5.77062E-06	0.005705577
---	242628_at	2.420499564	3.67761E-06	0.004278154
ANK1	205389_s_at	2.390066219	2.11953E-07	0.000965713
ADRB2	206170_at	2.372204579	3.9177E-05	0.01215513
GYG1	211275_s_at	2.37183625	3.17722E-05	0.011207375
NCS1	222570_at	2.326098913	1.12328E-05	0.0069006
PRF1	214617_at	2.321523549	2.90979E-06	0.004131554
PRF1	1553681_a_at	2.297708719	4.85562E-06	0.005105399
PTGDR	215937_at	2.282109238	0.000416893	0.029640618
PHACTR2	204048_s_at	2.269213167	7.59553E-07	0.002040156
PHACTR2	204047_s_at	2.236464638	4.52917E-05	0.012454981
RORC	228806_at	2.222917724	1.63906E-07	0.000814688

DLG5	229689_s_at	2.21549375	5.47385E-05	0.013542212
PRDM1	228964_at	2.192793646	1.51565E-05	0.007968097
NEO1	204321_at	2.192570865	8.26638E-05	0.015372928
FASLG	210865_at	2.189771539	0.000770645	0.039341755
KLRG1	210288_at	2.156958491	2.60077E-05	0.010772517
NKG7	213915_at	2.1461783	0.000439481	0.030531919
SLAMF7	219159_s_at	2.13347905	0.000216135	0.022901538
ANK1	208353_x_at	2.125124986	6.29985E-07	0.001913579
DLG5	201681_s_at	2.122689481	2.55488E-05	0.010663216
MCTP2	229021_at	2.093849561	0.000777739	0.039380485
FEZ1	205973_at	2.084097033	4.14406E-05	0.012181537
TNFSF14	207907_at	2.066660466	5.02896E-06	0.005187898
SIPA1L2	1559469_s_at	2.041598033	4.02063E-05	0.01215513
CACNA2D2	204811_s_at	2.016905323	2.86876E-06	0.004131554
---	241069_at	2.009902783	2.75724E-06	0.004131554

Table 1: Microarray data comparing up regulated genes between CD161++CD8+ and CD161-CD8+ T cells in cord blood (>2 log fold change in expression). Genes corresponding to the type 17 genotype are highlighted in bold.

Gene.Symbol	ID	logFC	P.Value	adj.P.Val
PLXDC1	PLXDC1	-2.033088359	3.02263E-06	0.004131554
LRRN3	LRRN3	-2.066288885	3.62748E-06	0.004278154
GAL3ST4	GAL3ST4	-2.079067556	2.42434E-05	0.010322657
MEST	MEST	-2.081931346	1.6788E-05	0.008661579
CACHD1	CACHD1	-2.129815354	0.000178485	0.021168497
FOXP1	FOXP1	-2.130959177	8.26508E-05	0.015372928
ARMCX1	ARMCX1	-2.152341358	8.2233E-06	0.006422985
FLT1	FLT1	-2.157302047	6.12686E-05	0.01389494
TBC1D4	TBC1D4	-2.162556529	4.75249E-06	0.005094952
RIPK4	RIPK4	-2.193809491	3.09527E-05	0.011207375
RAPGEF6	RAPGEF6	-2.194939034	4.34534E-05	0.012200778
MAL	MAL	-2.247913233	9.11856E-06	0.006827766
TTN	TTN	-2.257545761	2.58101E-06	0.004131554
NOG	NOG	-2.311614156	9.4603E-06	0.006827766
ADRB1	ADRB1	-2.335536626	1.07816E-05	0.0069006
AGBL3	AGBL3	-2.349275199	3.82505E-05	0.012144452
PPIL4 /// ZC3H12D	PPIL4 /// ZC3H12D	-2.377667545	8.34756E-08	0.000570504
CDR1	CDR1	-2.431596259	9.18368E-06	0.006827766
LOC100292909	LOC100292909	-2.472682708	0.000119891	0.017945768
---	---	-2.501928501	6.88719E-07	0.001981879
PLXDC1	PLXDC1	-2.510473042	3.83982E-07	0.001614939
REG4	REG4	-2.975466655	7.82883E-06	0.006334957
DSC1	DSC1	-3.343793481	1.02609E-06	0.002244056

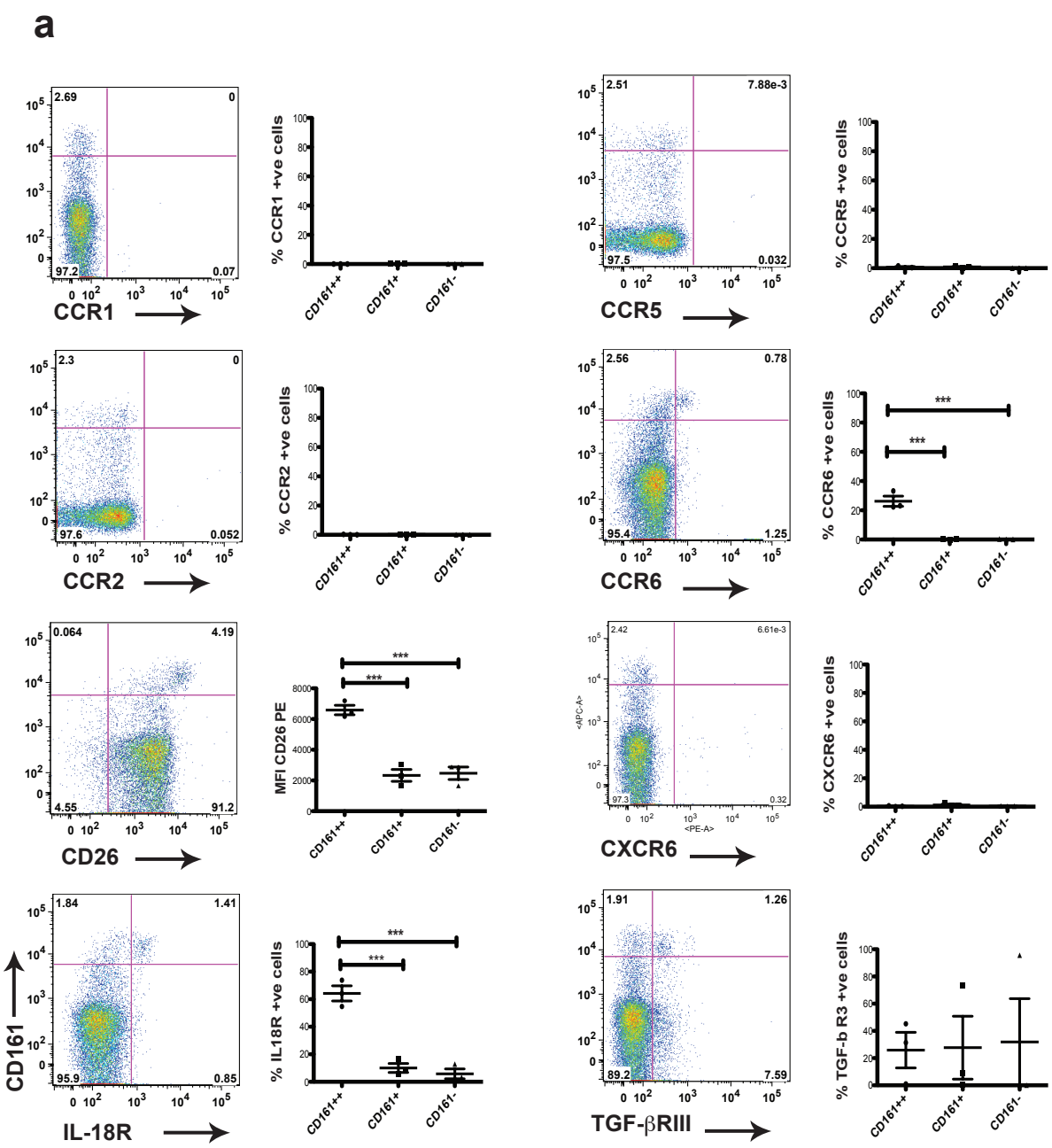
Table 2: Microarray data comparing down regulated genes between CD161++CD8+ and CD161-CD8+ T cells in cord blood (>2 log fold change in expression).

No expression of TGFβ-RIII, CCR1, CCR2, CCR5 or CXCR6 could be demonstrated by FACS, despite up-regulation at the gene expression level. I was also unable to demonstrate expression of RORγt or ZBTB16 by intracellular antibody staining or immunofluoresence (data not shown). Real-time PCR was used to increased relative gene expression for RORC, ZBTB16, IL18RAP and IL23R (**Figure 3.4b**).

3.4.4 MAIT cell/ CD161++CD8α+ T cell co-receptor expression

Mucosal associated invariant T (MAIT) cells in humans have been previously defined by their invariant use of the T-cell receptor (TCR) Vα7.2 chain (Treiner, Duban et al. 2003) and have more recently been shown to express high levels of CD161 and to have type-17 properties (Dusseaux, Martin et al. 2010). There is growing understanding that the cellular subset described as MAIT cells bears striking similarity to that previously described as CD161++CD8α+ T cells (Billerbeck, Kang et al. 2010) (**Appendix 1**), although this has not previously been fully explored.

MAIT cells have so far been described to be either CD8αβ, CD8αα or double negative populations. Differences in modes of FACS-based description of MAIT cells and CD161++CD8α+ T cells have made direct comparisons difficult to date. Analysis of MAIT cells has previously used a system of gating based on CD3, CD4 and CD8β antibodies. Here, by additional use of a CD8α antibody, I show the CD3+CD161++Vα 7.2+ population to be almost


a
CCR1
% CCR1 +ve cells
CCR5
% CCR5 +ve cells
CCR2
% CCR2 +ve cells
CCR6
% CCR6 +ve cells
CD26
MFI CD26 PE
CXCR6
% CXCR6 +ve cells
CD161
IL-18R
% IL18R +ve cells
TGF-βRIII
% TGF-b R3 +ve cells
CD161++
CD161+
CD161-

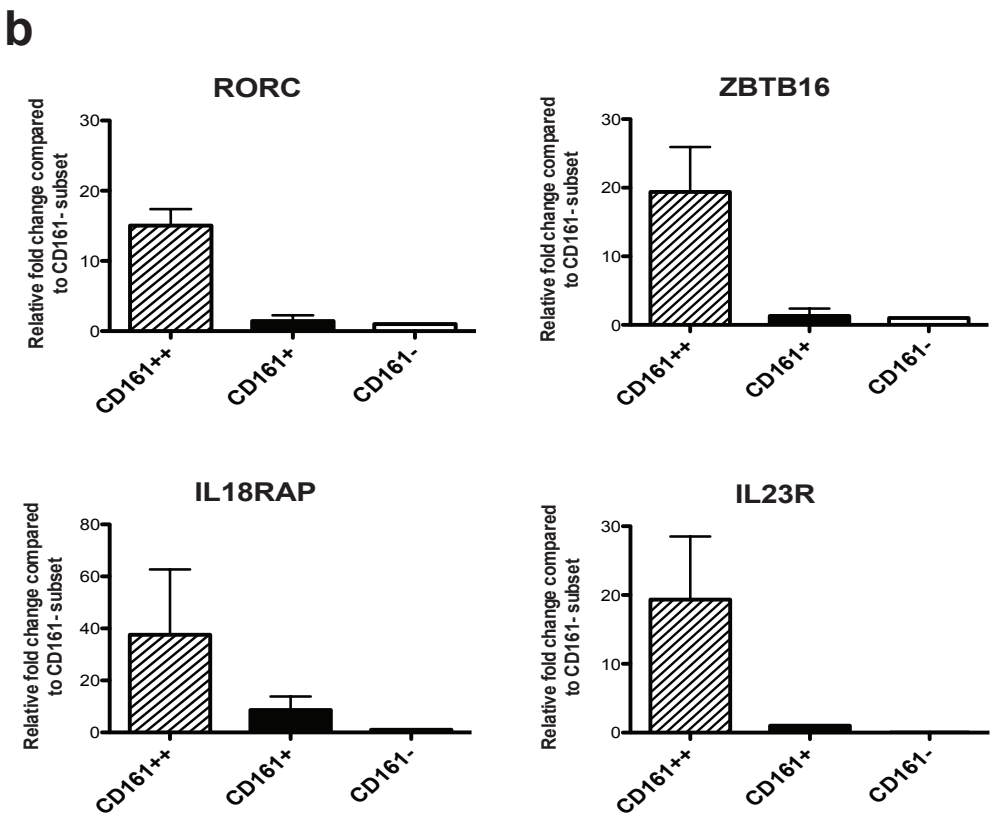


Figure 3.4. CD161++CD8α+ T cells are a pre-programmed type-17 subset

(a) Representative FACS plots and cumulative data showing expression of surface markers on CD161++/CD161+/CD161- subsets in cord blood up-regulated on microarray comparison of CD161++ vs CD161-CD8α+ datasets. ***p< 0.001 (one way ANOVA) (n=3). (b) Relative fold change in gene expression for RORC, ZBTB16, IL18RAP and IL23R in CD161++CD8α+ compared to the CD161+ and CD161-CD8α+ subsets in cord blood by real time PCR analysis (n=3).

exclusively CD8α+CD8β- or CD8α+CD8β+ (49% and 42% of CD3+CD161++Vα 7.2+ subset respectively). Other cell types, including CD4+ and double negative cells, represented less than 10% of the subset (**Figure 3.5**).

3.4.5 T cell receptor usage of CD161++ CD8α+ T cells

To further investigate the relationship of the CD161++CD8α+ and MAIT cell subsets, I analysed to what extent CD161++CD8α+ T cells express the MAIT TCR. I found the CD161++CD8α+ subset to have predominant but, interestingly, not exclusive usage of the TCR Vα7.2 chain (mean of 87% usage) (**Figure 3.6a**). This is significantly greater compared to the CD161+ and CD161-CD8α+ subsets (**Figure 3.6b**). I found, using a panel of Vβ antibodies, that the CD161++ CD8α+ population consistently used the TCR Vβ chains 2 and 13.2 (17.8% and 9.4% respectively) as had been previously suggested using a PCR approach (Tilloy, Treiner et al. 1999) (**Figure 3.7**). However, I also show that Vα7.2+ cells did not exclusively use the Vβ chains 2 and 13.2, with these chains only accounting for 33% of the usage by Vα7.2+ CD161++ T cells (**Figure 3.8a**).

To further investigate the relationship of the cord blood CD161++CD8α+ T cell subset to that of adult peripheral blood, I compared the TCR usage between in these two age groups. I show that in comparison to

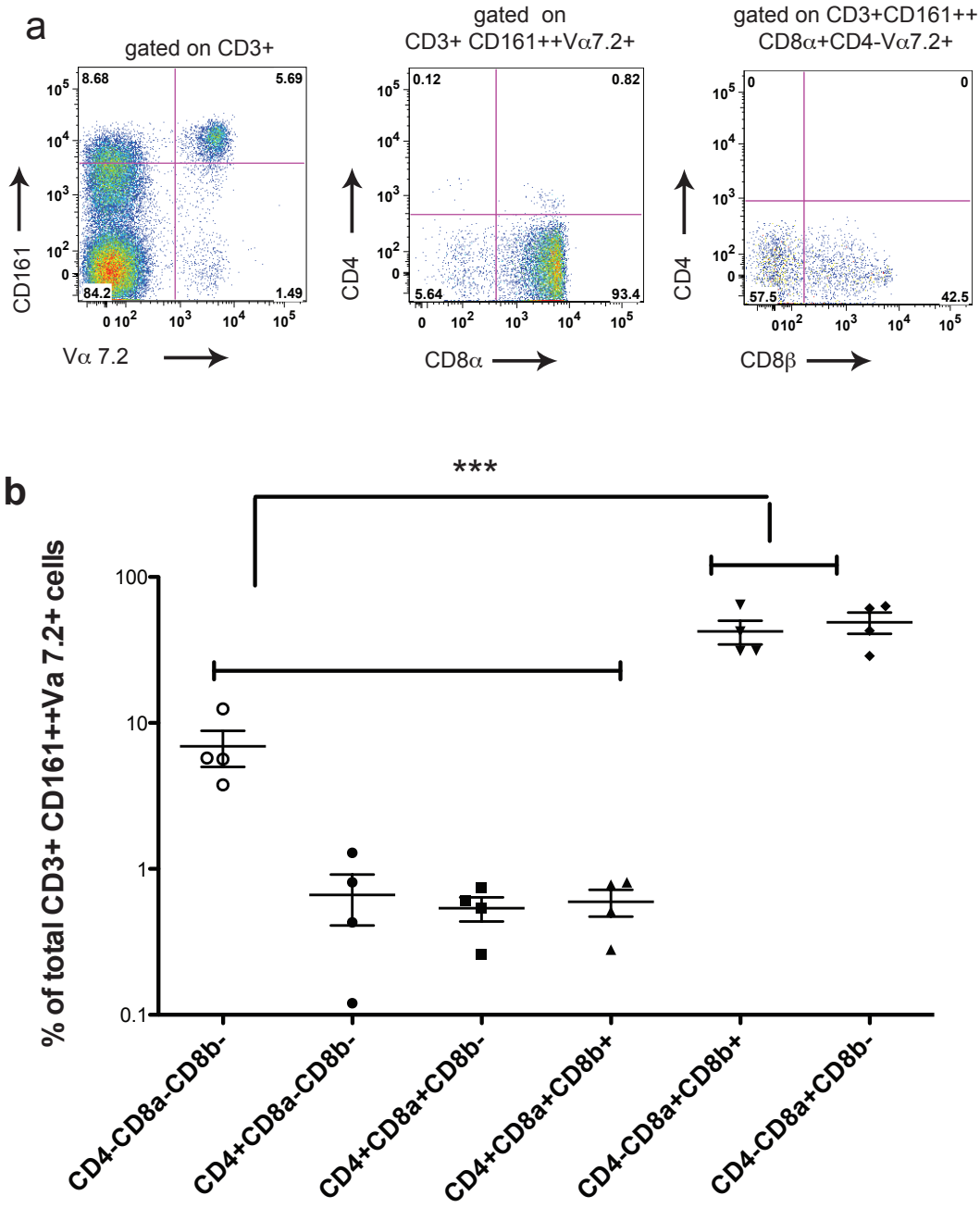


Figure 3.5. CD3+Vα7.2+ T cells are predominantly CD8αα and CD8αβ cells. (a) Representative FACS plots of adult CD3+CD161++Va7.2+ cells co-receptor expression. (b) Cumulative data demonstrates CD3+CD161++ Va7.2+ cells are predominantly CD8αα and CD8αβ cells. ***p<0.001 (one way ANOVA) (n=4).

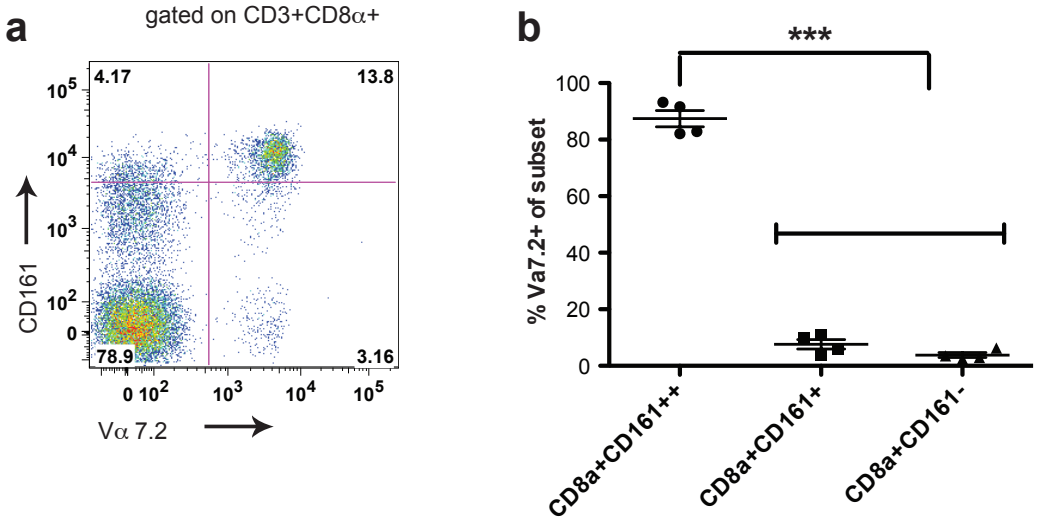
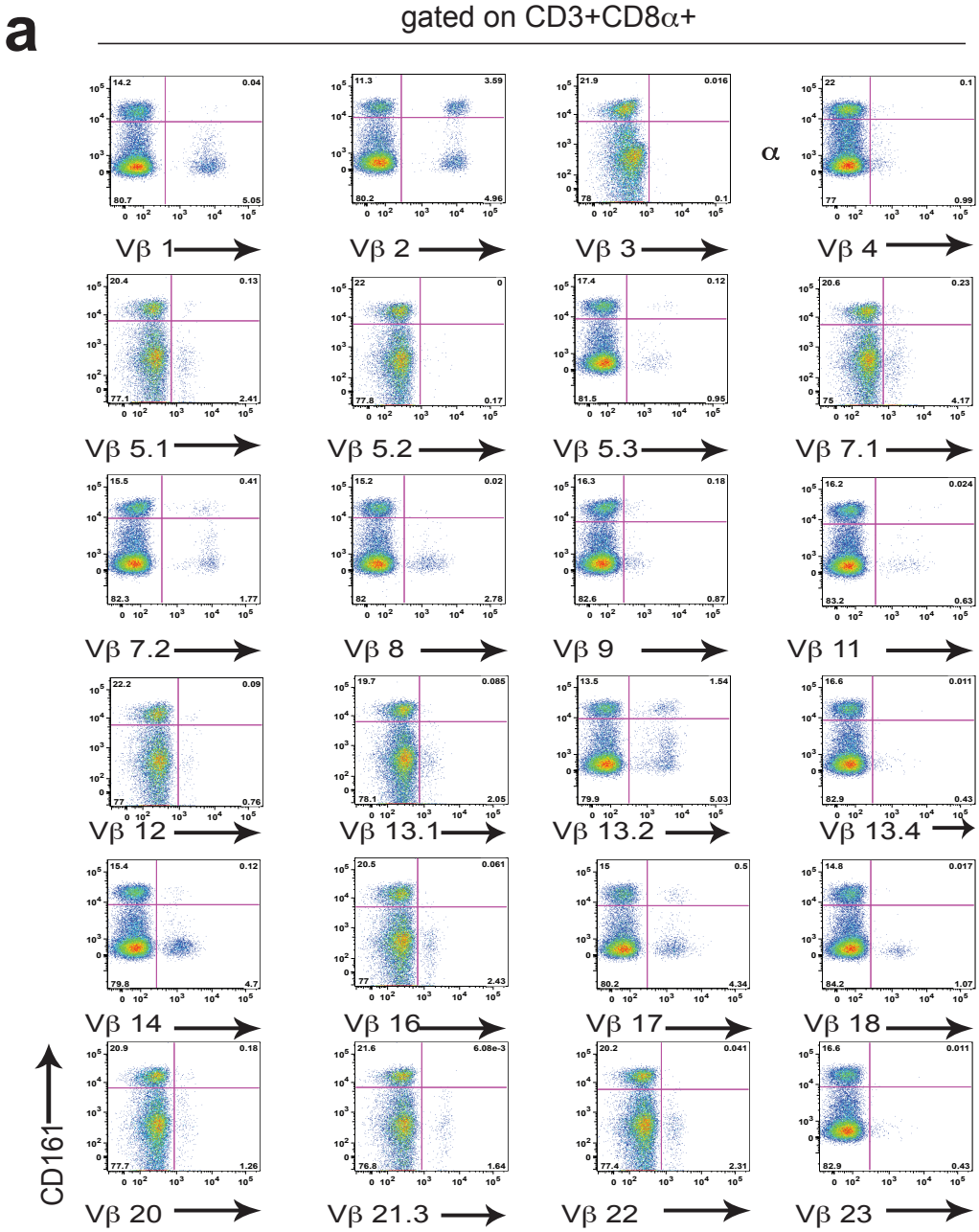


Figure 3.6. TCR Vα7.2 usage by adult CD3+CD161++CD8α+ T cells. (a) Representative FACS plot showing Vα7.2 usage by adult CD3+CD8α+ T cells. (b) Cumulative data comparing Vα7.2 usage between adult CD3+CD161++/CD161+/CD161- CD8α+ subsets. ***p<0.001 (one way ANOVA) (n=4).


a
gated on CD3+CD8α+
CD161
Vβ 1
Vβ 2
Vβ 3
α
Vβ 4
Vβ 5.1
Vβ 5.2
Vβ 5.3
Vβ 7.1
Vβ 7.2
Vβ 8
Vβ 9
Vβ 11
Vβ 12
Vβ 13.1
Vβ 13.2
Vβ 13.4
Vβ 14
Vβ 16
Vβ 17
Vβ 18
Vβ 20
Vβ 21.3
Vβ 22
Vβ 23

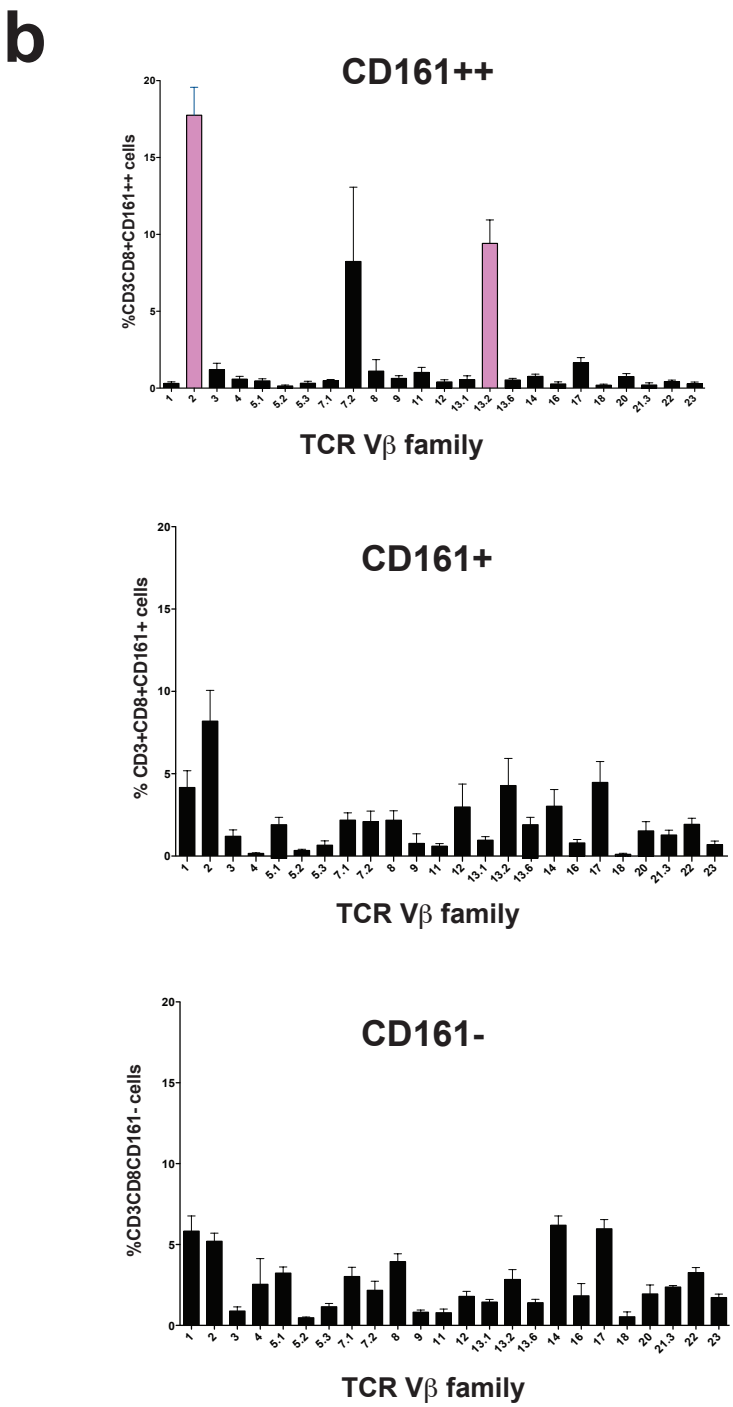


Figure 3.7. CD161++CD8α+ T cells have predominant TCR Vβ 2 and 13.2 usage. (a) Representative FACS plots showing TCR Vβ panel staining of PBMCs from one individual. (b) Cumulative data from 10 individuals shows predominant usage of Vβ 2 and 13.2 by CD161++CD8α+ T cells. Pink bars represent significant difference from other Vβs in CD161++ subsets. $p<0.001$ (one way ANOVA). No significant predominance of Vβ usage was seen in CD161+ and CD161- subsets (n=10).

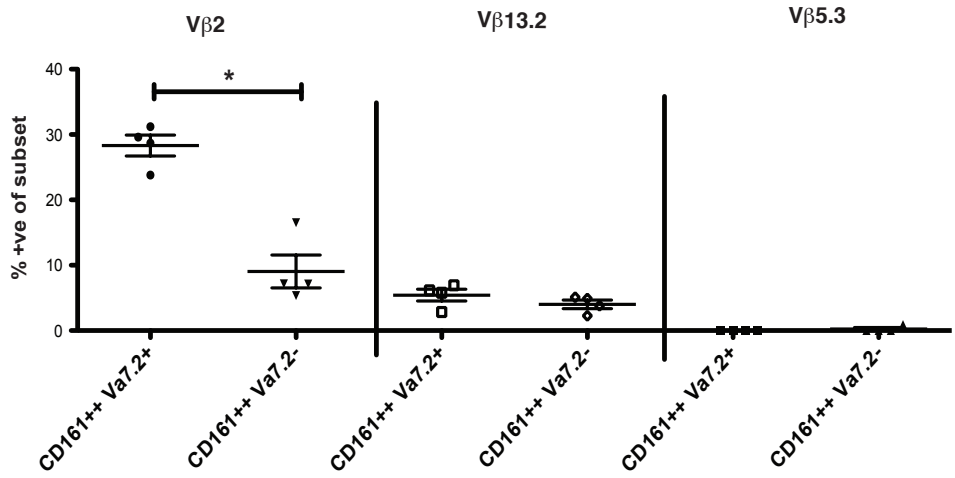


Figure 3.8. CD161++Vα7.2+ T cell subsets do not exclusively use Vβ2 and 13.2. Cumulative data from FACS analysis of Vβ2, 13.2 and 5.3 usage for CD161++Vα7.2+ and Vα7.2- subsets. Vβ 5.3 was used as a negative control. *p=0.0286 (Mann Whitney) (n=4).

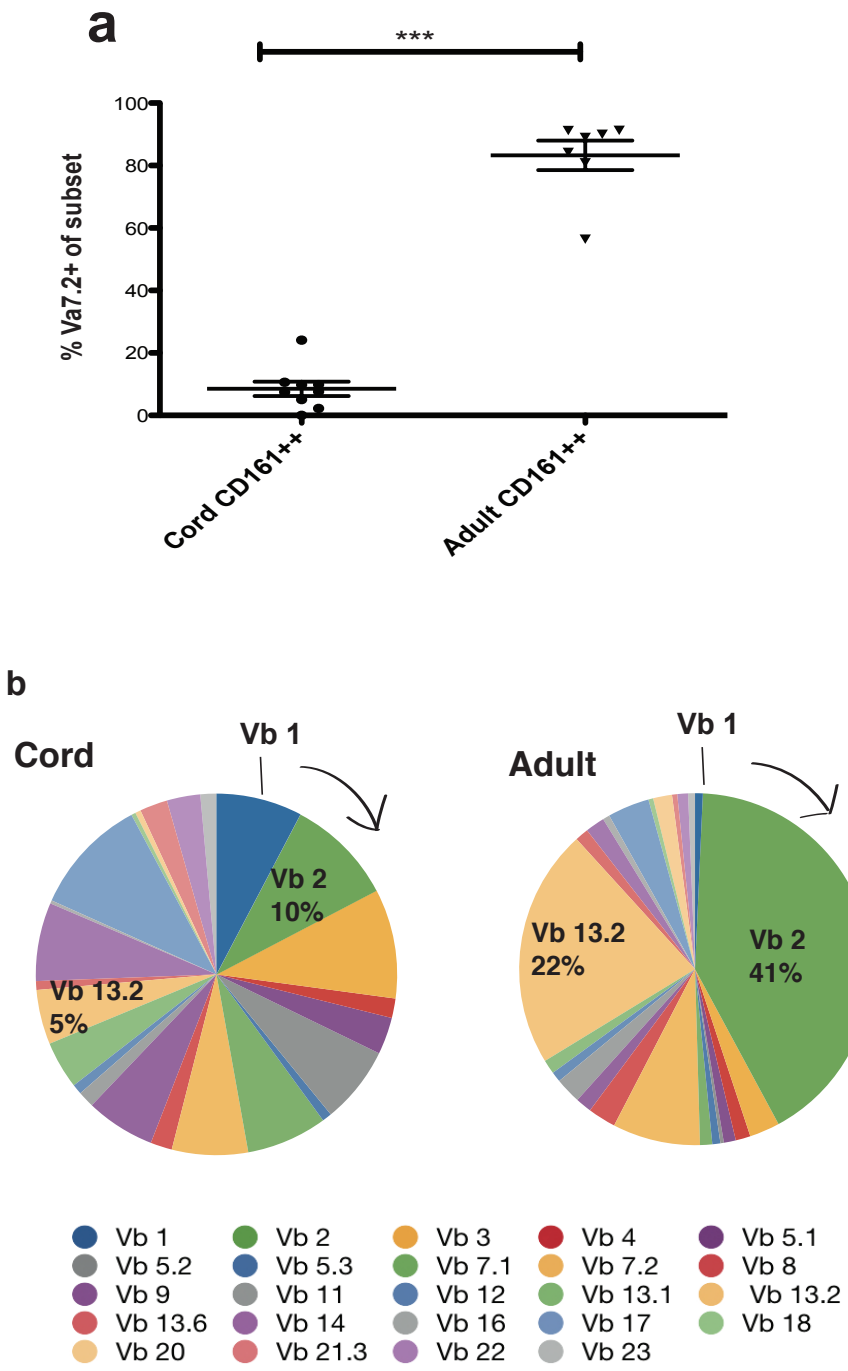


Figure 3.9. CD161++CD8α+ T cells in cord blood have broad T cell receptor usage compared to adults. (a) Comparison of Vα7.2 usage between CD161++CD8α+ subsets in cord (n=9) and adult (n=7) blood. ***p=0.002 (Mann Whitney). (b) Comparison of proportion of Vβ usage by CD161++CD8α+ T cells in adult (n=10) and cord (n=8) blood using TCR Vβ antibody panel. Vβ usage represented by the colours as shown in the key, running clockwise from Vβ1 as marked and indicated by the arrows.

CD161++CD8α+ T cells in adults, cord blood TCR usage is broad (**Figure 3.9a and b)** suggesting the expansion of the subset seen is antigen driven, likely linked to MR1, which MAIT cells are reported to be restricted by.

3.5 Discussion

CD161++CD8+ T-cells, defined by high expression of the C-type lectin, CD161, a pattern of phenotypic markers shared with Th17 cells and (in adults) predominant invariant TCR usage (Vα 7.2 and Vβ 2/13.2), are emerging as a IL18R, IL23R, RORγt and ZBTB16 in cord blood suggests that this population is a pre-committed subset, rather than cells that differentiate later from conventional T cells, a finding similar to that for Th17 CD4+ T cells (Cosmi, De Palma et al. 2008). CD161++CD8+ T cells have a specific chemokine receptor signature, which appears to be 'pre-conditioned' in their expression of CCR6 as naïve cells. Acquisition of further chemokine receptors (CXCR6, CCR2) occurs post-activation as they are not expressed by the CD161++CD8αβ cells of cord blood. As naïve cells they express low levels of CCR7 and CD62L, despite being CD45RA+, indicating that they have an intrinsic tissue-, rather than lymph node-, homing phenotype.

The relationship of CD161++CD8α+ T cell subset to MAIT cells has been further clarified here. What to date have been described as MAIT cells (CD161++Vα7.2+), whilst describing the majority of cells in CD161++CD8+ T cell subset, fails to account for those cells which share the same functional and phenotypic features, but do not express the MAIT TCR. Gene expression and phenotyping data from both cord blood and adults indicates that the their

genetic signature is strong at both stages, despite there being minimal Vα7.2+ cells in cord blood. The predominant, but not exclusive usage by Vα7.2+ T cells of Vβ2 and 13.2 indicates some flexibility in Vβ chain usage, which may reflect variable MR1 ligand-dependent TCR restriction with a couple of ligands predominating, whilst overall MR1 restriction requires expression of Vα7.2. This would fit with the idea that MR1 might be presenting conserved common epitopes from extra-cellular pathogens.

In addition, the MAIT cell literature has so far loosely described CD161++Vα7.2+ cells to be CD8αα, CD8αβ or double negative. This has been based on use of a limited anchor antibody panel of CD3, CD4 and CD8β. By the use of a CD8α antibody I have been able to more clearly demonstrate that CD161++Vα7.2+ cells are predominantly CD8αα or CD8αβ, with other co-receptor combinations making up less than 10% of the population (the majority of which are double negative). The CD161++CD8α+ definition therefore encompasses the majority of the MAIT cell subset. In combining these findings, the definition of these cells could be extended from CD161++CD8+ or MAIT cells to be more accurately described as CD161++CD4- T cells. This thesis focuses on the CD8αβ and CD8αα expressing CD161++ T cells. The double-negative subset may represent a continuum of the CD8β down-regulation observed in this subset, as further discussed in chapter 4.

The differentiation pathway of MAIT cells has previously been explored in both mice and humans (Martin, Treiner et al. 2009). Unlike NKT cells, MAIT

cells do not exit the thymus a mature, ready selected and expanded population (Bendelac, Savage et al. 2007). Small numbers of CD161++Vα7.2+ T cells have been identified in the human thymus and cord blood and are described to be naïve (CD45RA+CD45RO-). Intra-thymic selection on MR1 has been demonstrated in both transgenic mice expressing the murine MAIT cell defining TCR (Vα19-J33/Vβ 6 or 8) on MR1+/+ or MR1-/- backgrounds and fetal thymic organ cultures. Peripheral expansion of MAIT cells has been described to be reliant on MR1 expressing B cells using an experiment of Vα19-J33/Vβ6 transgenic Rag-/- mice treated with either MR1+ or MR1- splenocyte transfer. My data, although encompassing an extended definition of this subset to all CD161++CD8α+ T cells, is in keeping with this model. In cord blood this subset is naïve and TCR usage broad. With age it undergoes expansion to become an effector memory population with narrow TCR usage. Preferential encounter with antigen presented by a non-classical MHC class I molecule, such as MR1, would explain the expansion of the CD161++CD8α+ subset and the predominant TCR-usage observed.

NKT cells express high levels of the transcription factor ZBTB16 compared to other conventional T cells, and intrathymic expression has been demonstrated from an early stage in their differentiation (Kovalovsky, Uche et al. 2008), (Savage, Constantinides et al. 2008). Expression is associated with the ability of this subset to undergo intra-thymic expansion and effector differentiation. In ZBTB16 deficient mice, NKT cells remain naïve, fail to expand and become predominantly lymph node homing rather than migrating to non-lymphoid tissue. Under conditions of forced ZBTB16 expression, conventional T cells

are able to perform memory and effector functions without antigenic stimulation or proliferation, indicating an important role for this transcription factor in readying innate-like cells for action. Interestingly, under conditions of forced expression T cells also produce significantly increased amounts of IL-17 (Kovalovsky, Alonzo et al. 2010). From my microarray data, ZBTB16 was found to be one of the most up regulated genes in cord and adult CD161++CD8α+ T cells (Billerbeck, Kang et al. 2010) (**Appendix 1**). Although previously reported in MAIT cells from adult donors, expression at this earlier stage of development has not been described (Savage, Constantinides et al. 2008). Expression of IL18R by the CD161++CD8α+ T cell population would suggest that these cells already have the ability to respond to cytokine stimulation in an innate manner. A role of ZBTB16 in this context should also be explored.

CD26 (Dipeptidyl peptidase-4) is a ubiquitously expressed membrane glycoprotein and serine exopeptidase that cleaves X-proline dipeptides from the N-terminus of polypeptides. It is involved in immune regulation through cleavage and inactivation of chemokines and by acting as a co-stimulatory molecule (Ohnuma, Dang et al. 2008). In this study we show very high CD26 expression on CD161++CD8α+ T cells even in cord blood. CD26 is up regulated on T cells following activation. CD26^{high} cells have been shown to have enhanced proliferation and IL-2 production on CD3/CD28 cross linkage by antibody (Tanaka, Camerini et al. 1992) and high production of IFN-γ (Reinhold, Kahne et al. 1997). Increased levels of CD26+ T cells have been identified in the inflamed tissue of a number of autoimmune diseases,

including multiple sclerosis, Grave's disease and rheumatoid arthritis (Ohnuma, Dang et al. 2008). This would be in keeping with its expression on activated T cells, but may also reflect enrichment at these tissue sites of particular subsets of cells, such as CD161++CD8+ T cells. Therapeutic use of a CD26 inhibitor as a treatment for type-2 diabetes has recently been the subject of human trials (Matteucci and Giampietro 2009). One observation made was that patients taking the active drug suffered increased opportunistic infection compared to those taking placebo, providing interesting insight into the immune functions of this molecule.

These data further define the programming and differentiation of the distinctive CD161++CD8α+ T cell subset, setting the population apart from conventional CD8 T cells. I have identified a naïve pre-committed subset of CD161++CD8α+ T cells in cord blood, which bear strong resemblance at a gene and protein expression level to the more numerous subset observed in adults. Expansion of the CD161++CD8α+ population with age corresponds to the emergence of a predominant subset with narrow TCR usage (Vα7.2+, Vβ2/ 13.2+), as described for MAIT cells, which would suggest that this is an antigen driven process related to restriction of this TCR to MR1.

3.6 Conclusions

1. **CD161++CD8α+ T cells exist as a naïve, polyclonal, pre-determined type-17 subset in cord blood that is closely related to the CD161++CD8α+ T cell subset found in adults.**

2. **The CD161++CD8α+ T cell population expands with age.**

3. **Expansion of the CD161++CD8α+ T cell subset is associated with narrowing of the TCR usage to predominant usage of the MAIT TCR (Vα7.2+ and Vβ2+ or 13.2+). This strongly indicates that the subset expansion is driven by MR1-presented antigen.**

4. **Vα7.2+ MAIT cells predominantly (>90%) express the co-receptors CD8αα and CD8αβ.**

4 Human CD8αα cells

4.1 Introduction

CD8+ T cells form a key pillar of host defense against infection, but are highly heterogeneous, with a range of functions and phenotypes as well as specificities. Most TCRαβ+ CD8+ T cells express CD8 as a heterodimer of CD8α and β chains. However, it is recognized that a sub-group of CD8+ T cells exists which express CD8α as a homodimer, so-called CD8αα cells. The CD8αα homodimer is believed to act as a co-repressor and experimental models support a potential regulatory role for these cells (Tang, Maricic et al. 2006),(Tang, Maricic et al. 2007).

In murine models single positive CD8αα cells have been demonstrated to be a developmentally distinct subset that undergoes positive thymic selection and are highly enriched amongst intra-epithelial lymphocytes (IELs). CD8αα can also be co-expressed with either CD8αβ or CD4 on conventionally selected T cells within the environment of the intestine (Cheroutre and Lambolez 2008). Peripheral expression of IL-15 appears crucial for their development and maintenance. In the absence of the cytokine or its receptor components intraepithelial CD8αα cells numbers are severely reduced (Suzuki, Duncan et al. 1997; Lodolce, Boone et al. 1998; Kennedy, Glaccum et al. 2000) and its presence supports their proliferation and survival (Lai, Hou et al. 2008) (Lai, Gelfanov et al. 1999).

In humans, CD8αα/ CD8α+β^{low} cells are found exclusively within the memory cell population, with the overall proportion of these cells shown to increase with age (Konno, Okada et al. 2002). In tissue, CD8αα cells have been

identified among human fetal IELs (Latthe, Terry et al. 1994) and MAIT cells of the lamina propria, ascites and lung (Le Bourhis, Martin et al. 2010). The most extensive investigation of human CD8αα cells to date comes from literature on MAIT cells, which have been previously described to contain CD8αα, CD8αβ and double-negative T-cells (Treiner, Duban et al. 2003). Independently, a human CD161++CD8+ T-cell subset has been described to be Tc17 cells (Billerbeck, Kang et al. 2010) (**Appendix 1**) a subset recently confirmed in the MAIT cell population (Dusseaux, Martin et al. 2011); there is growing recognition that these data have been describing the same phenomenon in parallel or overlapping populations, covered in chapter 3 of this thesis. Study of the co-receptor phenotype of MAIT Vα7.2+ cells in chapter 3 of this thesis has shown that they express predominantly either CD8αα or CD8αβ. The CD8αα cell populations in humans have been little studied to date and whether they share the distinct phenotype, function and TCR usage of the CD161++CD8+ T cell subset has not been previously explored.

4.2 Hypothesis and Aims

I hypothesise that human CD161++CD8αα cells are a type 17 subset that share phenotype, function and TCR usage with their CD161++CD8αβ counterparts.

The aims of this chapter are:

1. To establish the relationship of human CD8αα cells to the CD161++ subset.
2. To further explore the tissue distribution of human CD8αα cells.

3. To explore the function, phenotype, gene expression profiles, TCR usage and differentiation of human CD161++CD8$\alpha\alpha$ cells in relation to their CD161++CD8$\alpha\beta$ counterparts.

4.3 Methods

4.3.1 Study subjects

20 adult healthy donors were enrolled in this study after informed consent. 22 umbilical cord blood samples were obtained from Stem Cell Services, NHS Blood and Transplant, Oxford, UK. PBMCs from 20 healthy 10 week-old infants were obtained from the South African TB Vaccine Initiative field site in Worcester, near Cape Town, South Africa. 5 paired PBMC and explant liver samples from patients with chronic hepatitis C were obtained from the transplantation programme, Boston, USA and 8 explant liver samples from patients with a variety of etiology of liver disease (4 Alcoholic liver disease, 3 Non-alcoholic fatty liver disease and 1 primary biliary cirrhosis) were obtained from the transplantation programme, Birmingham, UK. 3 colonic and 1 terminal ileal biopsy samples were obtained during colonoscopy from patients with normal findings on colonoscopy and histology. All study subjects were recruited following informed consent and in agreement with local ethics committees.

4.3.2 Lymphocyte recovery and sample preparation

Mononuclear cells from EDTA peripheral blood and cord blood samples were isolated as detailed in chapter 2 section 2.2.1. Cryopreserved samples from 10 week-old infants were thawed as per the protocol detailed in chapter 2.2.2 section.

LDLs were freshly isolated from explanted liver tissue from chronic liver diseases. LPMCs were isolated from endoscopic biopsy samples from human colon and small bowel. Detailed protocol of extraction techniques are found in chapter 2.

4.3.3 Fluorescent antibody staining for flow cytometry

Surface staining of separated lymphocytes, whole blood staining and intracellular staining for cytokines was performed as outlined in chapter 2 sections 2.3.1, 2.3.2 and 2.3.3 respectively.

Samples were acquired on either a FACSCaliber or LSRII cytometer (BD) using FACSDiva software (BD). FACS data was analysed using FloJo software (Treestar ltd). Gates were set using isotype and unstained control samples to identify positive populations following panel set up using a 'full minus one' strategy.

4.3.4 Cell sorting for microarray

Cell sorting of fresh healthy donor samples for micro-array analysis was performed by initial Ficoll-Histopaque density gradient centrifugation (Lymphoprep, Axis Sheild) (see chapter 2, section 2.2.1 for full protocol) followed by magnetic-bead CD8 enrichment (Easy-sep human CD8 enrichment kit, STEMCELL Technologies, Grenoble, France) (see chapter 2 section 2.4.1 for full protocol). Cells were labeled with fluorescent conjugated antibodies and sorted using a MoFlo MLS cell sorter (Dako), in collaboration with Andrew Worth, Jenner Institute, University of Oxford. Sorted cell populations were snap frozen and stored at -80^{0}C prior to RNA extraction.

4.3.4 RNA extraction

Total RNA was extracted from snap frozen sorted cell samples. These were lysed and homogenized using a QIAshredder spin column (Qiagen). Total RNA was extracted using an RNeasy mini kit (Qiagen) according to the manufacturer's instructions (see chapter 2 section 2.6 for full protocol).

4.3.5 Microarray

cDNA was amplified from total RNA using the Ovation Pico WTA System (NuGEN). Amplified cDNA was then fragmented and labeled using the Encore Biotin Module kit (NuGEN) (see chapter 2 section 2.7 for full protocol). Samples were then passed on to the Imperial College Genomics Laboratory for hybridization to GeneChip Human Genome U133 Plus 2.0 arrays (Affymetrix) using a hybridization, wash and stain kit (Affymetrix) and scanning with the GeneChip scanner 3000 7G (Affymetrix). Data analysis was performed in collaboration with the Natasha Sahgal, Wellcome Trust centre for human genetics, Oxford, UK as outlined in chapter 2 section 2.7.5.

4.3.6 Cell culture

PBMCs were CD8 enriched (see full protocol, chapter 2) and subsequently PE-positively selected using a CD8β–PE antibody (see full protocol, chapter 2) to obtain a >95% pure CD8αβ cell population, depleted of CD8αα cells. 2 x10^5 cells were then placed in 96 well culture plates at a concentration of 1 x 10^6 cells/ml in an incubator (5% CO_2, 37^0C). Cells were incubated in either R10 culture media alone or with anti-CD3/CD28 beads (Dyna beads, Invitrogen) at a bead to cell ration of 1:1 and with or without cytokines in different combinations as described under specific experiments; IL-

1β (10ng/ml), IL-2 (25ng/ml), IL-15 (10ng/ml) and IL-18 (40ng/ml). Media was changed and cytokines added on days 3 and 6. Cultures containing anti-CD3/CD28 beads were placed in an EasySep magnet for 1 min to remove the beads. Cells were then washed in PBS and prior to analysis by flow cytometry.

4.3.7 Statistical analysis

Statistical analysis was performed using GraftPad PRISM (GraphPad Software) version 4. A *p* value of <0.05 was considered significant.

4.4 Results

4.4.1 Human CD8αα cells are exclusive to the CD161++CD8+ T cell subset.

A significant reduction in the expression of CD8β by CD161++ cells compared to CD161+ and CD161- subsets (CD161++ vs CD161-: -4.43 Log_2 fold change; adjusted p=4.13 x 10^{-6}) (CD161++ vs CD161+: -2.08 Log_2 fold change; adjusted p=0.0053) was previously shown by gene expression profiling (Billerbeck, Kang et al. 2010) (**Appendix 1**). By FACS analysis of peripheral blood mono-nucleocytes (PBMCs) from healthy donors the CD8αα population in humans is demonstrated to be exclusive to the CD161++CD8α+ subset (**Figure 4.1a**). In fact, even the CD161++CD8αβ population expresses

lower amounts of CD8β than the CD161+ and CD161- subsets, indicating that there is likely expression of the CD8αα heterodimer on these cells as the CD8α molecule is expressed in excess (**Figure 4.1b**). The overall proportions of CD161++CD8αα and CD161++CD8αβ cells of the CD161++CD8α+ subset represent means of 33% and 67% respectively (**Figure 4.1c**).

4.4.2 Human CD8αα cells are present at diverse tissue sites.

Next, I identified this human CD8αα subset in both liver and small bowel tissue as also exclusive to the CD161++ subset, although I was unable to demonstrate CD161++CD8αα cells in the colon (**Figure 4.2a**). Similar proportions of CD161++/CD161+ and CD161-CD8α+ T cells are found in peripheral blood from healthy controls compared to in the LDLs of explant livers (**Figure 4.2b**). A significant difference in the proportions of

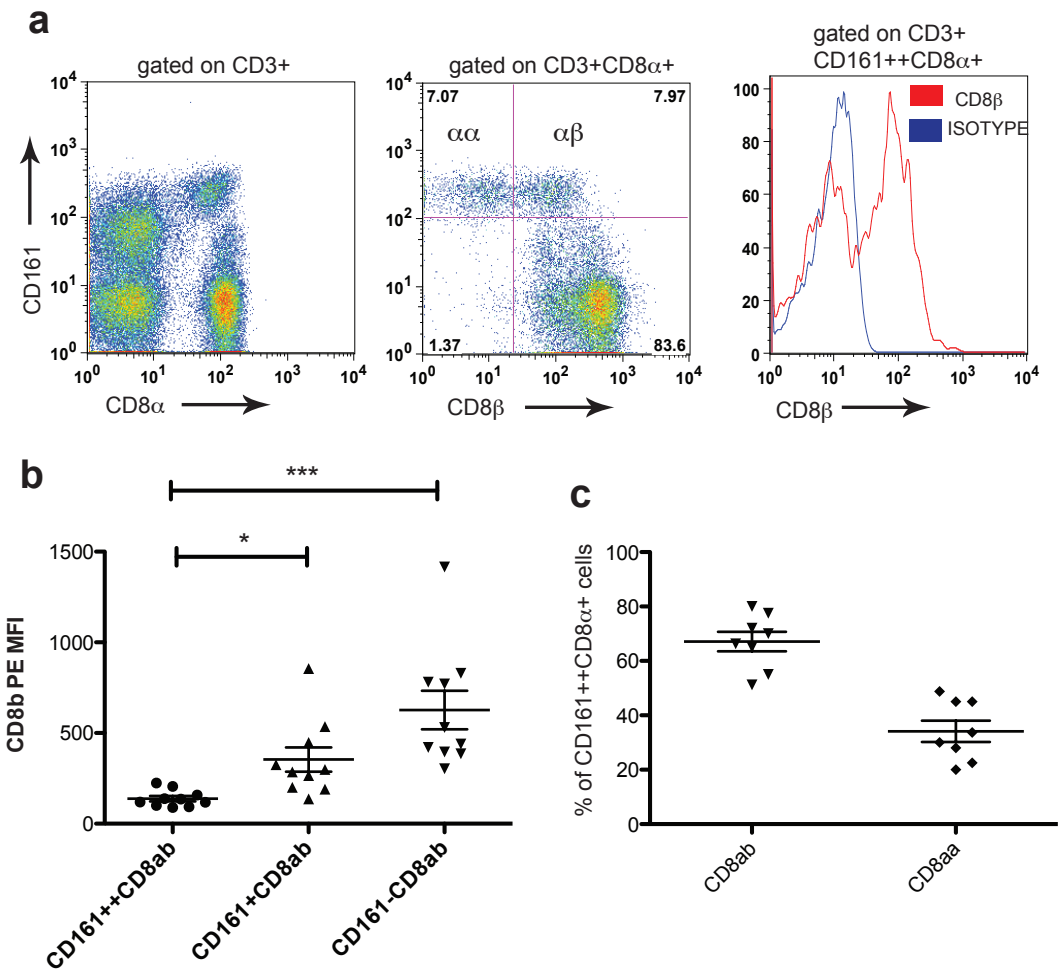


Figure 4.1. Human CD8αα cells are exclusive to the CD161++CD8α+ T cell subset. (a) Representative FACS plots show a prominent CD8α+ CD8β- population within the CD161++CD8α+ subset in peripheral blood (n=8). (b) Cumulative data comparing the mean fluorescent intensity (MFI) of CD8β expression on CD161++, CD161+ and CD161- CD8αβ subsets. *p<0.05, ***p<0.0001 (one way ANOVA). (c) Cumulative data showing distribution of CD161++CD8αβ and CD161++CD8αα cells in the CD161++CD8α+ subset.

CD161++CD8αβ and CD8αα cells are observed in peripheral blood from healthy controls compared to the LDL infiltrate with a smaller proportion of CD8αα cells seen in the liver (21%) compared to the blood (34%) (**Figure 4.2c**).

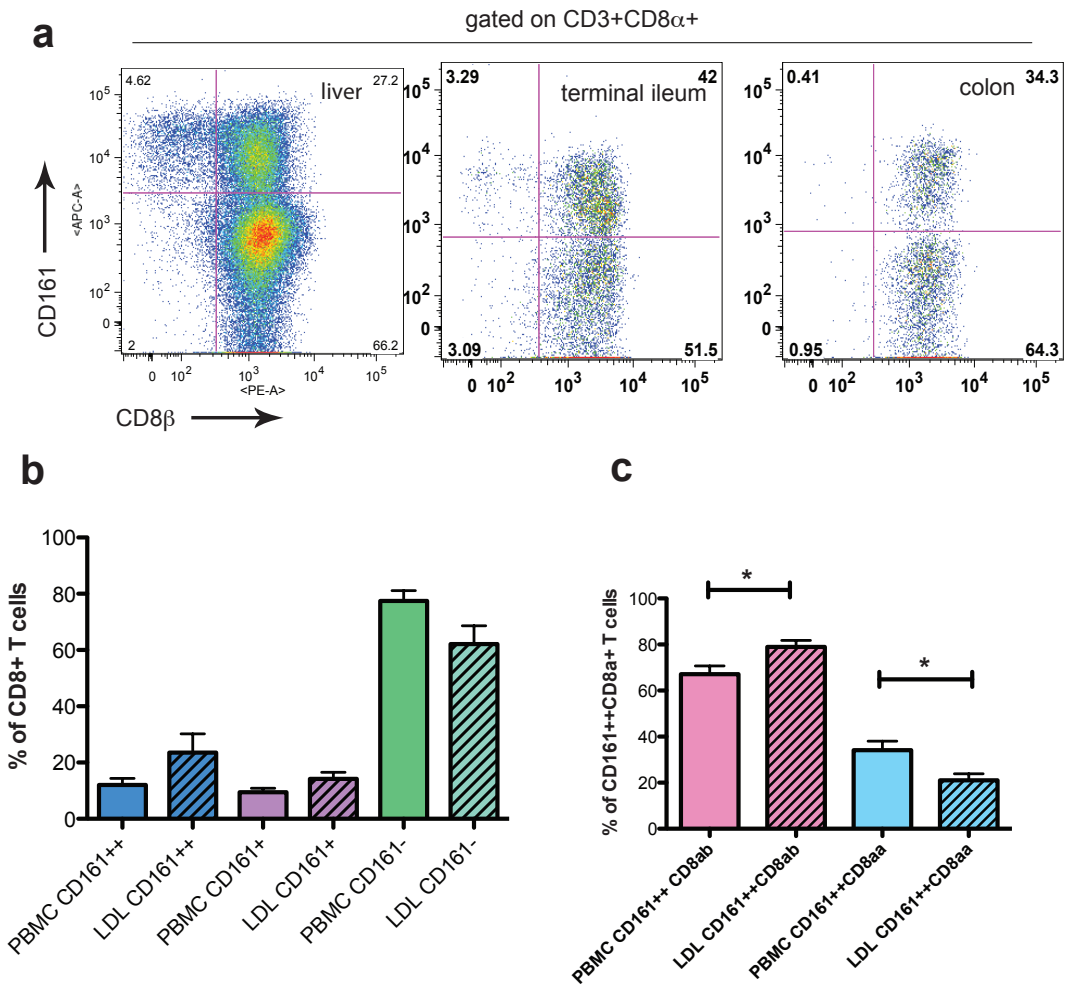


Figure 4.2. Human CD8αα cells are CD161++CD8α+ subset in the liver and terminal ileum. (a) CD8αα cells in the human liver (n=8) and terminal ileum (n=1) are found exclusively in the CD161+CD8+ subset. No CD8aa cells are found in the human colon (n=3). (b) Comparison of CD161++/CD161+/CD161- subsets between the liver (LDL) and peripheral blood (PBMC) of healthy controls as a proportion of CD8+ T cells. (c) Comparison of CD161++CD8αβ/CD8αα subsets between peripheral blood of healthy controls and liver as a proportion of CD8a+ T cells. *p<0.05 (Mann Whitney test).

4.4.3 Human CD161++CD8αα cells share Tc17 phenotype, function and gene expression profiles with CD161++CD8αβ cells.

It has been previously shown that CD161++CD8+ T cells are a unique functional subset with distinct chemokine receptor expression (CCR6, CXCR6 and CCR2) (**Figure 4.3a and 4.3b**) and cytokine secretion profile (IL-17A, IL-

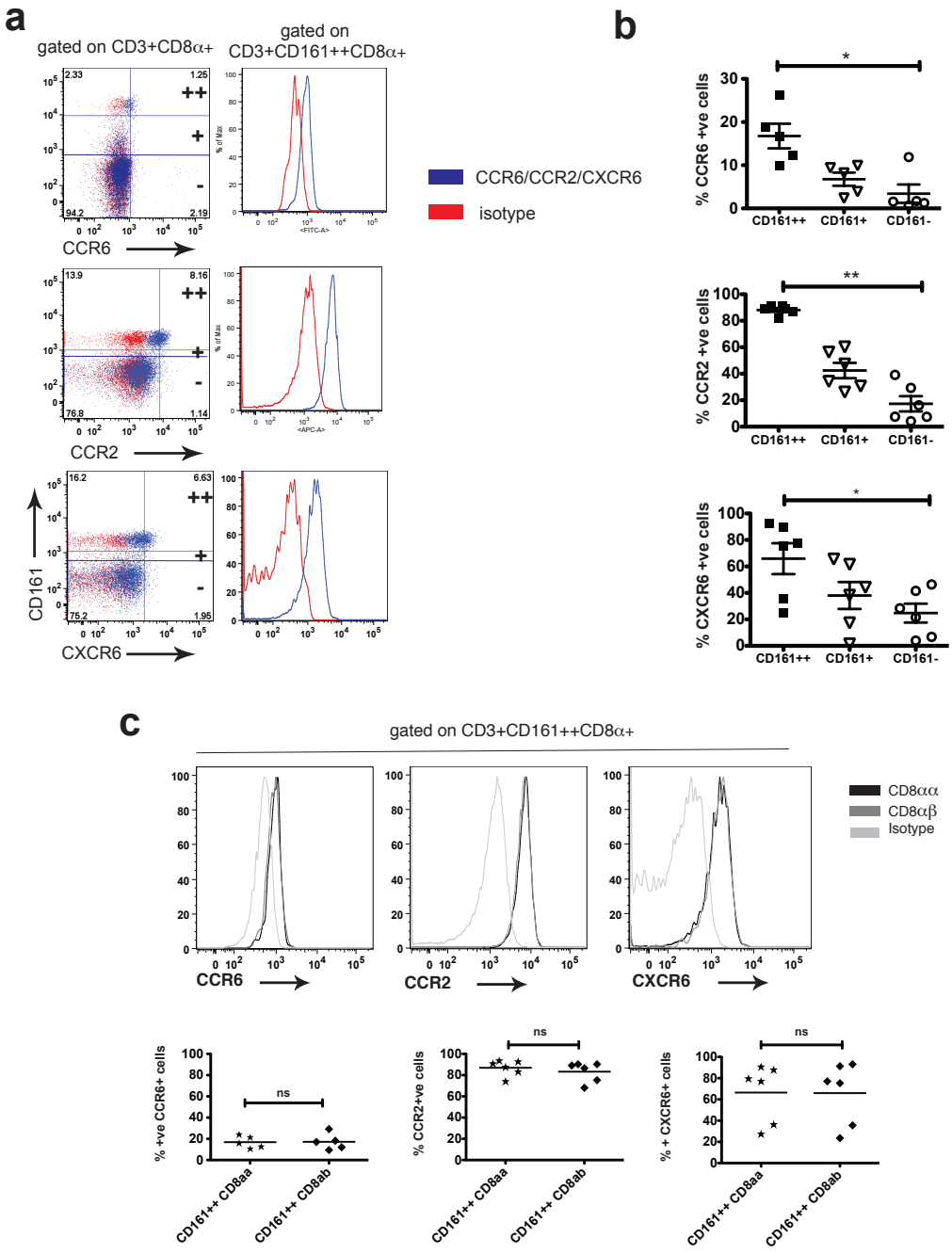


Figure 4.3. CD161++CD8ab and CD8aa cells share chemokine receptor expression profiles. (a) Representative FACS plots (left) and (b) histograms (right) showing CCR6, CCR2 and CXCR6 expression on CD161++CD8a+ T cells. *p<0.05, **p<0.001 (one way ANOVA). (c) Representative histograms showing CD161++CD8αα and CD8αβ cells to express CCR6, CCR2 and CXCR6. Cumulative data shown. NS = non significant (Mann-Whitney test).

22 and IFN-γ) (**Figure 4.4a and 4.4b**) (Billerbeck, Kang et al. 2010) (**Appendix 1**), as repeated here. I next analysed whether CD161++CD8αα T-cells shared these characteristics.

Firstly, I analysed the phenotype of the CD8αα cells, focusing on chemokine receptors. This demonstrated that in adult blood CD161++CD8αα T cells shared the chemokine-receptor expression profile of CD161++CD8αβ cells, with equivalent levels of CCR6, CCR2 and CXCR6 demonstrated in both subsets (**Figure 4.3c**).

The CD161++CD8αα subset also shared functional characteristics of the CD8αα subset defined by cytokine secretion; following stimulation with PMA/ionomycin, secreting IL-17A, IL-22 and IFNγ. CD161++CD8αα T cells secreted slightly more IL-17A than CD161++CD8αβ T cells (p= 0.0467), with no difference found in levels of IFN-γ or IL-22 secretion (**Figure 4.4c**).

To assess the differences at a global transcriptional level, I performed a microarray of sorted CD161++CD8αα and CD161++CD8αβ cells. Very few differences in the gene expression profiles of these two cell populations was observed, with none of the up- or down-regulated genes achieving a significant adjusted *p* value (**Figure 4.5 and Appendix 6**). Clustering of data to individuals rather than the cell subsets further supported the idea that these subsets are very closely related to one another phenotypically and functionally.

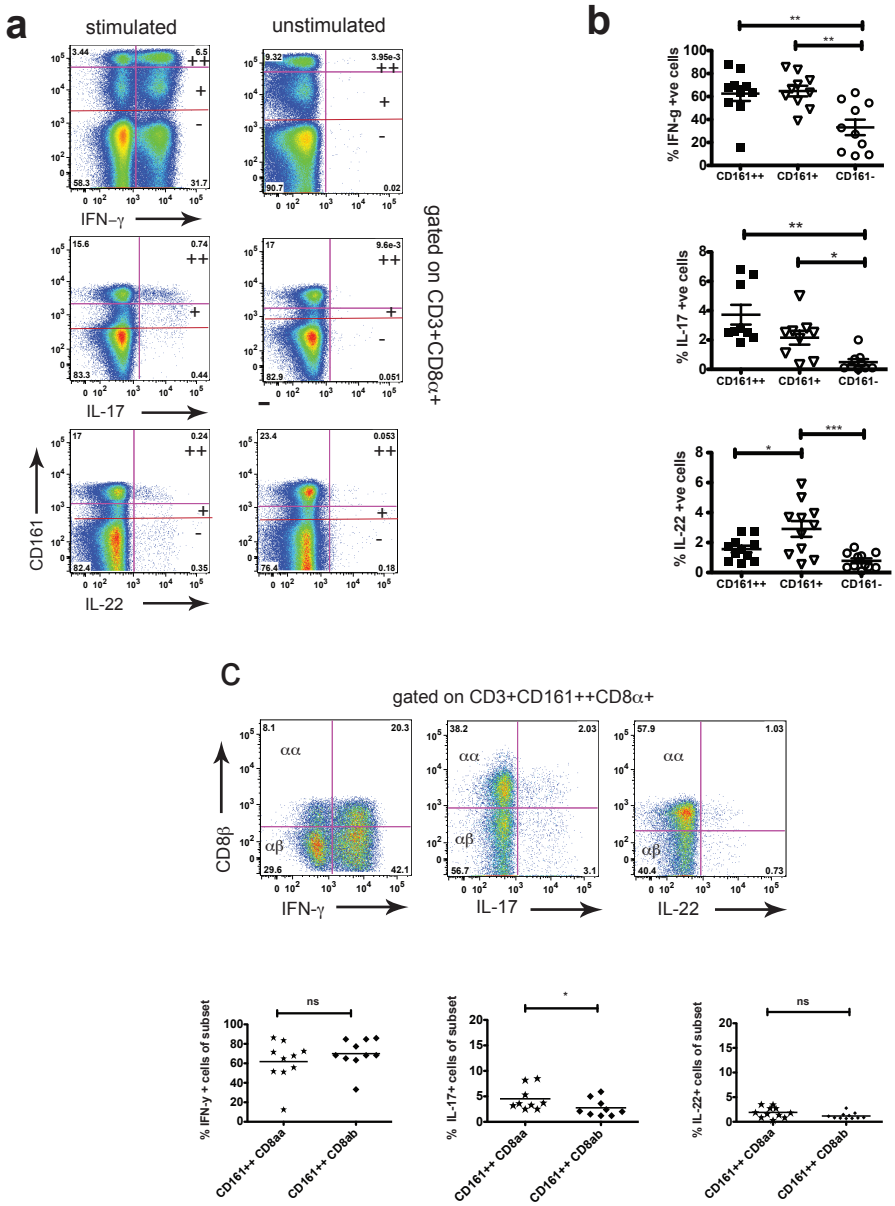


Figure 4.4. CD161++CD8αβ and CD8αα cells share cytokine expression profiles. (a) Representative FACS plots showing IFN-γ, IL-17 and IL-22 expression by CD161++/CD161+/CD161- subsets following stimulation with PMA/ionomycin (left). Unstimulated controls shown (right). (b) Cumulative data showing expression of IFN-γ, IL-17 and IL-22 by CD161++/CD161+/CD161- subsets following stimulation with PMA/ionomycin. *p<0.05, **p<0.01,***p<0.001 (one-way ANOVA). (c) Representative FACS plots (upper panel) and cumulative data and cumulative data (lower panel) showing IFN-γ, IL-17 and IL-22 expression by CD161++CD8αα and CD8αβ subsets. *p<0.05 (Mann Whitney).



Figure 4.5. CD161++CD8αα and CD8αβ cells share gene expression profiles. Microarray data presented as a heat-map showing up (red) and down (green) regulated gene expression of CD161++CD8αα (light blue) compared to CD8αβ (dark blue) cells. Individual study subjects numbered 1-4 at the bottom. Tree at the top indicates hierarchical clustering of samples. No significant differences found in gene expression between the two subsets.

4.4.4 Human CD8αα cells share a common differentiation pathway with CD161++CD8αβ cells.

In adult peripheral blood, the CD161++CD8α+ subset has a narrow TCR usage as demonstrated in chapter 3, with predominant usage of the Vα 7.2 chain and Vβ chains 2 and 13.2. In cord blood I found that such polarity of usage was not seen in the CD161++ CD8α+ population, which consistently showed broad usage of TCR Vβ chains. In addition, a very small proportion of cells used the Vα 7.2 chain compared to adult blood.

CD161++CD8αα cells were not detectable in cord or infant peripheral blood samples (**Figure 4.6a**). I observed a marked expansion of the CD161++CD8α+ T cell subset and the emergence of the CD161++CD8αα subset in adulthood (**Figure 4.6b**). To address the clonal relatedness of the populations, I analysed the Vβ usage of the CD161++CD8αα and CD161++ CD8αβ subsets using flow cytometry. The CD8αα subset shared very closely the narrow TCR usage of the CD161++CD8αβ subset (**Figure 4.6c**). Taken together, these data indicate a common origin of the CD161++CD8αβ and CD161++CD8αα subsets.

To further investigate the origin of the CD161++CD8αα cells, I isolated CD8αβ+ T cells and cultured them under a variety of conditions. Data from mouse models implicates peripheral IL-15 expression as an important factor in the development of CD8αα cells. However, I found that even without the addition of exogenous cytokines, by day 1 a significant reduction in

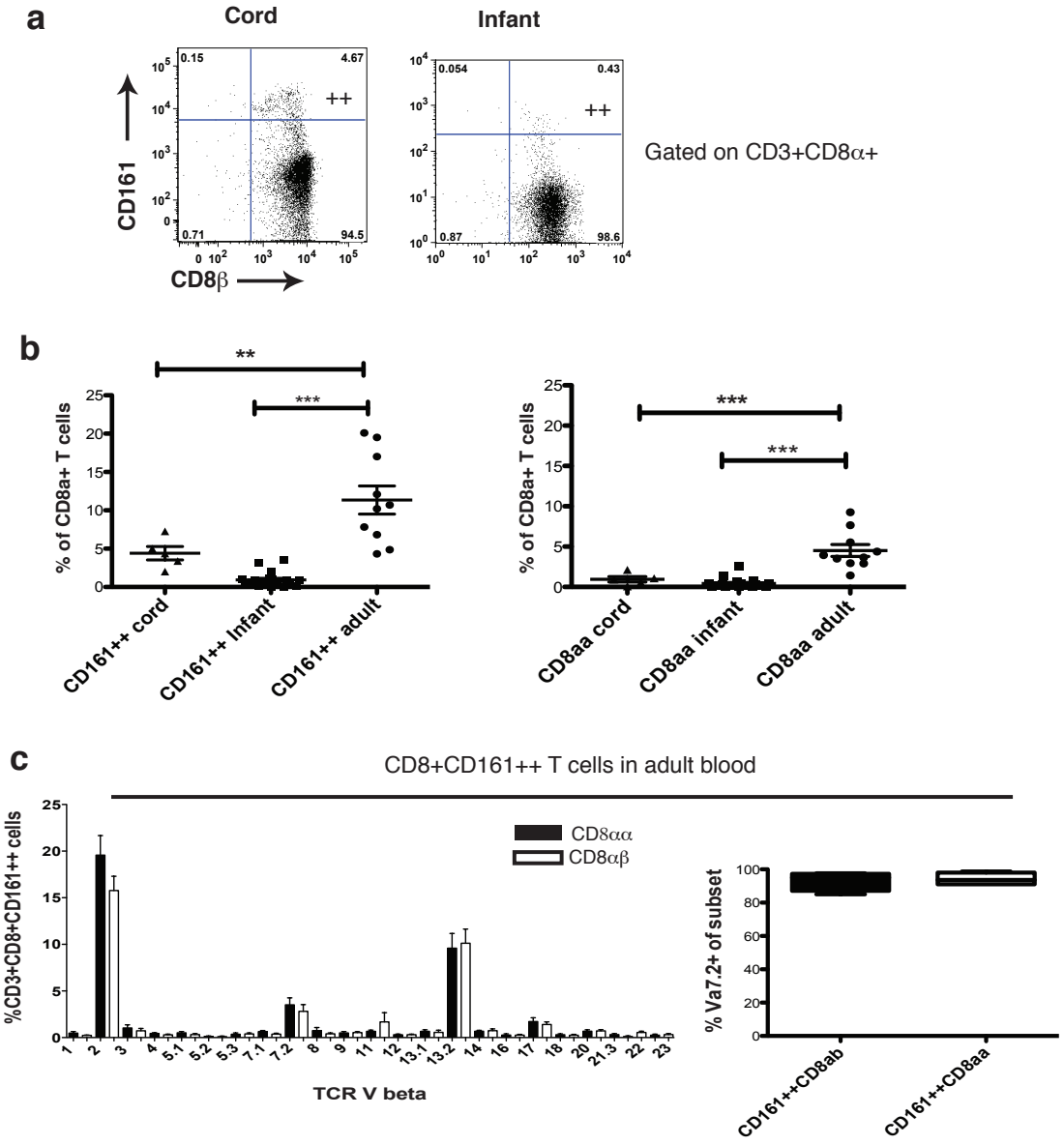
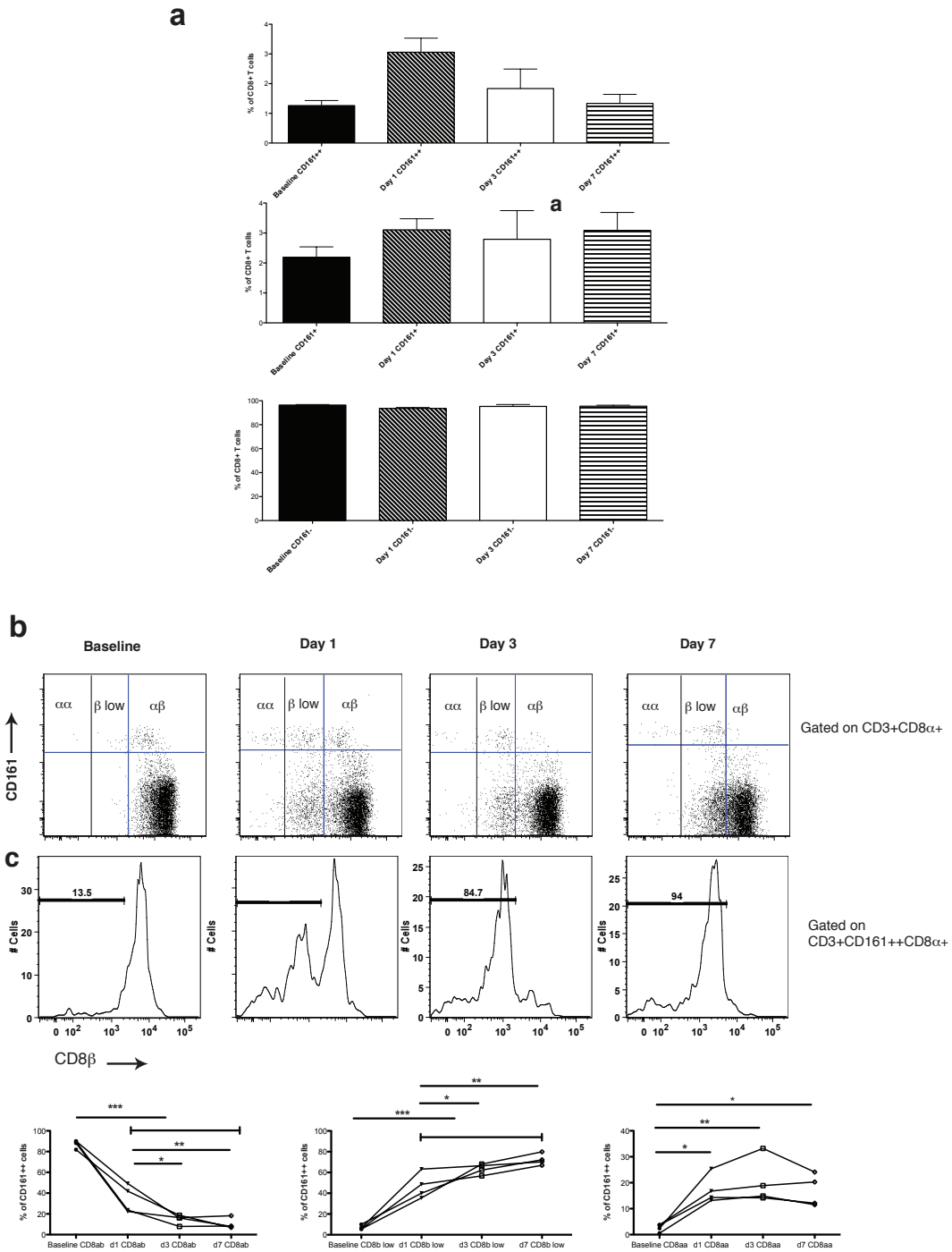


Figure 4.6. The CD161++ CD8αα population emerges on expansion of the CD161++CD8αβ subset with age. (a) CD161++ CD8αα cells are not found in cord or infant blood. (b) Comparison of CD161++CD8α+ and CD161++CD8αα populations in cord, infant and adult blood. **P<0.001, ***p<0.0001 (one-way ANOVA). (c) Comparison of TCR Vβ and Vα usage between CD161++ CD8αβ (black) and CD161++CD8αα (white) subsets in adult blood.


a
% of CD8+ T cells
Baseline CD161++
Day 1 CD161++
Day 3 CD161++
Day 7 CD161++
a
% of CD8+ T cells
Baseline CD161+
Day 1 CD161+
Day 3 CD161+
Day 7 CD161+
% of CD8+ T cells
Baseline CD161-
Day 1 CD161-
Day 3 CD161-
Day 7 CD161-
b
Baseline
Day 1
Day 3
Day 7
αα
β low
αβ
CD161
Gated on CD3+CD8α+
c
13.5
84.7
94
Cells
CD8β
Gated on CD3+CD161++CD8α+
% of CD161++ cells
Baseline CD8ab
d1 CD8ab
d3 CD8ab
d7 CD8ab
Baseline CD8b low
d1 CD8b low
d3 CD8b low
d7 CD8b low
Baseline CD8aa
d1 CD8aa
d3 CD8aa
d7 CD8aa

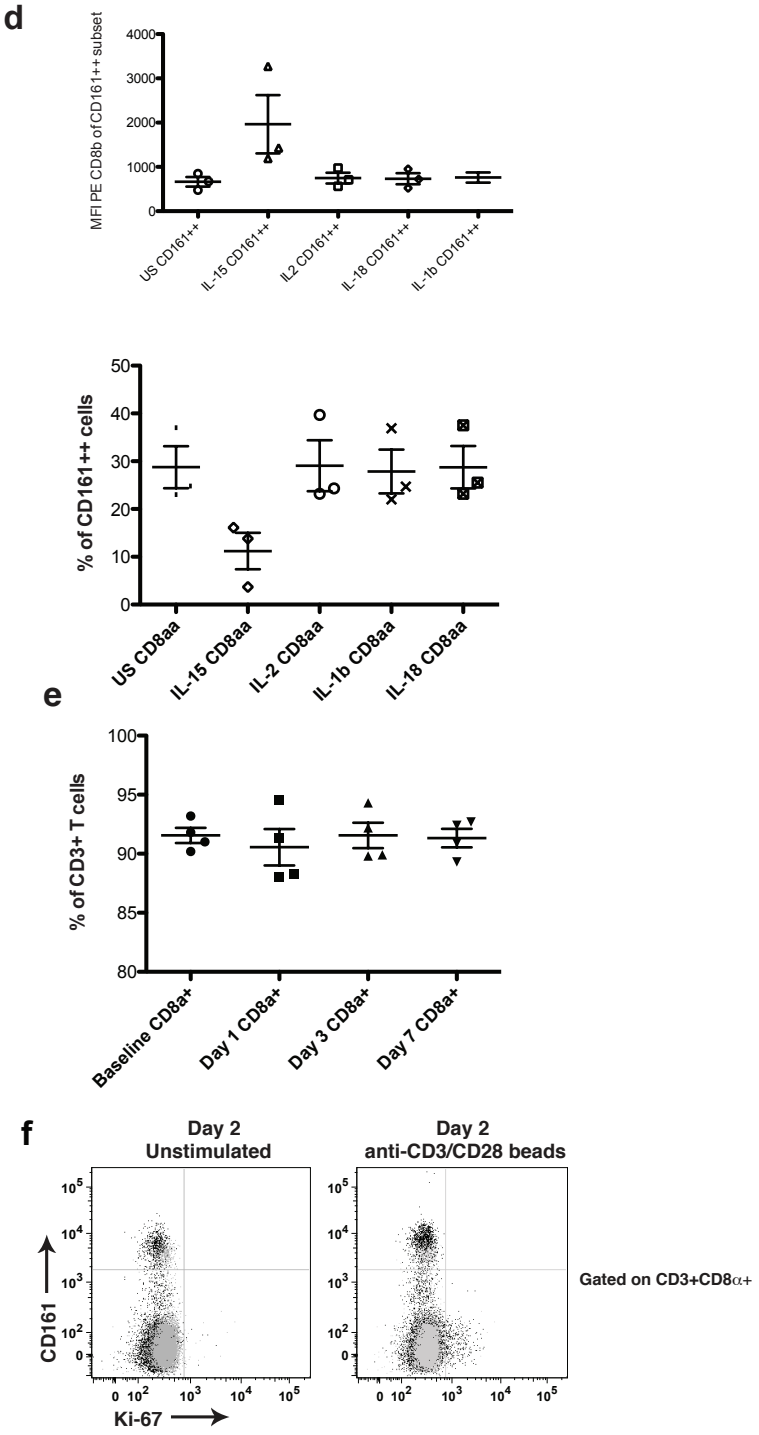


Figure 4.7. CD161++ CD8αα T-cells can be derived from CD161++CD8αβ cells in culture. (a) CD161++, CD161+ and CD161- populations of the CD8 enriched/CD8β+ selected PBMCs remain stable over the 7 days of culture in R10 media alone. (**b**) Representative FACS plots demonstrating change in CD8β expression of CD161++, CD161+ and CD161- populations of the CD8 enriched/CD8β+ selected PBMCs in media alone over 7 days of culture. CD8αα population seen only in CD161++ population. (**c**) Representative histograms showing change in CD8β expression of the CD161++CD8α+ population of the CD8 enriched/CD8β+ selected PBMCs over 7 days of culture (upper panel). Cumulative data shown (bottom panel), *p <0.05, **p<0.001, ***p<0.0001 (one-way anova). Data

representative of 4 experiments. (**d**) Comparison of CD8β down regulation and emergence of the CD8αα subset by CD8 enriched/CD8β+ selected PBMCs following culture in media alone, IL-2, IL-15, IL-18 or IL-1β. (**e**) Cumulative data showing no significant change in the CD8α+ T cell population of cultures over course of experiment (one way ANOVA). (**f**) Ki-67 proliferation data for sorted CD8β+ cells left in culture media alone or with CD3/CD28 beads for 48 hours. Baseline Ki-67 staining (grey), post culture Ki-67 staining (black). Data representative of 2 experiments.

CD8β expression and accumulation of CD8αα cells was seen overall. All three CD161 subsets developed a CD8β low population. No variation in the proportions of CD161++, CD161+ and CD161- cell populations was observed over the course of the experiment (**Figure 4.7a**). However, the emergence of a CD8β- population corresponding to CD8αα cells was only observed in the CD161++ population (**Figure 4.7b and c**). No significant impact on this phenomenon was observed with the addition of any cytokine to the culture over media alone, including IL-15 (**Figure 4.7d**). To verify that the loss of CD8β expression was not due to internalization of CD8αβ following antibody labeling for sorting I show that CD8α expression is stable over the course of the experiment. To ensure that the emergence of the CD8αα population was not the result of proliferation of a residual CD8αα population following sorting, using Ki-67 expression I demonstrate that the CD161++ cell population had not proliferated significantly over this period, even when co-cultured with anti-CD3+CD28+ beads (**Figure 4.7f**). This was in keeping with previous reports that this subset proliferates poorly in culture (Dusseaux, Martin et al. 2011), (Turtle, Swanson et al. 2009) (Northfield et al, 2008).

4.5 Discussion

In adult blood, CD8αα T-cells are found exclusively in the CD161++CD8α+ T cell subset. Low CD8β expression on the CD161++CD8αβ subset indicates

expression of CD8α in excess, and expression of both CD8αα and CD8αβ at the cell surface on this subset. In contrast to models of CD8αα cell differentiation in mouse models, the CD161++CD8αα and CD8αβ cell populations appear to be very closely developmentally related. I show human CD8αα cells to be present in the liver and small bowel and, based on previous data (Billerbeck, Kang et al. 2010) (**Appendix 1**), I would predict infiltrates of CD161++CD8αα cells will also be found at further diverse tissue sites (tonsil, inflammatory arthritis). Interestingly, I was unable to demonstrate CD161++CD8αα cells in the colon, which might indicate preferential homing to, or CD8β down regulation at particular tissue sites and not others.

CD161++CD8αα cells, like their CD161++CD8αβ counterparts, are differentiated down a type-17 pathway, with similar effector function (IFNγ, IL17, IL22) and chemokine receptor expression (CCR2, CCR6 and CXCR6). The overall function of the cells therefore appears to be potentially distinct from the regulatory one suggested for CD8αα T-cells found in murine models. In keeping with the idea that CD8αα acts as a co-repressor, rather than a co-receptor like Cd8αβ, CD8αα cells in mice have been shown to provide protection from autoimmune encephalitis and colitis (Poussier, Ning et al. 2002; Tang, Maricic et al. 2007). In humans, CD8αα may play a similar role in CD161++CD8α+ T cells - in imposing an important threshold of activation on these innate-like, effector-ready T cells in tissue or in determining the overall functional phenotype of the cells (e.g. predominant IL-17 vs IL-22 production) depending of the type of activation or homeostatic signals received, although I have not demonstrated that here.

The fact that little difference is observed between the phenotype, function, gene expression on microarray or TCR Vα and Vβ usage between CD161++CD8αβ+ and CD161++CD8αα+ cells suggests that the two populations are very closely linked. From these data it is proposed that the latter population emerges at a later stage from within the same cellular pool as CD161++CD8αβ+ cells, and CD8β expression is regulated within it. Firstly, in infant PBMCs and cord blood, broad TCR-usage of the CD161++ subset is observed – no different to other e.g. CD161- populations. Secondly, CD161++CD8αα cells are not present in cord or infant blood, but are detectable in adulthood, while precursor Tc17 lineage populations are present at both stages. Thirdly, I show that CD161++ CD8αα cells can be derived from CD161++ CD8αβ cells in culture. This is seen in the absence of specific stimulation or proliferation after just 24 hours and would suggest that the transition between CD161++CD8αα and CD8αβ cell populations is a rapid and simple process. Interestingly these data contrast with those from mouse models, which suggest that CD8αα cells, found predominantly within the epithelial compartment of the gut, are positively selected in the thymus and preferentially migrate to the gut as CD4-CD8- T cells that re-express CD8αα on exposure to IL-15 (Cheroutre and Lambolez 2008)' (Kennedy, Glaccum et al. 2000)' (Lai, Hou et al. 2008)' (Lodolce, Boone et al. 1998)' (Terabe, Tagaya et al. 2008). Here I show no enhanced benefit of the addition of IL-15 in culture to the generation or proliferation of CD8αα cells in man.

This is the first description of human CD8αα cells as an exclusive CD161++CD8α+ T cell subset. These data also define human CD8αα cells in healthy donors to have type-17 functional and phenotypic properties. Data relating CD161++CD8αα T cells to the CD161++CD8αβ population strongly

suggest a common origin for these cells, emerging from a pre-committed CD161++ naïve precursor. The true in vivo impact of CD161++CD8αα T cells requires further analysis, with many questions remaining unanswered. What drives the transition from CD161++CD8αβ to CD8αα? Why is the CD8αα population only seen in the CD161++CD8α+ subset? What differential function does the CD8αα molecule impart compared to CD8αβ? Why do I see a CD161++CD8αα population in some tissue and not others? Much further work is required to investigate the likely significant role played by this subset in inflammation and immunity at diverse tissue sites, including the gut and liver.

4.6 Conclusions

1. **Human CD8αα cells are exclusive to the CD161++CD8α+ subset in humans.**

2. **Human CD161++CD8αα cells share TCR usage and type-17 function and phenotype with their CD161++CD8αβ counterparts.**

3. **CD8αα cells are not present in cord or infant blood, but emerge as the CD161++CD8α+ subset expands with age and there is marked narrowing of their TCR usage to a predominant MAIT cell TCR.**

4. **Shared TCR usage, function, phenotype and ready transition of CD161++CD8αβ populations to CD161++CD8αα cells in culture strongly suggests a common origin of differentiation of these subsets.**

5. Activation of CD8 T cell subsets and regulation of CD8β expression in chronic viral hepatitis.

5.1 Introduction

It has been demonstrated in this thesis (chapter 4) and previously (Billerbeck, Kang et al. 2010) (**Appendix 1**) that the CD161++CD8α+ T cell population is a prominent peripheral and intra-hepatic T cell subset. In chronic HCV infection a striking loss from the peripheral circulation and enrichment in the liver is seen by analysis of paired patient blood and liver samples. In keeping with their type 17 functionality, these cells are shown to variably co-produce IL-17, IL-22 and IFN-γ. Levels of IL-17/IFN-γ co-producing CD161++CD8+ T cells inversely correlate with the degree of liver fibrosis observed, suggestive of a protective effect in terms of disease progression. A role in terms of viral control has not been demonstrated.

The CD161++CD8α+ T cell subset likely sits within an immunological niche linking innate to adaptive immunity - given their predominant expression of the MR1 restricted TCR, co-receptor profile, chemokine receptor expression and type-17 functionality. However, in terms of cytokine expression it is difficult to extrapolate data obtained by *ex-vivo* non-specific stimulation of cells with PMA/ionomycin as a true reflection of what is occurring *in vivo*, especially within the distinct immunological environment of the liver. Functional subtlety

is undoubtedly lost in such an experimental set up. Indeed, where they are associated with a particular infection whether they are playing an active role at all or just present in the inflammatory infiltrate is hard to decipher. Access to human liver samples is also difficult, with biopsy representing a significant risk to patients in terms of procedure related complications, and explant liver material obtained at transplant being distorted and fibrosed.

In addressing this issue, an initial approach is to phenotype the CD161++CD8α+ T cells in terms of expression of activation and exhaustion markers. These give an indication of active involvement in immunity (**Table 5.1**) in the setting of disease. Up-regulation of such markers on peripheral CD161++CD8α+ T cells in the context of chronic HBV and HCV infection compared to healthy controls would help to establish this, although may not be a true reflection of the state of intra-hepatic populations. However, the subset does express CXCR6 and CCR2, which are involved specifically in liver homing via their ligands CXCL16 and CCL16 respectively. Cells observed in the periphery may represent cells that are re-circulating to the liver, although this requires further investigation. A possible differential role for CD161++CD8$\alpha\alpha$ and CD8$\alpha\beta$ cells also warrants exploration. In this chapter I use samples from patients with chronic HBV as a control group to look for disease vs liver specific effects on the CD161++CD8+ T cell subset by comparison with samples from patients with chronic HCV infection.

Marker	Function
CD25	Intermediate activation marker: IL-2Rα
CD28	Activation marker: receptor for B7 co-stimulatory molecule.
CD38	Activation marker: linked with cell proliferation in the presence of IL-2
CD69	Early activation marker: no known function
HLA-DR	Late activation marker
PD-1	Exhaustion marker: engagement of receptor delivers negative signal to TCR activation pathway, leading to T-cell anergy.

Table 5.1. Functions of activation and exhaustion markers tested.

HBV, despite the availability of a prophylactic vaccine, is a serious global health issue with an estimated 350 million people are infected worldwide. HBV is a small, enveloped DNA virus that is transmitted both horizontally and vertically through infected blood products and blood contaminated body fluids. Most people who become infected as older children and adults clear the virus during acute infection, with about 5-10% progressing to chronic disease. This compares to 95% of those who acquire the virus vertically as infants (Dienstag 2008).

The clinical course of chronic HBV is complicated and reflects a complex relationship between the virus and the host immune system. Initial infection is characterised by expression of the HBV e antigen (eAg), high viral load and immune inertia and is termed the 'immunotolerant' phase. At some point this tolerance is broken and an immune response develops. This is characterised by loss of eAg expression and development of anti-eAg antibodies. Viral load is much reduced and patients can clear the virus at this stage. Transient liver damage is also observed, with elevation in the liver enzyme alanine transaminase (ALT). Those who don't clear at this stage have ongoing low level HBV replication, thought to be controlled by active immunity, with little evidence of ongoing liver damage termed inactive carriers. At either the e-

antigen negative (eAg-ve) or positive (eAg+ve) stage of the disease flares in activity of the virus and immune system can occur and unchecked by treatment leads to hepatocellular damage and fibrosis. Current treatment is based on use of either time-limited courses interferon injections to try to clear the virus or a choice of a limited number of life-long anti-viral agents with a view to long-term viral suppression, which in time risk the selection of drug-resistant virus (Dienstag 2008). Therapeutic vaccination and immunomodulatory therapy are important avenues of research in development of new treatments. Long-term viral control with drugs will not be an option for the majority of the world's population infected with HBV due to the costs involved. It is important that we research ways to clear the virus, which are less expensive, more widely available and likely to have a greater impact on the global burden of disease.

In acute HBV infection a marked absence of type 1 interferons and increased levels of IL-10 is observed allowing unchecked high level viral replication prior to the emergence of the adaptive response. In those who clear the virus in the acute phase, a strong and multi-specific CD8 T cell response is seen. This contrasts to the weak and transient response seen in those who develop chronic infection (Das and Maini, 2010), similar to chronic HCV. Antigen-specific CD8+ T cells from patients with chronic HBV infection display marked up-regulation of the pro-apoptotic protein, Bcl2-interacting protein (Bim)(Lopes, Kellam et al. 2008). This is likely a consequence rather than a cause of the weak response seen – possibly driven by high persistent antigenic load or ineffective antigen presentation within the liver.

In addition to the effects seen amongst antigen specific T cells, marked changes in the bulk CD8 T cell population in chronic HBV infection have also been observed. These cells proliferate poorly with impaired production of IL-2 and have down-regulated expression of CD28 and CD3-ζ (Das, Hoare et al. 2008). Such effects on the TCR signalling capacity are observed in other settings of chronic inflammation and antigenic exposure, such as autoimmunity (Krishnan, Kiang et al. 2005), chronic infection (Trimble and Lieberman 1998) and malignancy (Nakagomi, Petersson et al. 1993), although has not been reported in chronic HCV. Loss of CD28 expression has been associated with reduced expression of CD8β in autoimmune disease (Werwitzke, Tiede et al. 2008), however whether this occurs in chronic HBV infection has not previously been investigated.

5.2 Hypothesis and Aims

I hypothesise that CD161++CD8α+ T cell subsets play an active role in immunity in chronic HBV and HCV. In addition I predict that levels of CD8β expression on the bulk CD8 T cell population in chronic HBV are associated with activation/ exhaustion.

The aims of this chapter are:

1. To further investigate the loss of peripheral CD161++CD8α+ subsets (CD8αα and CD8αβ cells) in chronic HBV and HCV.

2. To investigate the role of the CD161++CD8α+ T cell subsets in chronic HBV and HCV compared to healthy controls using a panel of activation/ exhaustion markers.

3. To study changes in the bulk CD8+ T cell populations in chronic HBV and HCV, including changes in expression of activation/exhaustion markers in association with CD8β chain expression levels.

5.3 Methods

5.3.1 Study subjects

Peripheral blood samples were obtained from patients with treatment naïve chronic HBV (18) and HCV (24) and healthy controls (19) who were enrolled in the study after informed consent and in accordance with the local ethics committee. Patient demographics are detailed in table 5.2.

Disease group	Age (mean) (years)	Viral load (mean) (IU/L)	ALT (mean) (Units/L)	Genotype
HBV eAg+ (n=6)	39	$5.68x10^7$	52	unknown
HBV eAg- (n=12)	38	4974	31	unknown
HCV (n=24)	41	$8.2x10^6$	55	1a

Table 5.2. Demographics table giving information on HBV and HCV patients enrolled in the study.

5.3.2 Lymphocyte recovery and sample preparation

Mononuclear cells from from EDTA peripheral blood and cord blood samples were isolated as detailed in chapter 2 section 2.2.1 prior to immediate antibody staining for FACS analysis or were cryopreserved for future use. All analysis looking at activation/exhaustion marker expression was performed

using cryopreserved samples, thawed as per the protocol detailed in chapter 2.2.2 section. LDLs were freshly isolated from explanted liver tissue from chronic liver diseases. LPMCs we isolated from endoscopic biopsy samples from human colon and small bowel. Detailed protocol of extraction techniques are found in chapter 2.

5.3.3 Fluorescent antibody staining for flow cytometry

Surface staining of separated lymphocytes, whole blood staining and intracellular staining for cytokines was performed as outlined in chapter 2 sections 2.3.1, 2.3.2 and 2.3.3 respectively. Samples were acquired on either a FACSCaliber or LSRII cytometer (BD) using FACSDiva software (BD). FACS data was analysed using FloJo software (Treestar ltd). Gates were set using isotype and unstained control samples to identify positive populations following panel set up using a 'full minus one' strategy.

4.3.4 Cell culture

PBMCs were CD8 enriched (see full protocol, chapter 2) and subsequently PE-positively selected using a CD8β–PE antibody (see full protocol, chapter 2) to obtain a >95% pure CD8αβ cell population, depleted of CD8αα cells. 2 $x10^5$ cells were then placed in 96 well culture plates at a concentration of 1 x 10^6 cells/ml in an incubator (5% CO_2, 37^0C). Cells were incubated in either R10 culture media alone or with anti-CD3/CD28 beads (Dyna-beads, Invitrogen) at a bead to cell ratio of 1:1. Cultures were split and harvested on days 1 and 3. Cultures containing anti-CD3/CD28 beads were placed in an EasySep magnet for 1 min to remove the beads. Cells were then washed in PBS prior to analysis by flow cytometry.

4.3.5 Statistical analysis

Statistical analysis was performed using GraftPad PRISM (GraphPad Software) version 4. A *p* value of <0.05 was considered significant.

5.4 Results

5.4.1 CD161++CD8+ T cell subset redistribution in chronic HBV and HCV infection.

CD161++CD8$\alpha\alpha$ and CD8$\alpha\beta$ T cells are significantly reduced in the peripheral circulation of patients with chronic HBV and HCV compared to healthy controls (**Figure 5.1a and 5.1b**), contrasting with no reduction in CD161+ or CD161-CD8+ T cells (**Figure 5.1c**). This might be due to accumulation within the liver or due to actual loss of CD161++CD8+ T cells in these conditions. In order to address this I looked at distribution of the CD161++ T cell subsets between the blood and the liver in paired samples using explant liver tissue obtained at transplantation from patients with chronic HCV. This demonstrates significant enrichment in the liver of both CD161+CD8$\alpha\beta$ and CD8$\alpha\alpha$ T cells (**Figure 5.2**).

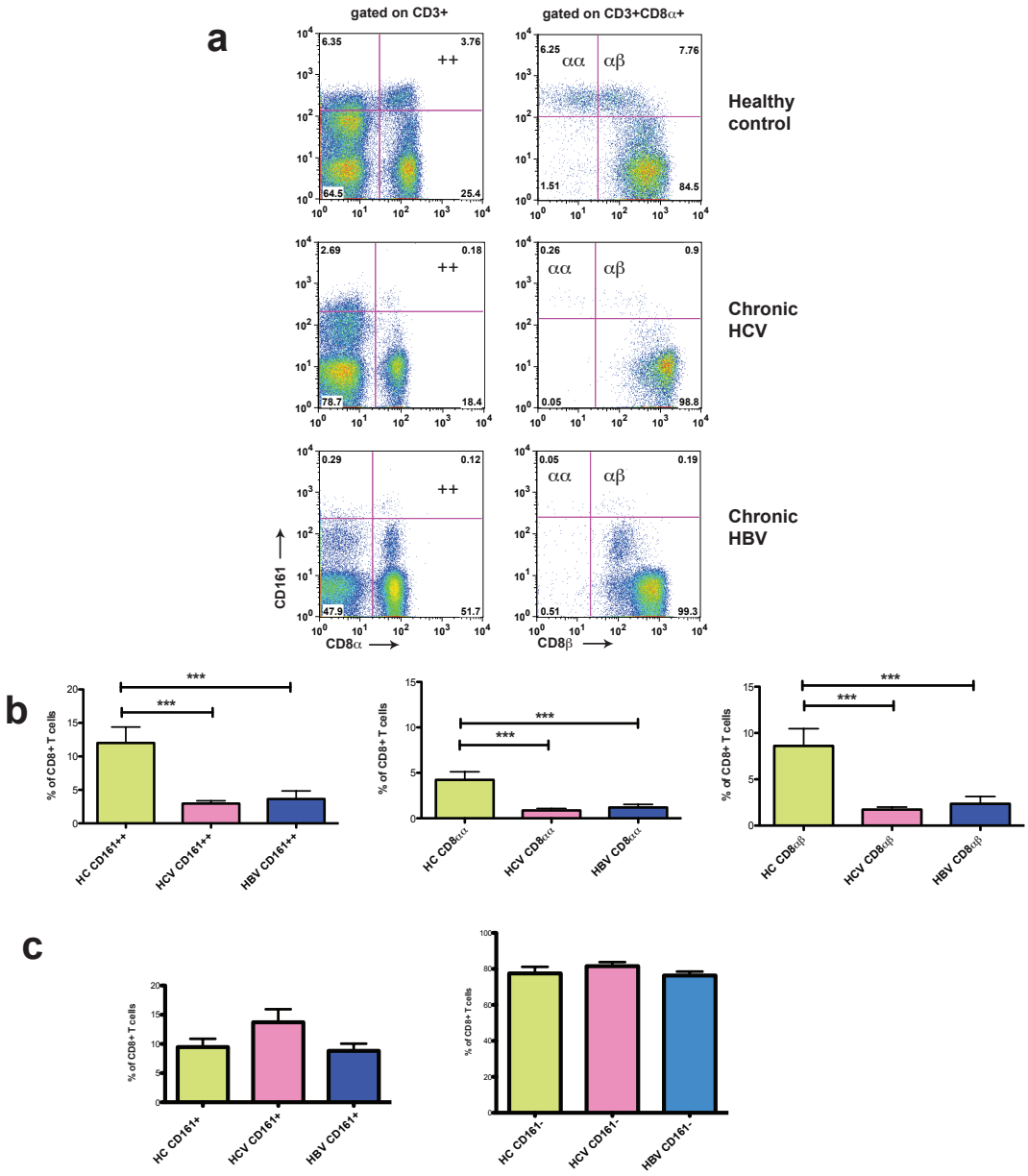


Figure 5.1. CD161++CD8+ T cells subsets are lost from peripheral blood in chronic HBV and HCV. (a) Representative FACS plots and (b) cumulative data showing the differences in CD161++CD8+ and CD161++CD8αα+/CD8αβ+ cell populations in peripheral blood between healthy controls and patients with chronic HBV and HCV. **p<0.001, ***p<0.0001 (one-way ANOVA). (c) Cumulative data demonstrating no loss of CD161+ or CD161- CD8 T cells from peripheral blood inpatients with chronic HBV or HCV.

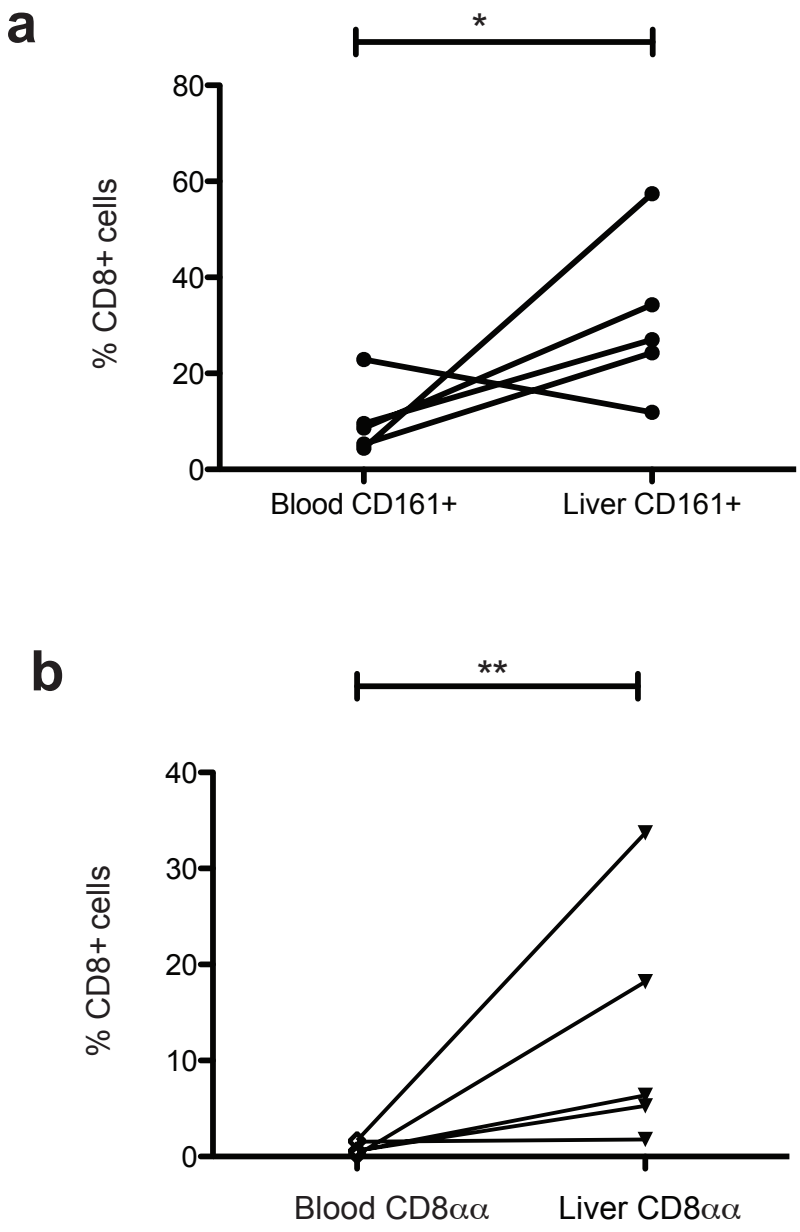
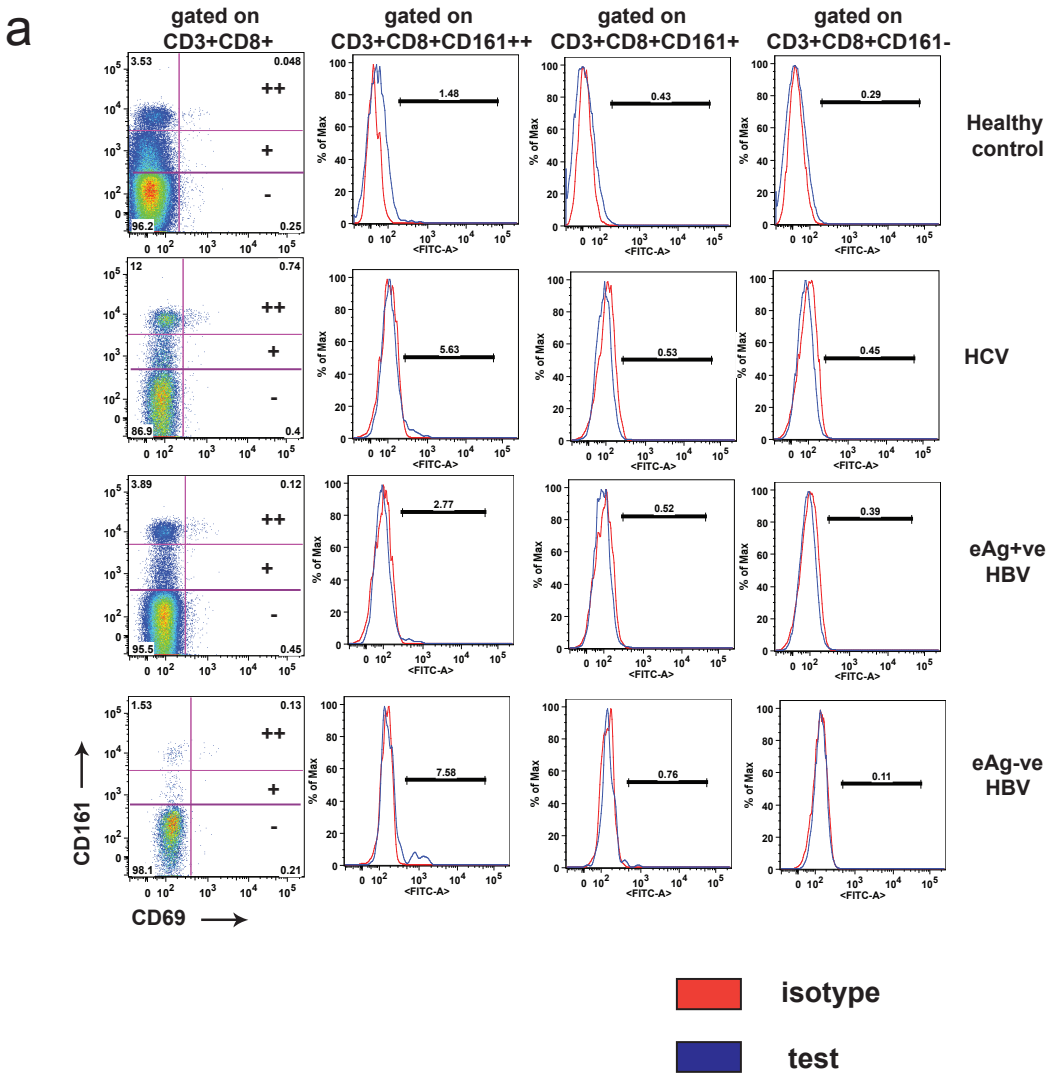


Figure 5.2. Relative enrichment of CD161++CD8+ T cell subsets in the liver in chronic HCV. Cumulative data obtained from paired peripheral blood and liver derived lymphocytes (obtained from explant livers at transplanation) showing relative enrichment of CD161+T cells (a) and CD161+CD8αα cells (b) in the liver compared to peripheral blood in patients with chronic HCV. *p=0.0159, **p=0.0079 (Mann Whitney test).

5.4.2 Expression of activation and exhaustion markers on CD161++/CD161+ and CD161- subsets in chronic HBV and HCV compared to healthy controls.

A panel of activation/ exhaustion markers (**Table 5.1**) was used to address the question of whether, given their loss from peripheral circulation and enrichment in the liver in chronic HBV/HCV, the CD161++CD8 T cell subset might be playing an active role in immunity to these infections. I looked at the following markers; CD69 (**Figure 5.3**), CD25 (**Figure 5.4**), CD38 (**Figure 5.5**), HLA-DR (**Figure 5.6**), PD-1 (**Figure 5.7**) and CD28 (**Figure 5.8**).

Here it is demonstrated that CD69 (**Figure 5.3a**), CD25 (**Figure 5.4**), HLA-DR (**Figure 5.6**) and PD-1 (**Figure 5.7**) are significantly up-regulated on the CD161++CD8+ T cell subset in chronic HBV and HCV compared to healthy controls indicating activation of this subset in disease. However, I also demonstrate up-regulation of a number of these markers on the CD161+ and CD161-CD8+ T cell subsets in HBV and HCV. CD25 is significantly up-regulated on CD161+ and CD161- CD8+ T cell subsets in HCV and eAg+ve/eAg-ve HBV (**Figure 5.4**). A marked shift in HLA-DR expression is observed in both CD161+ and CD161-CD8 T cell subsets in HBV, but not HCV (**Figure 5.6**). PD-1 is up regulated in eAg-ve HBV on CD161+CD8+ T cells and on both eAg+ve and eAg-ve HBV on CD161-CD8+ T cells (**Figure 5.7**). This suggests that potentially there is bulk CD8 T cell activation/ exhaustion, not specific to the CD161++CD8+ T cell subset in these conditions (and especially HBV), despite their particular re-distribution to the liver.


a
gated on CD3+CD8+
gated on CD3+CD8+CD161++
gated on CD3+CD8+CD161+
gated on CD3+CD8+CD161-
Healthy control
HCV
eAg+ve HBV
eAg-ve HBV
CD161
CD69
% of Max
<FITC-A>
isotype
test

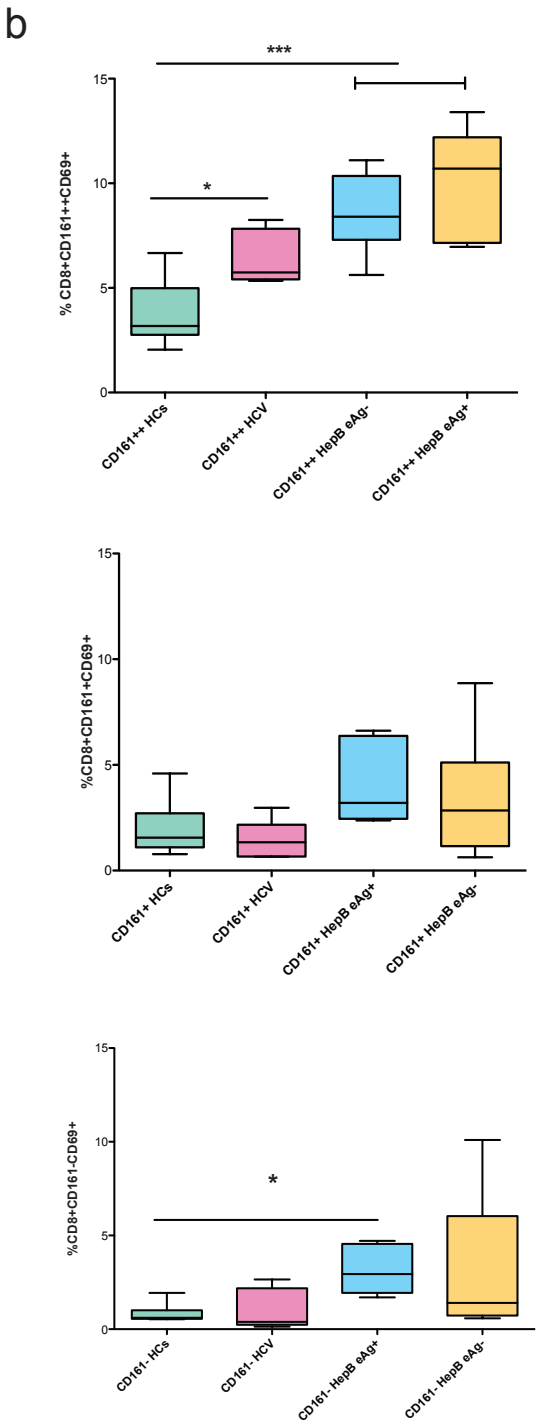
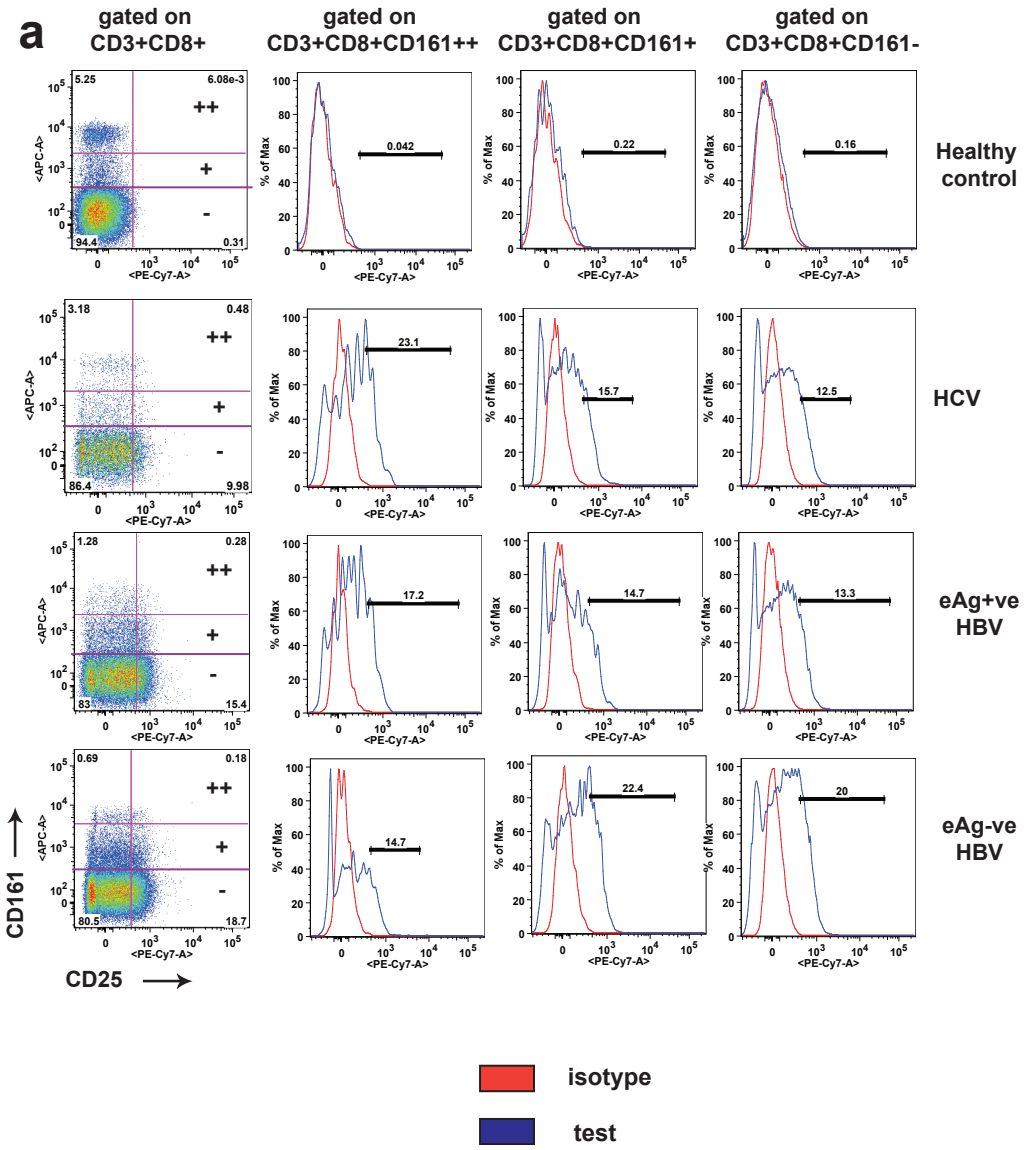


Figure 5.3. CD69 expression by CD161++, CD161+ and CD161-CD8+ PBMC T cell subsets in chronic HBV and HCV. Representative FACS plots (a) and cumulative data (b) comparing CD69 expression by the CD161++/CD161+/CD161- subsets in chronic HCV and eAg-ve/eAg+ve HBV. *p<0.05, ***p<0.0001 (one-way ANOVA).


a
gated on CD3+CD8+
gated on CD3+CD8+CD161++
gated on CD3+CD8+CD161+
gated on CD3+CD8+CD161-
Healthy control
HCV
eAg+ve HBV
eAg-ve HBV
CD161
CD25
<APC-A>
<PE-Cy7-A>
% of Max
5.25
6.08e-3
94.4
0.31
0.042
0.22
0.16
3.18
0.48
86.4
9.98
23.1
15.7
12.5
1.28
0.28
83
15.4
17.2
14.7
13.3
0.69
0.18
80.5
18.7
14.7
22.4
20
isotype
test

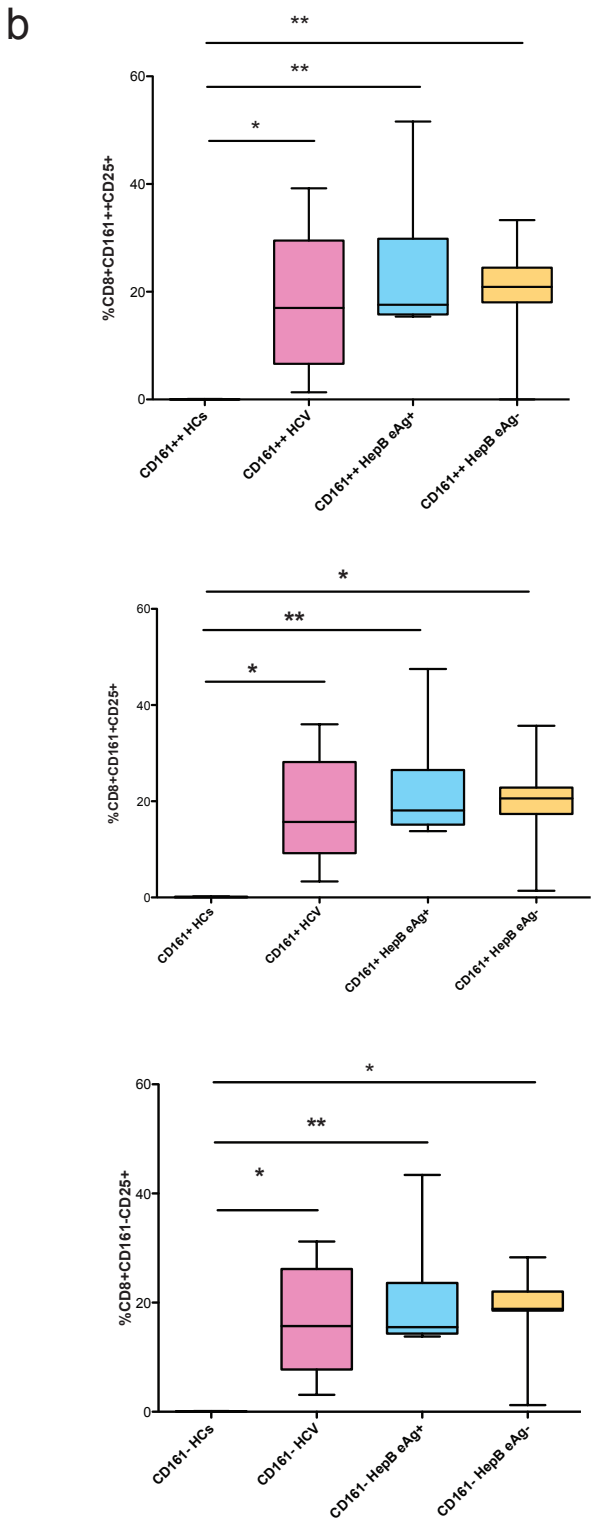
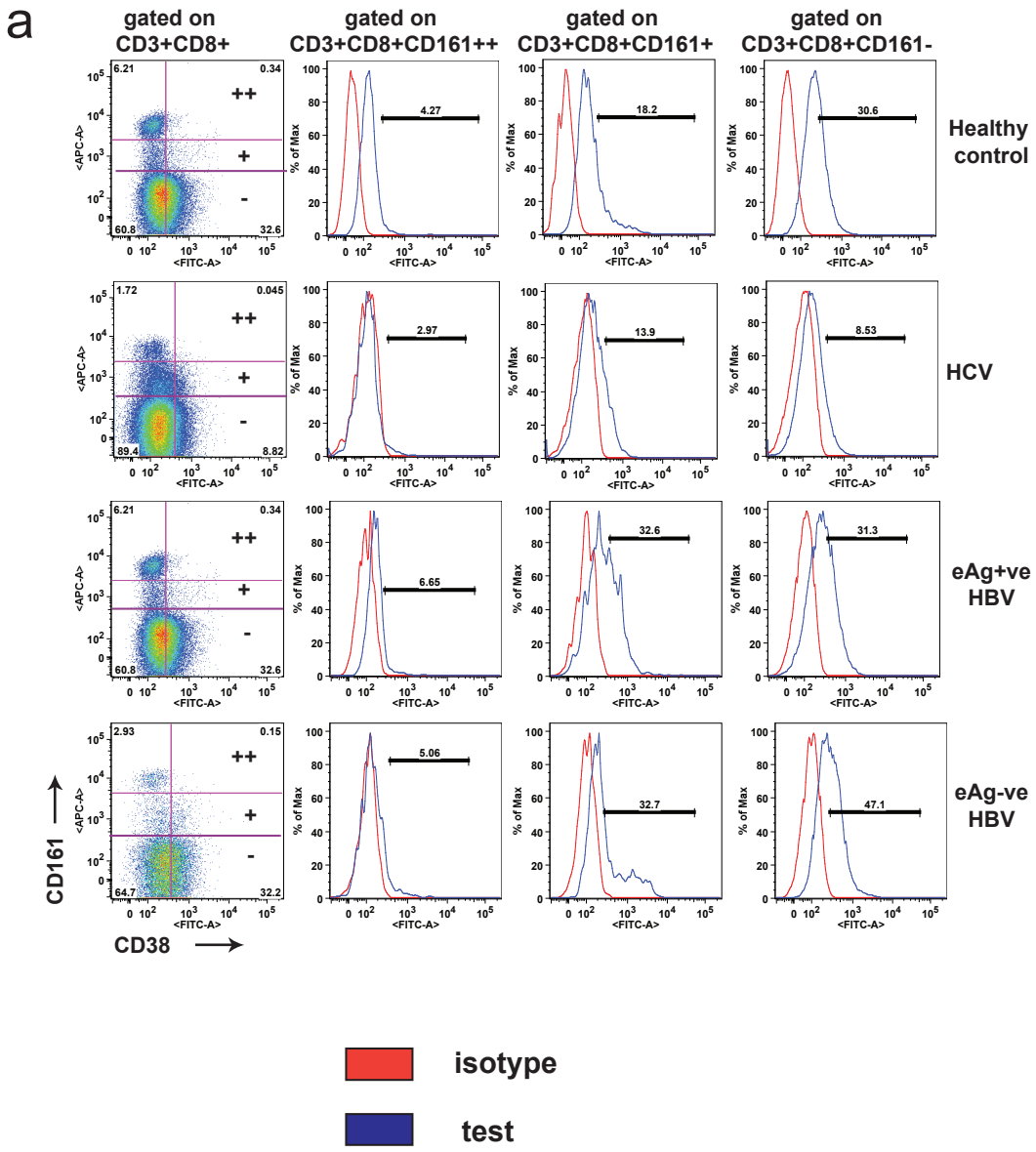


Figure 5.4. CD25 expression by CD161++, CD161+ and CD161- T cells subsets in chronic HBV and HCV. Representative FACS plots (a) and cumulative data (b) comparing CD25 expression by the CD161++/CD161+/CD161- subsets in chronic HCV and eAg-ve/eAg+ve HBV. *p<0.05,**p<0.001 (one way ANOVA).


a
gated on CD3+CD8+
gated on CD3+CD8+CD161++
gated on CD3+CD8+CD161+
gated on CD3+CD8+CD161-
Healthy control
HCV
eAg+ve HBV
eAg-ve HBV
CD161
CD38
<APC-A>
<FITC-A>
% of Max
6.21
0.34
60.8
32.6
4.27
18.2
30.6
1.72
0.045
89.4
8.82
2.97
13.9
8.53
6.21
0.34
60.8
32.6
6.65
32.6
31.3
2.93
0.15
64.7
32.2
5.06
32.7
47.1
isotype
test

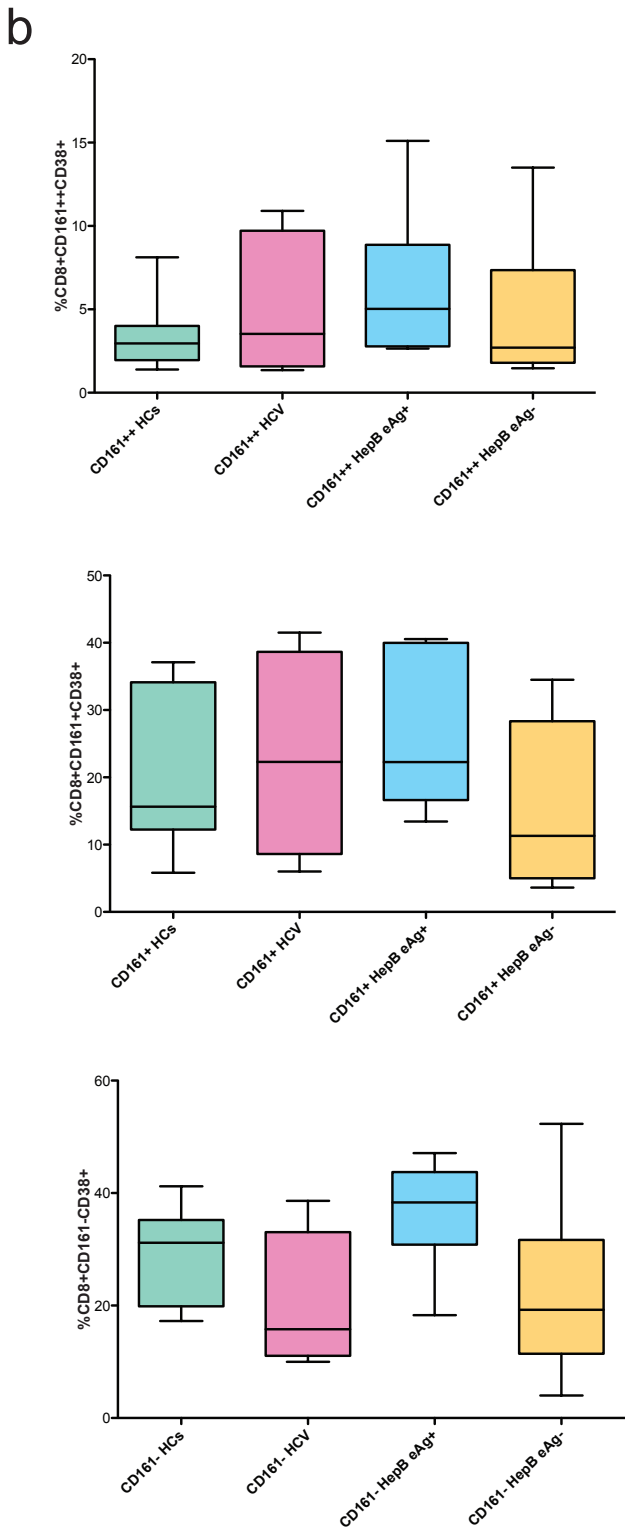
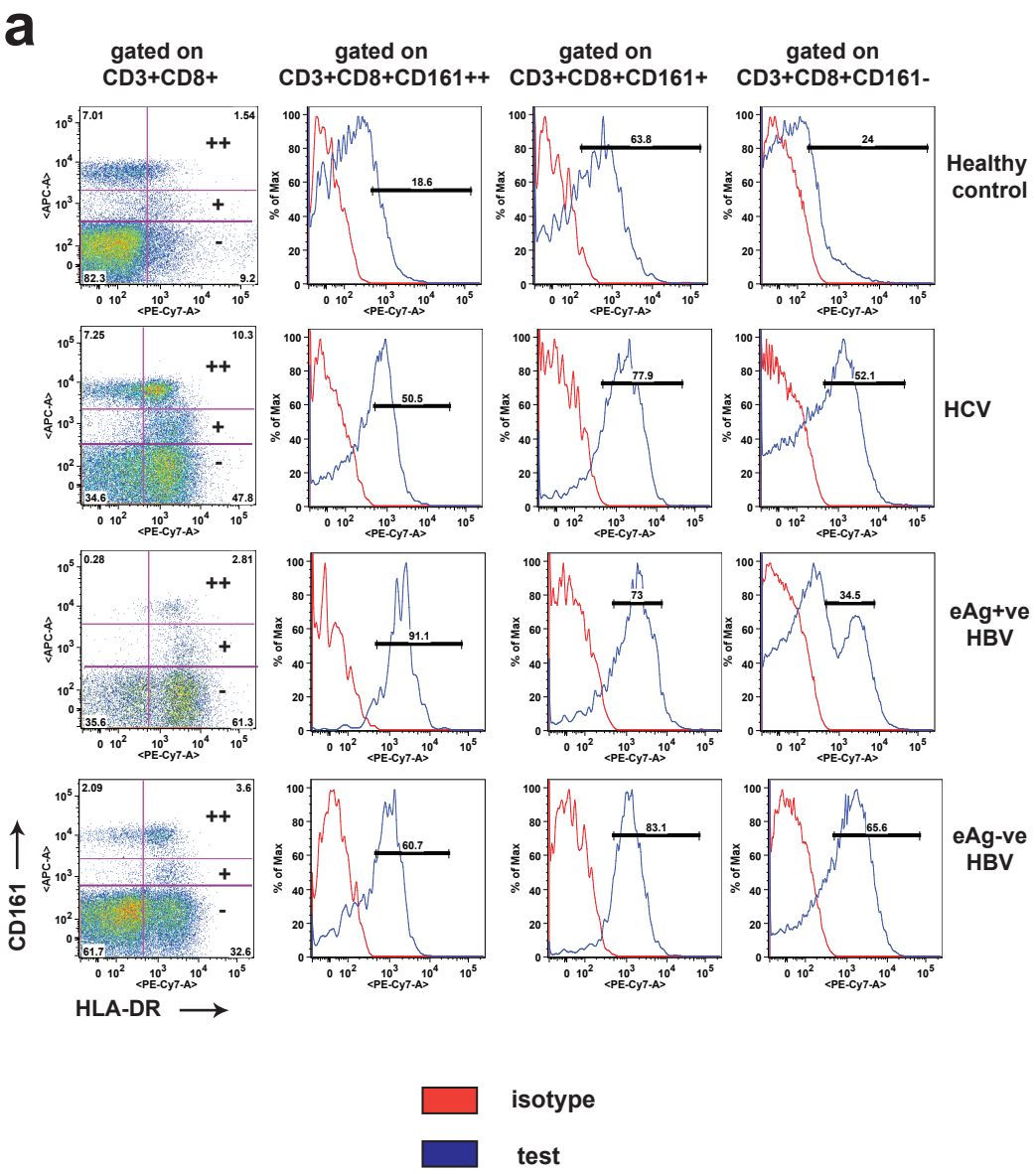


Figure 5.5. CD38 expression by CD161++, CD161+ and CD161- T cell subsets in chronic HBV and HCV. Representative FACS plots (a) and cumulative data (b) comparing CD38 expression by the CD161++/CD161+/CD161- subsets in chronic HCV and eAg-ve/eAg+ve HBV.


a
gated on CD3+CD8+
gated on CD3+CD8+CD161++
gated on CD3+CD8+CD161+
gated on CD3+CD8+CD161-
Healthy control
HCV
eAg+ve HBV
eAg-ve HBV
CD161
HLA-DR
<APC-A>
<PE-Cy7-A>
% of Max
7.01
1.54
82.3
9.2
18.6
63.8
24
7.25
10.3
34.6
47.8
50.5
77.9
52.1
0.28
2.81
35.6
61.3
91.1
73
34.5
2.09
3.6
61.7
32.6
60.7
83.1
65.6
isotype
test

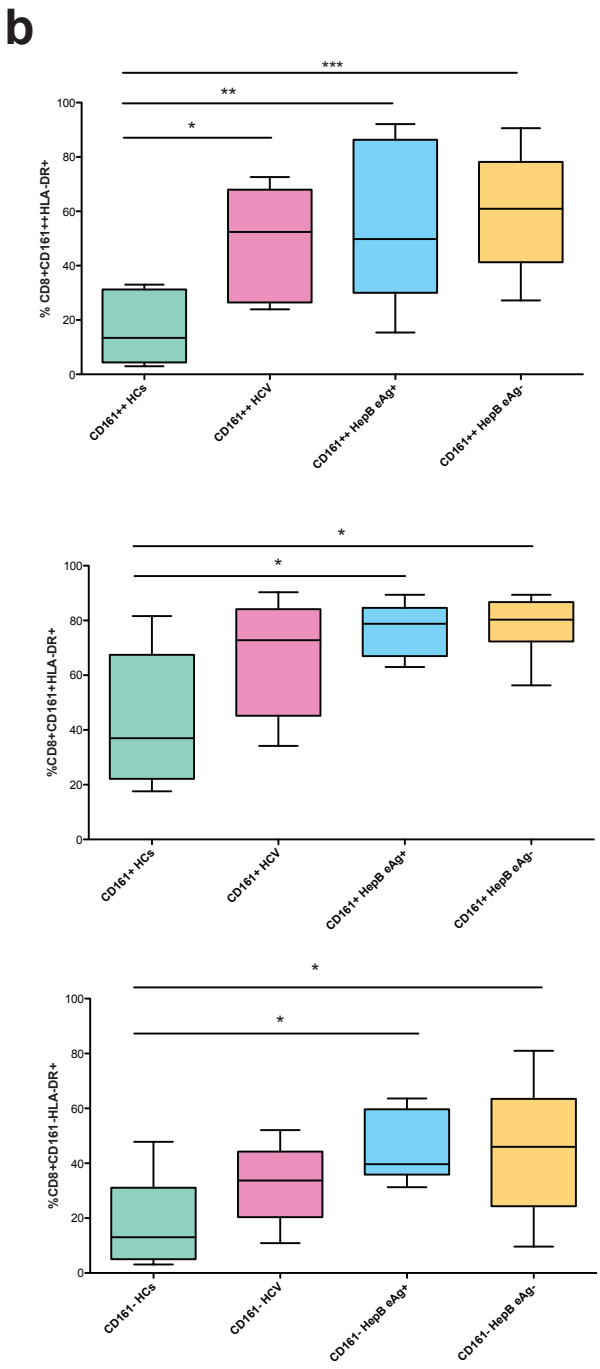
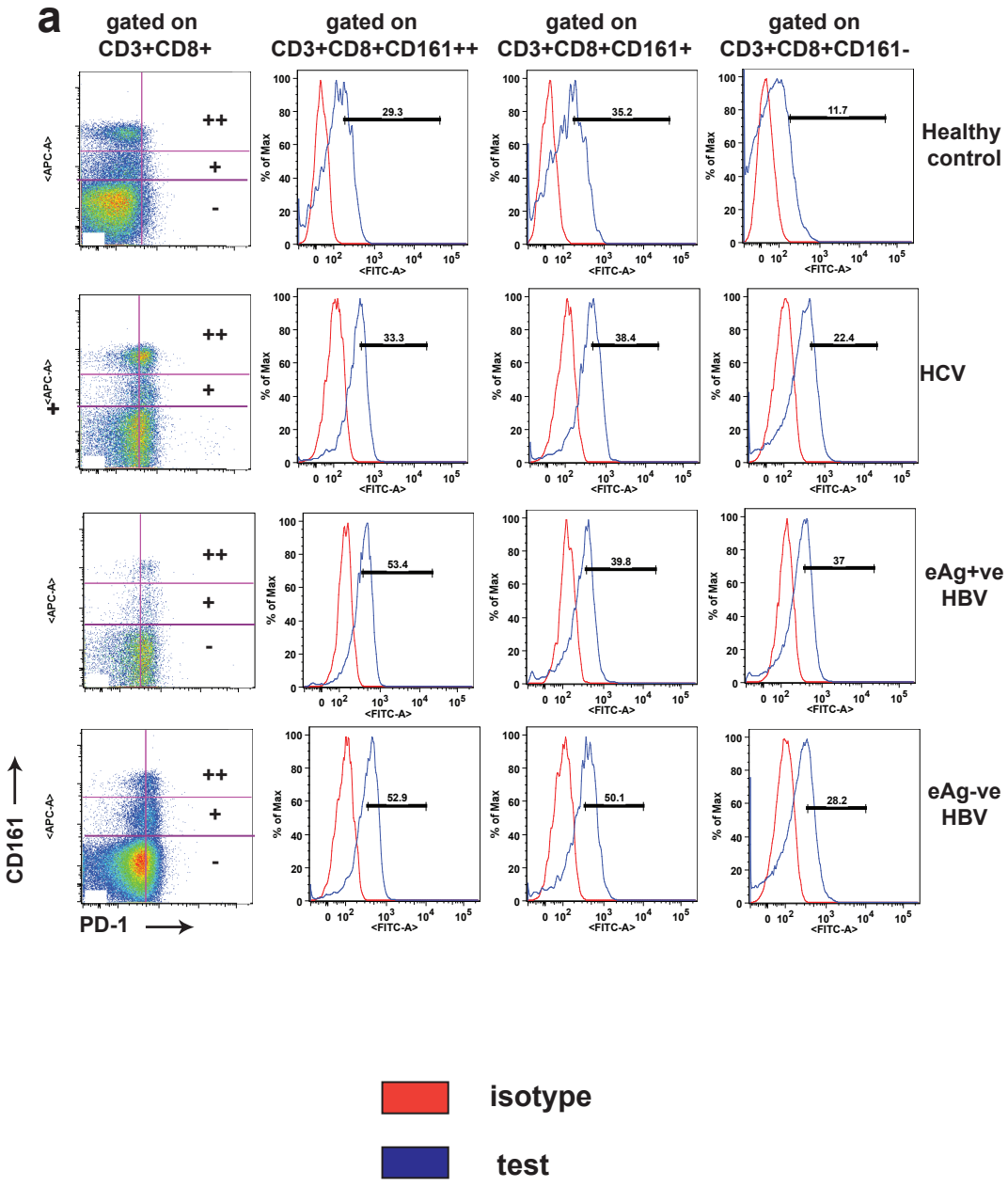


Figure 5.6. HLA-DR expression by CD161++, CD161+ and CD161- CD8+ T cells subsets in chronic HBV and HCV. Representative FACS plots (a) and cumulative data (b) comparing HLA-DR expression by CD161++/CD161+/CD161- CD8+ T cell subsets in chronic HCV and eAg+ve/eAg-ve HBV. *p<0.05, **p<0.001, ***p<0.0001 (one way ANOVA).


a
gated on CD3+CD8+
gated on CD3+CD8+CD161++
gated on CD3+CD8+CD161+
gated on CD3+CD8+CD161-
Healthy control
HCV
eAg+ve HBV
eAg-ve HBV
CD161
PD-1
<APC-A>
<FITC-A>
% of Max
29.3
35.2
11.7
33.3
38.4
22.4
53.4
39.8
37
52.9
50.1
28.2
isotype
test

b

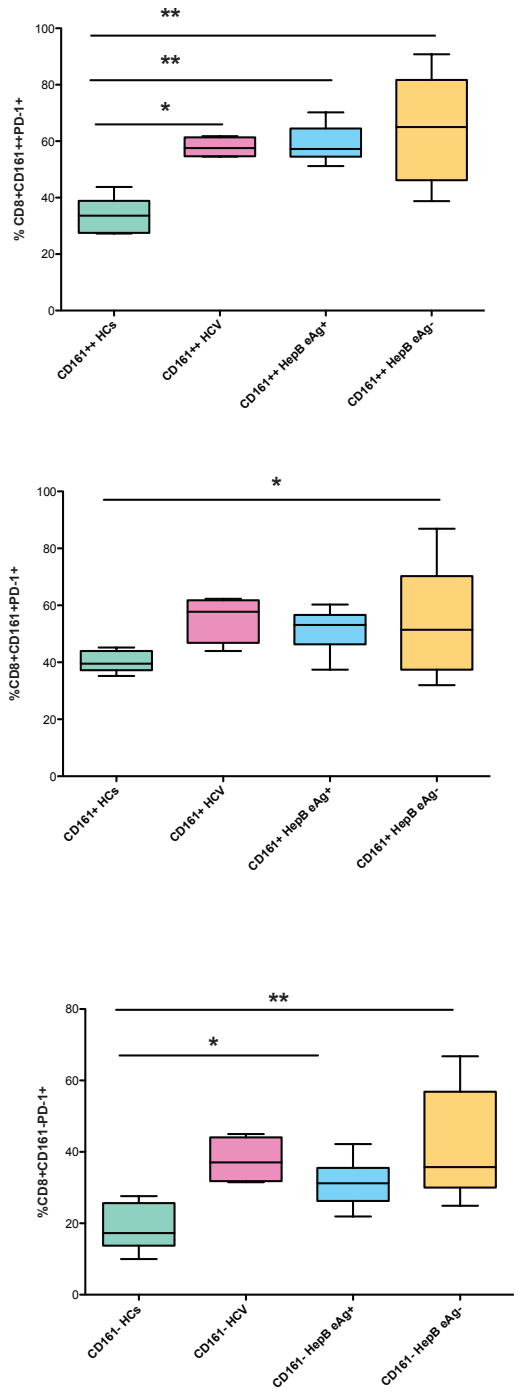
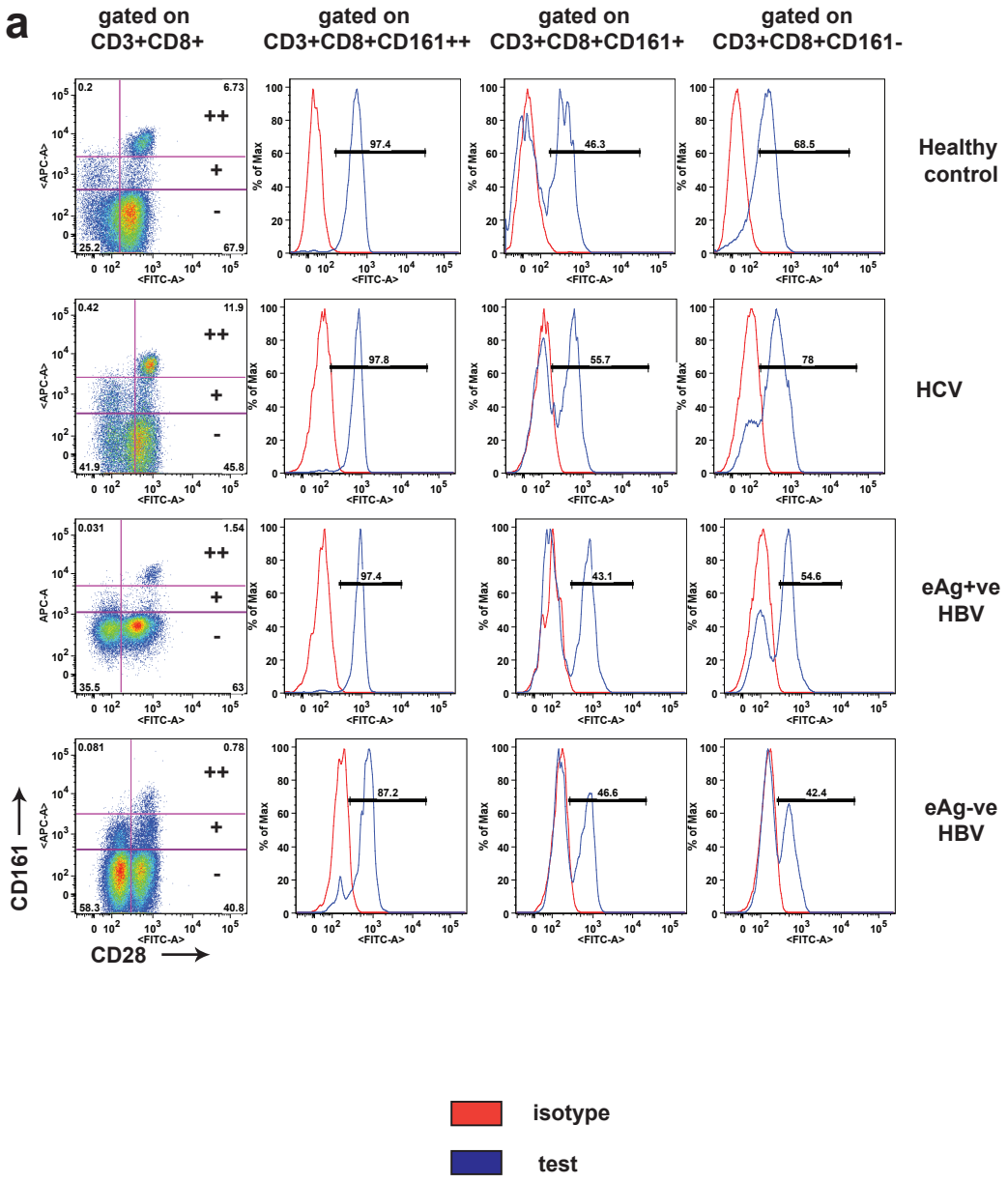


Figure 5.7. PD-1 expression by CD161++, CD161+ and CD161- CD8+ T cell subsets in chronic HBV and HCV. Representative FACS plots (a) and cumulative data (b) comparing PD-1 expression by CD161++/CD161+/CD161- CD8+ T cell subsets in chronic HBV and HCV.*p<0.05, **p<0.001 (one way ANOVA).


a
gated on CD3+CD8+
gated on CD3+CD8+CD161++
gated on CD3+CD8+CD161+
gated on CD3+CD8+CD161-
Healthy control
HCV
eAg+ve HBV
eAg-ve HBV
CD161
CD28
<APC-A>
<FITC-A>
% of Max
0.2
6.73
25.2
67.9
97.4
46.3
68.5
0.42
11.9
41.9
45.8
97.8
55.7
78
0.031
1.54
35.5
63
97.4
43.1
54.6
0.081
0.78
58.3
40.8
87.2
46.6
42.4
isotype
test

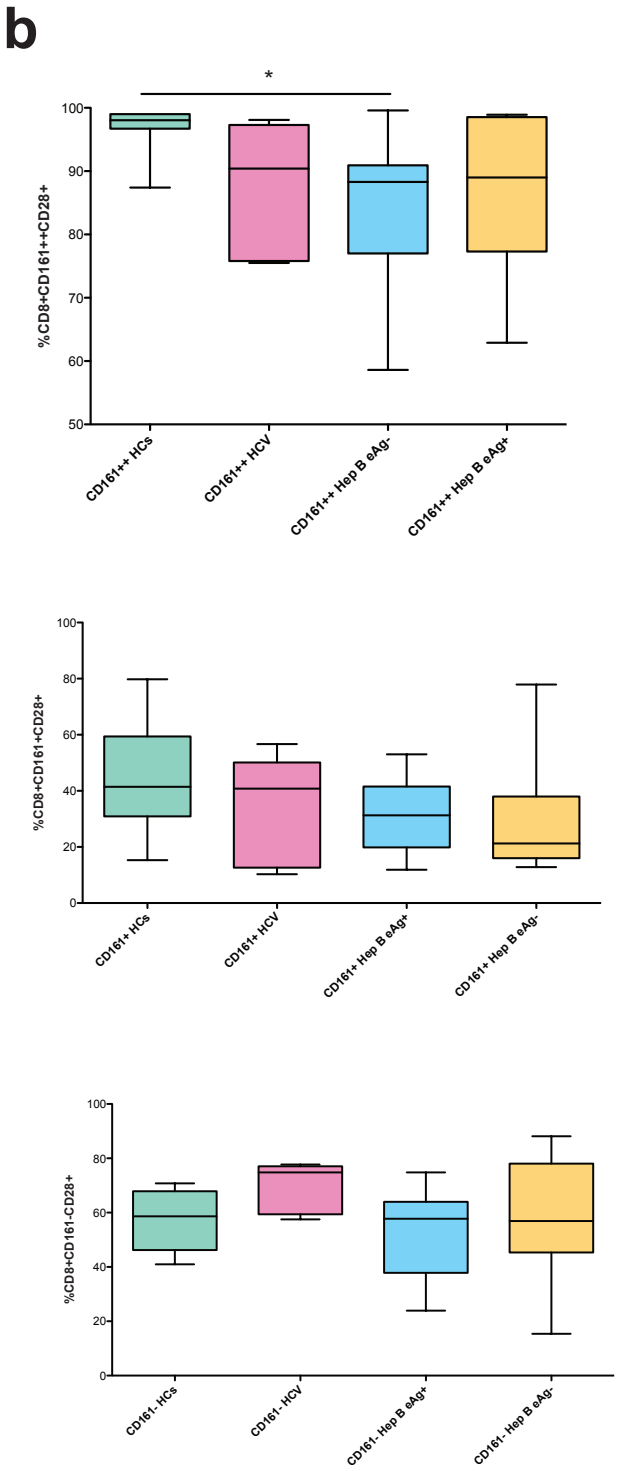
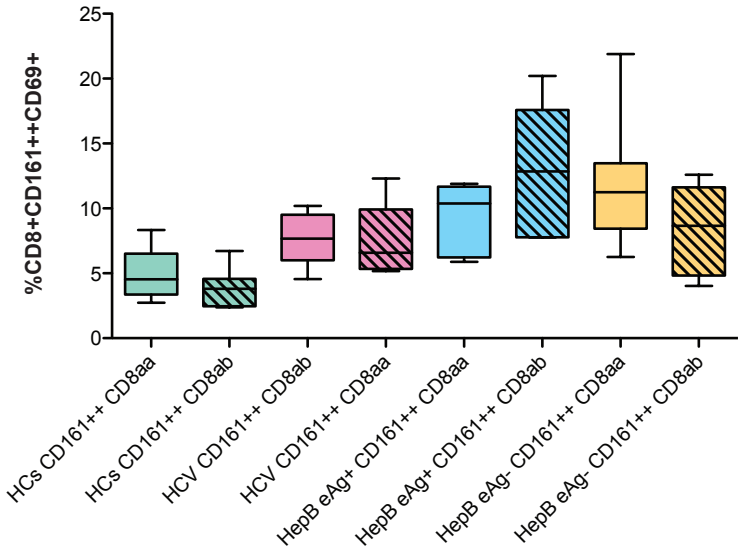
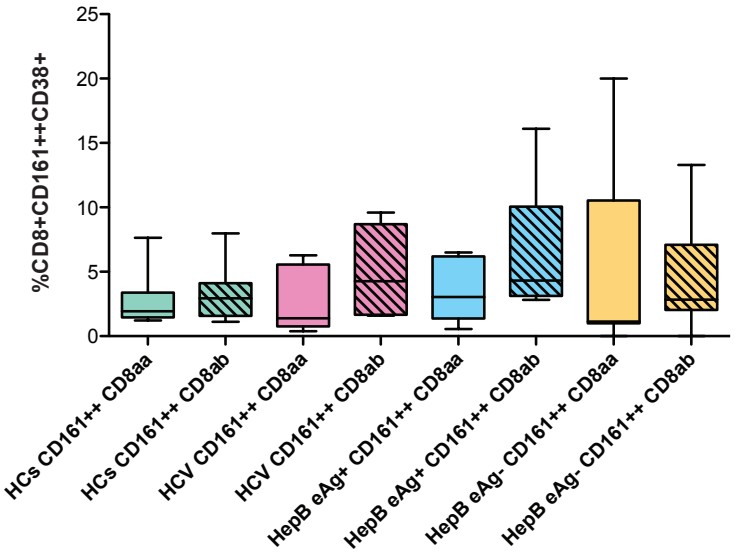
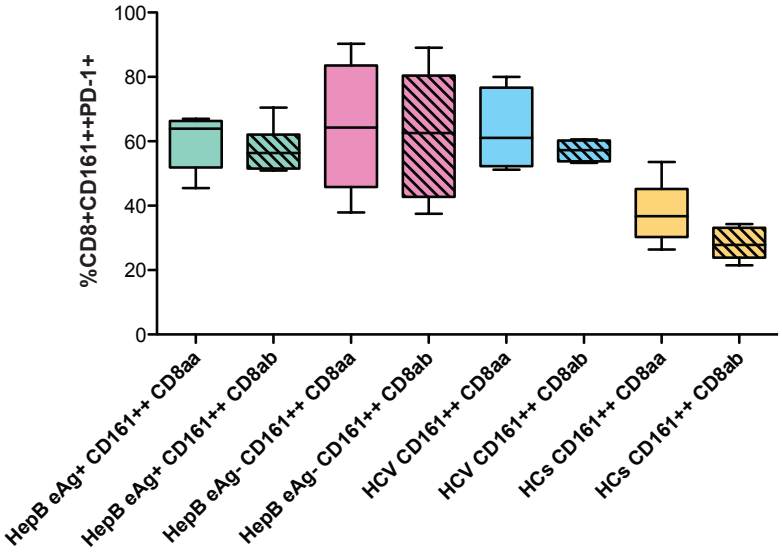


Figure 5.8. CD28 expression by CD161++, CD161+ and CD161- CD8 T cell subsets in chronic HBV and HCV. Representative FACS plots (a) and cumulative data (b) comparing expression of CD28 by CD161++/CD161+/CD161- CD8 T cell subsets in chronic HCV and HBV.*p<0.05 (one way ANOVA).


%CD8+CD161++CD69+
25
20
15
10
5
0
HCs CD161++ CD8aa
HCs CD161++ CD8ab
HCV CD161++ CD8ab
HCV CD161++ CD8aa
HepB eAg+ CD161++ CD8aa
HepB eAg+ CD161++ CD8ab
HepB eAg- CD161++ CD8aa
HepB eAg- CD161++ CD8ab


%CD8+CD161++CD38+
25
20
15
10
5
0
HCs CD161++ CD8aa
HCs CD161++ CD8ab
HCV CD161++ CD8aa
HCV CD161++ CD8ab
HepB eAg+ CD161++ CD8aa
HepB eAg+ CD161++ CD8ab
HepB eAg- CD161++ CD8aa
HepB eAg- CD161++ CD8ab


%CD8+CD161++PD-1+
100
80
60
40
20
0
HepB eAg+ CD161++ CD8aa
HepB eAg+ CD161++ CD8ab
HepB eAg- CD161++ CD8aa
HepB eAg- CD161++ CD8ab
HCV CD161++ CD8aa
HCV CD161++ CD8ab
HCs CD161++ CD8aa
HCs CD161++ CD8ab

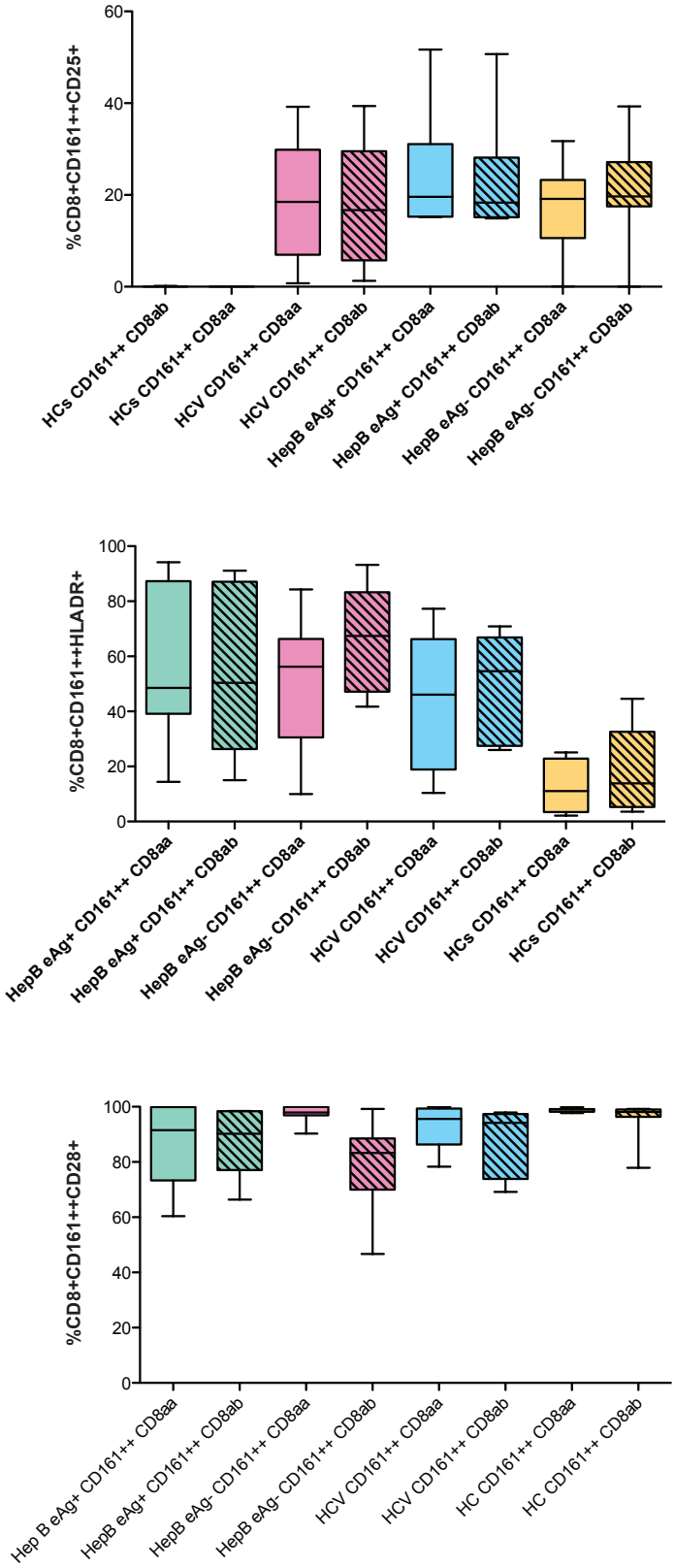


Figure 5.9. No difference in activation/ exhaustion marker expression between CD161++CD8αα and CD8αβ T cells. Cumulative data comparing activation/ exhaustion marker (CD69, CD25, CD38, HLA-DR, PD-1, CD28) expression between CD161++CD8αα and CD8αβ cells.

No difference in terms of activation/exhaustion marker expression between CD161++CD8αα and CD8αβ cells **(Figure 5.9**) is demonstrated, in keeping with the findings of chapter 4 of this thesis which demonstrates little difference between the two subsets in terms of phenotype, function, location and gene expression profiles.

In chronic HCV the CD161++CD8+ T cell subset, as in healthy controls, predominantly use Vβ 2 and 13.2 (**Figure 5.10**). Non-expansion of other Vβ usage in HCV is in keeping with likely continued restriction by MR1.

5.4.3 Patients with chronic HBV have a prominent CD161-CD8β^{low} population.

In analyzing the CD8αα/CD8αβ populations in the different disease groups, it was observed that in chronic HBV a prominent population of cells have reduced expression of CD8β. This is observed in the CD161+ and CD161- CD8+ T cell populations, regardless of eAg status, but only reached statistical significance in the CD161-CD8+ T subset (**Figure 5.11**). Bulk functional changes in the CD8 T cell population in chronic HBV have previously been described, with significant down regulation of CD28 associated with impaired IL-2 production (Das, Hoare et al. 2008).

I further investigated the relationship of CD8β down regulation to CD28 expression along with other activation/exhaustion markers (**Figure 5.12**). The findings were striking in that the CD161-CD8β^{low} population was associated with significantly increased expression of HLA-DR (**Figure 5.12e**) and

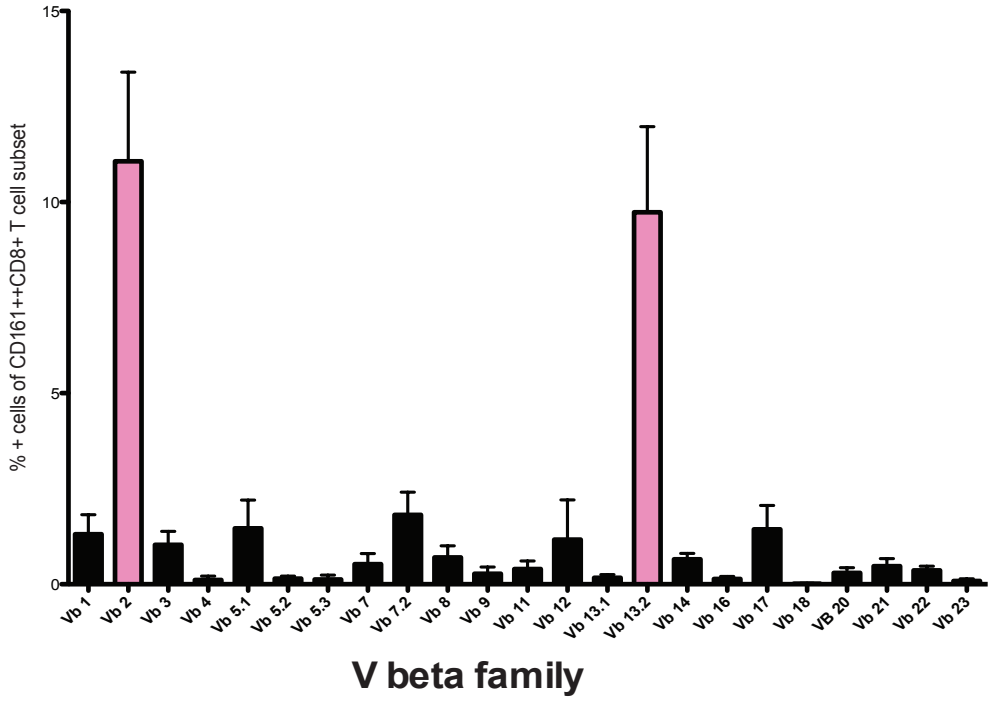


Figure 5.10. TCR Vβ usage of CD161++CD8+ T cell subset in chronic HCV. Cumulative data demonstrating predominant Vβ 2 and 13.2 usage by CD161++CD8+T cells in patients with chronic HCV. Pink bars indicatate significant difference from other TCR Vβ families except 2/13.2 $p<0.0001$ (one way ANOVA).

significantly reduced expression of CD28 (**Figure 5.12f**). This was observed in patients with both eAg-ve and eAg+ve HBV.

5.4.4 CD161-CD8β^{low} cells in chronic HBV produce greater amounts of IFN-γ than CD161-CD8β^{high} cells.

The functional status of the CD161-CD8β^{low} population was investigated by performing intracellular cytokine staining on cryopreserved PBMCs from patients with chronic HBV. I found no difference in IL-2 production between the CD161-CD8β^{high} and CD8β^{low} population, as previously described (Das, Hoare et al. 2008). However, a large difference in terms of IFN–γ production

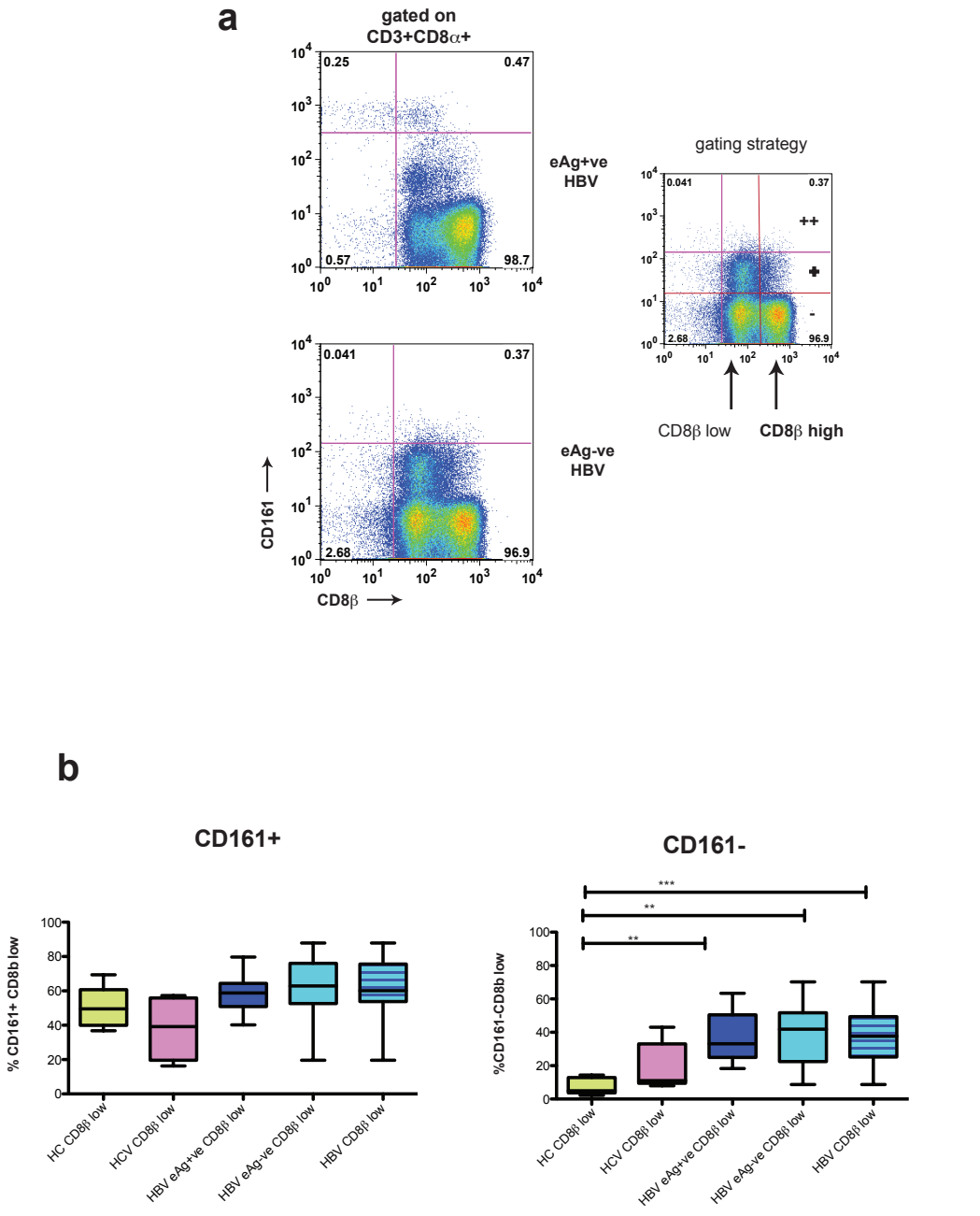
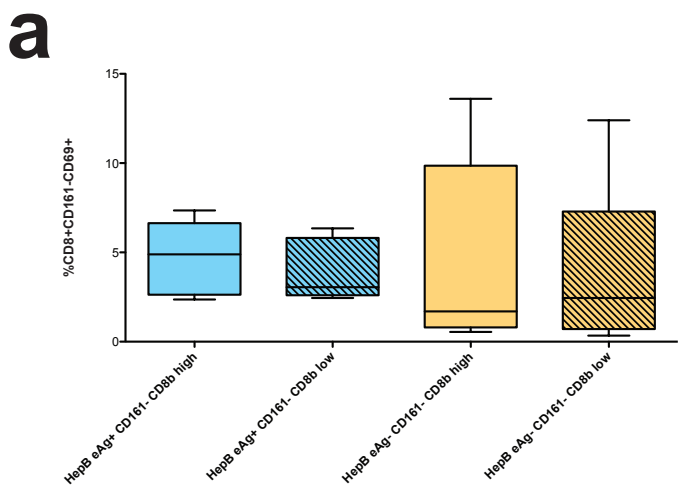
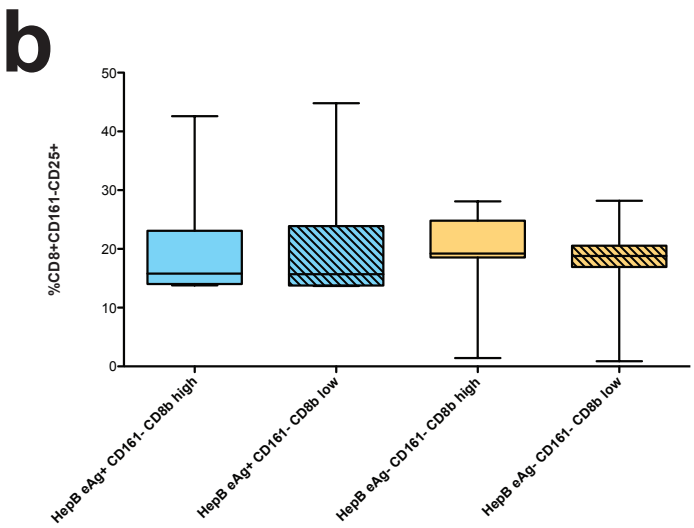
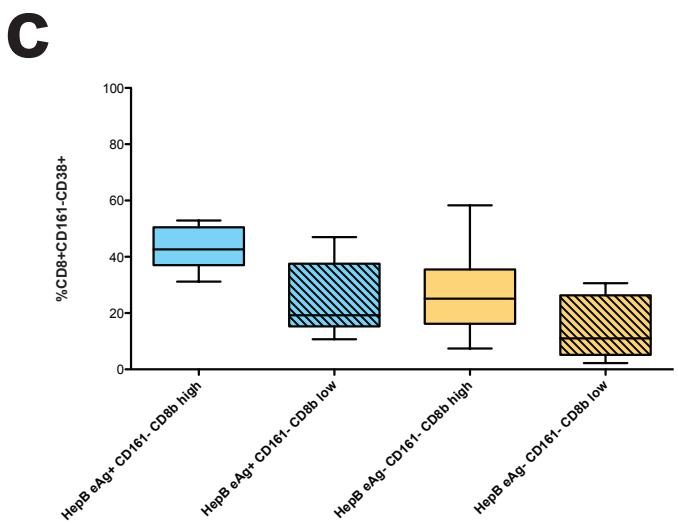


Figure 5.11. Prominent CD161-CD8β^{low} population identified in patients with chronic HBV. Representative FACS plots (a) and cumulative data (b) demonstrating that in chronic eAg+ve and eAg-ve HBV there is significant down regulation of CD8β on CD161-CD8+ T cells. **p<0.001, ***p<0.0001 (one way ANOVA).


a
%CD8+CD161-CD69+
15
10
5
0
HepB eAg+ CD161- CD8b high
HepB eAg+ CD161- CD8b low
HepB eAg- CD161- CD8b high
HepB eAg- CD161- CD8b low


b
%CD8+CD161-CD25+
50
40
30
20
10
0
HepB eAg+ CD161- CD8b high
HepB eAg+ CD161- CD8b low
HepB eAg- CD161- CD8b high
HepB eAg- CD161- CD8b low


c
%CD8+CD161-CD38+
100
80
60
40
20
0
HepB eAg+ CD161- CD8b high
HepB eAg+ CD161- CD8b low
HepB eAg- CD161- CD8b high
HepB eAg- CD161- CD8b low

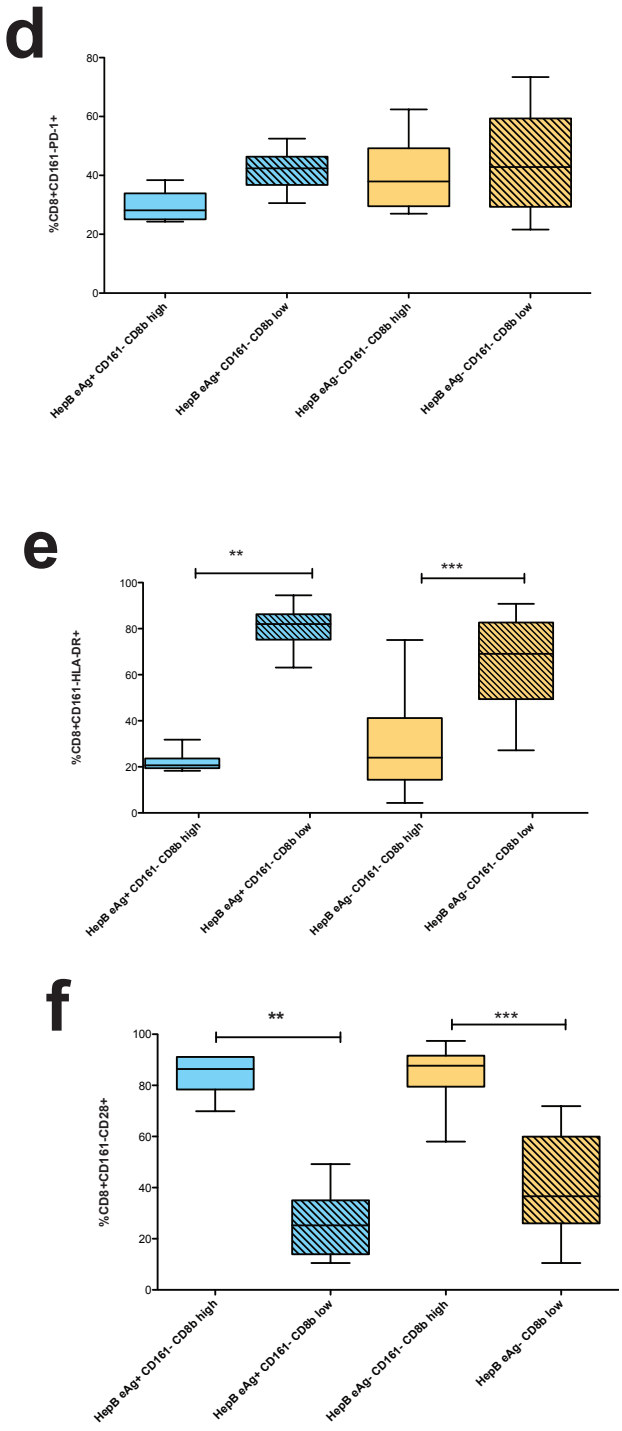


Figure 5.12. CD161-CD8αβ low T cells express high levels of HLA-DR and low levels of CD28 in chronic HBV. Cumulative data comparing activation/exhaustion marker expression (CD69, CD25, CD38, HLA-DR, PD-1 and CD28) between CD161-CD8β high and CD8β^{low} T cells in chronic HBV. (e) **p=0.0022 , ***p=0.009 (f) **p=0.005, ***p= 0.0001. (Mann Whitney test).

was observed between the two populations, with the CD161-CD8β^{low} population producing significantly more IFN-γ than the CD161-CD8β^{high} population (62.05% vs 12.4% respectively) (**Figure 5.13**).

5.4.5 CD8β down-regulation does not correlate with e antigen status, ALT or viral load.

In order to determine whether CD8β down-regulation was related to disease status in patients with chronic hepatitis B, we analysed the relationship of this to the markers of disease activity used in clinical practice; ALT, viral load and eAg status. In our sample pool, I was unable to find a correlation between the proportion of CD161-CD8+ T cells being CD8β^{low} and disease status (**Figure 5.14**).

5.4.6 CD8β is readily down regulated on CD161-CD8+ T cells in culture.

I investigated factors that may be involved in down-regulation of CD8β *in vivo* by comparing the effect of culture with R10 media alone or with anti-CD3/CD28 beads to look at the effect of TCR stimulation. It was found that in both culture conditions there is down-regulation of CD8β, which is more pronounced on the culture with beads (**Figure 5.15**). To look to see if this was a secondary effect of activation, I looked at activation and exhaustion marker expression on these cells post culture, but found no differences between CD8β^{high} and CD8β^{low} populations, although importantly failed to perform a baseline analysis for overall comparison (data not shown).

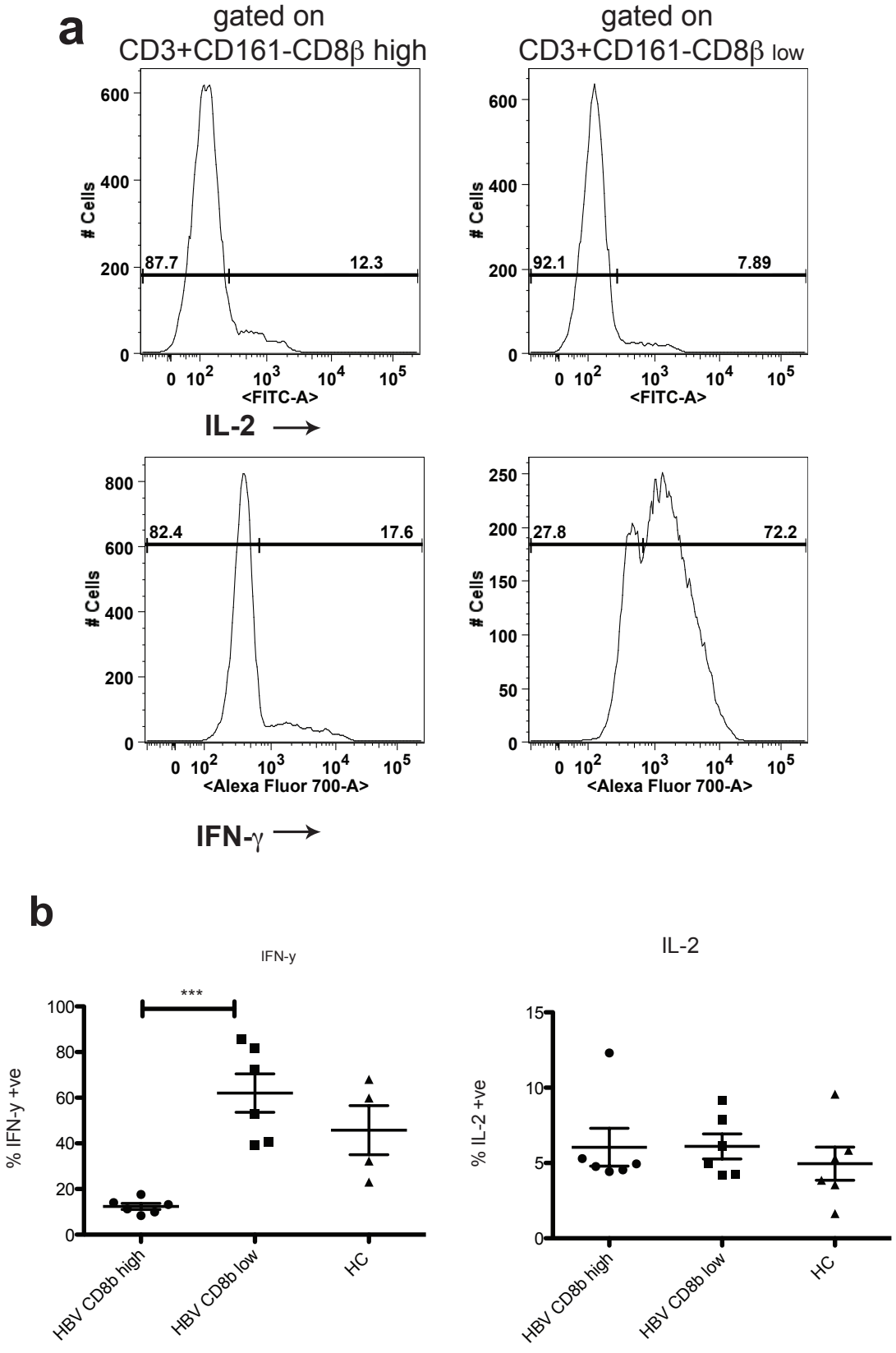


Figure 5.13. CD161-CD8β low cells from patients with chronic HBV make significantly more IFN-γ than CD161-CD8β high cells. Representative histograms (a) and cumulative data (b) comparing IL-2 and IFN-γ production between CD161-CD8β high and CD8β low cells. ***p<0.0001 (one way ANOVA).

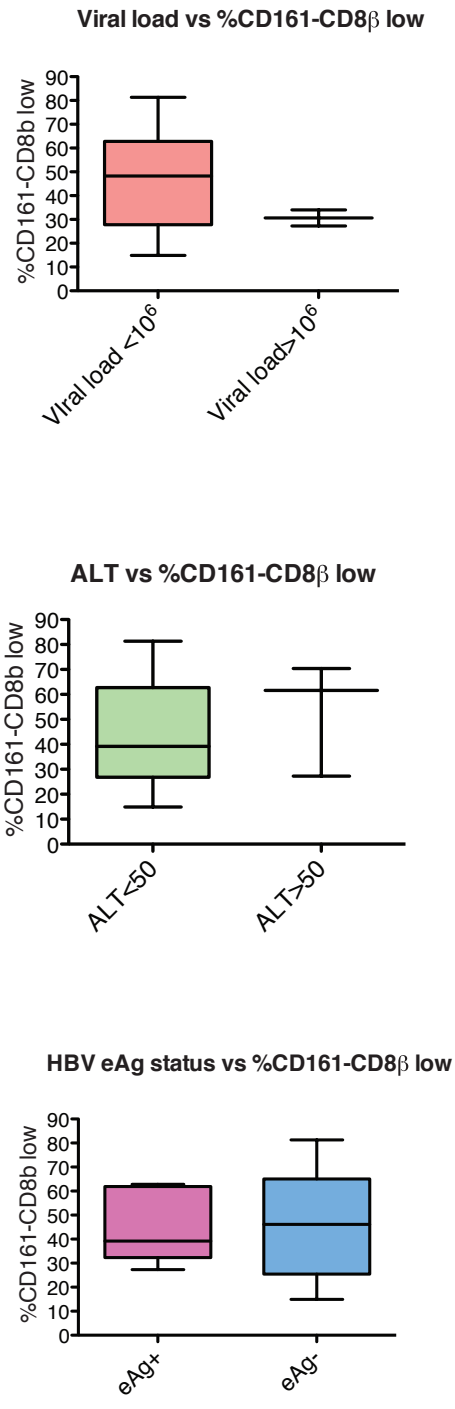


Figure 5.14. No difference between proportion of CD161-CD8β^{low} cells and disease activity in chronic HBV.

Proportion of CD161-CD8β^{low} T cells in chronic HBV to markers of disease activity viral load, ALT and e antigen status.

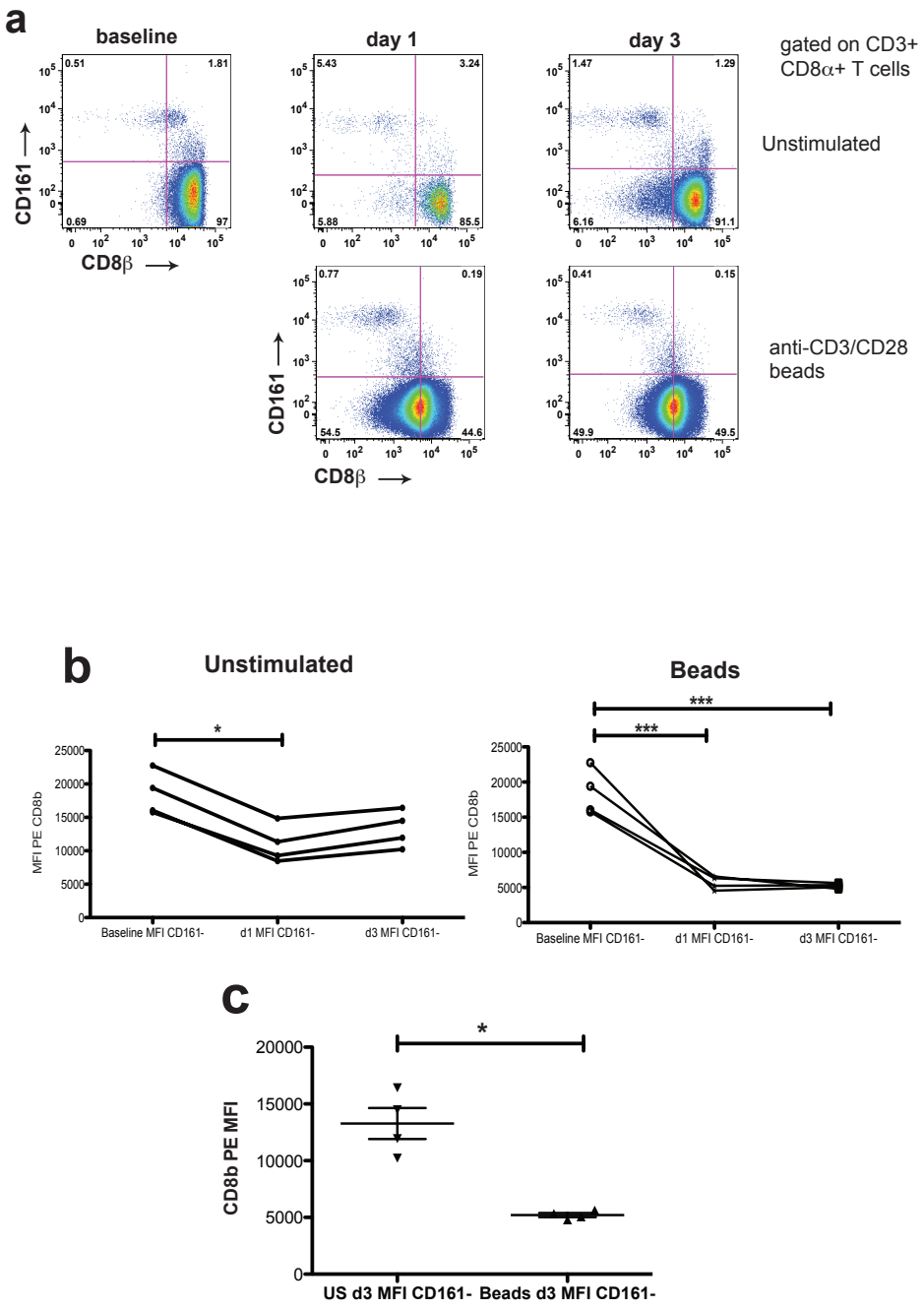


Figure 5.15. CD8β is readily down-regulated on CD8+ T cells in culture. (a) Representative FACS plots showing reduction in expression of CD8β on CD161- following initial CD8α enrichmentand CD8β positive selection at days 1 and 3 compared to baseline following intial sorting for cells cultured in media alone or with anti-CD3/CD28 beads. (b) Cumulative data showing change in CD8β PE MFI from baseline at days 1 and 3 for experiment described in (a). *p<0.05, ***p<0.0001 (oneway ANOVA). (c) Comparison of CD8β PE MFI at day 3 between cells cultured in media alone (US) and those cultured with anti-CD3/CD28 beads. *p = 0.0286 (Mann Whitney).

5.5 Discussion

Much work on defining the CD8 response to HBV and HCV has focused on the role and phenotypic/functional status of antigen-specific T cells. However, there is evidence in HBV infection to suggest that changes to the bulk CD8 T cell populations are also observed. This may be due infiltration of the liver by CD8 T cells in such infections (Maini, Boni et al. 2000) resulting in non-specific liver-related effects or bystander activation. Understanding these changes is important, as they may profoundly influence the immunological environment into which immunotherapy and vaccination is to be introduced.

In this chapter I first further explored the role of CD161++CD8+ T cells in HCV and HBV infection. Previous work has indicated that this subset is involved in intra-hepatic immunity in HCV, with a loss of CD161++CD8+ T cells demonstrated from the peripheral blood, CD161++CD8+ T cells shown to co-produce IL-17/IFN–γ on ex-vivo stimulation and the frequency of such cells to be inversely correlated with fibrosis in those patients (Billerbeck, Kang et al. 2010) (**Appendix 1**). Further to this loss of the CD161++CD8+ T cell subset from the peripheral blood in HBV and relative enrichment of both CD161++CD8$\alpha\beta$ and CD8$\alpha\alpha$ cells in HCV, using paired blood and liver samples, was demonstrated.

Using a panel of activation/exhaustion markers it was shown the CD161++CD8+ T cell subset in HCV/ HBV express higher levels of CD69, CD25, HLA-DR and PD-1 compared to healthy controls suggesting cells within the subset to be in a range of activation/exhaustion states. In

comparing activation states between HCV and eAg+ve and eAg-ve HBV, it seems that there was consistently significantly greater up-regulation in HBV compared to HCV and only a difference between eAg+ve and eAg-ve disease seen for HLA-DR expression. In comparing expression of these markers between CD161++CD8αα and CD8αβ cells, no difference was seen in any disease group. This is in keeping with data presented in chapter 4, which indicates a common function, phenotype, differentiation pathways and tissue location for these cells.

Ex-vivo determination of differential intra-hepatic function of the CD161++CD8αα and CD8αβ subsets in both health and disease is important and requires further work. Certainly I have been unable to study phenotypic or cytokine production profiles here due to difficulties with access to appropriate tissue samples. CD161++CD8+ T cells likely fulfill an innate-like functional niche and help to orchestrate the immune response. Differential expression of IL-22 over IL-17 or IFN-γ may occur in certain settings or by CD161++CD8αα vs CD8αβ cells for example, and be associated with a preferential as opposed to a progressive disease outcome, although our data so far would not suggest this (Billerbeck, Kang et al. 2010) (**Appendix 1**). Alternatively, CD8αα expression, acting as a co-repressor rather than a co-receptor, may impose a greater threshold to activation of the subsets that may be important in addition to the other tolerising mechanisms of the liver.

No difference was observed in the TCR usage of the CD161++CD8+ T cell subset in chronic HCV infection compared to healthy controls, indicating that

MR1 restriction in this setting is preserved. MAIT cells are activated *in vitro* following co-culture with both bacteria and fungus exposed monocyte-derived dendritic cells, however, a similar effect was not demonstrated for a number of viruses (Le Bourhis, Martin et al. 2010). Similar experiments have not been performed for HCV or HBV, and it would be interesting to investigate up-regulation of MR1 on infected hepatocytes and their ability to activate CD161++CD8+ T cells *in vitro*.

Activation/exhaustion marker expression was not exclusive to the CD161++CD8+ T cell subset. Increased expression of CD25 was observed on both CD161+ and CD161- subsets across HCV and HBV disease groups. Increased expression of HLA-DR was observed only in HBV in both CD161+ and CD161- subsets, and was the same for both eAg+ve and eAg-ve disease. PD-1 expression was increased in eAg-ve HBV in the CD161+ and CD161- subsets but only in the CD161- subset in eAg+ve disease. This would suggest activation the CD161+ and CD161- CD8+ T cell populations in HBV, with greater exhaustion observed in eAg-ve compared to eAg+ve disease. Such phenomenon have previously been described for bulk CD8 T cells in HBV for PD-1 expression (Ye, Weng et al. 2008) and in HCV for PD-1 and HLA-DR (Shen, Zheng et al. 2010), although I have been unable to replicate this here in HCV.

In addition to changes in activation marker expression, I observed a marked down-regulation of CD8β on CD161-CD8+ T cells in both eAg-ve and eAg+ve HBV, but not HCV (suggesting that this is a not necessarily a liver-specific

effect) compared to healthy controls. This correlated with significant up-regulation of HLA-DR, down-regulation of CD28 and an enhanced capacity to produce IFN-γ on stimulation with PMA and ionomycin. Previous study of the global CD8 population in chronic HBV found peripheral and intra-hepatic CD8 T cells from patients with chronic HBV had preserved IFN-γ, but impaired IL-2 production, and to proliferate poorly following TCR stimulation. CD3ζ and CD28 was also found to be down-regulated and that this was more marked in the hepatic compartment (Das, Hoare et al. 2008).

CD28-CD8+ T cells are a well-described phenomenon of the aging immune system in primates. In cord blood virtually all T cells express the co-receptor CD28, however by the time an individual is >80 years old approximately 50-60% of their CD8 T cells have lost CD28 expression. These cells are memory cells *in vivo*, but can be derived from naïve cells *in vitro* by antigenic stimulation. Enhanced loss of CD28 on co-exposure to IL-2, IL-17, IL-15 , type 1 interferons and TNF-α would suggest that both homeostatic maintenance of memory populations and persistent inflammation/infection might be responsible for driving their accumulation. In keeping with this hypothesis, in older people the CD28-CD8+ T cell subset has a reduced diversity of TCR usage (Azuma, Phillips et al. 1993), and a large proportion of these cells are specific for the chronic viral infections cytomegalovirus (CMV) and Epstein-Barr virus (EBV). Such loss of T cell diversity is associated with impaired immune function in the elderly. This may be associated with reduced capacity within the CD8+ T cell pool to deal with new pathogens, but other mechanisms might also be at play. In vaccination studies the frequency of

CD28-CD8+ T cells was found to be a good predictor of a poor humoral response to the influenza vaccine (Fann, Chiu et al. 2005). This indicates a possible wider immunomodulatory effect, supported by data from pigs suggesting CD28-CD8+ T cells were able to tolerize dendritic cells and suppress CD4 T cell responses (Ciubotariu, Colovai et al. 1998).

Microarray studies have allowed the study of differential gene expression by CD28+ and CD28- T cell subsets. These have highlighted differences in gene expression including CD28- T cells demonstrating down-regulation of other co-stimulatory receptors, ICOS and CTLA-4, up-regulation of a number of both activatory and inhibitory NK receptors, changes in cytokine, chemokine and chemokine receptor expression (enhanced expression of IL12A, CCL4, CX3CR1 and reduced expression of IL3, IL-23A, IL12Rβ2, CCR6 and CCR7) and an increase in effector molecule (perforin, granzyme B and H) expression. Functionally loss of CD28 expression is associated with reduced proliferative response to stimulation, defective IL-2 and IFN-γ production, decreased ability to up-regulate telomerase after activation and resistance to apoptosis (Weng, Akbar et al. 2009).

In addition to aging, CD3ζ/CD28 down regulation is also a feature described in a number diseases characterized by chronic inflammation and antigen persistence, including malignancy (Nakagomi, Petersson et al. 1993), infection (Trimble and Lieberman 1998) and autoimmunity (Krishnan, Kiang et al. 2005). It has also been observed in acute viral infection with

gastroenteritis, Epstein-Barr and cytomegalovirus (Trimble, Kam et al. 2000), where CD3ζ-CD28- cells also expressed high levels of HLA-DR. In acute viral infection the CD3ζ-/CD28- cells had impaired IL-2 production, a preserved ability to make IFN-γ, as in HBV, and required overnight culture with IL-2 to become cytotoxic, despite being perforin/ granzyme B positive when stained directly *ex-vivo*. This would suggest that the CD3ζ/ CD28 down-regulation occurs as an immuno-modulatory mechanism, preventing uncontrolled T cell proliferation, whilst maintaining anti-viral function. The fact that this is observed in a number of different settings would also indicate that it is a normal mechanism of regulation of T cell responses and not a disease specific anomaly.

These data demonstrate that a CD28-CD8β^{low} population is expanded in chronic HBV and likely analogous to the CD28-CD3ζ^{low} population previously described (Das, Hoare et al. 2008). CD28-CD8β^{low} T cells are also a distinct T cell subset in healthy controls (Werwitzke, Tiede et al. 2003) and an expansion in this population has also been observed in systemic lupus erthematosus, correlating with disease activity (Werwitzke, Tiede et al. 2008). CD28-CD8β^{low} cells have been generated from CD28+CD8β^{high} T cells in culture following TCR mediated activation of both adult T cells and from cord blood, in keeping with the previously discussed mechanisms for generation on CD28- T cells. The cause of this in the bulk CD8 T cell population of HBV is not clear. My *in vitro* data would suggest that this process is accelerated but not dependent on TCR activation. However where I see this bulk effect in HBV *ex-vivo*, such TCR-mediated activation seems unlikely, although

arginine-deficiency, which is observed in chronic HBV, has been proposed as one possible mechanism (Das, Hoare et al. 2008) as arginine has been shown to be required for CD3ζ expression by T cells (Rodriguez, Zea et al. 2003). The tolerizing environment of the liver or inflammatory cytokine exposure may also have an effect, although does not explain why this is seen in HBV and not HCV. CD28 down regulation on bulk CD8 T cells in HBV has been previously associated with a higher HBV viral load (Das, Hoare et al. 2008), although I was unable to demonstrate this here. In looking for correlations with other markers of disease activity, I found no association with ALT or e-antigen status, although the cohort studied had predominantly inactive hepatitis and so it is difficult to draw any real conclusions from the analysis with regards to this.

Understanding the role of CD8+ T cell populations in chronic viral hepatitis is important, especially where immunotherapy and vaccination are being considered as avenues of research for the discovery of further treatment options. Previous studies have focused on the failed antigen-specific responses, but these data suggest that wider effects are occurring and understanding these will be important in developing this area of research.

5.6 Conclusions

1. **CD161++CD8α+ T cell subsets are significantly reduced in the peripheral circulation in chronic HBV and HCV infection.**

2. **CD161++CD8α+ T cell subsets are relatively enriched in the liver in chronic HCV infection.**

3. **CD161++CD8α+ T cell subsets have an activated/exhausted phenotype in chronic HBV and HCV infection.**

4. **No difference between the activation status of CD161++CD8αα and CD8αβ T cells in chronic HBV or HCV infection is observed.**

5. **A prominent CD8β^{low} population is observed within the CD161-CD8+ T cell subset in chronic HBV infection.**

6. **CD161-CD8β^{low} T cells in chronic HBV have significantly reduced expression of CD28, increased expression of HLA-DR and produce significantly greater amounts of IFN-γ compared to CD161-CD8β^{high} T cells.**

6 Conclusions and further work

6.1 CD161++CD8αα and CD161++CD8αβ cell development and their role in human health and disease

6.1.1 Conclusions

- **CD161++CD8α+ T cells are a distinct pre-determined population in cord blood.**

  CD161++CD8α+ T cells in cord blood appear already a distinct subset in their expression of CCR6, IL18R, IL23R, RORγt and ZBTB16. This suggests that they are a pre-committed subset, rather than cells that differentiate later from conventional T cells, a finding similar to that in CD4+ T cells (Cosmi, De Palma et al. 2008). Gene expression and phenotyping data from both the cord and adults indicates that their genetic signature is strong at both stages, despite there being minimal MAIT Vα7.2+ cells in cord blood. Their chemokine receptor expression profile (CCR6+, $CCR7^{low}$, $CD62L^{low}$) at this stage would suggest preferential tissue, rather than lymph node, homing as naïve cells.

  Strong correlation in gene expression between the CD161+CD8α+ vs CD161-CD8α+ T cell subsets in cord and adult blood, indicates that the CD161+CD8α+ subset may also be a pre-determined subset in cord blood, although this subset requires further study. This is of interest

with regard to antigen-specific cells in chronic HCV, which appear to be found within the CD161+ subset.

- **CD161++CD8α+ and MAIT cells are overlapping T cell populations.**

  These data have clarified the relationship of the CD161++CD8α+ T cell subset to MAIT cells. CD161++CD8α+ T-cells (in adults) in addition to being defined by high expression of the C-type lectin CD161 and a pattern of phenotypic markers shared with Th17 cells, predominantly share the invariant TCR usage (Vα 7.2 and Vβ 2/13.2) of MAIT cells.

- **MAIT cells expand from the population of naïve CD161++CD8α+ T cells.**

  MAIT cells appear to expand from the pool of naïve CD161++CD8α+ T cells, suggesting that it is the phenotype/transcriptional signature that defines the subset primarily, and not the TCR. From these data it is not known at what stage in the development of the CD161++ signature occurs, i.e. pre- or intra-thymically. The requirement for gut flora and peripheral MR1 expression for development of the homologous MAIT cells in murine models (Treiner, Duban et al. 2003) supports the idea that this narrowing of TCR usage with age is due to antigen-driven peripheral expansion. Our data, although encompassing an extended definition of this subset to all CD161++CD8α+ T cells, is in keeping with this. In cord blood the population has broad TCR usage and chemokine receptor expression (CCR6+, $CCR7^{low}$, $CD62L^{low}$), which would suggest preferential migration to tissue and not lymph nodes as

naïve cells. Peripheral encounter with antigen/MR1 likely drives the expansion seen with age of cells within the CD161++CD8α+ subset expressing the MAIT TCR.

- **MAIT cells are predominantly CD8αβ and CD8αα expressing T cells.**

  By the use of an extended antibody panel, it has been clearly demonstrated that MAIT (CD161++Vα7.2+) cells express CD8αα or CD8αβ, with other co-receptor combinations (primarily double-negative cells) making up less than 10% of this population and the CD8αα cell population in humans to be exclusive to this subset. The CD161++CD8α+ T cell pool therefore largely encompasses the MAIT cell population. The CD161++ double negative population may represent a continuum of CD8β down-regulation in subset.

- **Human CD8αα cells are type-17 cells.**

  These data have made significant headway in describing the CD8αα subset in humans. Although I have not demonstrated any clear differences compared to CD161++CD8αβ cells, it has been shown that they clearly share type-17 differentiation, TCR usage, effector function (IFNγ, IL-17, IL-22) and chemokine receptor expression (CCR2, CCR6 and CXCR6). There is much work to do on further understanding their differential *in vivo* role in man. Data from mice would suggest an immunomodulatory role for CD8αα, which requires further exploration in man.

- **CD161++CD8αβ and CD161++CD8αα T cells are developmentally closely linked.**

  These data suggest that the CD161++CD8αα and CD8αβ cell populations are developmentally very closely linked, in contrast to the proposed pathways published in murine models. I suggest that the CD161++CD8αα cell population emerges from within the same cellular pool as CD161++CD8αβ+ cells, and CD8β expression is regulated within it. In cord blood and infant PBMCs the CD161++CD8αβ subset is a small population and its TCR-usage broad. CD161++CD8αα cells are not present at this stage, but become detectable in adulthood as the CD161++CD8α+ T cell subset has undergone an approximate ten-fold expansion. The two populations share phenotype, function, gene expression on microarray and TCR Vα/Vβ usage. CD161++ CD8αα cells can be readily derived from CD161++ CD8αβ cells in culture in the absence of specific stimulation or proliferation after just 24 hours, suggesting that the transition between CD161++CD8αα and CD8αβ cell populations is a rapid and simple process.

- **CD161++CD8α+ T cells are redistributed to the liver in chronic HCV infection.**

  The redistribution of human CD161++CD8α+ T cells to the liver seen in chronic HCV is intriguing and their expression of activation and exhaustion markers in both HCV and HBV compared to healthy controls clearly points to an active role in inflammation or immunity, although requires much further work. Overall, their significance in chronic hepatitis is not yet known, although the inverse correlation between fibrosis score and the frequency of CD8+ T cells co-secreting

IL17 and IFNγ (Billerbeck, Kang et al.) (**Appendix 1**) described is likely to be of importance. Defining a specific differential role for CD8αα cells in such settings remains an important and unanswered question.

6.1.2 Overall model for CD161++CD8α+ T cell development and role in immunity

These data have defined the origins and relationships of CD161++/CD8αα+/MAIT TCR+ T cells and I propose a model whereby there is primary expression of CD161 and its associated phenotype on a pre-committed naïve T cell population with diverse TCRs. This is followed by postnatal expansion of MAIT TCR+ populations within this pool after preferential tissue homing, encounter with MR1/antigen, and ready transition to a CD8αα status. Once expanded, the potent cytokine secretory activity and homing pattern of the CD8+ T cell populations studied here suggests a central role in host defense and tissue inflammation in human health and disease (**Figure 6.1**).

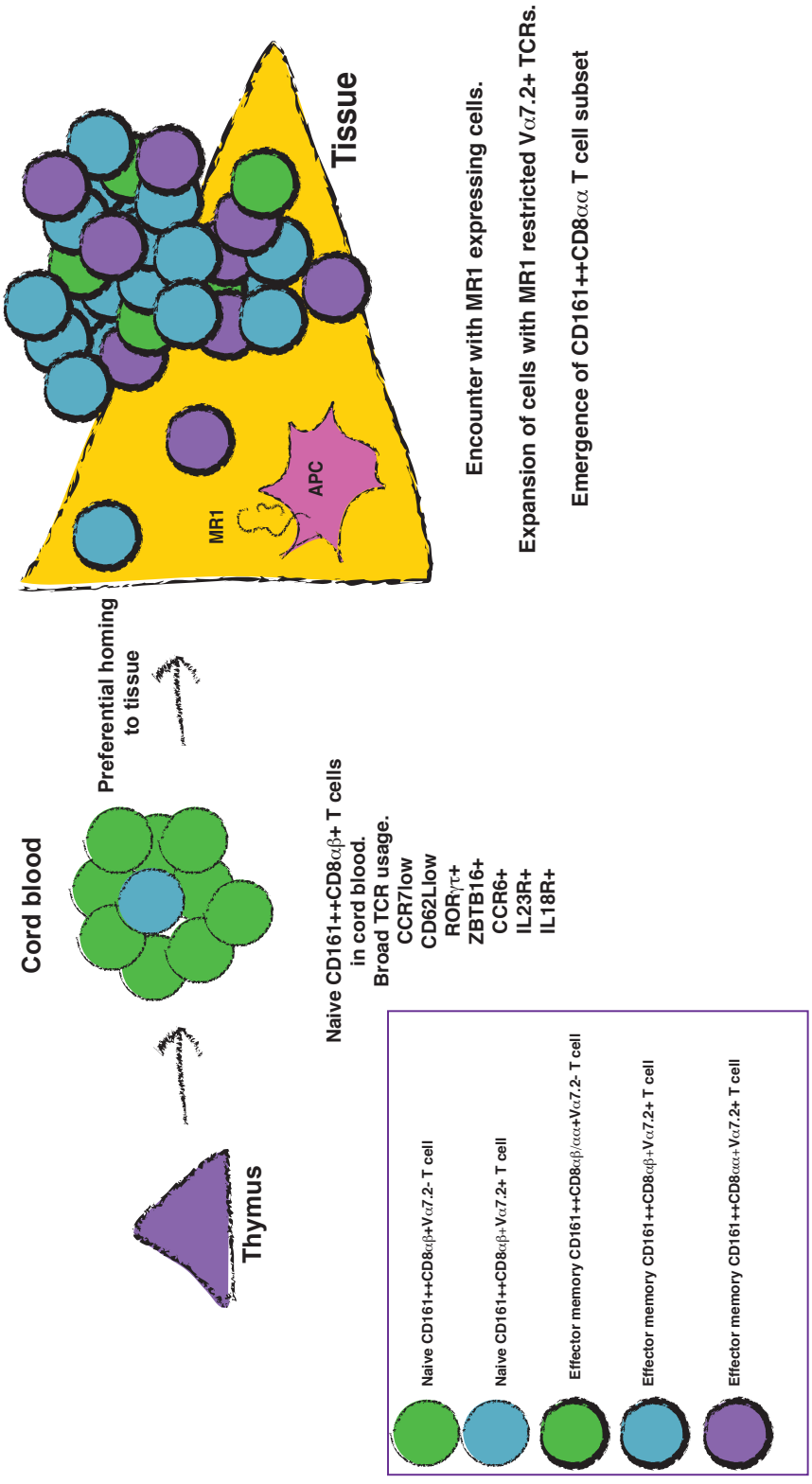


Figure 6.1 Model for CD161++CD8+ T cell population development and expansion. Type-17 pre-committed CD161++CD8αβ T cells emerge from the thymus in cord blood. Naive cells preferentially home to tissue, where they encounter MR1 and cells expressing the Vα7.2 MR1 restricted TCRs proliferate. Emergence of CD161++CD8αα cells is seen in conjunction with this expansion.

6.1.3 Further work

There is clearly much work to be done in further understanding the CD161++CD8α+ human T cell lineage and its role in health and disease. Beyond work on the differentiation of these cells, their *in vivo* role in immunity and immunopathology, MR1 ligand identification and study of MR1 cell surface expression triggers require further study. The relative enrichment seen in chronic HCV in the liver and activation/exhaustion of the subset in both chronic HCV and HBV is of great interest. More extensive study of CD161++CD8αβ and CD8αα cells in the liver is important, including the ability of these viruses to stimulate MR1 expression on hepatocytes with subsequent activation of the CD161++CD8α+ population. Study of the subset at other tissue sites in both health and disease is also required, such as the small intestine, joints and skin. Given the conserved reactivity to MR1 between individuals and species, I think a very interesting avenue for further research would also be their role in relation to organ rejection after transplantation, especially given their reported resistance to chemotherapeutic agents (Turtle, Swanson et al. 2009).

6.2 Bulk CD8+ T cell effects in chronic Hepatitis B infection

6.2.1 Conclusions

- **CD161-CD8β^{low} T cells are a prominent population in chronic HBV infection**

An unexpected finding of this work was the prominent population of cells within the CD161-CD8+ T cell subset in chronic HBV that were CD8β^{low}.

- **CD161-CD8β^{low} T cells are CD28^{low} and HLA-DR^{high}**

  The CD161-CD8β^{low} population had significantly reduced expression of CD28 and increased expression of HLA-DR in chronic HBV infection. This has not previously been described, although bulk changes in the CD8+ T cell population in HBV have been identified, including CD28 down-regulation (Das, Hoare et al. 2008).

- **CD8β is readily down-regulated on CD8+ T cells in culture.**

  It was found that CD8β was readily down-regulated on sorted CD8$\alpha\beta$ cells cultured in media alone. The process was potentiated in culture with the addition of anti-CD3/CD28 beads, which suggests a role for T cell activation in transition from CD8β^{high} to CD8β^{low} status.

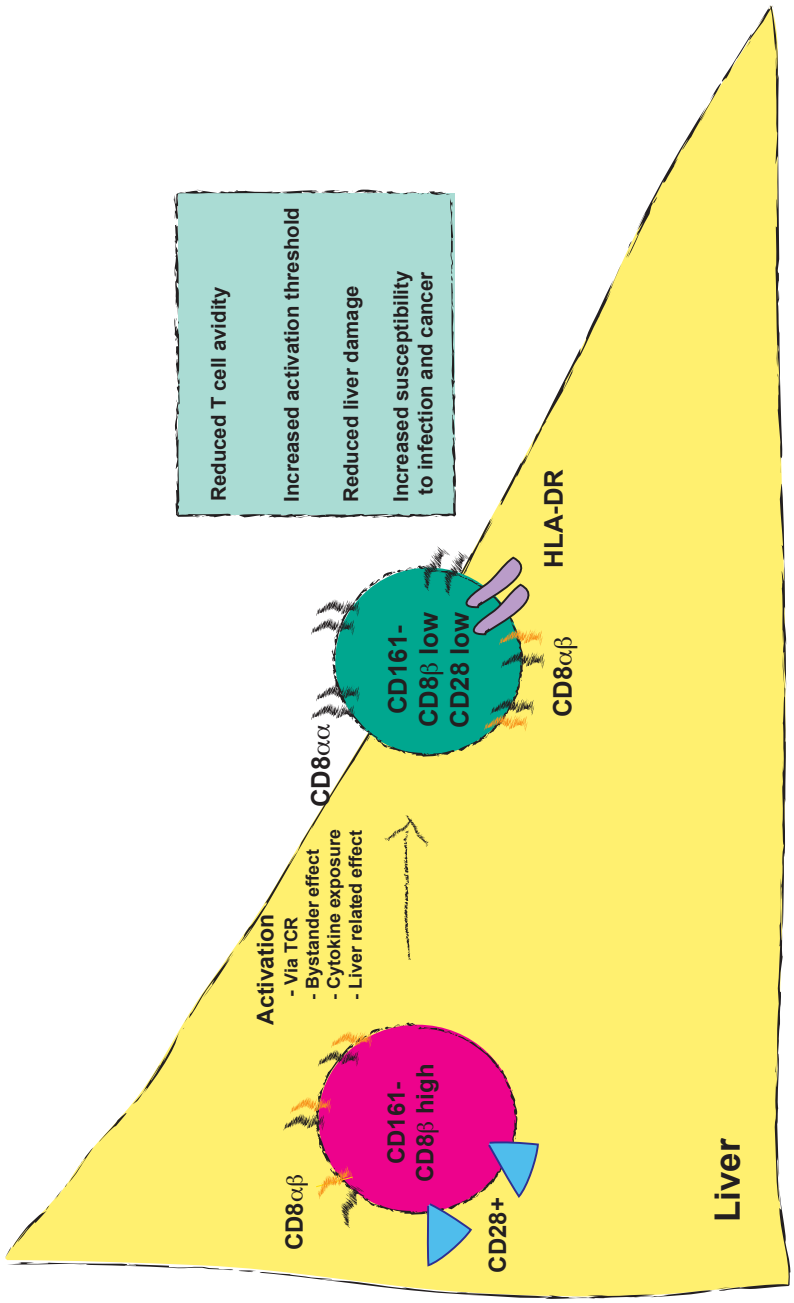


Figure 6.2 Model for generation and role of CD161- CD8β low T cells in chronic HBV infection. CD161-CD8β low T cells are generated through chronic activation. These cells up-regulate HLA-DR and down-regulate CD28. The increased proportion of CD8αα expressed on the cell surface acts to reduce T cell avidity for antigen and increase the activation threshold. This may play an immunomodulatory role, protecting the liver from immune mediated damage and progression of liver disease. Side effects of this might be increased susceptibility to infection or cancer development.

6.2.2 Overall model for generation and role of CD161- CD8β^{low}CD28^{low}HLADR^{high} T cells in chronic HBV infection.

From these data, I propose that the CD161-CD8β^{low}CD28^{low}HLADR^{high} population in chronic HBV occurs as a result of a homeostatic response to chronic activation. Where CD8β is down regulated, there is increased relative expression of CD8α and thus a presumed increased density of CD8$\alpha\alpha$ molecules at the cell surface, which may play an immunomodulatory role in reducing the avidity of those cells for their cognate antigen (**Figure 6.2**). This in turn would act to control ongoing antigen-specific responses to HBV antigens in the liver and reduce the risk of flares of hepatitis, resultant liver damage and progression of liver fibrosis. The association of CD28-CD8+ T cells with the ageing immune system, malignancy, autoimmunity and chronic infection suggests that this may not be a disease or liver specific effect, although why it is not seen in chronic HCV is of interest.

6.2.3 Further work

The CD161-CD8β^{low}CD28^{low}HLADR^{high} population in chronic HBV infection requires further study. Firstly the population needs to be studied in a wider range of disease states in the context of chronic HBV. It may be that the patients looked at here, who all had stable disease, were a self-selected group for whom such an immune tolerance mechanism may be important in controlling immune-mediated disease flares and subsequent progression to fibrosis. Study of this phenomenon during a phase of active hepatitis would shed interesting light on the causes and mechanisms involved, as well as presenting a possible target for treatment.

Should the CD161-CD8β^{low} population represent bulk tolerisation of these cells, it would be important to study the susceptibility of patients to other

infections and their risk of cancer development. I have developed an *in vitro* model with which to work on these cells, which provides a good starting point from which to study the factors driving CD8β down-regulation and the effects of this on cell function. An important first experiment would be to correlate CD8β down-regulation in culture to CD28 and HLA-DR expression. I also propose performing microarray experiments to look at differential gene expression by the bulk CD8+ T cell populations of chronic HBV and HCV compared to healthy controls as a first step in casting a wide net in terms of identifying further avenues of investigation.

6.3 Final thesis conclusions

- **CD161++CD8α+ T cells/MAIT cells are a prominent innate-like semi-invariant type-17 human T cell population that develops from a pre-committed precursor population in cord blood.**

- **CD161++CD8α+ T cells are found at diverse tissue sites and are predicted to play an important front-line role in immunity.**

- **The type-17 properties of the CD161++CD8α+ T cells point to a primary role in defense against extracellular bacteria and fungi through neutrophil recruitment and maintenance of epithelial barrier function. Their influence on control of viral infection and also in the pathogenesis of autoimmune and inflammatory disease requires further study.**

- **Human CD8αα T cells are exclusive to the CD161++CD8α+ T cell subset and share the type-17 properties of their CD161++CD8αβ counterparts. The CD8αα molecule may act in an immunomodulatory capacity - imposing a threshold to activation through the MR1 restricted TCR (Figure 6.3).**

- **CD8β expression is reduced on CD161-CD8+ T cells in chronic HBV infection that in addition have a $CD28^{low}HLADR^{high}$ phenotype.**

- **An increase in proportion of CD8αα expression on CD161-$CD8\beta^{low}$ T cells in conjunction with increased expression of HLA-DR and reduced expression of CD28 is a likely homeostatic response to chronic stimulation/activation of CD8 T cells in HBV infection. This may represent an important pathway to promote in the development of immunomodulatory treatments to prevent disease progression.**

Figure 6.3 CD161++CD8+ T cell subsets; phenotype and function. CD161++CD8αβ and CD8αα cells are a semi-invariant, innate-like T cell subset with Type-17 effector functions and phenotype. Expression of CD8αα, acting as a co-repressor, likely imposes a threshold of activation, which provides intrinsic immunomodulation of the subset.

7 References

Aberle, J. H., E. Formann, et al. (2006). "Prospective study of viral clearance and CD4(+) T-cell response in acute hepatitis C primary infection and reinfection." J Clin Virol 36(1): 24-31.

Aldemir, H., V. Prod'homme, et al. (2005). "Cutting edge: lectin-like transcript 1 is a ligand for the CD161 receptor." J Immunol 175(12): 7791-5.

Amadei, B., S. Urbani, et al. "Activation of natural killer cells during acute infection with hepatitis C virus." Gastroenterology 138(4): 1536-45.

Arcaro, A., C. Gregoire, et al. (2000). "Essential role of CD8 palmitoylation in CD8 coreceptor function." J Immunol 165(4): 2068-76.

Aujla, S. J., Y. R. Chan, et al. (2008). "IL-22 mediates mucosal host defense against Gram-negative bacterial pneumonia." Nat Med 14(3): 275-81.

Azuma, M., J. H. Phillips, et al. (1993). "CD28- T lymphocytes. Antigenic and functional properties." J Immunol 150(4): 1147-59.

Bendelac, A., P. B. Savage, et al. (2007). "The biology of NKT cells." Annu Rev Immunol 25: 297-336.

BENJAMINI, Y. and Y. HOCHBERG (1995). "CONTROLLING THE FALSE DISCOVERY RATE : A PRACTICAL AND POWERFUL APPROACH TO MULTIPLE TESTING." JOURNAL OF THE ROYAL STATISTICAL SOCIETY SERIES B 57(1): 289-300.

Bertolino, P., D. G. Bowen, et al. (2007). "T cells in the liver: there is life beyond the graveyard." Hepatology 45(6): 1580-2.

Billerbeck, E., Y. H. Kang, et al. (2010). "Analysis of CD161 expression on human CD8+ T cells defines a distinct functional subset with tissue-homing properties." Proc Natl Acad Sci U S A 107(7): 3006-11.

Boniface, K., F. X. Bernard, et al. (2005). "IL-22 inhibits epidermal differentiation and induces proinflammatory gene expression and migration of human keratinocytes." J Immunol 174(6): 3695-702.

Bosselut, R., S. Kubo, et al. (2000). "Role of CD8beta domains in CD8 coreceptor function: importance for MHC I binding, signaling, and positive selection of CD8+ T cells in the thymus." Immunity 12(4): 409-18.

Bosselut, R., W. Zhang, et al. (1999). "Association of the adaptor molecule LAT with CD4 and CD8 coreceptors identifies a new coreceptor function in T cell receptor signal transduction." J Exp Med 190(10): 1517-26.

Bowen, D. G. and C. M. Walker (2005). "Adaptive immune responses in acute and chronic hepatitis C virus infection." Nature 436(7053): 946-52.

Brand, S., F. Beigel, et al. (2006). "IL-22 is increased in active Crohn's disease and promotes proinflammatory gene expression and intestinal epithelial cell migration." Am J Physiol Gastrointest Liver Physiol 290(4): G827-38.

Breous, E., S. Somanathan, et al. (2009). "Hepatic regulatory T cells and Kupffer cells are crucial mediators of systemic T cell tolerance to antigens targeting murine liver." Hepatology 50(2): 612-21.

Brustle, A., S. Heink, et al. (2007). "The development of inflammatory T(H)-17 cells requires interferon-regulatory factor 4." Nat Immunol 8(9): 958-66.

Calne, R. Y., R. A. Sells, et al. (1969). "Induction of immunological tolerance by porcine liver allografts." Nature 223(5205): 472-6.

Cantor, H. and E. A. Boyse (1975). "Functional subclasses of T-lymphocytes bearing different Ly antigens. I. The generation of functionally distinct T-cell subclasses is a differentiative process independent of antigen." J Exp Med 141(6): 1376-89.

Cantor, H. and E. A. Boyse (1977). "Regulation of cellular and humoral immune responses by T-cell subclasses." Cold Spring Harb Symp Quant Biol 41 Pt 1: 23-32.

Cawthon, A. G. and M. A. Alexander-Miller (2002). "Optimal colocalization of TCR and CD8 as a novel mechanism for the control of functional avidity." J Immunol 169(7): 3492-8.

Chang, H., H. Hanawa, et al. (2006). "Hydrodynamic-based delivery of an interleukin-22-Ig fusion gene ameliorates experimental autoimmune myocarditis in rats." J Immunol 177(6): 3635-43.

Cheent, K. and S. I. Khakoo. (2011), "Natural killer cells and hepatitis C: action and reaction." Gut 60(2): 268-78.

Chen, Z., C. M. Tato, et al. (2007). "Distinct regulation of interleukin-17 in human T helper lymphocytes." Arthritis Rheum 56(9): 2936-46.

Cheroutre, H. and F. Lambolez (2008). "Doubting the TCR coreceptor function of CD8alphaalpha." Immunity 28(2): 149-59.

Ciubotariu, R., A. I. Colovai, et al. (1998). "Specific suppression of human CD4+ Th cell responses to pig MHC antigens by CD8+CD28- regulatory T cells." J Immunol 161(10): 5193-202.

Cosmi, L., R. De Palma, et al. (2008). "Human interleukin 17-producing cells originate from a CD161+CD4+ T cell precursor." J Exp Med 205(8): 1903-16.

Crispe, I. N. (2009). "The liver as a lymphoid organ." Annu Rev Immunol 27: 147-63.

Crome, S. Q., A. Y. Wang, et al. (2009). "The role of retinoic acid-related orphan receptor variant 2 and IL-17 in the development and function of human CD4+ T cells." Eur J Immunol 39(6): 1480-93.

Crome, S. Q., A. Y. Wang, et al. "Translational mini-review series on Th17 cells: function and regulation of human T helper 17 cells in health and disease." Clin Exp Immunol 159(2): 109-19.

Cua, D. J., J. Sherlock, et al. (2003). "Interleukin-23 rather than interleukin-12 is the critical cytokine for autoimmune inflammation of the brain." Nature 421(6924): 744-8.

Das, A., M. Hoare, et al. (2008). "Functional skewing of the global CD8 T cell population in chronic hepatitis B virus infection." J Exp Med 205(9): 2111-24.

Das, A. and M. K. Maini (2010). "Innate and adaptive immune responses in hepatitis B virus infection." Dig Dis 28(1): 126-32.

Dao, T., W. Z. Mehal, et al. (1998). "IL-18 augments perforin-dependent cytotoxicity of liver NK-T cells." J Immunol 161(5): 2217-22.

Denning, T. L., S. W. Granger, et al. (2007). "Mouse TCRalphabeta+CD8alphaalpha intraepithelial lymphocytes express genes that down-regulate their antigen reactivity and suppress immune responses." J Immunol 178(7): 4230-9.

Dessouki, O., Y. Kamiya, et al. (2010). "Chronic hepatitis C viral infection reduces NK cell frequency and suppresses cytokine secretion: Reversion by anti-viral treatment." Biochem Biophys Res Commun 393(2): 331-7.

Dienstag, J. L. (2008). "Hepatitis B virus infection." N Engl J Med 359(14): 1486-500.

Dubin, P. J. and J. K. Kolls (2007). "IL-23 mediates inflammatory responses to mucoid Pseudomonas aeruginosa lung infection in mice." Am J Physiol Lung Cell Mol Physiol 292(2): L519-28.

Duerr, R. H., K. D. Taylor, et al. (2006). "A genome-wide association study identifies IL23R as an inflammatory bowel disease gene." Science 314(5804): 1461-3.

Dusseaux, M., E. Martin, et al (2011). "Human MAIT cells are xenobiotic-resistant, tissue-targeted, CD161hi IL-17-secreting T cells." Blood 117(4): 1250-9.

Fann, M., W. K. Chiu, et al. (2005). "Gene expression characteristics of CD28null memory phenotype CD8+ T cells and its implication in T-cell aging." Immunol Rev 205: 190-206.

Fujino, S., A. Andoh, et al. (2003). "Increased expression of interleukin 17 in inflammatory bowel disease." Gut 52(1): 65-70.

Gao, G. F., J. Tormo, et al. (1997). "Crystal structure of the complex between human CD8alpha(alpha) and HLA-A2." Nature 387(6633): 630-4.

Garcia, K. C., C. A. Scott, et al. (1996). "CD8 enhances formation of stable T-cell receptor/MHC class I molecule complexes." Nature 384(6609): 577-81.

Ge, D., J. Fellay, et al. (2009). "Genetic variation in IL28B predicts hepatitis C treatment-induced viral clearance." Nature 461(7262): 399-401.

Gentleman, R. C., V. J. Carey, et al. (2004). "Bioconductor: open software development for computational biology and bioinformatics." Genome Biol 5(10): R80.

Gold, M. C., S. Cerri, et al. (2010). "Human mucosal associated invariant T cells detect bacterially infected cells." PLoS Biol 8(6): e1000407.

Goldfinch, N., P. Reinink, et al. (2010). "Conservation of mucosal associated invariant T (MAIT) cells and the MR1 restriction element in ruminants, and abundance of MAIT cells in spleen." Vet Res 41(5): 62.

Gran, B., G. X. Zhang, et al. (2002). "IL-12p35-deficient mice are susceptible to experimental autoimmune encephalomyelitis: evidence for redundancy in the IL-12 system in the induction of central nervous system autoimmune demyelination." J Immunol 169(12): 7104-10.

Gross, G. G., V. L. Schwartz, et al. (1994). "Distribution of dominant T cell receptor beta chains in human intestinal mucosa." J Exp Med 180(4): 1337-44.

Hamada, H., L. Garcia-Hernandez Mde, et al. (2009). "Tc17, a unique subset of CD8 T cells that can protect against lethal influenza challenge." J Immunol 182(6): 3469-81.

Hanvesakul, R., N. Spencer, et al. (2008). "Donor HLA-C genotype has a profound impact on the clinical outcome following liver transplantation." Am J Transplant 8(9): 1931-41.

Happel, K. I., P. J. Dubin, et al. (2005). "Divergent roles of IL-23 and IL-12 in host defense against Klebsiella pneumoniae." J Exp Med 202(6): 761-9.

Harrington, L. E., R. D. Hatton, et al. (2005). "Interleukin 17-producing CD4+ effector T cells develop via a lineage distinct from the T helper type 1 and 2 lineages." Nat Immunol 6(11): 1123-32.

Helgeland, L., P. Brandtzaeg, et al. (1997). "Sequential development of intraepithelial gamma delta and alpha beta T lymphocytes expressing CD8 alpha beta in neonatal rat intestine: requirement for the thymus." Immunology 92(4): 447-56.

Helgeland, L., E. Dissen, et al. (2004). "Microbial colonization induces oligoclonal expansions of intraepithelial CD8 T cells in the gut." Eur J Immunol 34(12): 3389-400.

Helgeland, L., F. E. Johansen, et al. (1999). "Oligoclonality of rat intestinal intraepithelial T lymphocytes: overlapping TCR beta-chain repertoires in the CD4 single-positive and CD4/CD8 double-positive subsets." J Immunol 162(5): 2683-92.

Hershberg, R., P. Eghtesady, et al. (1990). "Expression of the thymus leukemia antigen in mouse intestinal epithelium." Proc Natl Acad Sci U S A 87(24): 9727-31.

Heydtmann, M., P. F. Lalor, et al. (2005). "CXC chemokine ligand 16 promotes integrin-mediated adhesion of liver-infiltrating lymphocytes to cholangiocytes and hepatocytes within the inflamed human liver." J Immunol 174(2): 1055-62.

Huang, S., S. Gilfillan, et al. (2005). "Evidence for MR1 antigen presentation to mucosal-associated invariant T cells." J Biol Chem 280(22): 21183-93.

Huang, S., S. Gilfillan, et al. (2008). "MR1 uses an endocytic pathway to activate mucosal-associated invariant T cells." J Exp Med 205(5): 1201-11.

Huang, W., L. Na, et al. (2004). "Requirement of interleukin-17A for systemic anti-Candida albicans host defense in mice." J Infect Dis 190(3): 624-31.

Huarte, E., J. R. Cubillos-Ruiz, et al. (2008). "PILAR is a novel modulator of human T-cell expansion." Blood 112(4): 1259-68.

Ishikawa, S., K. Ikejima, et al (2010). "CD1d-restricted natural killer T cells contribute to hepatic inflammation and fibrogenesis in mice." J Hepatol. ePub ahead of print.

Ivanov, II, B. S. McKenzie, et al. (2006). "The orphan nuclear receptor RORgammat directs the differentiation program of proinflammatory IL-17+ T helper cells." Cell 126(6): 1121-33.

Irizarry, R. A., B. M. Bolstad, et al. (2003). "Summaries of Affymetrix GeneChip probe level data." Nucleic Acids Res 31(4): e15.

Kawachi, I., J. Maldonado, et al. (2006). "MR1-restricted V alpha 19i mucosal-associated invariant T cells are innate T cells in the gut lamina propria that provide a rapid and diverse cytokine response." J Immunol 176(3): 1618-27.

Kennedy, M. K., M. Glaccum, et al. (2000). "Reversible defects in natural killer and memory CD8 T cell lineages in interleukin 15-deficient mice." J Exp Med 191(5): 771-80.

Kern, P., R. E. Hussey, et al. (1999). "Expression, purification, and functional analysis of murine ectodomain fragments of CD8alphaalpha and CD8alphabeta dimers." J Biol Chem 274(38): 27237-43.

Kern, P. S., M. K. Teng, et al. (1998). "Structural basis of CD8 coreceptor function revealed by crystallographic analysis of a murine CD8alphaalpha ectodomain fragment in complex with H-2Kb." Immunity 9(4): 519-30.

Khakoo, S. I., C. L. Thio, et al. (2004). "HLA and NK cell inhibitory receptor genes in resolving hepatitis C virus infection." Science 305(5685): 872-4.

Klein, I. and I. N. Crispe (2006). "Complete differentiation of CD8+ T cells activated locally within the transplanted liver." J Exp Med 203(2): 437-47.

Kleinschek, M. A., K. Boniface, et al. (2009). "Circulating and gut-resident human Th17 cells express CD161 and promote intestinal inflammation." J Exp Med 206(3): 525-34.

Kondo, T., H. Takata, et al. (2009). "Cutting edge: Phenotypic characterization and differentiation of human CD8+ T cells producing IL-17." J Immunol 182(4): 1794-8.

Konno, A., K. Okada, et al. (2002). "CD8alpha alpha memory effector T cells descend directly from clonally expanded CD8alpha +beta high TCRalpha beta T cells in vivo." Blood 100(12): 4090-7.

Korn, T., E. Bettelli, et al. (2009). "IL-17 and Th17 Cells." Annu Rev Immunol 27: 485-517.

Kotenko, S. V., L. S. Izotova, et al. (2001). "Identification of the functional interleukin-22 (IL-22) receptor complex: the IL-10R2 chain (IL-10Rbeta) is a common chain of both the IL-10 and IL-22 (IL-10-related T cell-derived inducible factor, IL-TIF) receptor complexes." J Biol Chem 276(4): 2725-32

Kovalovsky, D., E. S. Alonzo, et al. (2010). "PLZF induces the spontaneous acquisition of memory/effector functions in T cells independently of NKT cell-related signals." J Immunol 184(12): 6746-55.

Kovalovsky, D., O. U. Uche, et al. (2008). "The BTB-zinc finger transcriptional regulator PLZF controls the development of invariant natural killer T cell effector functions." Nat Immunol 9(9): 1055-64.

Krakowski, M. and T. Owens (1996). "Interferon-gamma confers resistance to experimental allergic encephalomyelitis." Eur J Immunol 26(7): 1641-6.

Krishnan, S., J. G. Kiang, et al. (2005). "Increased caspase-3 expression and activity contribute to reduced CD3zeta expression in systemic lupus erythematosus T cells." J Immunol 175(5): 3417-23.

Krueger, G. G., R. G. Langley, et al. (2007). "A human interleukin-12/23 monoclonal antibody for the treatment of psoriasis." N Engl J Med 356(6): 580-92.

Lai, Y. G., V. Gelfanov, et al. (1999). "IL-15 promotes survival but not effector function differentiation of CD8+ TCRalphabeta+ intestinal intraepithelial lymphocytes." J Immunol 163(11): 5843-50.

Lai, Y. G., M. S. Hou, et al. (2008). "IL-15 does not affect IEL development in the thymus but regulates homeostasis of putative precursors and mature CD8 alpha alpha+ IELs in the intestine." J Immunol 180(6): 3757-65.

Lan, R. Y., C. Cheng, et al. (2006). "Liver-targeted and peripheral blood alterations of regulatory T cells in primary biliary cirrhosis." Hepatology 43(4): 729-37.

Langrish, C. L., Y. Chen, et al. (2005). "IL-23 drives a pathogenic T cell population that induces autoimmune inflammation." J Exp Med 201(2): 233-40.

Latthe, M., L. Terry, et al. (1994). "High frequency of CD8 alpha alpha homodimer-bearing T cells in human fetal intestine." Eur J Immunol 24(7): 1703-5.

Lauer, G. M. and B. D. Walker (2001). "Hepatitis C virus infection." N Engl J Med 345(1): 41-52.

Le Bourhis, L., E. Martin, et al. (2010). "Antimicrobial activity of mucosal-associated invariant T cells." Nat Immunol 11(8): 701-8.

Lee, Y. C., L. Lu, et al. (1999). "Hepatocytes and liver nonparenchymal cells induce apoptosis in activated T cells." Transplant Proc 31(1-2): 784.

Leishman, A. J., O. V. Naidenko, et al. (2001). "T cell responses modulated through interaction between CD8alphaalpha and the nonclassical MHC class I molecule, TL." Science 294(5548): 1936-9.

Liang, S. C., X. Y. Tan, et al. (2006). "Interleukin (IL)-22 and IL-17 are coexpressed by Th17 cells and cooperatively enhance expression of antimicrobial peptides." J Exp Med 203(10): 2271-9.

Liu, H. and C. Rohowsky-Kochan (2008). "Regulation of IL-17 in human CCR6+ effector memory T cells." J Immunol 180(12): 7948-57.

Liu, Y., Y. Xiong, et al. (2003). "The crystal structure of a TL/CD8alphaalpha complex at 2.1 A resolution: implications for modulation of T cell activation and memory." Immunity 18(2): 205-15.

Livak, K. J. and T. D. Schmittgen (2001). "Analysis of relative gene expression data using real-time quantitative PCR and the 2(-Delta Delta C(T)) Method." Methods 25(4): 402-8.

Lodolce, J. P., D. L. Boone, et al. (1998). "IL-15 receptor maintains lymphoid homeostasis by supporting lymphocyte homing and proliferation." Immunity 9(5): 669-76.

Longhi, M. S., M. J. Hussain, et al. (2006). "Functional study of CD4+CD25+ regulatory T cells in health and autoimmune hepatitis." J Immunol 176(7): 4484-91.

Lopes, A. R., P. Kellam, et al. (2008). "Bim-mediated deletion of antigen-specific CD8 T cells in patients unable to control HBV infection." J Clin Invest 118(5): 1835-45.

Luzza, F., T. Parrello, et al. (2000). "Up-regulation of IL-17 is associated with bioactive IL-8 expression in Helicobacter pylori-infected human gastric mucosa." J Immunol 165(9): 5332-7.

Ma, C. S., G. Y. Chew, et al. (2008). "Deficiency of Th17 cells in hyper IgE syndrome due to mutations in STAT3." J Exp Med 205(7): 1551-7.

Madakamutil, L. T., U. Christen, et al. (2004). "CD8alphaalpha-mediated survival and differentiation of CD8 memory T cell precursors." Science 304(5670): 590-3.

Maggi, L., V. Santarlasci, et al (2010). "CD161 is a marker of all human IL-17-producing T-cell subsets and is induced by RORC." Eur J Immunol 40(8): 2174-81.

Maini, M. K., C. Boni, et al. (2000). "The role of virus-specific CD8(+) cells in liver damage and viral control during persistent hepatitis B virus infection." J Exp Med 191(8): 1269-80.

Major, M. E., K. Mihalik, et al. (2002). "Previously infected and recovered chimpanzees exhibit rapid responses that control hepatitis C virus replication upon rechallenge." J Virol 76(13): 6586-95.

Mannon, P. J., I. J. Fuss, et al. (2004). "Anti-interleukin-12 antibody for active Crohn's disease." N Engl J Med 351(20): 2069-79.

Martin, E., E. Treiner, et al. (2009). "Stepwise development of MAIT cells in mouse and human." PLoS Biol 7(3): e54.

Matteucci, E. and O. Giampietro (2009). "Dipeptidyl peptidase-4 (CD26): knowing the function before inhibiting the enzyme." Curr Med Chem 16(23): 2943-51.

McKiernan, S. M., R. Hagan, et al. (2004). "Distinct MHC class I and II alleles are associated with hepatitis C viral clearance, originating from a single source." Hepatology 40(1): 108-14.

McNicol, A. M., G. Bendle, et al. (2007). "CD8alpha/alpha homodimers fail to function as co-receptor for a CD8-dependent TCR." Eur J Immunol 37(6): 1634-41.

Meier, U. C., R. E. Owen, et al. (2005). "Shared alterations in NK cell frequency, phenotype, and function in chronic human

immunodeficiency virus and hepatitis C virus infections." J Virol 79(19): 12365-74.

Miley, M. J., S. M. Truscott, et al. (2003). "Biochemical features of the MHC-related protein 1 consistent with an immunological function." J Immunol 170(12): 6090-8.

Morishima, C., D. M. Paschal, et al. (2006). "Decreased NK cell frequency in chronic hepatitis C does not affect ex vivo cytolytic killing." Hepatology 43(3): 573-80.

Mootha, V. K., C. M. Lindgren, et al. (2003). "PGC-1alpha-responsive genes involved in oxidative phosphorylation are coordinately downregulated in human diabetes." Nat Genet 34(3): 267-73.

Nakagomi, H., M. Petersson, et al. (1993). "Decreased expression of the signal-transducing zeta chains in tumor-infiltrating T-cells and NK cells of patients with colorectal carcinoma." Cancer Res 53(23): 5610-2.

Nguyen, K. B., T. P. Salazar-Mather, et al. (2002). "Coordinated and distinct roles for IFN-alpha beta, IL-12, and IL-15 regulation of NK cell responses to viral infection." J Immunol 169(8): 4279-87.

Northfield, J. W., V. Kasprowicz, et al. (2008). "CD161 expression on hepatitis C virus-specific CD8+ T cells suggests a distinct pathway of T cell differentiation." Hepatology 47(2): 396-406.

Ohnuma, K., N. H. Dang, et al. (2008). "Revisiting an old acquaintance: CD26 and its molecular mechanisms in T cell function." Trends Immunol 29(6): 295-301.

Olivares-Villagomez, D., Y. V. Mendez-Fernandez, et al. (2008). "Thymus leukemia antigen controls intraepithelial lymphocyte function and

inflammatory bowel disease." Proc Natl Acad Sci U S A 105(46): 17931-6.

Oo, Y. H., C. J. Weston, et al. (2010). "Distinct roles for CCR4 and CXCR3 in the recruitment and positioning of regulatory T cells in the inflamed human liver." J Immunol 184(6): 2886-98.

Oppmann, B., R. Lesley, et al. (2000). "Novel p19 protein engages IL-12p40 to form a cytokine, IL-23, with biological activities similar as well as distinct from IL-12." Immunity 13(5): 715-25.

Pang, D. J., A. C. Hayday, et al. (2007). "CD8 Raft localization is induced by its assembly into CD8alpha beta heterodimers, Not CD8alpha alpha homodimers." J Biol Chem 282(18): 13884-94.

Parra-Cuadrado, J. F., P. Navarro, et al. (2000). "A study on the polymorphism of human MHC class I-related MR1 gene and identification of an MR1-like pseudogene." Tissue Antigens 56(2): 170-2.

Pestka, J. M., M. B. Zeisel, et al. (2007). "Rapid induction of virus-neutralizing antibodies and viral clearance in a single-source outbreak of hepatitis C." Proc Natl Acad Sci U S A 104(14): 6025-30.

Podd, B. S., C. Aberg, et al. (2004). "Late postnatal expansion of self-reactive CD8alphaalpha+ intestinal intraepithelial lymphocytes in mice." Autoimmunity 37(8): 537-47.

Polakos, N. K., I. Klein, et al. (2007). "Early intrahepatic accumulation of CD8+ T cells provides a source of effectors for nonhepatic immune responses." J Immunol 179(1): 201-10.

Poussier, P., T. Ning, et al. (2002). "A unique subset of self-specific intraintestinal T cells maintains gut integrity." J Exp Med 195(11): 1491-7.

Qian, S., L. Lu, et al. (1997). "Apoptosis within spontaneously accepted mouse liver allografts: evidence for deletion of cytotoxic T cells and implications for tolerance induction." J Immunol 158(10): 4654-61.

Quintana, F. J., A. S. Basso, et al. (2008). "Control of T(reg) and T(H)17 cell differentiation by the aryl hydrocarbon receptor." Nature 453(7191): 65-71.

Radaeva, S., R. Sun, et al. (2004). "Interleukin 22 (IL-22) plays a protective role in T cell-mediated murine hepatitis: IL-22 is a survival factor for hepatocytes via STAT3 activation." Hepatology 39(5): 1332-42.

Regnault, A., A. Cumano, et al. (1994). "Oligoclonal repertoire of the CD8 alpha alpha and the CD8 alpha beta TCR-alpha/beta murine intestinal intraepithelial T lymphocytes: evidence for the random emergence of T cells." J Exp Med 180(4): 1345-58.

Regnault, A., P. Kourilsky, et al. (1995). "The TCR-beta chain repertoire of gut-derived T lymphocytes." Semin Immunol 7(5): 307-19.

Rehermann, B. (2009). "Hepatitis C virus versus innate and adaptive immune responses: a tale of coevolution and coexistence." J Clin Invest 119(7): 1745-54.

Reinhold, D., T. Kahne, et al. (1997). "The effect of anti-CD26 antibodies on DNA synthesis and cytokine production (IL-2, IL-10 and IFN-gamma) depends on enzymatic activity of DP IV/CD26." Adv Exp Med Biol 421: 149-55.

Romani, L., F. Fallarino, et al. (2008). "Defective tryptophan catabolism underlies inflammation in mouse chronic granulomatous disease." Nature 451(7175): 211-5.

Rosen, D. B., J. Bettadapura, et al. (2005). "Cutting edge: lectin-like transcript-1 is a ligand for the inhibitory human NKR-P1A receptor." J Immunol 175(12): 7796-9.

Rodriguez, P. C., A. H. Zea, et al. (2003). "L-arginine consumption by macrophages modulates the expression of CD3 zeta chain in T lymphocytes." J Immunol 171(3): 1232-9.

Rosen, D. B., W. Cao, et al. (2008). "Functional consequences of interactions between human NKR-P1A and its ligand LLT1 expressed on activated dendritic cells and B cells." J Immunol 180(10): 6508-17.

Rushbrook, S. M., M. Hoare, et al. (2007). "T-regulatory lymphocytes and chronic viral hepatitis." Expert Opin Biol Ther 7(11): 1689-703.

Salazar-Mather, T. P., J. S. Orange, et al. (1998). "Early murine cytomegalovirus (MCMV) infection induces liver natural killer (NK) cell inflammation and protection through macrophage inflammatory protein 1alpha (MIP-1alpha)-dependent pathways." J Exp Med 187(1): 1-14.

Sallusto, F., A Lanavecchia (2009). " Human Th17 cells in infection and autoimmunity." Microbes and Infection 11:620-624.

Savage, A. K., M. G. Constantinides, et al. (2008). "The transcription factor PLZF directs the effector program of the NKT cell lineage." Immunity 29(3): 391-403.

Shen, T., J. Zheng, et al. (2010). "PD-1 expression on peripheral CD8+ TEM/TEMRA subsets closely correlated with HCV viral load in chronic hepatitis C patients." Virol J 7: 310.

Shin, T., T. Nakayama, et al. (2001). "Inhibition of tumor metastasis by adoptive transfer of IL-12-activated Valpha14 NKT cells." Int J Cancer 91(4): 523-8.

SMYTH, G. K. (2005). LIMMA: LINEAR MODELS FOR MICROARRAY DATA. BIOINFORMATICS AND COMPUTATIONAL BIOLOGY SOLUTIONS USING R AND BIOCONDUCTOR. G. R. NEW YORK, SPRINGER-VERLAG: 397-420.

Spangenberg, H. C., S. Viazov, et al. (2005). "Intrahepatic CD8+ T-cell failure during chronic hepatitis C virus infection." Hepatology 42(4): 828-37.

Spits, H. and J. P. Di Santo. (2011). "The expanding family of innate lymphoid cells: regulators and effectors of immunity and tissue remodeling." Nat Immunol 12(1): 21-7.

Subramanian, A., P. Tamayo, et al. (2005). "Gene set enrichment analysis: a knowledge-based approach for interpreting genome-wide expression profiles." Proc Natl Acad Sci U S A 102(43): 15545-50.

Sugimoto, K., A. Ogawa, et al. (2008). "IL-22 ameliorates intestinal inflammation in a mouse model of ulcerative colitis." J Clin Invest 118(2): 534-44.

Suzuki, H., G. S. Duncan, et al. (1997). "Abnormal development of intestinal intraepithelial lymphocytes and peripheral natural killer cells in mice lacking the IL-2 receptor beta chain." J Exp Med 185(3): 499-505.

Takahashi, T., S. Dejbakhsh-Jones, et al. (2006). "Expression of CD161 (NKR-P1A) defines subsets of human CD4 and CD8 T cells with different functional activities." J Immunol 176(1): 211-6.

Takaki, A., M. Wiese, et al. (2000). "Cellular immune responses persist and humoral responses decrease two decades after recovery from a single-source outbreak of hepatitis C." Nat Med 6(5): 578-82.

Tanaka, T., D. Camerini, et al. (1992). "Cloning and functional expression of the T cell activation antigen CD26." J Immunol 149(2): 481-6.

Tang, X., I. Maricic, et al. (2007). "Anti-TCR antibody treatment activates a novel population of nonintestinal CD8 alpha alpha+ TCR alpha beta+ regulatory T cells and prevents experimental autoimmune encephalomyelitis." J Immunol 178(10): 6043-50.

Tang, X., I. Maricic, et al. (2006). "Regulation of immunity by a novel population of Qa-1-restricted CD8alphaalpha+TCRalphabeta+ T cells." J Immunol 177(11): 7645-55.

Terabe, M., Y. Tagaya, et al. (2008). "IL-15 expands unconventional CD8alphaalphaNK1.1+ T cells but not Valpha14Jalpha18+ NKT cells." J Immunol 180(11): 7276-86.

Tesmer, L. A., S. K. Lundy, et al. (2008). "Th17 cells in human disease." Immunol Rev 223: 87-113.

Thimme, R., J. Bukh, et al. (2002). "Viral and immunological determinants of hepatitis C virus clearance, persistence, and disease." Proc Natl Acad Sci U S A 99(24): 15661-8.

Thimme, R., C. Neumann-Haefelin, et al. (2008). "Adaptive immune responses to hepatitis C virus: from viral immunobiology to a vaccine." Biol Chem 389(5): 457-67.

Thimme, R., D. Oldach, et al. (2001). "Determinants of viral clearance and persistence during acute hepatitis C virus infection." J Exp Med 194(10): 1395-406.

Thomas, D. L., C. L. Thio, et al. (2009). "Genetic variation in IL28B and spontaneous clearance of hepatitis C virus." Nature 461(7265): 798-801.

Tilloy, F., E. Treiner, et al. (1999). "An invariant T cell receptor alpha chain defines a novel TAP-independent major histocompatibility complex class Ib-restricted alpha/beta T cell subpopulation in mammals." J Exp Med 189(12): 1907-21.

Tran, E. H., E. N. Prince, et al. (2000). "IFN-gamma shapes immune invasion of the central nervous system via regulation of chemokines." J Immunol 164(5): 2759-68.

Treiner, E., L. Duban, et al. (2003). "Selection of evolutionarily conserved mucosal-associated invariant T cells by MR1." Nature 422(6928): 164-9.

Trimble, L. A., L. W. Kam, et al. (2000). "CD3zeta and CD28 down-modulation on CD8 T cells during viral infection." Blood 96(3): 1021-9.

Trimble, L. A. and J. Lieberman (1998). "Circulating CD8 T lymphocytes in human immunodeficiency virus-infected individuals have impaired function and downmodulate CD3 zeta, the signaling chain of the T-cell receptor complex." Blood 91(2): 585-94.

Tu, Z., A. Bozorgzadeh, et al. (2008). "TLR-dependent cross talk between human Kupffer cells and NK cells." J Exp Med 205(1): 233-44.

Turtle, C. J., H. M. Swanson, et al. (2009). "A distinct subset of self-renewing human memory CD8+ T cells survives cytotoxic chemotherapy." Immunity 31(5): 834-44.

Unitt, E., S. M. Rushbrook, et al. (2005). "Compromised lymphocytes infiltrate hepatocellular carcinoma: the role of T-regulatory cells." Hepatology 41(4): 722-30.

Weber G, H. C. (1998). CD8. Roitt I. London, Elsevier: 475 - 478.

Weng, N. P., A. N. Akbar, et al. (2009). "CD28(-) T cells: their role in the age-associated decline of immune function." Trends Immunol 30(7): 306-12.

Werwitzke, S., A. Tiede, et al. (2003). "CD8beta/CD28 expression defines functionally distinct populations of peripheral blood T lymphocytes." Clin Exp Immunol 133(3): 334-43.

Werwitzke, S., A. Tiede, et al. (2008). "CD8alpha+beta(low) effector T cells in systemic lupus erythematosus." Scand J Immunol 67(5): 501-8.

Witte, T., R. Spoeri, et al (1999). " The CD8beta ectodomain contributes to the augmented coreceptor function of CD8alphabeta heterodimers relative to CD8alphaalpha homodimers." Cell Immunol 191(2): 90-96.

Wolk, K., E. Witte, et al. (2006). "IL-22 regulates the expression of genes responsible for antimicrobial defense, cellular differentiation, and mobility in keratinocytes: a potential role in psoriasis." Eur J Immunol 36(5): 1309-23.

Wong, J. S., X. Wang, et al. (2003). "Stalk region of beta-chain enhances the coreceptor function of CD8." J Immunol 171(2): 867-74.

Yamamoto, M., K. Fujihashi, et al. (1998). "A mucosal intranet: intestinal epithelial cells down-regulate intraepithelial, but not peripheral, T lymphocytes." J Immunol 160(5): 2188-96.

Yang, X. O., A. D. Panopoulos, et al. (2007). "STAT3 regulates cytokine-mediated generation of inflammatory helper T cells." J Biol Chem 282(13): 9358-63.

Yang, X. O., B. P. Pappu, et al. (2008). "T helper 17 lineage differentiation is programmed by orphan nuclear receptors ROR alpha and ROR gamma." Immunity 28(1): 29-39.

Yao, Z., W. C. Fanslow, et al. (1995). "Herpesvirus Saimiri encodes a new cytokine, IL-17, which binds to a novel cytokine receptor." Immunity 3(6): 811-21.

Ye, P., Z. H. Weng, et al. (2008). "Programmed death-1 expression is associated with the disease status in hepatitis B virus infection." World J Gastroenterol 14(28): 4551-7.

Yen, D., J. Cheung, et al. (2006). "IL-23 is essential for T cell-mediated colitis and promotes inflammation via IL-17 and IL-6." J Clin Invest 116(5): 1310-6.

Zaba, L. C., I. Cardinale, et al. (2007). "Amelioration of epidermal hyperplasia by TNF inhibition is associated with reduced Th17 responses." J Exp Med 204(13): 3183-94.

Zenewicz, L. A., G. D. Yancopoulos, et al. (2007). "Interleukin-22 but not interleukin-17 provides protection to hepatocytes during acute liver inflammation." Immunity 27(4): 647-59.

Zhang, G. X., B. Gran, et al. (2003). "Induction of experimental autoimmune encephalomyelitis in IL-12 receptor-beta 2-deficient mice: IL-12 responsiveness is not required in the pathogenesis of inflammatory demyelination in the central nervous system." J Immunol 170(4): 2153-60.

Zheng, Y., D. M. Danilenko, et al. (2007). "Interleukin-22, a T(H)17 cytokine, mediates IL-23-induced dermal inflammation and acanthosis." Nature 445(7128): 648-51.

Zheng, Y., P. A. Valdez, et al. (2008). "Interleukin-22 mediates early host defense against attaching and effacing bacterial pathogens." Nat Med 14(3): 282-9.

Zhu, J., H. Yamane, et al. (2010). "Differentiation of effector CD4 T cell populations. " Ann Rev Immunol 28:445-89

Appendix 1

Analysis of CD161 expression on human CD8$^+$ T cells defines a distinct functional subset with tissue-homing properties

Eva Billerbeck[a,1], Yu-Hoi Kang[b,1], Lucy Walker[b], Helen Lockstone[c], Stefanie Grafmueller[a], Vicki Fleming[b], Jonathan Flint[c], Chris B. Willberg[b], Bertram Bengsch[a], Bianca Seigel[a], Narayan Ramamurthy[b], Nicole Zitzmann[b], Eleanor J. Barnes[b], Jonarthan Thevanayagam[b], Anisha Bhagwanani[b], Alasdair Leslie[d], Ye H. Oo[e], Simon Kollnberger[d], Paul Bowness[d], Oliver Drognitz[f], David H. Adams[e], Hubert E. Blum[a], Robert Thimme[a,2], and Paul Klenerman[b,g,2,3]

[a]Department of Medicine II and Spemann Graduate School of Biology and Medicine, University of Freiburg, 79106 Freiburg, Germany; [b]Peter Medawar Building for Pathogen Research, Oxford OX1 3SY, United Kingdom; [c]Wellcome Trust Centre for Human Genetics, Oxford OX3 7BN, United Kingdom; [d]Weatherall Institute for Molecular Medicine, Oxford OX3 9TU, United Kingdom; [e]Institute for Biomedical Research, University of Birmingham, Birmingham B15 2TT, United Kingdom; [f]Department of Surgery, University Hospital Freiburg, 79106 Freiburg, Germany; and [g]Biomedical Research Centre, John Radcliffe Hospital, Oxford OX3 9TU, United Kingdom

Communicated by Rolf M. Zinkernagel, University Hospital Zurich, Zurich, Switzerland, December 28, 2009 (received for review August 5, 2009)

CD8$^+$ T lymphocytes play a key role in host defense, in particular against important persistent viruses, although the critical functional properties of such cells in tissue are not fully defined. We have previously observed that CD8$^+$ T cells specific for tissue-localized viruses such as hepatitis C virus express high levels of the C-type lectin CD161. To explore the significance of this, we examined CD8$^+$CD161$^+$ T cells in healthy donors and those with hepatitis C virus and defined a population of CD8$^+$ T cells with distinct homing and functional properties. These cells express high levels of CD161 and a pattern of molecules consistent with type 17 differentiation, including cytokines (e.g., IL-17, IL-22), transcription factors (e.g., retinoic acid-related orphan receptor γ-t, $P = 6 \times 10^{-9}$; RUNX2, $P = 0.004$), cytokine receptors (e.g., IL-23R, $P = 2 \times 10^{-7}$; IL-18 receptor, $P = 4 \times 10^{-6}$), and chemokine receptors (e.g., CCR6, $P = 3 \times 10^{-8}$; CXCR6, $P = 3 \times 10^{-7}$; CCR2, $P = 4 \times 10^{-7}$). CD161$^+$CD8$^+$ T cells were markedly enriched in tissue samples and coexpressed IL-17 with high levels of IFN-γ and/or IL-22. The levels of polyfunctional cells in tissue was most marked in those with mild disease ($P = 0.0006$). These data define a T cell lineage that is present already in cord blood and represents as many as one in six circulating CD8$^+$ T cells in normal humans and a substantial fraction of tissue-infiltrating CD8$^+$ T cells in chronic inflammation. Such cells play a role in the pathogenesis of chronic hepatitis and arthritis and potentially in other infectious and inflammatory diseases of man.

hepatitis | hepatitis C virus | IL-17 | IL-22 | arthritis

The CD8$^+$ T lymphocyte response against human virus infections has been under intense scrutiny since the emergence of HIV and hepatitis C virus (HCV) as global health threats in the 1980s (1). In the past decade, the emergence of MHC class I peptide tetramer technology allowed, for the first time, detailed ex vivo analysis of the T cell responses to such infections, and comparisons of frequency and also phenotype. A common differentiation pathway for antiviral responses has been proposed (2), although it has been difficult to link differences in cellular phenotype to functions, and more importantly to clinical outcomes.

HCV infects nearly 200 million people globally and sets up persistent hepatitis leading over time to a high burden of liver failure and cancer (3). The outcome of infection is related to the CD4$^+$ and CD8$^+$ T cell response, as indicated by a wealth of studies involving host genetics, chimpanzee model infections, and human correlative analyses (4). In those in which persistence is established, CD8$^+$ T cell responses are weak or undetectable in blood, although they may be enriched in the liver (5). A number of potential viral mechanisms for evasion of CD8$^+$ T cell responses have been proposed, although most are common to all persistent virus models (including HIV and lymphocytic choriomeningitis virus in the mouse). These include escape in immunodominant peptides, immune exhaustion, induction of regulatory responses, and loss of CD4$^+$ T cell help (1). However, an alternative explanation is that this outcome reflects the induction of a CD8$^+$ T cell response of a distinct lineage as a result of the localized tissue expression of the virus.

We previously observed expression of CD161 (NKRP1A) (6) on circulating virus-specific T cells in patients with hepatitis B and C, and the levels were higher on the tissue-infiltrating populations of such cells (7). Such expression was not found on T cells specific for most other viruses tested, including HIV, CMV, and EBV. CD161 expression therefore represents a unique potential marker of CD8$^+$ T cells that might potentially differentiate responses targeting specific organs, e.g., the liver. This idea is supported by the close association between CD161 and CXCR6 expression in peripheral blood CD8$^+$ T cells (7). CXCR6 is a chemokine receptor, which binds CXCL16, a chemokine that is constitutively expressed in organs such liver and respiratory tract (8), although it can be induced in other inflamed tissues such as joints (9). Modulation of CXCR6 signaling in murine models disrupts normal tissue immunosurveillance and impairs local immune responses (10–12).

We therefore tested the hypothesis that CD161 expression might define a subset of CD8$^+$ T cells with a distinct differentiation program, leading to a novel phenotype, homing, and function.

Results

CD161^{++} CD8$^+$T Cell Populations Contain the T_C17 Subset. We first examined CD161$^+$CD8$^+$CD3$^+$ T cell populations from healthy donors. We observed two populations of CD161$^+$CD8$^+$CD3$^+$ T cells based on the staining intensity of CD161 (13), CD161^{bright} (CD161^{++}) cells (15% of total CD8 T cells), and CD161^{mid} (CD161$^+$) cells (10% of CD8$^+$ T cells; Fig. 1*A*). After PMA/ionomycin stimulation, CD161^{++} CD8$^+$ T cells secreted IFN-γ and high levels of TNFα (Fig. 1*B*).

It has recently been shown independently that CD161 is highly expressed on human CD4$^+$ T helper cells of the type 17 lineage

Author contributions: N.Z., P.B., D.H.A., H.B., R.T., and P.K. designed research; E. Billerbeck, Y.-H.K., L.W., S.G., V.F., C.B.W., B.B., B.S., N.R., E.J. Barnes, J.T., A.B., A.J.L., Y.O., S.K., and O.D. performed research; H.L. and J.F. analyzed data; and H.B., R.T., and P.K. wrote the paper.

The authors declare no conflict of interest.

Freely available online through the PNAS open access option.

[1]E.B. and Y.-H.K. contributed equally to this work.

[2]R.T. and P.K. contributed equally to this work.

[3]To whom correspondence should be addressed. E-mail: paul.klenerman@ndm.ox.ac.uk.

This article contains supporting information online at www.pnas.org/cgi/content/full/0914839107/DCSupplemental.

IMMUNOLOGY

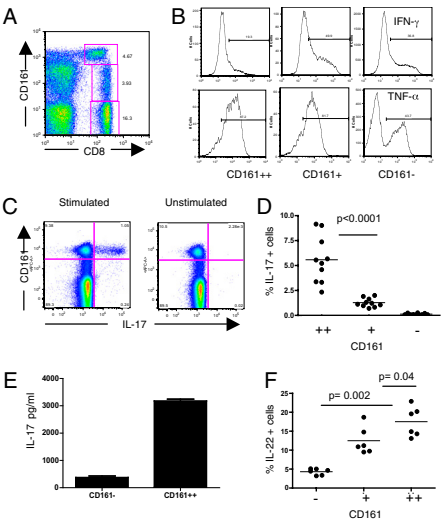


Fig. 1. Function of CD161-expressing CD8$^+$ T cells. (*A*) FACS profile of CD161 expression on CD3$^+$CD8$^+$ T cells in healthy donors. Cells within the live lymphocyte CD3$^+$ gate are shown. The gates shown here were also the gates used for sorting (*B*). Panels show PMA/ionomycin–stimulated expression of IFN-γ (*Upper*) and TNF-α (*Lower*) according to CD161 expression, using gates as indicated in Fig 1*A*. Unstimulated controls are shown in Fig. S1*D*. (*C*) IL-17 production in PMA/ionomycin–stimulated cells (gated as in Fig 1*A*). (*D*) Group data from 10 healthy control subjects showing percentage of IL-17 production in CD161^{++}, CD161$^+$, and CD161$^-$ CD8$^+$ T cells. (*E*). Secretion of IL-17 as measured by ELISA after stimulation of sorted cells. ICS is shown below for comparison. One representative experiment of two is shown. (*F*) Expression of IL-22 in healthy donors. Healthy donor PBMCs were stimulated as in Fig 1*B* and IL-22 secretion determined in CD161^{++} cells. The percentage of cells staining positive is indicated.

(T_H17) (14, 15). T_H17 cells are defined by secretion of the cytokine IL-17 (16) and play an important role in tissue inflammation. T_H17 cells are characterized by, among others, the expression of the transcription factor retinoic acid–related orphan receptor γ-t (RORγt) (17, 18), the IL-23 receptor (IL23R) (19) and the chemokine receptor CCR6 (20). IL-17 is secreted not only by T_H17 cells but may also be produced by several other cell types, including CD8$^+$ T cells in mouse (21) and man (22). We therefore tested for IL-17 secretion in stimulated CD8$^+$ T cells and observed striking populations of IL-17–secreting CD8$^+$ T cells restricted to the CD161^{++} T cell subset (Fig. 1*C*), consistent across all donors (Fig. 1*D*; $P < 0.0001$). IL-17 secretion by CD161^{++}CD8$^+$ T cells was confirmed by analysis of supernatants in sorted, stimulated cells (Fig. 1*E*).

IL-17–secreting human T lymphocytes may also cosecrete IFN-γ (14, 15, 22). CD161^{++} CD8$^+$ T cells showed three populations of IFN-γ$^+$, IL-17$^+$, and IFN-γ/IL-17–cosecreting cells (Fig. S1*A*). Among CD4$^+$ T cells, IL-17 secretion and IFN-γ/IL-17 cosecretion was also associated with CD161 expression (although a CD161^{++} population is not distinct; Fig S1 *B* and *C*) (14, 15). In these assays, IL-17 was produced by 4.5% of CD161^{++} CD8$^+$ T cells in healthy blood, (range, 2.1% to 7.1%). This compares to 5.5% of CD161$^+$ CD4$^+$ T cells [range, 2.6% to 8.9%; *P* value not significant (NS); Fig. S1*C*].

We also showed that CD161$^{+/++}$ CD8$^+$ T cell populations secrete high levels of IL-22, a cytokine involved in tissue repair and epithelial defense (23) and linked to a Th17 phenotype (Fig. 1*F*).

Expression and Phenotypic Analysis of CD161^{++} CD8$^+$ T Cells. To define the detailed characteristics of the CD161^{++} CD8$^+$ T cell subset, we performed expression profiling of sorted lymphocytes ex vivo (Fig. 2 and Table S1). Differential gene expression among CD161^{++}, CD161$^+$, and CD161$^-$ cells was assessed for the three possible group comparisons. We identified a number of up-regulated genes relating to type 17 cell differentiation. First, RORγt (RORC)—the key transcription factor—was the most highly discriminatory transcript comparing CD161^{++} and CD161$^-$ cells (5.88 $\log_2$ fold change; adjusted $P = 5.78 \times 10^{-9}$; Fig. 2*A*). Comparing CD161^{++} versus CD161$^+$, RORγt was expressed as the second most significant differential signal (3.91 $\log_2$ fold change; adjusted $P = 1.87 \times 10^{-6}$). Elevated expression was confirmed by qRT-PCR, and RORγt staining was observed using flow cytometry (Fig. 2*B*) and immunofluorescence on sorted CD161^{++} cells (Fig. 2*C*).

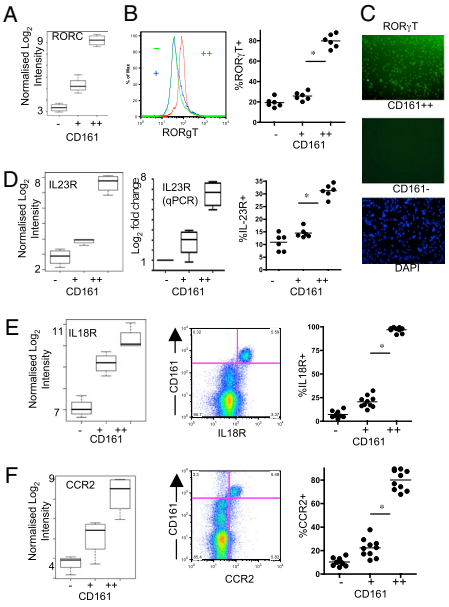


Fig. 2. Phenotype of CD161^{++} cells (*A*) Relative expression of levels of RORC (RORγt) in CD161$^-$, CD161$^+$, and CD161^{++} sorted CD8$^+$ T cells (shown as –, $^+$, and $^{++}$). Data are derived from the RNA expression analyses after normalization among the 12 samples ($n = 4$ per group). (*B*) Expression of RORγT by flow cytometry in CD161^{++}, CD161$^+$, and CD161$^-$ CD3$^+$CD8$^+$ T cells. Representative histogram plot (*Left*) and combined data (*Right*); *$P = 0.002$. (*C*) Expression of RORγT by immunofluorescence of sorted CD161^{++} cells (*Upper*) and CD161$^-$ cells (*Lower*); DAPI staining is shown for CD161$^-$ cells. Magnification: ×200. (*D*) Expression of IL23R by gene array (*Left*), qRT-PCR (*Center*), and flow cytometry (*Right*). Combined staining from six healthy donors is shown. (*E*) IL-18 receptor (IL18R) expression on CD161^{++} cells: gene expression (*Left*), example flow cytometry (*Center*), and group flow cytometry data (*Right*). *$P < 0.0001$. (*F*) CCR2 expression on CD161^{++} cells displayed as in Fig 1*E*.

We also observed clear up-regulation of relevant chemokine receptors: IL23R was up-regulated in the gene array (confirmed by qRT-PCR and flow cytometry; Fig. 2*D*) and also IL-18 receptor, shown to be coordinately important in type 17 differentiation (20, 24) (Fig. 2*E*). Chemokine receptors CCR6 (20) and CCR2 (25), both associated with IL-17–secreting T cells, were up-regulated at the RNA and protein level (Fig. 2*F* and Fig. S2*A*). Expression of the chemokine receptor CXCR6 was also tightly linked to $CD161^{++}$ (but not $CD161^{+}$ $CD161^{+}$) expression on $CD8^{+}$ T cells (Fig. S2*B*). CXCR6 is of specific interest for tissue homing T cells through triggering via locally expressed CXCL16 (7–10).

A number of other genes potentially contributing to type 17 differentiation, including the transcription factors RORα (18) (log_2 fold change, 1.6; adjusted $P = 0.02$) and RUNX2 (26) (log_2 fold change, 1.3; adjusted $P = 0.004$) were up-regulated; elevated RUNX2 expression was confirmed by flow cytometry (mean fluorescence intensity, 988 vs. 392; $P = 0.03$). Additionally, CYP1B1 (downstream of the aryl hydrocarbon receptor) was overexpressed in $CD161^{++}$ cells (log_2 fold change, 1.9; adjusted $P = 0.007$) (27).

We also observed down-regulation of specific molecules in $CD161^{++}$ cells. This included reduction in the expression of CXCR3 in $CD161^{++}CD8^{+}$ T cells (Fig S2*C*); additionally CCR7 was low in both $CD161^{+}$ and $CD161^{++}$ subsets (Fig S2*D*). We also observed low expression of granzyme B and perforin (Fig S3 *A* and *B*). Degranulation, as assessed by CD107a up-regulation, was seen in this population, although the level of CD107a staining was lower than in $CD161^{+}$ cells (Fig S3*C*). A similar phenotype of T_C17 cells with low levels of cytolytic granules and limited cytolytic capacity has been recently reported in the mouse (21).

Further analysis of memory and maturation markers in healthy donors was consistent with $CD161^{++}$ cells representing an "effector" memory population (7, 13), with a distinct phenotype that was not "exhausted" or "terminally differentiated" ($PD\text{-}1^{lo}$, $CD127^{hi}$, $KLRG1^{hi}$, $CD45R0^{+}$, $CD27^{hi}$, $CD28^{hi}$; Figs. S3 and S4).

We confirmed that the populations studied represented conventional TCR-αβ T cells, rather than TCR-γδ T cells or natural killer (NK) T cells (Fig. S5): we have previously shown that conventional CD1d-restricted NKT cells in man constitute only a very small fraction (<0.1%) of total $CD3^{+}$ T cells in blood and typically <0.5% in liver, and most are $CD8^{-}$ (28, 29). Additionally, although the $CD161^{++}$ subset showed reduced CD8 expression, they were $CD4^{-}$ (Fig. S5*D*).

Enrichment of $CD161^{++}$ T_C17 Cells in the Liver During Chronic Hepatitis C. To address the question of whether IL-17–secreting $CD8^{+}$ T cells (T_C17) are involved in the immunopathogenesis of tissue-localized persistent virus infection, we examined the frequency of T_C17 cells in $CD8^{+}$ populations, initially expanded from blood and liver of chronically HCV-infected patients (30), upon stimulation with PMA/ionomycin (Fig. 3). In this well established method, $CD8^{+}$ T cells are stimulated using anti-CD3 and feeder cells for 3 weeks in vitro with supplementary IL-2 but without antigen. Exactly the same procedure is performed in parallel using peripheral blood mononuclear cells (PBMCs) and liver-infiltrating lymphocytes (LILs; *SI Methods*). We found a marked enrichment of such Tc17 cells in liver compared with blood ($P < 0.0001$; Fig. 3*A* and *B*). This enrichment was much more significant than that of total IFN-γ–secreting cells (P = NS; Fig. 3*A* and *B*). Intrahepatic IL-17–secreting $CD8^{+}$ T cells expressed high levels of CD161 (Fig. 3*C*).

Because in vitro expansion can modulate the functions of T cells and could have been responsible for induction of a Tc17 phenotype, we analyzed these populations ex vivo by using liver explant tissue. Similarly, substantial populations of $CD8^{+}CD161^{++}$ T cells secreting IL-17 were found in liver-infiltrating lymphocytes tested directly ex vivo after PMA/ionomycin stimulation (Fig. S6). Among these cells, substantial IFN-γ/IL-17 coexpression was also observed: we noted that the highest levels of IFN-γ were seen among the dual IFN-γ/IL-17–secreting cell subset compared with IFN-γ monosecretors (Fig. S6*B*; $P = 0.006$). Enrichment of $CD161^{++}$ $CD8^{+}$ T cells in the liver was associated with substantial reductions of the same populations in peripheral blood, and was not seen for $CD161^{+}$ cells, suggestive of specific redistribution in vivo (Fig. S6 *C* and *D*).

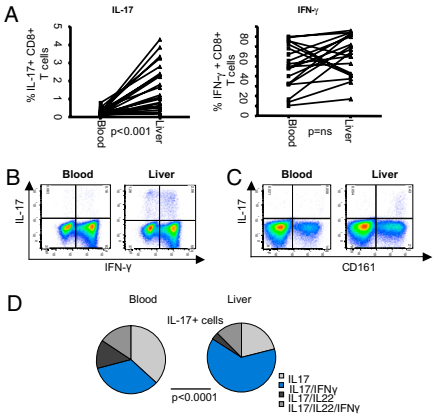


Fig. 3. Peripheral and intrahepatic distribution of IL-17–secreting $CD8^{+}$ T cells during chronic HCV infection. (*A*) Analysis of intracellular production of IL-17 and IFN-γ after stimulation with PMA/ionomycin in $CD8^{+}$ T cells expanded from PBMCs and livers of HCV-infected patients. (*B*) FACS plot from one representative subject showing the distribution of IL-17– and IFN-γ–secreting $CD8^{+}$ T cells in blood and liver. (*C*) Representative FACS plot showing CD161 expression on peripheral and intrahepatic IL-17–secreting $CD8^{+}$ T cells. (*D*) Polyfunctionality of $IL17^{+}$ cells: Percentages of IL-17–secreting, IL-17/IFN-γ–secreting, IL-17/IL-22–secreting, and IL-17/IL-22/IFN-γ–secreting cells among the liver and blood-derived IL-17–producing $CD8^{+}$ T cell populations.

Analysis of IL-22, IFN-γ Secretion, and IL-17 Secretion in Tissue-Homing Cells. IL-22 is also highly expressed by $CD161^{+}$ cells (Fig. 1*F*). We analyzed coexpression of IL-22 and IFN-γ with IL-17 in T_C17 populations expanded from blood and liver of chronically HCV infected patients as described earlier (Fig. 3*D*). IL-22 was coexpressed with IL-17 in a substantial proportion of cells, especially in those derived from liver. The majority of $IL\text{-}22^{+}$ cells also expressed IFN-γ. Comparing the fractions of cells coexpressing IL-22 and IFN-γ among T_C17 populations identified in blood and liver, the following features were noted: a significant intrahepatic enrichment of IL-17/IFN-γ dual secretors ($P = 0.0005$) and a reduction in intrahepatic IL-17 monosecretors ($P = 0.02$). Triple IL-17/IL-22/IFN-γ secretors were present in similar proportions in blood and liver.

Antigen-specific $CD8^{+}$ T cells constitute only only a fraction of the total $CD8^{+}$ T cell infiltrate during chronic hepatitis (5, 30). We therefore asked whether we could observe HCV-specific $CD8^{+}$ T cell populations in liver-infiltrating $CD8^{+}$ T cell populations using a modification of previously established methods to define IFN-γ–secreting populations (*Methods*). As described earlier, $CD8^{+}$ T cells from liver and peripheral blood were expanded using non-specific stimulation only for 3 weeks, supported by IL-2 supplementation. Expanded T cell populations were then tested against HCV-derived peptides to assess cytokine release. Analysis using

IMMUNOLOGY

cells found in normal humans and even in cord blood. As these cells in adults express RORγt and IL23R—both critical steps in differentiation (17–19, 26, 36)—we propose that the $CD161^{++}$ subset are polarized toward the type 17 lineage, even as naive cells, but may require other signals in vivo, e.g., through the aryl hydrocarbon receptor (27), to develop IL-17 and/or IL-22 secretion. The overexpression of RUNX2, another transcription factor, is consistent with a previously described interaction between this protein (as well as RUNX1) and RORγt, which leads to up-regulation of IL-17 (26).

Studies in Tbet- and Eomes-deficient mice have recently indicated that type 17 $CD8^+$ T cells occur under certain polarized conditions, and suggested that they may play a role in viral infection (37). In the lymphocytic choriomeningitis virus model used, cytolysis through perforin and granzyme B is critical to control of viremia; in contrast, in human HBV and HCV infection, there is good in vivo and in vitro evidence that IFN-γ secretion plays a dominant antiviral role (38, 39). The environment of specific organs may favor noncytolytic clearance mechanisms to avoid severe immunopathology (38). A recent report also shows a protective effect of T_C17 in a murine influenza challenge (21), driven by noncytolytic mechanisms. Overall, the protective or pathogenic role in any given clinical setting is likely to depend on the tissue concerned, the degree of viral cytopathic effect, and the chronicity of infection.

As far as HCV is concerned, the overall effect of $CD161^{-/+/++}$ populations in disease outcome and the role of antigen-specific versus antigen-nonspecific cells in tissue infiltrates still need to be defined; however, a potentially important association between $CD161^+$ Tc17 subsets and limited disease progression is reproducibly observed. If the effect is causal, the mechanism for this is not yet clear, even though the association was robust and reproducible. An alternative explanation for our findings, however, is that such functionality declines as disease progresses; further longitudinal studies are required to address this. Loss of functionality of $CD8^+$ T cells in the liver of HCV is known to occur, although we were unable to address this directly in this study.

More generally, $CD161^{++}$ $CD8^+$ T cells in vivo could possess critical functions in diverse tissues as a result of their specific tissue-homing and chemokine receptor expression (e.g., CXCR6 and CCR6). CCL20 (the ligand for CCR6) is constitutively highly expressed in the liver and tonsillar epithelia—consistent with the results shown—although it may be up-regulated at many peripheral sites during inflammation, as is CXCR6 (9, 34). We also show very striking enrichment of $CD161^{++}$Tc17 cells in inflamed joints from patients with autoimmune arthritis, in which they may play an important role in disease pathogenesis either directly or through recruitment of other cell types.

A key function is likely to be elevated secretion of cytoprotective IL-22 (33), which has specific protective activity in those tissues expressing IL22R (e.g., liver, gut, kidney) (23). Their action in such organs could also be indirect via activity of other inflammatory infiltrating cells (as appears to be the case in the murine lung) (21). Although IFN-γ is antiviral, IL-17 and IL-22 are not thought to have direct antiviral effects (40), but the latter can induce secretion of antibacterial peptides at epithelial surfaces (32).

Although culture conditions could have affected the results from the cytokine assays, we were able to robustly demonstrate IL-17/IFN-γ–coproducing cells in LILs studied directly ex vivo and thus it is clear the populations are detectable without further cytokine or proliferation-induced artifact. Currently, the ex vivo antigen-specific T cell populations were too infrequent to assay reliably by using flow cytometry for cosecretion of IFN-γ/IL-17, and further work, together with MHC class I peptide tetramer staining, is required to define their full functionality.

Studies are also required to define the mechanisms leading to the origin of the naïve $CD161^{++}$ T cells, their priming, and their role in healthy humans. The presence of "preconditioned" naive $CD8^+$ T cells with a distinct chemokine receptor profile ($CCR6^+$) is a striking result of this study and suggests that the transcriptional program associated with CD161 is of general significance. In this context, the roles of the known CD161 ligands [LLT-1 (41) and PILAR (42)] are not yet defined. CD161 triggering may inhibit lymphocyte activation (41, 43), although its impact on T_C17 functions has not been examined.

Finally, in addition to the data presented indicating enrichment of $CD161^+$ T cells in liver, upper respiratory tract, kidney, and joint, the finding of $CXCR6^+$ and/or $CCR6^+$ T cells in other organs suggest that the answers to such questions may be of widespread interest immunologically (44–46). Interestingly, polymorphisms in CD161 itself are implicated in multiple sclerosis (47). We therefore speculate that further definition of the lineage may provide novel therapeutic avenues in a number of important human diseases..

Methods

Chronically HCV-infected patients ($n = 81$), patients with nonviral hepatitis ($n = 12$), and healthy normal donors ($n = 15$) were enrolled in this study after informed consent and after appropriate ethical review in the authors' three institutions. The patient characteristics of the liver biopsy study cohorts (in Freiburg, Germany) are summarized in Table S2. PBMCs, liver cells, and liver-derived cell lines were prepared as described previously (30). Lymphocyte staining was performed on whole blood as described previously (7), using antibodies as indicated in *Methods*. Intracellular cytokine staining after PMA/ionomycin stimulation was performed as described previously (7, 30). Cells were analyzed on an LSRII machine, FACSCanto, or FACSCalibur machine (BD Biosciences) using FlowJo software. For immunologic studies, Spearman rank correlation and unpaired and paired Student *t* tests were used. For cell sorting experiments PBMCs (1×10^8) from four healthy donors were stained with CD161, CD3, and CD8 and sorted to >95% purity on a MoFlo MLS cell sorter (Dako). Three sorted CD8 cell subsets from each donor (12 in total) were lysed and homogenized using a QIAshredder spin column (Qiagen). Total RNA was extracted using an RNeasy Mini Kit (Qiagen) according to the manufacturer's instructions. cDNA was synthesized and cRNA was amplified and purified using Illumina TotalPrep RNA amplification kit (Ambion). cRNA was hybridized to Illumina Sentrix Human Whole Genome 6 BeadChips (Illumina) and scanned with an Illumina BeadArray Reader. Details of the downstream analysis are included in *SI Methods*. Antiviral assays were performed using the HCV replicon system as previously described (48), using human recombinant IFNγ (Biomol) or IL-17 (Immunotools). After 48 h of incubation at 37°C, luciferase activity was assessed by using the Steady-Glo Luciferase Assay System (Promega) according to the manufacturer's instructions and a Lumat LB 9507 (Berthold). Further details are available in *SI Methods*.

ACKNOWLEDGMENTS. We are grateful to Marella de Bruin, Chris Norbury, Arian Laurence, Rodney Phillips, and Philip Goulder for helpful comments, and Hanspeter Pircher for providing the KLRG1 antibody. This study was funded by the Wellcome Trust; the Medical Research Council; the James Martin School of the 21st Century, Oxford; The Deutsche Forschungsgemeinschaft; National Institute for Health Research Biomedical Research Centre Program; and National Institutes of Health Grant U19 AI082630.

1. Klenerman P, Hill A (2005) T cells and viral persistence: lessons from diverse infections. *Nat Immunol* 6:873–879.
2. Appay V, et al. (2002) Memory $CD8^+$ T cells vary in differentiation phenotype in different persistent virus infections. *Nat Med* 8:379–385.
3. Lauer GM, Walker BD (2001) Hepatitis C virus infection. *N Engl J Med* 345:41–52.
4. Bowen DG, Walker CM (2005) Adaptive immune responses in acute and chronic hepatitis C virus infection. *Nature* 436:946–952.
5. He XS, et al. (1999) Quantitative analysis of hepatitis C virus-specific CD8(+) T cells in peripheral blood and liver using peptide-MHC tetramers. *Proc Natl Acad Sci USA* 96: 5692–5697.
6. Lanier LL, Chang C, Phillips JH (1994) Human NKR-P1A. A disulfide-linked homodimer of the C-type lectin superfamily expressed by a subset of NK and T lymphocytes. *J Immunol* 153:2417–2428.
7. Northfield JW, et al. (2008) CD161 expression on hepatitis C virus-specific CD8+ T cells suggests a distinct pathway of T cell differentiation. *Hepatology* 47:396–406.
8. Freeman CM, Curtis JL, Chensue SW (2007) CC chemokine receptor 5 and CXC chemokine receptor 6 expression by lung CD8+ cells correlates with chronic obstructive pulmonary disease severity. *Am J Pathol* 171:767–776.
9. Nanki T, et al. (2005) Pathogenic role of the CXCL16-CXCR6 pathway in rheumatoid arthritis. *Arthritis Rheum* 52:3004–3014.

10. Geissmann F, et al. (2005) Intravascular immune surveillance by CXCR6+ NKT cells patrolling liver sinusoids. *PLoS Biol* 3:e113.
11. Sato T, et al. (2005) Role for CXCR6 in recruitment of activated CD8+ lymphocytes to inflamed liver. *J Immunol* 174:277–283.
12. Kim CH, et al. (2001) Bonzo/CXCR6 expression defines type 1-polarized T-cell subsets with extralymphoid tissue homing potential. *J Clin Invest* 107:595–601.
13. Takahashi T, Dejbakhsh-Jones S, Strober S (2006) Expression of CD161 (NKR-P1A) defines subsets of human CD4 and CD8 T cells with different functional activities. *J Immunol* 176:211–216.
14. Cosmi L, et al. (2008) Human interleukin 17-producing cells originate from a CD161+ CD4+ T cell precursor. *J Exp Med* 205:1903–1916.
15. Kleinschek MA, Boniface K, Sadekova S, Grein J, Murphy EE, et al. (2009) Circulating and gut-resident human Th17 cells express CD161 and promote intestinal inflammation *J Exp Med*.
16. Yao Z, et al. (1995) Herpesvirus Saimiri encodes a new cytokine, IL-17, which binds to a novel cytokine receptor. *Immunity* 3:811–821.
17. Ivanov II, et al. (2006) The orphan nuclear receptor RORgammat directs the differentiation program of proinflammatory IL-17+ T helper cells. *Cell* 126:1121–1133.
18. Yang XO, et al. (2008) T helper 17 lineage differentiation is programmed by orphan nuclear receptors ROR alpha and ROR gamma. *Immunity* 28:29–39.
19. Veldhoen M, Hocking RJ, Atkins CJ, Locksley RM, Stockinger B (2006) TGFbeta in the context of an inflammatory cytokine milieu supports de novo differentiation of IL-17-producing T cells. *Immunity* 24:179–189.
20. Acosta-Rodriguez EV, et al. (2007) Surface phenotype and antigenic specificity of human interleukin 17-producing T helper memory cells. *Nat Immunol* 8:639–646.
21. Hamada H, et al. (2009) Tc17, a unique subset of CD8 T cells that can protect against lethal influenza challenge. *J Immunol* 182:3469–3481.
22. Kondo T, Takata H, Matsuki F, Takiguchi M (2009) Cutting edge: Phenotypic characterization and differentiation of human CD8+ T cells producing IL-17.*J Immunol* 182:1794–1798.
23. Wolk K, et al. (2004) IL-22 increases the innate immunity of tissues. *Immunity* 21: 241–254.
24. Mathur AN, et al. (2007) Stat3 and Stat4 direct development of IL-17-secreting Th cells. *J Immunol* 178:4901–4907.
25. Sato W, Aranami T, Yamamura T (2007) Cutting edge: Human Th17 cells are identified as bearing CCR2+CCR5- phenotype. *J Immunol* 178:7525–7529.
26. Zhang F, Meng G, Strober W (2008) Interactions among the transcription factors Runx1, RORgammat and Foxp3 regulate the differentiation of interleukin 17-producing T cells. *Nat Immunol* 9:1297–1306.
27. Veldhoen M, et al. (2008) The aryl hydrocarbon receptor links TH17-cell-mediated autoimmunity to environmental toxins. *Nature* 453:106–109.
28. Lucas M, et al. (2003) Frequency and phenotype of circulating Valpha24/Vbeta11 double-positive natural killer T cells during hepatitis C virus infection. *J Virol* 77: 2251–2257.
29. Karadimitris A, et al. (2001) Human CD1d-glycolipid tetramers generated by in vitro oxidative refolding chromatography. *Proc Natl Acad Sci USA* 98:3294–3298.
30. Spangenberg HC, et al. (2005) Intrahepatic CD8+ T-cell failure during chronic hepatitis C virus infection. *Hepatology* 42:828–837.
31. Rowan AG, et al. (2008) Hepatitis C virus-specific Th17 cells are suppressed by virus-induced TGF-beta. *J Immunol* 181:4485–4494.
32. Aujla SJ, et al. (2008) IL-22 mediates mucosal host defense against Gram-negative bacterial pneumonia. *Nat Med* 14:275–281.
33. Zenewicz LA, et al. (2007) Interleukin-22 but not interleukin-17 provides protection to hepatocytes during acute liver inflammation. *Immunity* 27:647–659.
34. Schutyser E, Struyf S, Van Damme J (2003) The CC chemokine CCL20 and its receptor CCR6. *Cytokine Growth Factor Rev* 14:409–426.
35. Liu H, Rohowsky-Kochan C (2008) Regulation of IL-17 in human CCR6+ effector memory T cells. *J Immunol* 180:7948–7957.
36. McGeachy MJ, Cua DJ (2008) Th17 cell differentiation: the long and winding road. *Immunity* 28:445–453.
37. Intlekofer AM, et al. (2008) Anomalous type 17 response to viral infection by CD8+ T cells lacking T-bet and eomesodermin. *Science* 321:408–411.
38. Guidotti LG, et al. (1999) Viral clearance without destruction of infected cells during acute HBV infection. *Science* 284:825–829.
39. Jo J, et al. (2008) Analysis of CD8(+) T cell-mediated inhibition of hepatitis c virus replication using a novel immunological model. *Gastroenterology* 136:1391–1401.
40. Dambacher J, et al. (2008) The role of interleukin-22 in hepatitis C virus infection. *Cytokine* 41:209–216.
41. Aldemir H, et al. (2005) Cutting edge: lectin-like transcript 1 is a ligand for the CD161 receptor. *J Immunol* 175:7791–7795.
42. Huarte E, et al. (2008) PILAR is a novel modulator of human T-cell expansion. *Blood* 112:1259–1268.
43. Rosen DB, et al. (2005) Cutting edge: lectin-like transcript-1 is a ligand for the inhibitory human NKR-P1A receptor. *J Immunol* 175:7796–7799.
44. van der Voort R, et al. (2005) Elevated CXCL16 expression by synovial macrophages recruits memory T cells into rheumatoid joints. *Arthritis Rheum* 52:1381–1391.
45. Ludwig A, et al. (2005) Enhanced expression and shedding of the transmembrane chemokine CXCL16 by reactive astrocytes and glioma cells. *J Neurochem* 93: 1293–1303.
46. Morgan AJ, et al. (2005) Expression of CXCR6 and its ligand CXCL16 in the lung in health and disease. *Clin Exp Allergy* 35:1572–1580.
47. Hafler DA, et al.; International Multiple Sclerosis Genetics Consortium (2007) Risk alleles for multiple sclerosis identified by a genomewide study. *N Engl J Med* 357: 851–862.
48. Schaller T, et al. (2007) Analysis of hepatitis C virus superinfection exclusion by using novel fluorochrome gene-tagged viral genomes. *J Virol* 81:4591–4603.

Supporting Information

Billerbeck et al. 10.1073/pnas.0914839107

SI Methods

Antibodies and Staining. Anti–CD8-PerCP, anti–CD8-PE, anti–CD8-PerCP-Cy5.5, anti–CD8-Alexa Fluor 700–anti–CD4-PerCP, anti–CD4-FITC, anti–CD4-APC, anti–IFN-γ-FITC, anti–TCRγδ-PE, anti–TCRαβ-PE, anti–TNF-α, isotype PE, isotype FITC, and isotype APC were obtained from BD Pharmingen. Anti-CD3-FITC/APC, anti–IL-22-APC, anti–CCR6-APC, anti–CCR2-APC, anti–CXCR6-PE, anti–CXCR3-FITC, anti–CCR7-FITC, biotinylated polyclonal goat anti–IL-23R, and anti–IFN-γ-FITC were obtained from R & D Systems; and anti–CD161-APC from Miltenyi Biotech. Anti–IL-17A-PE, anti–IL-17A-Alexa 647, anti-TCRαβ-APC, anti–CD127-PE, anti–RORγT-PE, and anti–IL18R-FITC were from eBioscience. Anti–CD161-PE, anti–CD3-ECD, and anti–TCRγδ-FITC were obtained from Immunotech/Beckman Coulter. Anti–granzyme B-APC and anti–CD3-Pacific Orange were obtained from Caltag Laboratories and anti–Vα24-FITC from Serotec. Anti-Runx2 was obtained from Santa Cruz Biotechnology. Anti-RORγT-Alexa 488 was obtained from Cambridge Biosciences. FITC- or APC-conjugated antibodies to CD45RA, CD45RO, CD38, CD62L, CD56, CD103, TGFβRII, PD-1, ICOS, GITR, CD38, CD62L, CCR5, CXCR4, CCR9, CD85j, CD27, and CD28 for studies in Fig. S4 were obtained from BD Pharmingen and R & D Systems. Extravidin-PE was obtained from Sigma.

For immunofluorescence experiments, $CD8^+$ T cells were isolated using an EasySep CD8 negative selection kit and positive PE selection beads (Stem Cell Technologies) following anti-IL18R or anti-CD161 staining. Cells were plated in eight-chamber slides coated with CC2 (Nunc), fixed with methanol/acetone, air dried, blocked with 1% BSA, and washed with PBS/Tween 1% solution before staining. For intracellular staining by flow cytometry permeabilization buffers from BD Biosciences and eBiosciences were used according to the manufacturer's instructions.

CD8 selection and polyclonal expansion of PBMCs. PBMCs (4×10^6) were resuspended in 5 mL PBS solution and incubated with CD8 Dynabeads (Invitrogen) for 20 min at 4 °C. Bound $CD4^+$ T cells were isolated by a particle magnetic concentrator. The purity of $CD4^+$ T cells was >95% by FACS analysis. The $CD4^+$ T cells were plated into one well of a 24-well plate (Greiner) in 1 mL complete medium (RPMI medium 1640 containing 10% FCS, 1% streptomycin/penicillin, and 1.5% 1 M Hepes containing 100 U/mL IL-2; Hoffmann-La Roche), 0.04 g/mL anti–human CD3 monoclonal antibody (Immunotech), and 2×10^6 irradiated autologous PBMCs as feeder cells. Twice per week, 1 mL of medium was exchanged and 100 U/mL IL-2 was added. After 3 weeks, the expanded $CD8^+$ PBMCs and intrahepatic lymphocytes were analyzed.

CD8 selection and polyclonal expansion of LILs. Briefly, the liver biopsy specimens were homogenized using a 70-m Dounce tissue grinder (BD Biosciences). Cell suspensions were incubated with CD8 Dynabeads (Invitrogen) for 20 min at 4 °C. Bound $CD8^+$ cells were isolated using a particle magnetic concentrator. The purity of $CD8^+$ cells was >95% by FACS analysis. The intrahepatic $CD4^+$ T cells were then expanded as described earlier for $CD8^+$ PBMCs. Importantly, the expansion of peripheral and intrahepatic $CD8^+$ T cells from a given patient was always performed in parallel and for the same time before analysis to obtain comparable results for both compartments. Tonsil/kidney–derived lymphocytes were prepared similarly, although without $CD8^+$ T cell selection and culture, and joint-derived lymphocytes prepared without the homogenization step.

ELISpot. To analyze HCV-specific cytokine–secreting $CD8^+$ T cells, ELISpot assays were performed with intrahepatic and peripheral $CD8^+$ T cells from chronically HCV-infected patients. Intrahepatic and peripheral $CD8^+$ T cells were isolated and expanded in an antigen nonspecific way (2 to 4 weeks). IL-17 ELISpot kits (R & D Systems) and IFN-γ ELISpot kits (Diaclone) were used according to the manufacturers' instructions, and 1×10^5 cells were plated per well. Peptides were added at a final concentration of 10 μg/mL per peptide and were combined in pools of 10 peptides, with each peptide being contained in two different pools in a matrix setup, allowing the identification of single positive peptides. Tests with peptide pools were performed in duplicates; two wells without peptides served as negative controls; four wells each stimulated with PMA/ionomycin served as positive controls. Responses were considered positive if the number of spots per well was at least three times as high as the mean of negative controls (typically 0 to 2 spots per well). Overlapping peptides derived from HCV strain H77 (genotype 1a) spanning 18 aa and overlapping by 11 aa were obtained from Beiresources (National Institutes of Health Biodefense and Emerging Infections Research Resources Repository).

ELISA. Purified $CD161^-$ or $CD161^+$ $CD8^+$ T cells (1×10^5 per well) were cultured in a 96-well plate and stimulated with PMA/ionomycin for 48 h. The concentrations of IL-17 and IFN-γ in the supernatants were analyzed using human IL-17 or INF-γ Duoset ELISA (R & D Systems) according to the manufacturer's instructions.

Microarray Data Analysis. Gene expression profiles for three sorted CD8 cell subsets from each of four healthy donors were obtained using Illumina Sentrix Human Whole Genome 6 BeadChips. Raw data were exported from the BeadStudio software (v3.3.7; Illumina) for further processing and analysis using the R statistical software and BioConductor packages (1–5). Signal data and detection scores were extracted for each of the 12 samples. Signal data were background corrected using array-specific measures of background intensity based on negative control probes before being transformed and normalized using the vs.n2 BioConductor package.

After filtering out probes not detected in any of the 12 samples (detection score <0.95), 32,159 probes were retained for further analysis.

Statistical testing was performed using the Linear Models for Microarray Analysis (limma) BioConductor package. Three contrasts were generated corresponding to the possible cell type comparisons ($CD161^{++}$ vs. $CD161^+$, $CD161^{++}$ vs. $CD161^-$, $CD161^+$ vs. $CD161^-$), each using a paired design. Raw *P* values were corrected for multiple testing using the false discovery rate controlling procedure of Benjamini and Hochberg. Gene details were added to final probe lists using the relevant annotation file (HumanWG-6_V3_0_R0_11282955_A.txt) downloaded from the Illumina Web site (*http://www.illumina.com*).

RNA Isolation, cDNA Synthesis, and Quantitative RT-PCR. RNA was isolated from sorted cells using the miRNeasy Mini Kit (Qiagen). cDNA synthesis was performed using a mixture of random and oligo(dT) primers and SuperScript III reverse transcriptase (Invitogen). Quantitative real-time PCR reactions were carried out using a LightCycler 480 (Roche Diagnostics) and a combination of preoptimized Qiagen QuantiTect Primer Assays [IL-23R (Hs_IL23R_1_SG) and HPRT1 as an internal control

(Hs_HPRT1_1_SG)] and primers designed using Primer3[6] (RORc, 5′-AGAAGGACAGGGAGCCAAG-3′ for forward and 5′-CAAGGGATCACTTCAATTTGTG-3′ for reverse). LightCycler 480 SYBR Green I Master Mix (Roche) was used according to the manufacturer's instructions, with cycling conditions as follows: 95 °C for 15 min and 40 cycles of 94 °C for 15 s, 54 °C for 30 s, and 72 °C for 30 s. Fold expression changes were determined by the 2-ΔΔCT method (7).

1. R Development Core Team (2007) R: a language and environment for statistical computing (R Foundation, Vienna).
2. Gentleman RC, et al. (2004) Bioconductor: open software development for computational biology and bioinformatics. *Genome Biol* 5:R80.
3. Huber W, von Heydebreck A, Sültmann H, Poustka A, Vingron M (2002) Variance stabilization applied to microarray data calibration and to the quantification of differential expression. *Bioinformatics* 18 (suppl 1):S96–S104.
4. Smyth GK (2005) Limma: linear models for microarray data. In *Bioinformatics and computational biology solutions using R and Bioconductor*, ed Gentleman R (Springer-Verlag, New York), pp 397–420.
5. Benjamini Y, Hochberg Y (1995) Controlling the false discovery rate: a practical and powerful approach to multiple testing. *J R Stat Soc, B* 57:289–300.
6. Rozen S, Skaletsky H (2000) Primer3 on the WWW for general users and for biologist programmers. In *Bioinformatics methods and protocols: methods in molecular biology*, eds Krawetz S, Misener S (Humana Press, Totowa, NJ), pp 365–386.
7. Livak KJ, Schmittgen TD (2001) Analysis of relative gene expression data using real-time quantitative PCR and the 2(-delta delta C(T)) method. *Methods* 25: 402–408.

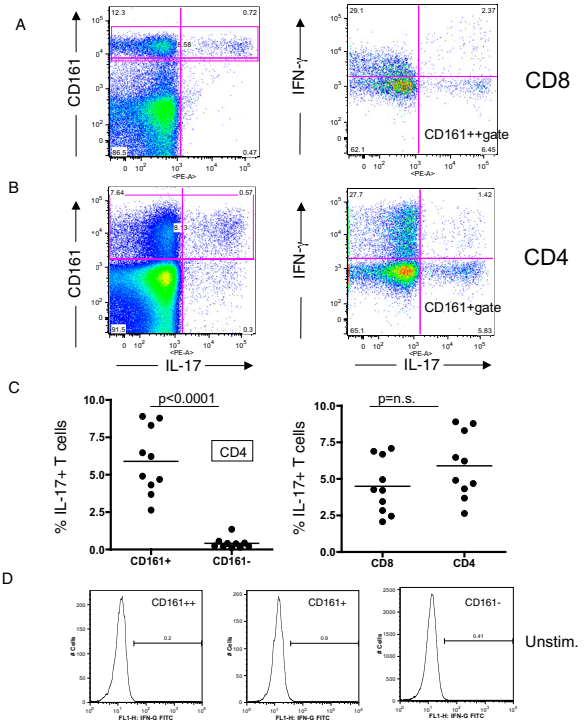


Fig. S1. Comparative secretion of IL-17 by CD161^{+} CD4^{+}, and CD8^{+} T cells in healthy donors. (*A*) IL-17 secretion in CD3^{+}CD8^{+} T cells after PMA/ionomycin stimulation (*Left*). Gating on CD161^{++} cells is indicated (*Left*) with analysis of secretion of IFN-γ and IL-17 in parallel (*Right*). Secretion of IFN-γ alone and IL-17 alone, and cosecretion of IL-17/IFN-γ is indicated among CD161^{++} T cells. (*B*) Identical experimental conditions and FACS display for CD3^{+}CD4^{+} T cells. (*C*) Distribution of IL-17–secreting cells according to CD161 expression (*Left*). CD161 expression in CD4^{+} T cells does not show clear distinction between bright and mid-staining populations as for CD8^{+} T cells. (*Right*) Comparison between IL-17 secretion in CD4^{+} and CD8^{+} CD161-expressing T cells (combined CD161^{+} and CD161^{++} in case of CD8^{+} T cells). No significant difference was found. (*D*) Unstimulated PBMCs gated according to CD161 expression among CD8^{+} T cells and stained for IFN-γ as example controls.

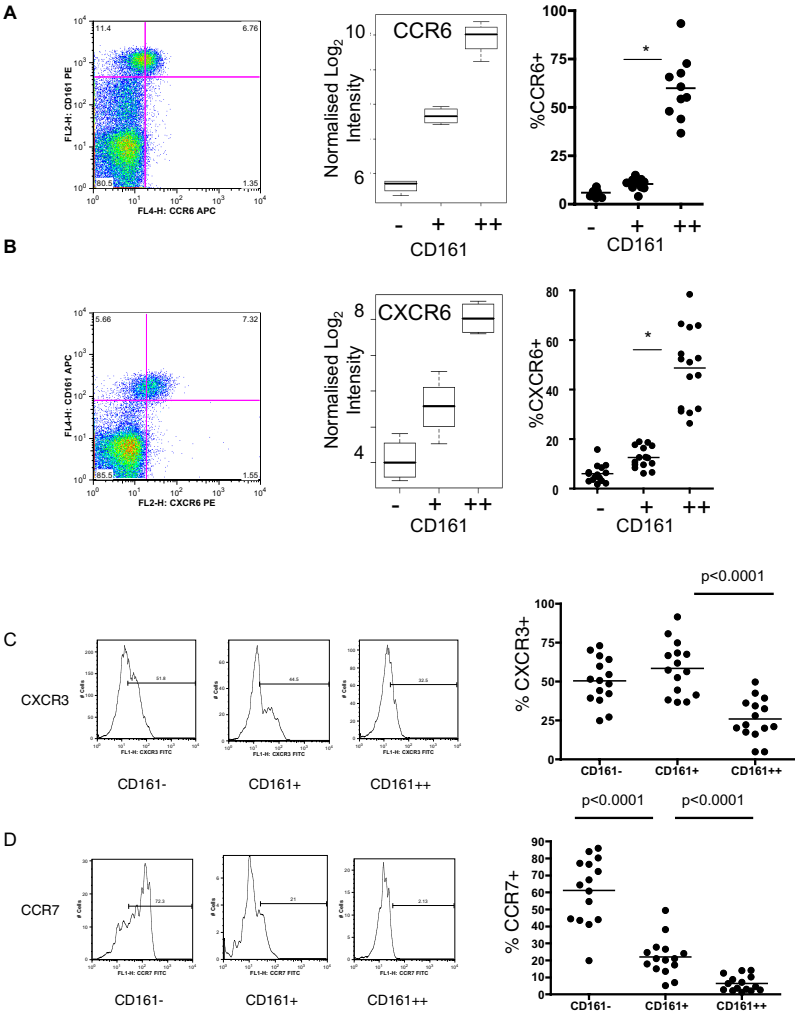


Fig. S2. Chemokine receptor expression on CD161^{++} CD8^{+} T cells. (*A*) Expression of CCR6: (*Right*) representative stain from healthy donor blood, gated on CD3^{+}CD8^{+} T cells; (*Middle*) normalized RNA expression from the microarrray as in Fig. 2 in the main text; (*Right*) group data from FACS staining from healthy donors (*$P < 0.0001$). (*B*) Expression of CXCR6. The data from healthy donors is displayed as for *A*. (*C*) Analysis of CXCR3 expression on CD161^{++}, CD161^{+}, and CD161^{-} CD8^{+} CD3^{+} T cells. Healthy donor PBMCs were analyzed using gates as in Fig. 1*A* in the main text and staining for chemokine receptor expression. Representative expression of CXCR3 is shown. (*Right*) Group expression data for CXCR3. (*D*) Analysis of CCR7 expression on CD161^{++}, CD161^{+}, and CD161^{-} cells. The data are displayed and analyzed exactly as in *C*.

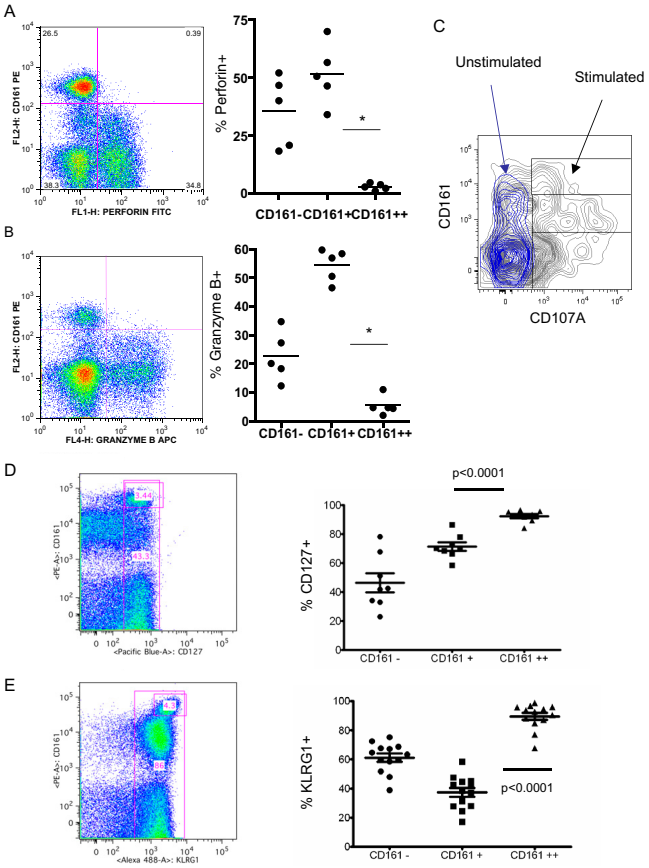


Fig. S3. Analysis of memory and maturation state. (*A*) Expression of perforin: (*Left*) example of low perforin expression in CD161^{++} CD8^{+} T cells; (*Right*) group data from healthy donors (*$P < 0.0001$). (*B*) Expression of granzyme B: data are displayed as in *A*. (*C*) CD107a up-regulation in CD161^{++} cells. The blue staining shows unstimulated cells and the black after PMA/ionomycin stimulation (one representative stain of three is shown). (*D* and *E*) For expression of CD127 and KLRG1, data are displayed as for *A*.

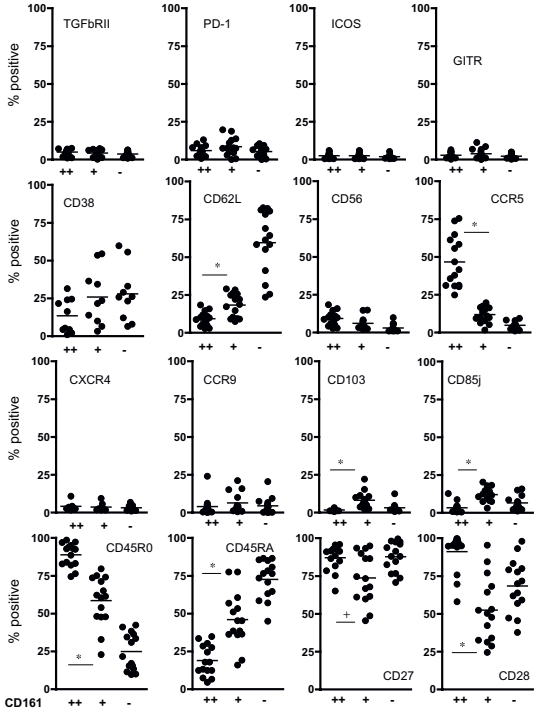


Fig. S4. Further analysis of phenotype of CD161^{++} CD8^{+} T cells CD3^{+}CD8^{+} T cells were costained with antibodies to surface receptors as shown. (Significant at $^{*}P < 0.001$; $^{+}P < 0.01$.)

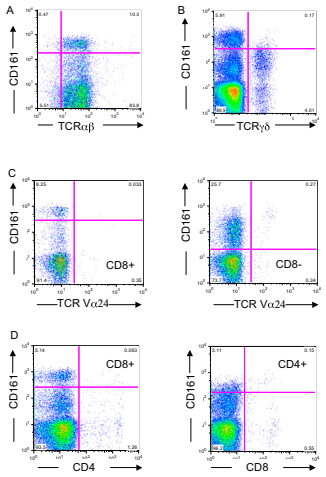


Fig. S5. Analysis of TCRαβ, TCRγδ, TCRVα24, and CD4 expression on CD161^{++} cells. (*A*) Analysis of TCRαβ expression in relation to CD161 expression on CD3$^+$CD8$^+$ T cells. A representative healthy donor is shown. (*B*) Analysis of TCRγδ expression as for *A*. A population of human TCRγδ cells is shown, which show CD161$^+$ expression only. (*C*) Analysis of Vα24 expression on CD161$^+$ CD8$^+$ CD3$^+$ T cells (*Left*) and CD8$^-$CD3$^+$ T cells (*Right*). We have previously extensively analyzed human PBMC for invariant chain Vα24/Vβ11 costaining and CD1d-α galactosyl ceramide tetramer staining, typical for classical human NKT cells. These populations represent, on average, 0.05% of T cells and only 20% express CD8; thus approximately 0.01% of CD8 T cells, compared with, typically, 15% CD161^{++} and 10% CD161$^+$ cells. (*D*) Analysis of CD4 expression on CD8$^+$CD161^{++} cells: (*Left*) analysis of CD4 on CD3$^+$ cells gated on CD8$^+$ population and (*Right*) expression of CD8 on CD3$^+$ cells gated on the CD4$^+$ population.

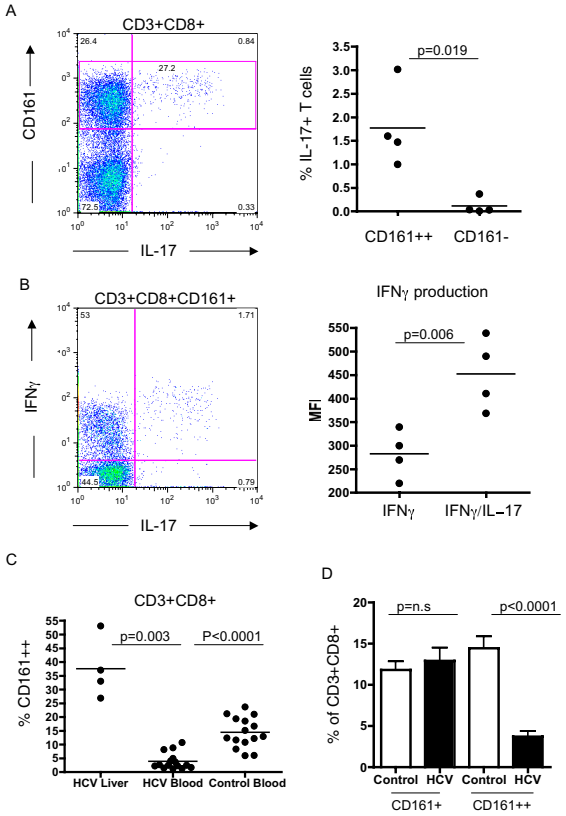


Fig. S6. Ex vivo staining of CD161$^+$ IL-17–secreting CD8$^+$ T cells from liver. Liver-infiltrating lymphocytes were separated from four livers taken at explant during transplantation for end-stage HCV. (*A*) (*Left*) Live CD3$^+$ CD8$^+$ T cells are gated and staining for IL-17 production is shown after PMA/ionomycin stimulation as in Fig S1. A representative plot is shown. (*Right*) Association of CD161 expression and IL-17 secretion in liver infiltrating CD8$^+$ T lymphocytes from four explanted HCV-positive cirrhotic livers. (*B*) Coexpression of IFN-γ and IL-17 after PMA/ionomycin stimulation. (*Left*) Plot is gated on CD161$^+$ CD8$^+$ T cells; a representative experiment is shown. (*Right*) Expression level (mean fluorescence intensity, *MFI*) of IFN-γ in single positive cells versus IFN-γ-IL-17–coexpressing cells is plotted. A significant difference in the level of expressed IFN-γ is shown (Wilcoxon test). (*C*) Enrichment of CD161^{++} CD8$^+$ T cells in HCV liver. Percentages of CD161^{++} cells among CD8$^+$ T cells in liver explants, PBMCs from HCV-positive donors, and PBMCs from healthy donors are shown. A significant reduction of CD161^{++} CD8$^+$ T cells in PBMC from HCV-positive donors is seen compared with healthy donors and a significant enrichment within liver tissue. The 15 HCV-positive donors studied in the analysis of PBMC were persistently infected donors (n = 8 genotype 1, n = 6 genotype 3, n = 1 genotype 2), of whom five had Ishak histologic scores of 5$^+$/6 and/or clinical cirrhosis. Groups were compared by Mann-Whitney tests. (*D*) Data as in *C* displayed comparing CD161^{++} cells and CD161$^+$ cells in peripheral blood.

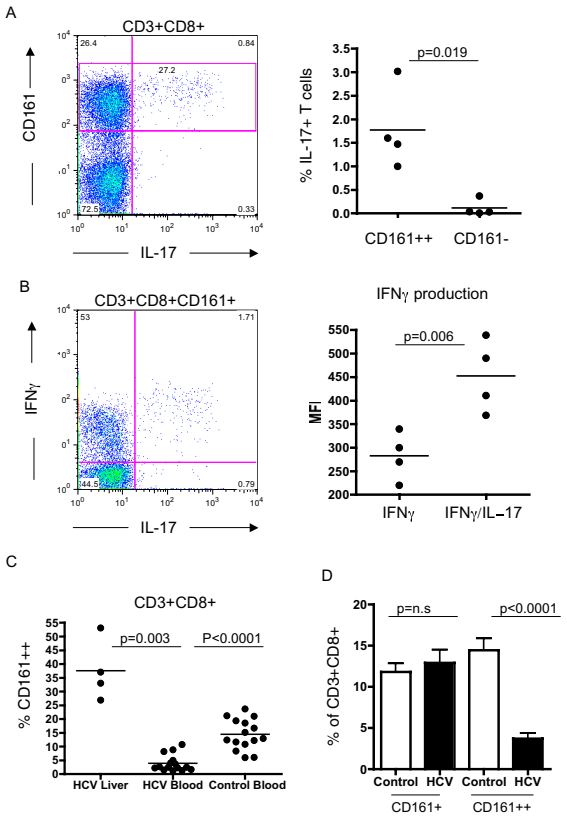


Fig. S6. Ex vivo staining of CD161$^+$ IL-17–secreting CD8$^+$ T cells from liver. Liver-infiltrating lymphocytes were separated from four livers taken at explant during transplantation for end-stage HCV. (*A*) (*Left*) Live CD3$^+$ CD8$^+$ T cells are gated and staining for IL-17 production is shown after PMA/ionomycin stimulation as in Fig S1. A representative plot is shown. (*Right*) Association of CD161 expression and IL-17 secretion in liver infiltrating CD8$^+$ T lymphocytes from four explanted HCV-positive cirrhotic livers. (*B*) Coexpression of IFN-γ and IL-17 after PMA/ionomycin stimulation. (*Left*) Plot is gated on CD161$^+$ CD8$^+$ T cells; a representative experiment is shown. (*Right*) Expression level (mean fluorescence intensity, *MFI*) of IFN-γ in single positive cells versus IFN-γ-IL-17–coexpressing cells is plotted. A significant difference in the level of expressed IFN-γ is shown (Wilcoxon test). (*C*) Enrichment of CD161^{++} CD8$^+$ T cells in HCV liver. Percentages of CD161^{++} cells among CD8$^+$ T cells in liver explants, PBMCs from HCV-positive donors, and PBMCs from healthy donors are shown. A significant reduction of CD161^{++} CD8$^+$ T cells in PBMC from HCV-positive donors is seen compared with healthy donors and a significant enrichment within liver tissue. The 15 HCV-positive donors studied in the analysis of PBMC were persistently infected donors (n = 8 genotype 1, n = 6 genotype 3, n = 1 genotype 2), of whom five had Ishak histologic scores of 5$^+$/6 and/or clinical cirrhosis. Groups were compared by Mann-Whitney tests. (*D*) Data as in *C* displayed comparing CD161^{++} cells and CD161$^+$ cells in peripheral blood.

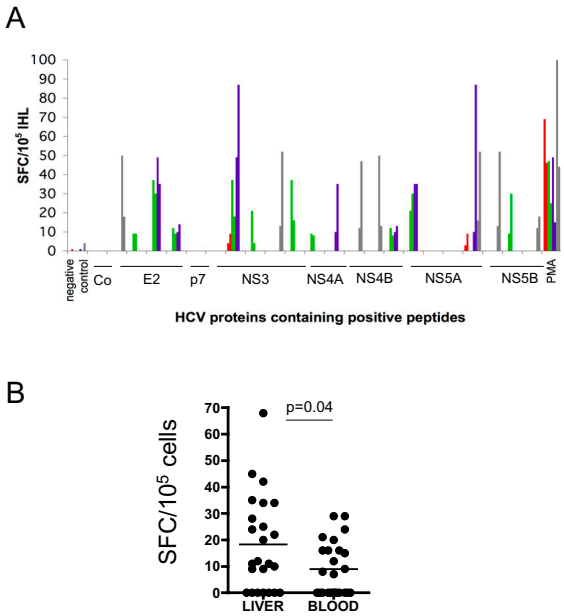


Fig. S7. Antigen-specific CD8$^+$ T cells in blood and liver. (*A*) Raw ELISpot data from nonspecifically expanded CD8$^+$ T cell lines from blood and liver in four donors. (*Left*) Each donor is represented by a different color. CD8$^+$ T cells were assayed against an overlapping peptide set of HCV peptides and responses obtained as indicated (*Co*, core). Each peptide pool was tested in duplicate and both results are displayed. Parallel studies were performed on blood. (*B*) Responses positive in either compartment from the four donors are indicated and compared between the two compartments using a Wilcoxon matched-pairs test.

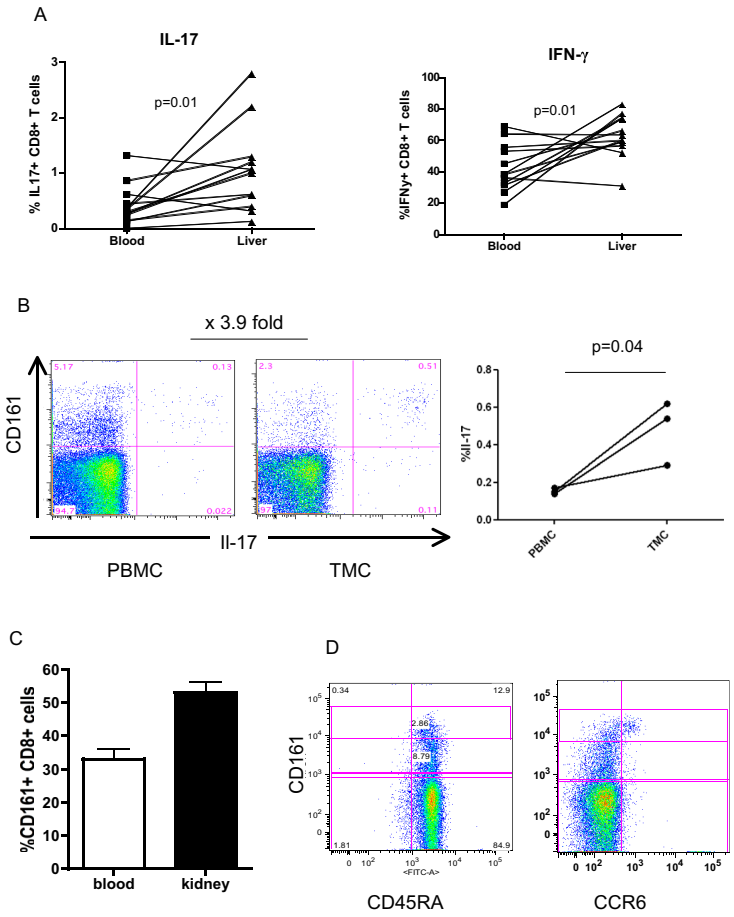


Fig. S8. CD161^{+} CD8^{+}T cells are not restricted to viral hepatitis. (*A*) CD8^{+} T cells isolated from PBMCs and liver biopsies of patients with nonalcoholic steatohepatitis were expanded with anti-CD3 and 100 U/mL IL-2 for 14 d before 5 h of stimulation with PMA/ionomycin and analysis of intracellular production of IL-17 and IFN-γ. (*B*) Secretion of IL-17 by CD161^{++} CD8^{+} T cells studied ex vivo from tonsil compared with PBMCs. Stimulation was as described earlier. (*Right*) Group data (n = 3, paired t test). (*C*) Expression of CD161 on CD8^{+} T cells in lymphocytes derived from kidney tissue (n = 2). (*D*) Expression of CD161^{++} in naive cord blood cells. Gating is on CD3^{+}CD8^{+} T cells and costaing for CD45RA and CCR6 is shown. One representative example among three is shown.

Table S1. Transcriptional comparison among CD161^{++}, CD161^{+}, and CD161^{-} CD8^{+}CD3^{+} T cells

logFC	Adjusted *P* value	Entrez_Gene_ID	Symbol
5.88	**5.78E−09**	**6097**	**RORC**
6.42	5.78E−09	4058	LTK
5.10	**1.02E−08**	**3820**	**KLRB1**
4.64	1.02E−08	8292	COLQ
5.74	1.39E−08	4199	ME1
4.9	2.83E−08	7704	ZBTB16
4.92	2.83E−08	642181	LOC642181
4.69	2.83E−08	4147	MATN2
4.29	**2.83E−08**	**1235**	**CCR6**
4.39	**4.22E−08**	**6097**	**RORC**
4.64	4.40E−08	59277	NTN4
3.88	1.63E−07	619207	LOC619207
3.54	2.08E−07	57568	SIPA1L2
4.80	**2.19E−07**	**149233**	**IL23R**
4.62	**3.32E−07**	**8807**	**IL18RAP**
4.23	3.32E−07	5121	PCP4
3.97	**3.32E−07**	**10663**	**CXCR6**
3.48	3.32E−07	10418	SPON1
4.47	4.23E−07	8292	COLQ
4.75	**5.22E−07**	**149233**	**IL23R**
4.78	8.00E−07	7704	ZBTB16
3.48	**8.12E−07**	**1231**	**CCR2**
3.24	8.12E−07	3800	KIF5C
4.60	9.47E−07	50509	COL5A3
3.10	1.29E−06	653518	LOC653518
3.68	1.72E−06	1289	COL5A1
3.20	1.74E−06	134285	PRP2
3.06	2.10E−06	259197	NCR3
3.73	2.20E−06	959	CD40LG
4.04	2.79E−06	259307	IL4I1
3.70	2.79E−06	1052	CEBPD
2.79	2.79E−06	79187	FSD1
3.21	**3.93E−06**	**8809**	**IL18R1**
2.70	4.13E−06	3487	IGFBP4
2.94	6.33E−06	167681	PRSS35
2.85	7.41E−06	120196	MGC34830
4.49	1.87E−06	4058	LTK
3.91	1.87E−06	6097	RORC
3.88	1.87E−06	642181	LOC642181
3.55	1.87E−06	619207	LOC619207
3.41	5.31E−06	4147	MATN2
3.17	6.83E−06	6097	RORC
2.96	6.83E−06	79187	FSD1
3.75	9.59E−06	149233	IL23R
3.49	9.59E−06	4199	ME1
2.78	9.59E−06	8292	COLQ
3.93	1.45E−05	149233	IL23R
3.00	1.99E−05	59277	NTN4
2.63	2.04E−05	9805	SCRN1
2.60	2.36E−05	10418	SPON1
3.65	2.54E−05	259307	IL4I1
3.43	3.20E−05	640	BLK
2.67	3.21E−05	134285	PRP2
3.02	3.38E−05	1289	COL5A1
2.34	3.38E−05	57568	SIPA1L2
2.44	5.08E−05	2352	FOLR3
2.25	6.01E−05	1235	CCR6
3.22	6.07E−05	221662	RBM24
3.18	6.07E−05	3706	ITPKA
2.76	6.07E−05	144100	PLEKHA7
3.51	0.00010	650761	LOC650761
2.48	0.00010	10663	CXCR6
2.41	0.00010	146722	CD300LF

Table S1. Cont.

logFC	Adjusted *P* value	Entrez_Gene_ID	Symbol
2.20	0.00010	84446	BRSK1
2.24	0.00013	7940	LST1
2.19	0.00013	259197	NCR3
3.48	0.00013	760	CA2
2.09	0.00014	649635	LOC649635
3.22	0.00016	1571	CYP2E1
2.46	0.00016	3101	HK3
2.10	0.00016	23261	CAMTA1
2.41	0.00016	166012	CHST13
2.35	0.00017	7704	ZBTB16
2.24	0.00017	167681	PRSS35
2.10	0.00018	221	ALDH3B1
2.02	0.00020	3800	KIF5C
2.86	0.00020	1441	CSF3R
2.23	0.00020	11213	IRAK3
2.16	0.00020	1231	CCR2
2.45	0.00020	23166	STAB1
2.60	0.00021	8292	COLQ
2.86	0.00022	50509	COL5A3
2.78	0.00029	760	CA2
2.16	0.00036	6785	ELOVL4
2.24	0.00041	7940	LST1
2.25	0.00042	91662	NALP12
2.32	0.00042	3055	HCK
2.24	0.00059	433	ASGR2
2.57	0.00060	116362	RBP7
2.29	0.00060	6556	SLC11A1
2.04	0.00062	644365	LOC644365
2.06	0.00064	9450	LY86
2.39	0.00065	929	CD14
2.32	0.00076	11027	LILRA2
2.76	0.00078	353514	LILRA5
2.19	0.00084	160364	CLEC12A
2.15	0.00085	959	CD40LG
2.15	0.00086	7940	LST1
2.23	0.00087	929	CD14
2.22	0.00090	6252	RTN1
2.48	0.00091	64231	MS4A6A
2.25	0.0011	2357	FPR1
2.44	0.0011	199	AIF1
2.34	0.0011	55799	CACNA2D3
2.12	0.0011	968	CD68
2.66	0.0012	10979	PLEKHC1
2.40	0.0012	1436	CSF1R
2.05	0.0012	2205	FCER1A
2.16	0.0013	10437	IFI30
2.13	0.0013	3728	JUP
2.19	0.0013	432	ASGR1
2.28	0.0013	2219	FCN1
2.18	0.0014	8707	B3GALT2
2.17	0.0014	11025	LILRB3
2.12	0.0014	11026	LILRA3
2.36	0.0015	6283	S100A12
2.24	0.0017	6279	S100A8
2.27	0.0017	2769	GNA15
2.24	0.0017	10261	IGSF6
2.01	0.0017	6916	TBXAS1
2.45	0.0017	11031	RAB31
2.23	0.0017	126259	TMIGD2
2.42	0.0019	5265	SERPINA1
2.04	0.0019	51313	C4orf18
2.66	0.0020	6688	SPI1

Table S1. Cont.

logFC	Adjusted *P* value	Entrez_Gene_ID	Symbol
2.21	0.0021	9056	SLC7A7
2.04	0.0022	132014	IL17RE
2.75	0.0022	221662	RBM24
2.19	0.0023	7704	ZBTB16
2.29	0.0024	6280	S100A9
2.05	0.0026	57698	KIAA1598
2.71	0.0027	6364	CCL20
2.07	0.0029	4082	MARCKS
2.21	0.0030	4055	LTBR
2.31	0.0031	1536	CYBB
2.47	0.0033	6688	SPI1
2.55	0.0034	256236	NAPSB
2.09	0.0034	30817	EMR2
2.62	0.0037	51363	GALNAC4S-6ST
2.18	0.0037	5265	SERPINA1
2.32	0.0042	3597	IL13RA1
2.28	0.0042	4005	LMO2
2.03	0.0047	54504	CPVL
2.00	0.0047	10981	RAB32
2.03	0.0048	9935	MAFB
2.02	0.0048	5337	PLD1
2.61	0.0050	140885	PTPNS1
2.28	0.0050	10409	BASP1
2.35	0.0050	58475	MS4A7
2.07	0.0054	5836	PYGL
2.19	0.0057	1462	CSPG2
2.07	0.0061	54504	CPVL
2.19	0.0062	948	CD36
2.22	0.0065	57282	SLC4A10
2.25	0.0067	9934	P2RY14
2.00	0.0067	4920	ROR2
2.18	0.0069	4778	NFE2
2.31	0.0089	64231	MS4A6A
2.50	0.0089	64231	MS4A6A

At the top, $CD161^{++}$ vs. CD161-: Log_2 Fold change is indicated among the most highly differentially expressed genes from the microarray analysis. Only genes with adjusted *P* value $<10^{-5}$ are indicated. Genes are arranged in order of adjusted *P* value. At the bottom, comparisons of gene expression profiles of $CD8^{+}$ $CD161^{++}$ vs. $CD161^{+}$ T cells Up-regulated genes with fold change >4 and adjusted $P < 0.01$ are indicated. Full datasets are available on request. Genes related to type 17 development and/or analyzed in the main text are in bold.

Table S2. Clinical characteristics of HCV and control (nonalcoholic steatohepatitis) donors studied in blood and liver analyses

Subject	Age, y	Sex	Viral load, U/mL	Fibrosis
Ex vivo analysis				
1	36	M	998027	1
2	50	M	2088920	2
3	56	F	89499	1
4	45	F	536864	1
5	48	F	1480000	2
6	36	M	677588	0
7	52	M	310098	2
8	54	M	1291992	3
9	56	F	477496	3
10	40	F	–	1
11	53	M	558835	3
12	53	F	–	2
13	50	M	5074737	0
14	53	F	208729	2
15	32	M	912622	1
16	29	M	771272	1
17	61	M	453483	3
18	42	F	127565	1
19	43	F	1900000	1
20	53	F	85777	2
21	34	M	365708	3
22	57	M	1259990	2
23	44	F	883657	2
In vitro stimulated lines				
1	36	M	677588	1
2	31	F	–	2
3	53	M	–	2
4	51	F	75341	1
5	63	F	2428420	3
6	28	F	900121	2
7	29	F	–	1
8	42	F	174618	1
9	36	M	1312790	2
10	56	M	4769592	2
11	30	M	587174	2
12	44	M	1300000	1
13	42	M	22098	1
14	56	F	89499	1
15	51	M	26884	2
16	48	M	559017	1
17	48	M	7311644	1
18	48	F	1480000	2
19	52	M	1438180	2
20	54	M	1500000	2
21	63	F	2568188	2
22	56	F	938114	2
23	43	M	915735	3
24	28	M	999416	1
25	62	M	–	1
26	57	M	123277	3
27	50	M	737087	3
28	44	F	572472	1
29	50	M	4011231	2
30	66	F	639838	3
31	72	F	2904622	3
32	49	M	15800000	3
33	65	F	208729	1
34	32	M	112622	1
35	43	M	864679	1
36	33	W	184445	2

Table S2. Cont.

Subject	Age, y	Sex	Viral load, U/mL	Fibrosis
Nonalcoholic steatohepatitis				
1	29	–	–	–
2	53	–	–	–
3	32	–	–	–
4	56	–	–	–
5	55	–	–	–
6	40	–	–	–
7	54	–	–	–
8	51	–	–	–
9	39	–	–	–
11	53	–	–	–
12	32	–	–	–

Appendix 2

Microarray data comparing up and down regulated genes between CD161+ and CD161- CD8+ T cell subsets in cord blood.

A2.1 CD161+CD8+ vs CD161-CD8+

Gene.Symbol	logFC	adj.P.Val
CCR6	3.952335969	0.000697368
---	3.483938801	0.000956486
---	3.220170274	0.00059088
---	3.2018926	0.000633501
ADAM12	2.986843228	0.007313664
LOC619207	2.87949304	0.003934873
KIF5C	2.660773381	0.00246745
KIT	2.65934342	0.000925041
NCR3	2.648876807	0.001909946
---	2.590234398	0.000484933
KIF5C	2.546575757	0.001226533
NCR3	2.505550001	0.002833198
ZBTB16	2.489295181	0.000484933
NCR3	2.40125561	0.001194069
CFH /// CFHR1	2.35052116	0.025183809
CXCR6	2.294614301	0.013870812
ANK1	2.277976138	0.000484933
ZNF462	2.221785215	0.000748259
POLR1E	2.219686368	0.001169735
FAM43A	2.18655332	0.001200822
SLAMF1	2.180152788	0.001219334
RORC	2.158716405	0.000484933
CYB561	2.13651252	0.00383074

Table A2.1 Comparison of gene expression profiles of CD161++CD8+ vs CD161+CD8+ T cells in cord blood. Genes with >2 $\log_2$ fold up regulation shown.

Gene.Symbol	logFC	adj.P.Val
EREG	-3.256983222	0.000484933
MARCKS	-3.189268639	0.00121565
THBD	-3.185101959	0.001220734
CXCL2	-3.16306979	0.001469274
DOCK4	-3.159496624	0.000633501
RNASE6	-3.123284916	0.001543784
VCAN	-3.058884162	0.000484933
PPBP	-3.052722443	0.004246222
MS4A7	-3.012383027	0.000484933
NRP2	-2.995734781	0.000633501
IL13RA1	-2.993278539	0.001362645
KYNU	-2.986169459	0.004860927
EPB41L3	-2.977341991	0.000484933
MS4A7	-2.970704179	0.000484933
RAB31	-2.964269303	0.000484933
KMO	-2.951333703	0.001200822
KYNU	-2.944089229	0.000484933
MMP19	-2.933706365	0.000484933
SERPINB2	-2.912356073	0.001346008

THBD	-2.903700931	0.001164958
TLR4	-2.886451847	0.001226533
EPB41L3	-2.872119255	0.000484933
CSF2RB	-2.859272109	0.000518028
---	-2.859079196	0.001194069
HLA-DQA1	-2.847454154	0.001137045
CD36	-2.840250701	0.000484933
CLEC7A	-2.835888917	0.001191367
---	-2.823314745	0.000889121
EMR2	-2.82207588	0.000484933
PLA2G7	-2.818457341	0.000545305
AQP9	-2.814904783	0.001194069
MYOF	-2.813524322	0.001420424
VCAN	-2.806168597	0.000748259
SERPINA1	-2.798952441	0.002008015
DMXL2	-2.786532099	0.000484933
C5AR1	-2.779762921	0.000633501
TNS3	-2.774251901	0.002930479
CD300LF	-2.771840204	0.000580441
SPP1	-2.763022742	0.031168356
LHFPL2	-2.756322477	0.000633501
CLEC7A	-2.750955916	0.000545305
CD163	-2.726412142	0.001500111
KMO	-2.721207077	0.000648639
IL13RA1	-2.714025745	0.000484933
RIN2	-2.710985907	0.000580441
IL1RN	-2.708439	0.003200393
TNS1	-2.704172149	0.002569584
CYP1B1	-2.692152739	0.000698626
RBM47	-2.680855724	0.000633501
ZNF697	-2.68030682	0.000941631
CD86	-2.675170846	0.000484933
FN1	-2.674595075	0.007355325
TNFAIP6	-2.672430599	0.003154153
GPR109B	-2.671313588	0.000484933
CXCL1	-2.670228125	0.001072173
HCK	-2.661850472	0.001346008
LY96	-2.660044981	0.001220734
KCTD12	-2.659020717	0.007883214
BASP1	-2.650545807	0.000633501
DOK3	-2.648359021	0.000545305
TNFAIP6	-2.64785938	0.002601555
FPR3	-2.641315232	0.000580441
CD163	-2.639401498	0.000484933
TGFBI	-2.636858144	0.000545305
IL1RN	-2.62948727	0.000849422
TFEC	-2.626027983	0.001194069
KYNU	-2.621816073	0.001666836
CCL2	-2.616769759	0.001368715
LILRA2	-2.616631127	0.000799279
PTX3	-2.610680514	0.010697339
CD36	-2.604819121	0.000484933
PROK2	-2.603614999	0.004576429
RAB31	-2.600564268	0.001137045
CLEC5A	-2.599012067	0.021998866
THBS1	-2.590444872	0.000484933
MS4A7	-2.58662012	0.000484933
SPP1	-2.583297889	0.001194069

MS4A6A	-2.581417609	0.000799279
CYP1B1	-2.581063893	0.000545305
CXCL9	-2.573211837	0.000484933
CD86	-2.5720841	0.001220734
ADAM28	-2.571891499	0.000484933
VCAN	-2.57125405	0.000484933
CD86	-2.568122859	0.002135772
C15orf48	-2.564865325	0.000484933
ADAMDEC1	-2.562100185	0.015254122
EPB41L3	-2.561257056	0.000484933
ZNF385A	-2.556133029	0.000633501
S100A12	-2.551804485	0.001592804
SERPINA1	-2.551341108	0.001116414
CD14	-2.544395056	0.000799279
MAFB	-2.540039555	0.000941631
FGL2	-2.533146409	0.001699901
INHBA	-2.532784933	0.001232311
PTGS1	-2.527831229	0.001200822
PTGS2	-2.526745522	0.001566397
---	-2.523432792	0.002366484
---	-2.521980429	0.017575341
SLC7A11	-2.521936879	0.001368715
C13orf18	-2.514529755	0.007611679
PTGS2	-2.514187468	0.000681042
---	-2.513987701	0.000484933
FAM26F	-2.51378987	0.005070258
MPEG1	-2.510321672	0.000545305
F3	-2.507972864	0.002863678
HLA-DQB1	-2.507646832	0.003773824
---	-2.501096691	0.00238816
SULF2	-2.500657129	0.000484933
VCAN	-2.495215242	0.000681042
FGR	-2.49195741	0.002681571
HLA-DQA1 /// HLA-DQA2 /// LOC100294224 /// LOC100294317	-2.487159232	0.000484933
CSF2RA	-2.481726756	0.001362645
IL13RA1	-2.47735248	0.003384708
MSR1	-2.477294371	0.005043536
CD109	-2.473493422	0.004950593
IL13RA1	-2.464954929	0.007664245
OLR1	-2.463601632	0.000873377
ANPEP	-2.459941968	0.000484933
GK3P	-2.456367101	0.00054622
MNDA	-2.454579017	0.000511628
GK	-2.446545547	0.000484933
HLA-DQA1	-2.44588984	0.007028915
FCGR1B	-2.438952356	0.001103471
IRG1	-2.437084877	0.04565779
ICAM1	-2.437064779	0.000633501
CXCL10	-2.434554028	0.028991601
FN1	-2.429920065	0.014217902
CLEC7A	-2.429448789	0.002381004
PTGS1	-2.426198139	0.003049175
CD93	-2.42313728	0.003589884
FGL2	-2.421508947	0.003155354
TUBB6	-2.4201209	0.001238847
SLC7A7	-2.417598052	0.000484933

S100A8	-2.416793684	0.002331843
MPEG1	-2.416508562	0.000874736
SLC15A3	-2.413521469	0.001404099
RBM47	-2.398466728	0.000950726
FPR2	-2.394916822	0.002398506
GJB2	-2.393318721	0.008456805
CTSL1	-2.391624874	0.000633501
CYP1B1	-2.390182154	0.002366484
LILRB1	-2.389015634	0.000484933
DAPP1	-2.387500788	0.005043536
ABCA1	-2.379005457	0.008494139
HLA-DRB1 /// HLA-DRB3 /// HLA-DRB4	-2.378213231	0.001192484
S100A8	-2.371215587	0.001220734
CHST15	-2.37042469	0.001270762
HLA-DRB4	-2.367477083	0.000484933
APOBEC3A	-2.364786225	0.001404026
LGALS2	-2.362381126	0.000545305
LILRB1	-2.361621483	0.002887459
TREM1	-2.36156581	0.001200822
KYNU	-2.356305056	0.001280973
CYBB	-2.355935469	0.000906869
IFNGR2	-2.352456909	0.004310183
TNFAIP2	-2.347502767	0.000537161
FAM26F	-2.347080059	0.000484933
NOD2	-2.344791857	0.00602921
IL1A	-2.342825865	0.012176002
HLA-DRA	-2.339110189	0.000849422
SIGLEC1	-2.338742779	0.013073817
GPNMB	-2.333182608	0.008943479
RAB20	-2.329712677	0.004180217
TJP2	-2.327558843	0.024525678
CCL7	-2.325741732	0.000897583
---	-2.325607248	0.002286716
IL1RN	-2.325166481	0.000484933
TLR8	-2.315289941	0.007063866
KIAA1598	-2.310386857	0.000748259
PTAFR	-2.306926066	0.003384708
RNF144B	-2.30541436	0.026936878
H1F0	-2.304507429	0.000986162
B3GNT5	-2.302625842	0.000986276
THBS1	-2.30116589	0.000484933
LILRB2	-2.300947264	0.002681571
MARCKS	-2.299733963	0.002323086
CSTA	-2.297036139	0.001169735
HLA-DPA1	-2.296505742	0.000633501
FPR1	-2.295495848	0.000721871
LILRB3	-2.294857837	0.000518028
BCAT1	-2.290078463	0.001346008
VCAN	-2.288387603	0.001116414
IRAK3	-2.287540463	0.000897583
HLA-DRB1 /// HLA-DRB4 /// HLA-DRB5	-2.285967848	0.000799279
NCF2	-2.28238775	0.000772305
SLC11A1	-2.280584842	0.001362645
CPVL	-2.280234813	0.000681042
CXCL3	-2.270560786	0.001200822
FCGR2A	-2.26965768	0.001220734
INHBA	-2.266014569	0.008183488

HLA-DMB	-2.265064731	0.006627124
CXCL2	-2.264761629	0.000874736
ETS2	-2.264609096	0.000484933
ADAM9	-2.263977259	0.001200822
IGSF6	-2.263158506	0.001524579
CD1C	-2.258793578	0.042225468
TLR4	-2.257720877	0.001000293
TMEM176B	-2.256524149	0.000849422
CD1D	-2.254154907	0.007028915
ACSL1	-2.253800256	0.000484933
CSF1R	-2.249740955	0.000484933
RNF144B	-2.248935863	0.022408603
DOCK5	-2.247965525	0.000681042
NPL	-2.247695102	0.005597413
HLA-DQB1 /// LOC100294318	-2.247562828	0.001481729
ST3GAL6	-2.24417019	0.032993981
GPR84	-2.242972829	0.021743183
---	-2.241860648	0.048787751
CLEC4E	-2.239095312	0.002088751
ALDH2	-2.238707778	0.001368715
IL6	-2.234175705	0.001469274
PLAUR	-2.232198659	0.000497639
---	-2.229832418	0.005702965
SLC8A1	-2.229621599	0.003070576
DUSP6	-2.22835479	0.000633501
CTSB	-2.225852632	0.001169735
PLAUR	-2.225052265	0.000748259
HLA-DMA	-2.224870054	0.001368715
IRAK3	-2.220695463	0.005616678
LILRA1	-2.220353646	0.000986162
AKAP2 /// PALM2-AKAP2	-2.22031848	0.008313228
FCN1	-2.21743692	0.002381004
TLR2	-2.216634074	0.000484933
PYGL	-2.214891868	0.0069524
TIMP1	-2.209108373	0.000484933
MS4A6A	-2.208819555	0.01299111
LILRB2	-2.20283449	0.000484933
IFI30	-2.202497474	0.000484933
PTAFR	-2.200870341	0.000484933
FAM26F	-2.200131277	0.002318118
PILRA	-2.197464013	0.001070575
ALOX5	-2.195006357	0.001729444
RAB32	-2.192614815	0.002887459
ABCC3	-2.191579791	0.001816261
LPCAT2	-2.186305673	0.002827203
CLEC7A	-2.182966223	0.007736699
SMPDL3A	-2.18272681	0.015328248
FCGR2C	-2.180368664	0.001368715
HLA-DRA	-2.17426756	0.000633501
FGD2	-2.174006536	0.000580441
BCAT1	-2.169080552	0.024237729
HLA-DQB1	-2.168732868	0.001194069
GK	-2.168438072	0.000545305
DHRS9	-2.168274061	0.021743183
RHOU	-2.162674262	0.006935097
ZC3H12C	-2.162059723	0.040023719
PLXDC2	-2.16053599	0.00174029

ALDH1A1	-2.158401522	0.021743183
GM2A	-2.156844358	0.001388726
VEGFA	-2.155792201	0.008135283
CYBB	-2.152996556	0.001647074
SDC2	-2.152481428	0.044667093
SRC	-2.151334846	0.001481729
THBS1	-2.14888537	0.000846593
HLA-DQB1	-2.148125499	0.000849422
LILRB3	-2.145235417	0.000484933
MARCH1	-2.140645146	0.012313162
ALDH3B1	-2.139992825	0.005502581
SIGLEC5	-2.139161848	0.016765687
NLRP3	-2.13908686	0.003524585
THBS1	-2.135695413	0.001259192
RTN1	-2.129379431	0.041835638
LAMB3	-2.127862103	0.0080922
---	-2.126989186	0.001262352
---	-2.126725417	0.00870359
---	-2.126547179	0.001013043
IL1RN	-2.121619093	0.001755636
HLA-DRB1 /// HLA-DRB4	-2.116514888	0.001220734
MSR1	-2.115321584	0.009939873
MSR1	-2.114648896	0.001592804
RAB31	-2.108948008	0.001404099
LILRB3	-2.102117683	0.000484933
SLC16A6	-2.100479606	0.003050373
---	-2.099510881	0.003104921
HLA-DQB1	-2.095792698	0.011240304
DUSP6	-2.095604397	0.000484933
TMEM176A	-2.09557023	0.038722372
LILRA2	-2.095109609	0.000986276
CIITA	-2.094858289	0.001913842
PLAUR	-2.093628201	0.000648639
MAFB	-2.093198158	0.003138179
ASPH	-2.09145231	0.014506777
FCAR	-2.090596536	0.000871437
SIRPB1	-2.087233528	0.017916371
SLC31A2	-2.085248507	0.006473229
S100A9	-2.083830596	0.00118928
LMO2	-2.07584375	0.001362645
C3	-2.0737929	0.036148971
HMOX1	-2.071237249	0.004153402
C1orf38	-2.06722926	0.007176851
MPP1	-2.062927063	0.001362645
RBP7	-2.058839044	0.007207825
MS4A6A	-2.051000653	0.041051904
DUSP6	-2.043745996	0.000633501
G0S2	-2.042626143	0.003035498
FCAR	-2.041085411	0.000849422
HLA-DPA1	-2.037744614	0.001238847
IL1R1	-2.037421144	0.034076777
FCGR2C	-2.035370371	0.002588764
CIITA	-2.035116005	0.000772305
GK	-2.033633679	0.001220734
PMP22	-2.030928829	0.002625819
TRIB1	-2.030317216	0.00876019
LILRB1	-2.030040495	0.004071467

CCRL2	-2.024714986	0.022261371
BTK	-2.02422035	0.006186453
IL1B	-2.019124889	0.003524585
KCTD12	-2.017888699	0.024210147
ABCA1	-2.017733181	0.00078913
PHACTR1	-2.014417649	0.043358277
DRAM1	-2.011103044	0.003050373
PRO2964	-2.006966753	0.003061105
CST3	-2.006571928	0.001402592
LYZ	-2.001794493	0.001755301

Table A2.2: Comparison of gene expression profiles of CD161++CD8+ vs CD161+CD8+ T cells in cord blood. Genes with >2 log_2 fold dwon regulation shown.

A2.2 CD161+CD8+ T cells vs CD161-CD8+ T cells

Gene.Symbol	logFC	adj.P.Val
KLRB1	4.040418184	9.10037E-05
CLEC7A	4.030682964	0.000103623
CLEC7A	3.984022944	0.000110773
CD163	3.979666339	0.000127067
PPBP	3.968787741	0.000669338
IL13RA1	3.968132211	0.000183752
CYP1B1	3.931821896	5.77481E-05
MS4A7	3.917762608	5.77481E-05
EPB41L3	3.842533505	5.77481E-05
RIN2	3.783571178	6.13279E-05
PTGS2	3.732864735	0.000126687
EREG	3.710876261	7.46427E-05
CD163	3.709066433	5.77481E-05
VCAN	3.688085415	6.13279E-05
ZNF697	3.68007775	9.42487E-05
SERPINB2	3.6772464	0.000224766
MPEG1	3.6653069	6.50035E-05
RBM47	3.657372107	6.77846E-05
CYP1B1	3.653271749	7.46427E-05
LILRA2	3.650513689	7.46427E-05
FPR3	3.641746475	6.14246E-05
ITGB3	3.614763401	0.021642398
CSF1R	3.606396181	5.77481E-05
MS4A7	3.601894471	6.74054E-05
SRC	3.5913895	7.46427E-05
VCAN	3.589427551	9.77313E-05
CHST15	3.583058355	9.29249E-05
CD36	3.582121996	5.77481E-05
SERPINA1	3.57017261	0.00034104
IL1RN	3.55966921	0.000476899
CXCL9	3.559069042	5.77481E-05
CYBB	3.543214976	6.77846E-05
GPR109B	3.523084999	5.77481E-05
OLR1	3.517161223	7.46427E-05
C15orf48	3.51699963	5.77481E-05
MAFB	3.510160726	0.000127067
IL13RA1	3.508260945	0.000750114
PLA2G7	3.505738371	7.46427E-05
KYNU	3.505447731	0.001409661
KYNU	3.503918794	0.000100913

SLC7A11	3.486686577	0.000147195
TGFBI	3.485721465	6.4414E-05
CYBB	3.479208806	9.20368E-05
VCAN	3.471347849	7.02303E-05
MMP19	3.462394486	7.17095E-05
CCR1	3.462128869	5.77481E-05
HCK	3.453623023	0.000192616
LILRB2	3.444954867	0.000191841
THBS1	3.442437439	5.77481E-05
PLAUR	3.433295892	5.77481E-05
MAFB	3.427499056	0.00010222
FCN1	3.417881896	0.000146671
FGL2	3.40656325	0.000220794
CSF2RB	3.406181373	8.24967E-05
CXCL2	3.402347938	0.000635883
FGR	3.397815713	0.000321922
SLC11A1	3.395095196	0.000106477
IL13RA1	3.38497318	5.77481E-05
IL13RA1	3.382686039	0.00041286
MARCKS	3.371280707	0.00050403
SERPINA1	3.370133737	0.000127067
CPVL	3.367154411	6.13279E-05
CYP1B1	3.3541539	0.000235936
TNFAIP6	3.35148609	0.000612717
TNFAIP2	3.350649044	5.77481E-05
CEBPD	3.347850154	0.000379473
CCL2	3.337755268	0.000224766
PILRA	3.332397222	7.46427E-05
ALDH2	3.327176582	0.000108216
ABCA1	3.324954591	0.000965485
IL1RN	3.314898735	0.000122204
VCAN	3.304344934	9.20368E-05
C5AR1	3.302476058	0.000107854
PTGS2	3.302088842	8.45864E-05
CLEC5A	3.302065965	0.004713191
TFEC	3.29997481	0.000186979
CXCL1	3.299213495	0.00017174
THBS1	3.297044266	6.13279E-05
RAB31	3.296023906	9.20368E-05
DUSP6	3.294686588	5.77481E-05
ANPEP	3.294673461	5.77481E-05
THBS1	3.293969394	8.9486E-05
VCAN	3.285755495	5.77481E-05
MPEG1	3.281357758	6.64581E-05
---	3.281078066	0.001079349
CXCL10	3.270720743	0.00480922
THBD	3.270459896	0.000620984
TREM1	3.270431947	0.000124208
CCR1	3.268799647	0.00012426
FCAR	3.263957412	6.13279E-05
LGALS3	3.263187828	6.1576E-05
THBS1	3.262682961	6.4414E-05
LYN	3.262488488	0.000293712
DSE	3.25825635	0.000144147
IL1R1	3.256435692	0.002276323
DUSP6	3.251878546	5.77481E-05
CD86	3.248712388	7.02303E-05
HLA-DQA1	3.246186848	0.000284744

LYN	3.244632662	0.00050403
F3	3.243272329	0.000461878
---	3.238175086	0.00122952
S100A12	3.229995367	0.000287132
BASP1	3.226909397	9.20368E-05
CLEC4E	3.224086801	0.000186979
---	3.223085651	0.000337221
CD14	3.218775687	0.000109465
CLEC7A	3.216126808	9.20368E-05
FCGR2A	3.21464406	0.000112835
CTSL1	3.212671621	7.17095E-05
KYNU	3.212427092	6.1576E-05
CCL7	3.211209369	9.10037E-05
CD300LF	3.205048553	0.000104336
FCAR	3.195983456	8.45864E-05
APOBEC3A	3.192053283	0.000173878
MYOF	3.187904296	0.000461878
CD93	3.186162386	0.000537161
TUBB6	3.183536714	0.000166807
DOK3	3.180946795	8.74929E-05
THBS1	3.177233892	5.77481E-05
EMR2	3.174578644	9.20368E-05
DMXL2	3.173212258	5.77481E-05
RAB31	3.171131298	0.000106681
THBD	3.170014896	0.000373206
PLEK	3.166121721	0.000147195
CCL20	3.164459902	0.006038638
NCF2	3.154571901	7.46427E-05
MNDA	3.153108623	6.4988E-05
RNASE6	3.153097903	0.00100628
CSTA	3.151234989	0.000118495
MS4A7	3.151148801	5.77481E-05
TLR2	3.1508833	5.77481E-05
SLC8A1	3.145712479	0.000313463
PTAFR	3.144303141	5.77481E-05
LYN	3.138646868	0.000386523
IL1R1	3.133943799	0.009092858
IRG1	3.124414884	0.010567654
CD36	3.119249702	9.77313E-05
ICAM1	3.116205304	8.45864E-05
PTGS1	3.112179387	0.000514078
RAB32	3.10482947	0.00028553
FPR2	3.097541093	0.000384509
AQP9	3.093021095	0.0003874
INHBA	3.089440009	0.001063613
LHFPL2	3.083772083	0.000144147
B3GNT5	3.082201707	0.000109465
KYNU	3.079171505	0.000461878
IFI30	3.074159937	5.77481E-05
HLA-DQA1	3.073548927	0.001409661
PTX3	3.071887202	0.00333103
FCGR3A /// FCGR3B	3.071206745	0.026133699
RASSF4	3.070011327	0.015617589
TLR4	3.067853314	0.000521905
KMO	3.067505565	0.000540936
HLA-DRA	3.067009145	0.000101531
LILRB3	3.055212172	6.13279E-05
TYROBP	3.053050208	5.77481E-05

INHBA	3.045776636	0.0002685
LILRB1	3.040525196	0.000476261
LYZ	3.039337674	0.00012426
FN1	3.036049966	0.04839095
LILRB2	3.031578034	5.77481E-05
ITGAX	3.027849541	0.00012426
CXCL3	3.026839155	0.000143145
EPB41L3	3.02683353	5.77481E-05
PLAUR	3.018717125	6.1576E-05
MARCKS	3.014659866	0.000338708
GRN	3.008178269	0.000104336
GJB2	3.001256746	0.001794263
PLXDC2	2.998733228	0.000189535
IL6	2.998089568	0.000189535
SPP1	2.996566968	0.015296771
PTGS1	2.995388589	0.0002685
LGALS2	2.995083859	7.02303E-05
DUSP6	2.993764944	6.13279E-05
MS4A6A	2.987566833	0.001816206
FCAR	2.985367986	7.46427E-05
IGSF6	2.980137408	0.000222692
KMO	2.969669586	0.000170525
---	2.965572703	0.000624952
MSR1	2.965555292	0.001130569
TNFAIP6	2.96542927	0.000946943
PLEK	2.964958236	0.002190269
SIRPB1	2.964435927	0.000630724
CD86	2.962215367	0.000327144
LILRB1	2.957068431	6.13279E-05
---	2.95051528	0.005714403
ADAM28	2.94929022	5.77481E-05
G0S2	2.947750286	0.0002685
PILRA	2.945410266	0.000144147
VEGFA	2.944355363	0.00054206
ALOX5	2.942872997	0.000224766
NOD2	2.942792374	0.001200198
PLBD1	2.942571407	0.000373206
FN1	2.938961783	0.003197445
---	2.937254535	0.005317115
NLRP3	2.93693714	0.000418114
LMO2	2.93458377	0.000129571
HLA-DRA	2.931336016	6.77846E-05
PLAUR	2.924777847	9.10037E-05
RAB31	2.923678158	0.000306271
TIMP1	2.923268134	6.13279E-05
IL8	2.911925969	0.000109465
MSR1	2.910797436	0.001454179
CST3	2.910639298	0.00012426
---	2.909888046	6.50035E-05
PIK3AP1	2.906625354	0.002133624
ZNF385A	2.904314711	0.000127067
S100A8	2.901260098	0.000547026
HLA-DRB4	2.90054667	5.77481E-05
ICAM1	2.900498762	5.77481E-05
IL1RN	2.89506393	6.13279E-05
IL1A	2.893155997	0.002864586
LPCAT2	2.886454804	0.000409066
---	2.881037048	0.000146671

CD86	2.877652088	0.000757117
SPP1	2.877032413	0.000366864
C10orf128	2.873993298	0.001789734
MN1	2.866866585	0.012440062
C13orf31	2.8637401	9.73111E-05
FPR1	2.861186699	0.000103923
CCL3 /// CCL3L1 /// CCL3L3	2.860107946	0.000223601
GK	2.859532676	6.50035E-05
---	2.85341955	0.0003874
IL1RN	2.852934277	0.000224766
LILRB3	2.845522775	5.77481E-05
IRAK2	2.840088581	0.003906213
FGD2	2.837829051	6.77846E-05
MARCKS	2.835896506	0.00023037
S100A8	2.823524879	0.000276426
LILRA1	2.822630446	0.000136825
HLA-DRB1 /// HLA-DRB3 /// HLA-DRB4	2.818352941	0.000249855
ZEB2	2.816252199	0.000612717
RBP7	2.814596815	0.000889936
FCGR2C	2.796574932	0.000292499
FCGR2A	2.796358634	0.001063613
HLA-DQA1 /// HLA-DQA2 /// LOC100294224 /// LOC100294317	2.792133112	8.14325E-05
CTSB	2.790926079	6.13279E-05
---	2.789124954	0.000345398
ITGB3	2.78657189	0.004670172
ADAMDEC1	2.782262251	0.007145934
IL1B	2.782206145	0.00041286
RAB20	2.780112965	0.001110742
CSF2RA	2.778992729	0.000461878
CTSB	2.777799296	0.000183752
---	2.777435965	0.020776591
---	2.776538279	0.00147234
PHACTR1	2.775119974	0.006856995
SIRPB1	2.766745874	0.00298686
CXCL2	2.762531102	0.000144147
SLC7A7	2.761996039	5.77481E-05
C13orf18	2.758894266	0.00333103
FN1	2.753272091	0.006441082
IRAK3	2.751268571	0.000157086
C13orf31	2.736634378	0.000795998
B3GNT5	2.736321042	0.000126687
GRN	2.735899235	6.50035E-05
ICAM1	2.735485621	9.10037E-05
NRP2	2.733851605	0.000386523
IL1B	2.732482875	0.000326871
SYK	2.725813543	0.000153379
SDC2	2.725682789	0.01091096
MS4A6A	2.72479217	0.00026837
LAMB3	2.722177083	0.001482631
NPL	2.721416604	0.001384283
HMOX1	2.71841432	0.000619865
TBC1D12	2.718076014	0.015410087
LOC731424	2.717772765	0.004342717
CEBPD	2.716458624	0.016945821
S100A9	2.715263376	0.000147195

ACSL1	2.709932066	6.14246E-05
CXCL16	2.70476702	0.000104336
F13A1	2.702265644	0.015348025
HLA-DRB1 /// HLA-DRB4 /// HLA-DRB5	2.702241209	0.000147195
GPNMB	2.694573601	0.003062089
---	2.688917111	0.00054981
IRAK3	2.684486215	0.019413972
CTSH	2.681758003	0.000305557
FPR3	2.679164534	0.036459668
TMEM176B	2.678972876	0.000153379
FCGR1B	2.671946164	0.000338708
SULF2	2.671263773	9.20368E-05
PHLDA1	2.670814785	0.00046332
MARCKS	2.66615364	0.000192616
LILRB3	2.665485896	9.10037E-05
C1orf38	2.664647621	0.001789734
FCGR2C	2.659932217	0.00028819
NLRP3	2.657606805	0.004308182
SLAMF7	2.651025775	0.004475748
SLAMF8	2.650011667	0.04310631
CLEC12A /// CLEC12B	2.649438915	0.007311408
GPR84	2.640964982	0.006860471
HLA-DRB1 /// HLA-DRB4	2.637287828	0.000220134
FN1	2.63629825	0.005484239
FN1	2.635035922	0.006727065
---	2.634118925	0.001602319
LPCAT2	2.633797197	0.001384283
---	2.63253786	0.029538602
TLR4	2.632525457	0.000220794
LILRB1	2.629877109	0.000650815
SIRPA	2.629124046	6.13279E-05
LILRB3	2.626500776	6.50035E-05
C11orf75	2.624794577	0.002099181
SLAMF7	2.624198086	0.004168604
RBM47	2.622336922	0.000287132
AGPAT9	2.621951805	0.010976203
SIGLEC1	2.61894443	0.005168659
EMILIN2	2.617202979	0.00012426
SLC16A6	2.614841284	0.000613322
WARS	2.613117429	7.02303E-05
DRAM1	2.613070365	0.000479373
TNS3	2.610288105	0.00298686
DOCK4	2.607612588	0.000697141
HLA-DPA1	2.602324785	0.000134803
---	2.593026612	0.000839296
DOCK5	2.585378709	0.000136825
FGL2	2.580356532	0.001576868
C1orf38	2.580287255	0.001482631
GAS7	2.577951768	0.00248251
GAS7	2.575106373	0.01131202
SH2D1B	2.574131951	0.034446242
MS4A6A	2.572393199	0.038925902
FNDC3B	2.568048869	0.00090424
HLA-DQB1	2.566726884	0.002418142
CD36	2.565048214	0.023447406
RTN1	2.563656257	0.023414859
HLA-DQB1	2.562956524	0.000147268

FAM49A	2.559852733	0.020559251
SIGLEC1	2.555519334	0.004470457
ZEB2	2.552780667	0.004027488
KIAA1598	2.552574008	0.000191841
HLA-DPA1	2.548905952	0.000220794
CLEC7A	2.547686609	0.00241651
---	2.544458437	0.003653649
CD93	2.543861049	6.77846E-05
MS4A6A	2.541859641	0.011007544
PMP22	2.539944447	0.000501866
LILRA3	2.537650844	0.004303796
TNS1	2.536331049	0.002598745
GNA15	2.534261334	0.000323775
SULF2	2.531403318	0.002259299
GK	2.52987559	0.000220134
CTNNA1	2.527601725	8.9486E-05
C3	2.526137539	0.01037798
LYZ	2.525718693	0.000925456
---	2.522426686	0.001558971
GK	2.521067041	9.73111E-05
BTK	2.518697671	0.001312749
SLC15A3	2.511794137	0.000729036
CTNNA1	2.500555153	0.000123601
ANXA5	2.499307735	0.000479246
PTGS1	2.496416777	0.001146627
CCRL2	2.495873825	0.005659921
PYGL	2.491801213	0.002637113
SLC31A2	2.491130769	0.0017324
PLAU	2.490384653	0.000750491
---	2.489147472	0.014767883
GAS7	2.487392828	0.003060893
RNF130	2.481929385	0.000129571
TJP2	2.480929276	0.013095789
MMP9	2.475047766	0.00203539
ITPRIPL2	2.470401933	0.0037816
PPIF	2.469039039	0.000220794
EPB41L3	2.465971023	0.000153379
WARS	2.465011064	0.001325061
GK3P	2.464048168	0.000189535
SLC16A6	2.463346303	0.00046332
H1F0	2.462171621	0.00034104
BCAT1	2.454326974	0.009648559
FAM49A	2.452116343	0.00023037
GRN	2.448340548	0.000142174
---	2.445542019	0.00243378
IL18RAP	2.440674903	0.004357957
LATS2	2.436896382	0.002174507
GAS7	2.432611237	0.011914543
CRLF2	2.432236672	0.001393812
FXYD6	2.428522265	0.005568493
NCF4	2.42785444	0.000903962
HLA-DRB1	2.426591367	0.000192616
ALDH3B1	2.421666213	0.002002053
---	2.418200353	0.000486049
PRDM1	2.416430968	0.0010353
MSR1	2.416151566	0.000501866
EMILIN2	2.415931731	0.002714837
HLA-DRB6	2.415607371	0.000325554

HLA-DQB1 /// LOC100294318	2.415128797	0.000650144
---	2.408253129	0.000262044
PIK3AP1	2.399103132	0.000431221
SIRPA	2.397035132	0.000100913
ITPRIPL2	2.396018878	0.001652892
HLA-DMA	2.395860563	0.000571803
PTAFR	2.393564368	0.002002157
RHOU	2.392193883	0.00289272
VEGFA	2.391426918	0.00506025
FAM26F	2.390807654	0.004755376
---	2.388483671	0.001747013
GLUL	2.388179559	0.000886214
---	2.385668089	0.006170343
CD109	2.384866803	0.004317863
CTSS	2.383964353	0.000375377
TNFSF13B	2.382292745	0.004257796
CSF3R	2.381053417	0.004522678
CORO1C	2.377936277	0.00012426
GLUL	2.377628985	0.001192813
ASPH	2.375319154	0.005384927
TLR8	2.374280388	0.004399803
MTMR11	2.371942564	0.000154773
HLA-DPA1	2.37173305	0.004271715
FCGR2B	2.370998574	0.028887134
CFP	2.370659558	0.000875191
TRIB1	2.368815751	0.00284018
LILRA2	2.368261154	0.000256462
C19orf59	2.368256007	0.003082129
PHLDA1	2.36766698	0.006038638
LILRA1	2.353065357	0.001395336
FCER1G	2.343070714	0.002227919
STEAP4	2.341943179	0.002898464
ACSL1	2.340413195	0.000693652
ABCC3	2.34018762	0.00086134
MAF	2.335311118	0.005786857
SMPDL3A	2.329652867	0.007879392
PSAP	2.327725342	0.000858787
ABCA1	2.323992134	0.018058818
SYK	2.321316503	0.000991237
CTSS	2.318365369	0.000501866
DHRS9	2.314963946	0.011240528
ALDH1A1	2.314756294	0.011007544
---	2.31379922	0.01503435
SLC22A4	2.30974016	0.001429316
CXCL5	2.308274043	0.027734283
RTN1	2.304668249	0.020298184
HLA-DRB4	2.303926167	0.00026837
FAM26F	2.303860131	0.000109465
NCF1 /// NCF1B /// NCF1C	2.302182003	0.000249921
PHLDA1	2.297048679	0.000521993
KMO	2.295108904	0.007359907
CYFIP1	2.293695564	0.001291738
RNF144B	2.288999773	0.019204296
IL8	2.288718105	0.000476648
LILRA2	2.282994481	0.0045273
HLA-DQB1	2.281576966	0.005261181
CD4	2.28084184	0.016451097

GNB4	2.275911505	0.009399778
ABCA1	2.273602237	0.000185276
CSF3R	2.272073461	0.019921425
OSM	2.266289057	0.002018584
RNF144B	2.265219014	0.015385513
---	2.264970404	0.014994933
TMEM176A	2.25744663	0.019119426
ADM	2.25374723	0.007777297
GAS2L1	2.253114254	0.006834061
LOC100288617	2.251288383	0.005466498
RBM47	2.250506644	0.000939254
SECTM1	2.248464731	0.003518857
---	2.248226145	0.021335195
CIITA	2.24577075	0.000884511
CLIC4	2.243175866	0.002064737
HAVCR2	2.243045857	0.010574248
BID	2.240463061	0.009488675
---	2.236334583	0.017149868
NRP2	2.235318462	0.034831625
PHLDA1	2.23516914	0.009509232
CTSB	2.233717962	0.001146627
HLA-DQB1	2.233048603	0.00054206
PPIF	2.23292309	0.001384283
ZEB2	2.230256053	0.031840444
ANKRD22	2.226337451	0.035407886
LAT2	2.225915771	0.016979366
NCF4	2.223493232	0.000228002
RGS18	2.22107262	0.024035372
FAM26F	2.220487664	0.001482631
ADAM9	2.219804914	0.002842934
ETS2	2.214635802	6.77846E-05
LILRA6	2.214225331	0.003904929
SLC11A1	2.213992175	9.10037E-05
CD68	2.212849176	0.005030046
LOC401233	2.21246306	0.002754349
ZEB2	2.211386792	0.006209702
IRAK3	2.208835646	0.004168604
GK	2.203185253	0.00034104
ETS2	2.201795382	0.013182997
TBXAS1	2.200417278	0.005475195
CIITA	2.19933266	0.000224766
CAPG	2.198824636	0.000287132
SPHK1	2.198304569	0.021335195
QPCT	2.196353425	0.003397833
PTAFR	2.187691645	0.001394889
LY86	2.185404565	0.027039142
ZC3H12C	2.184210757	0.025924576
RNF144B	2.183529486	0.01429024
SLC44A1	2.182648116	0.023704116
KCNJ15	2.17682867	0.009486154
MAP3K8	2.175075856	0.000839296
VEGFA	2.17454993	0.003242897
DOCK5	2.173049949	0.017615356
CREG1	2.170274725	9.29249E-05
IFIT3	2.168853216	0.00439352
SASH1	2.166491429	0.02248035
LILRB4	2.163713418	0.000471901
PSTPIP2	2.15147739	0.00056081

TBC1D12	2.151403738	0.004884201
RGL1	2.146972346	0.009789918
RAPH1	2.146410282	0.02518752
---	2.145485692	0.001312749
APOA2	2.144447592	0.012631494
FCER1G	2.144331642	0.00915835
NFAM1	2.143714142	0.004174988
ALCAM	2.140683029	0.001938139
FCGR2A /// FCGR2C	2.136180999	0.017254119
VEGFA	2.135069587	0.006209702
CTSZ	2.133736227	0.002898464
MARCKS	2.133204512	0.000435978
APLP2	2.131039976	0.001477242
MARCH1	2.121769512	0.009288856
CCL4	2.117420344	0.006856995
TLR4	2.117347327	0.020112377
TYMP	2.117346163	0.012116617
KCNJ2	2.116309913	0.006190559
CD302	2.112105681	0.043441074
GNS	2.110840164	0.001159696
DOCK4	2.108844451	0.017881692
SLC11A1	2.107456773	0.003084374
SIGLEC5	2.106656678	0.012880666
HLA-DMB	2.105516175	0.006952922
TNFSF13B	2.104220252	0.001075809
ANXA2	2.104166965	0.001048281
SLC24A4	2.092428025	0.035426972
SDC2	2.092021959	0.047274503
BCAT1	2.089838765	0.001429316
CCR6	2.085170128	0.010314612
CD1C	2.080855253	0.039205628
PRO2964	2.080776088	0.001803954
SIGLEC7	2.07903861	0.008667291
KIAA0146	2.075749908	0.016733689
BCL2A1	2.072718783	0.001225001
ZAK	2.068866946	0.001146627
LOC100289208 /// PHLDA1	2.067606298	0.013742988
ADAM9	2.067336742	0.001159696
IER3	2.066522086	0.000344111
PADI2	2.065687126	0.02116939
BID	2.065509667	0.006433969
FCGR1A /// FCGR1C	2.064028894	0.014492281
APOC1	2.063618346	0.037311644
PHLDA1	2.063479804	0.012897185
SOD2	2.062571256	0.000220794
SOD2	2.060669066	0.00095919
---	2.06059502	0.043914541
HLA-DPB1	2.059746981	0.002569582
CLEC4A	2.05400988	0.011316094
PTGER2	2.048336438	0.006170343
HLA-DRB1 /// HLA-DRB3 /// HLA-DRB4 /// HLA-DRB5 /// LOC100294036	2.048124424	0.009888958
GAS7	2.046401887	0.002898464
ANXA2	2.045863764	0.00122952
CORO1C	2.045753693	0.000461878
IFIT2	2.044696073	0.000619865
ANXA2	2.044151766	0.00194937

HSPC159	2.04377909	0.016158845
LST1	2.043523189	0.003144651
NPC2	2.042102371	0.000123092
MYOF	2.037148371	0.023939737
TUBB1	2.036611907	0.010209164
VPS37C	2.035908437	0.00054206
SLC2A6	2.035332868	0.00357648
LST1	2.03516995	0.003397833
ASAH1	2.032384646	0.00012426
FGD4	2.028705878	0.001482631
RNASE2	2.027194003	0.02291517
LST1	2.026527795	0.001482631
SNX10	2.022496257	0.001155447
IFNGR2	2.019826031	0.007061999
LIMS1	2.019152215	0.001110742
CTSS	2.018968089	0.001312749
ZNF503	2.017266544	0.012109661
DFNA5	2.016996117	0.000724691
---	2.015855287	0.00333103
CYP27A1	2.009451683	0.000220794
PLEKHO2	2.008197691	0.001906511
NCF1C	2.005583226	0.0003874
CD80	2.00369938	0.030960805

Table A2.3: Comparison of gene expression profiles of CD161+CD8+ vs CD161-CD8+ T cells in cord blood. Genes with >2 log_2 fold up regulation shown.

Gene.Symbol	logFC	adj.P.Val
DSC1	-2.903237142	0.000561933
FAM153A /// FAM153B	-2.021101865	0.008839375

Table A2.6: Comparison of gene expression profiles of CD161+CD8+ vs CD161-CD8+ T cells in cord blood. Genes with >2 log_2 fold down regulation shown.

Appendix 3:

Geneset enrichment analysis comparing CD161++CD8α+ vs CD161-CD8α+ datasets in cord and adult blood.

A3.1. Geneset enrichment analysis for UP-REGULATED GENES

A3.1.1 Statistics

Dataset	LucyW_E2_plusplus-minus_collapsed
Phenotype	NoPhenotypeAvailable
Upregulated in class	na_pos
GeneSet	UP REG RAW P 0.01
Enrichment Score (ES)	0.6803454
Normalized Enrichment Score (NES)	4.124273
Nominal p-value	0.0
FDR q-value	0.0
FWER p-Value	0.0

A3.1.2 Genes contributing to leading edge enrichment score

PROBE	RANK IN GENE LIST	RANK METRIC SCORE	RUNNING ES	CORE ENRICHMENT
KLRB1	0	21.80603981	0.008065439	Yes
ZBTB16	1	20.76554298	0.015746027	Yes
FAM43A	2	19.00238037	0.022774471	Yes
CCR6	3	18.37059212	0.029569235	Yes
RORC	5	15.40121746	0.035210796	Yes
NCR3	7	13.58539963	0.040180735	Yes
IL18RAP	9	13.27722359	0.045036692	Yes
KIT	10	13.18701839	0.0499142	Yes
PHACTR2	11	12.77184677	0.054638144	Yes
CEBPD	13	12.62705994	0.05925362	Yes
MAF	14	11.5253849	0.063516535	Yes
CACNA2D2	16	10.83139801	0.06746785	Yes
PRF1	17	10.81216812	0.07146697	Yes
LATS2	18	10.77336216	0.07545173	Yes
KIF5C	19	10.62022591	0.07937985	Yes
IL18R1	20	10.58071995	0.08329336	Yes
PRDM1	22	10.34609699	0.087065175	Yes
ERN1	23	10.25961494	0.09085992	Yes
CCR1	24	10.18205643	0.09462597	Yes
TNFSF14	25	10.09345818	0.09835926	Yes
PSCD3	26	9.919399261	0.10202816	Yes
KLRF1	27	9.689465523	0.105612025	Yes
GYG1	29	9.165244102	0.108947076	Yes

FREQ	31	9.112288475	0.11226254	Yes
LOC619207	32	9.061756134	0.11561423	Yes
RAB11FIP1	34	8.866705894	0.118838854	Yes
SLAMF1	35	8.837602615	0.12210763	Yes
CXCR6	36	8.592684746	0.12528582	Yes
TYROBP	37	8.547637939	0.12844735	Yes
BHLHB2	38	8.500946999	0.13159162	Yes
PRNP	39	8.43671608	0.13471211	Yes
MYO1F	40	8.320815086	0.13778976	Yes
FEZ1	41	8.301046371	0.14086008	Yes
CSF1R	43	8.253334045	0.14385784	Yes
KLRG1	45	8.173316002	0.146826	Yes
SCD5	46	8.129601479	0.1498329	Yes
TLE1	50	7.96795845	0.1526153	Yes
NCAM1	53	7.882385254	0.15542093	Yes
SLC16A3	57	7.752401352	0.15812358	Yes
ADRB2	58	7.744237423	0.16098796	Yes
SIPA1L2	59	7.717681885	0.16384251	Yes
ACTN4	60	7.704112053	0.16669205	Yes
CYB561	61	7.680686474	0.16953291	Yes
LRIG1	63	7.647157669	0.17230646	Yes
AHNAK	69	7.56463623	0.17482984	Yes
DUSP6	70	7.555166245	0.17762429	Yes
THBS1	71	7.546029568	0.18041535	Yes
PDZD4	73	7.388830185	0.18309334	Yes
PTGDR	74	7.385462284	0.18582502	Yes
CASP1	78	7.337090015	0.18837406	Yes
PLAUR	79	7.300203323	0.19107419	Yes
MAFF	80	7.291444778	0.1937711	Yes
FURIN	82	7.284314156	0.19641045	Yes
SART2	84	7.159857273	0.19900376	Yes
PIK3AP1	89	7.098859787	0.20140977	Yes
NEO1	91	7.007063866	0.20394656	Yes
CREB3L2	94	6.955151081	0.20640925	Yes
CYP1B1	97	6.852044582	0.2088338	Yes
FCAR	98	6.838677883	0.21136323	Yes
DUSP5	100	6.821020126	0.21383122	Yes
SLC4A4	102	6.769264221	0.21628007	Yes
CXXC5	103	6.762177944	0.2187812	Yes
PDE8A	104	6.760861397	0.22128186	Yes
CACNB3	105	6.703292847	0.22376122	Yes
LYN	108	6.659692764	0.22611462	Yes
LOC389634	109	6.655082703	0.22857614	Yes
CR1	110	6.648626328	0.23103529	Yes
CD151	112	6.6445508	0.233438	Yes
GNA15	114	6.622200966	0.23583245	Yes
EBI2	118	6.563209057	0.23809525	Yes
YPEL1	119	6.536242008	0.24051282	Yes
PPP2R2B	120	6.518707275	0.24292392	Yes
HM13	121	6.508321285	0.24533115	Yes
PHLDA1	122	6.495426178	0.24773362	Yes
GPR65	123	6.494598389	0.2501358	Yes
SRC	124	6.492931843	0.25253734	Yes

NPC1	126	6.481323242	0.25487968	Yes
DFNB31	128	6.465346813	0.25721613	Yes
SLCO3A1	130	6.431777477	0.25954014	Yes
LOC653127	131	6.424717426	0.26191646	Yes
EPB41L3	133	6.375169754	0.26421955	Yes
ADAM19	134	6.365929604	0.2665741	Yes
AUTS2	136	6.325740337	0.26885894	Yes
CTNNA1	137	6.310340881	0.27119294	Yes
PLD1	138	6.306882858	0.27352569	Yes
GZMA	139	6.268778324	0.27584434	Yes
GATA3	140	6.250342369	0.27815616	Yes
PLCB1	141	6.228885651	0.28046003	Yes
TNFRSF1B	142	6.22160387	0.28276125	Yes
LOC648470	146	6.177410126	0.28488135	Yes
SLAMF7	148	6.135259628	0.2870957	Yes
ALOX5AP	150	6.109394073	0.28930047	Yes
ZC3H12A	151	6.105469704	0.2915587	Yes
RRBP1	152	6.102072716	0.29381567	Yes
MGC14376	153	6.098640919	0.2960714	Yes
IL12RB2	154	6.095413208	0.29832593	Yes
ATP2B4	159	6.034834862	0.3003384	Yes
ADCY9	162	6.016711235	0.30245396	Yes
B4GALT5	163	6.016376495	0.30467924	Yes
EDG8	167	5.986781597	0.30672884	Yes
CD36	168	5.959416866	0.30893308	Yes
CCL20	170	5.942185879	0.311076	Yes
PMAIP1	177	5.857067585	0.31291288	Yes
CYBB	178	5.852308273	0.31507748	Yes
CSPG2	183	5.773425102	0.31699324	Yes
CPVL	184	5.765337467	0.31912568	Yes
MAPK8IP3	185	5.757008076	0.32125503	Yes
P2RY14	187	5.755743027	0.323329	Yes
EIF2C4	189	5.749152184	0.32540053	Yes
CD163	190	5.740252972	0.3275237	Yes
RAPGEF1	194	5.719049454	0.32947427	Yes
MAFB	196	5.695277214	0.33152586	Yes
CLEC7A	197	5.694661617	0.33363217	Yes
IL15RA	198	5.685540676	0.33573508	Yes
TNFAIP2	199	5.678168297	0.33783528	Yes
SLC7A5	201	5.671345234	0.33987805	Yes
TSPAN18	202	5.657338619	0.34197053	Yes
CDKN1A	204	5.6419034	0.3440024	Yes
PILRA	211	5.568434715	0.3457325	Yes
IFI30	213	5.562821865	0.34773514	Yes
S100A11	219	5.530720711	0.3495062	Yes
GUCY1A3	221	5.529561996	0.35149652	Yes
VCL	225	5.505429745	0.35336807	Yes
FHL1	227	5.473900318	0.3553378	Yes
LST1	229	5.465822697	0.35730454	Yes
SYK	232	5.420598984	0.35919964	Yes
B4GALT1	236	5.403229237	0.3610334	Yes
CCR2	237	5.402226925	0.36303154	Yes
LILRB2	247	5.335067749	0.3645106	Yes

ITGAX	248	5.332178593	0.36648282	Yes
TNF	252	5.321578503	0.36828637	Yes
APLP2	255	5.31012392	0.3701406	Yes
RHOC	262	5.275001526	0.3717622	Yes
STX11	266	5.255023479	0.37354115	Yes
ZDHHC14	267	5.229747772	0.37547547	Yes
ANXA2	268	5.211312294	0.377403	Yes
IL4I1	269	5.199875832	0.37932628	Yes
CST7	270	5.199486256	0.38124943	Yes
ELOVL6	273	5.184913635	0.38305733	Yes
CAMTA1	275	5.174298286	0.38491625	Yes
GALNAC4S-6ST	276	5.173745632	0.38682988	Yes
IFNGR1	277	5.172579288	0.38874307	Yes
FASLG	279	5.154631615	0.3905947	Yes
GALC	281	5.148880005	0.39244422	Yes
SMAD3	286	5.119298935	0.39411804	Yes
PLXNC1	287	5.11804533	0.39601105	Yes
RORA	291	5.083367825	0.3977265	Yes
CTSH	292	5.082153797	0.39960626	Yes
RIN2	293	5.080786705	0.4014855	Yes
CKLF	298	5.02649641	0.403125	Yes
SCRN1	300	5.019603729	0.4049267	Yes
COLQ	301	5.018210411	0.40678278	Yes
PLEKHG3	305	5.003352642	0.40846863	Yes
MAP3K5	310	4.979818821	0.41009086	Yes
DUSP1	311	4.977256775	0.4119318	Yes
ANXA5	313	4.961959839	0.4137122	Yes
RHOQ	318	4.95179081	0.41532406	Yes
RAB31	319	4.94507122	0.4171531	Yes
SYNE2	323	4.92378664	0.41880953	Yes
FOSL2	324	4.922563553	0.42063025	Yes
KYNU	325	4.914896965	0.42244813	Yes
ID2	334	4.879513741	0.4238136	Yes
LYZ	337	4.868513584	0.4255045	Yes
SLC11A1	340	4.852505207	0.42718947	Yes
ADAM8	348	4.82109642	0.42858827	Yes
FCN1	349	4.818413734	0.43037045	Yes
ALDH2	351	4.81163168	0.43209523	Yes
S100A4	354	4.806293964	0.43376312	Yes
ANPEP	355	4.80418396	0.43554005	Yes
ARNTL	356	4.801642895	0.43731603	Yes
DNAPTP6	357	4.799189568	0.43909112	Yes
IL8	361	4.78385973	0.4406958	Yes
CYP2E1	365	4.773283005	0.44229653	Yes
PODXL	368	4.767952919	0.44395024	Yes
GLB1	369	4.767878056	0.44571376	Yes
PTPRM	372	4.746851921	0.44735965	Yes
SLC4A10	376	4.738976002	0.44894773	Yes
IL23R	382	4.706979752	0.45041412	Yes
MARCKS	384	4.696851254	0.45209643	Yes
IL15	386	4.690071106	0.45377624	Yes
LILRA5	387	4.689428806	0.45551074	Yes
CERK	391	4.676886082	0.45707583	Yes

FAM38A	393	4.664768696	0.45874628	Yes
AGPAT4	400	4.631959915	0.46013004	Yes
LAMC1	403	4.628708839	0.46173224	Yes
SKAP2	404	4.62250042	0.46344197	Yes
LILRA2	410	4.581659794	0.46486202	Yes
DENND3	411	4.577863216	0.46655524	Yes
PTGS2	412	4.575853825	0.4682477	Yes
USP13	414	4.562480927	0.46988034	Yes
DUSP16	418	4.547562122	0.4713976	Yes
MAP3K8	421	4.535833359	0.47296545	Yes
FLJ20273	427	4.496328831	0.47435394	Yes
ME1	432	4.46567297	0.475786	Yes
SLC1A5	436	4.458178997	0.47727022	Yes
CHD9	438	4.449289799	0.47886097	Yes
MAN1A1	439	4.448132992	0.4805062	Yes
CST3	443	4.43739748	0.48198274	Yes
MS4A7	444	4.435190678	0.48362318	Yes
LONRF3	445	4.435074806	0.4852636	Yes
CAMK2N1	446	4.428312778	0.4869015	Yes
RXRA	449	4.404930115	0.48842093	Yes
CD40LG	456	4.373818398	0.4897092	Yes
PHLDB2	458	4.364257813	0.4912685	Yes
C3AR1	462	4.359340191	0.49271613	Yes
ARHGAP18	465	4.351591587	0.49421585	Yes
HLA-DRA	469	4.334348202	0.49565426	Yes
RDX	470	4.328900337	0.49725538	Yes
NPM2	471	4.327510357	0.498856	Yes
CA2	475	4.323923588	0.5002906	Yes
NBEAL2	476	4.32278204	0.50188947	Yes
KIAA0427	485	4.282352924	0.50303406	Yes
FCGR2A	487	4.276397228	0.5045608	Yes
GALNT10	489	4.271082878	0.5060857	Yes
ATF3	491	4.270321369	0.50761026	Yes
TGFBI	503	4.234194279	0.5085723	Yes
GALM	519	4.172367573	0.5092918	Yes
LIMS1	521	4.170872688	0.51077956	Yes
PPIF	522	4.170832634	0.51232225	Yes
DPP4	530	4.148039818	0.5134721	Yes
MESDC1	532	4.138533115	0.5149479	Yes
LMO2	538	4.113557339	0.5161948	Yes
STOM	543	4.108308315	0.51749474	Yes
PLEKHC1	544	4.106363297	0.5190135	Yes
ZFYVE28	545	4.105643272	0.5205321	Yes
QPCT	556	4.091723919	0.52149636	Yes
NTN4	562	4.074182987	0.52272874	Yes
LIMK1	571	4.05080986	0.5237877	Yes
FLJ22662	578	4.03028059	0.5249489	Yes
HIST2H2AA3	579	4.029924393	0.5264394	Yes
TSPAN15	595	4.003782749	0.52709657	Yes
CXCL16	596	4.000835896	0.5285764	Yes
CD58	599	3.995071173	0.52994424	Yes
HDAC9	615	3.961694956	0.5305858	Yes
CENTG2	619	3.948429346	0.5318815	Yes

FGD2	627	3.931590796	0.5329513	Yes
PLEKHA7	629	3.929061174	0.5343496	Yes
CSTA	639	3.916164398	0.53530383	Yes
NRIP1	641	3.905617476	0.5366935	Yes
SYTL2	647	3.897696972	0.5378606	Yes
NRIP3	658	3.870251894	0.5387429	Yes
PTGDS	663	3.858894587	0.53995055	Yes
MNDA	678	3.838764906	0.5406016	Yes
PRKCD	693	3.808148146	0.54124135	Yes
ZNF342	696	3.800458908	0.54253715	Yes
RIMS3	703	3.789741993	0.5436094	Yes
MXD1	706	3.778506279	0.54489714	Yes
GPR68	710	3.772855043	0.54612786	Yes
FOSB	712	3.76631546	0.547466	Yes
G0S2	715	3.759261131	0.54874665	Yes
PPGB	722	3.743608475	0.54980177	Yes
FLJ11292	723	3.741484165	0.55118567	Yes
PSEN2	727	3.728762865	0.55240005	Yes
IL13RA1	728	3.726619482	0.55377847	Yes
REC8L1	741	3.710196257	0.55449176	Yes
GAS7	747	3.701321602	0.5555862	Yes
RAB6B	750	3.698988676	0.55684453	Yes
PARVB	755	3.695915461	0.55799186	Yes
LYAR	765	3.683338881	0.55886	Yes
PLXDC2	777	3.649822235	0.5596059	Yes
EMILIN2	783	3.631172895	0.5606744	Yes
CLIC5	793	3.617364883	0.56151813	Yes
CFH	794	3.61705637	0.56285596	Yes
IL17RE	796	3.613489866	0.5641376	Yes
LTK	817	3.581984282	0.5643642	Yes
IER3	826	3.573546171	0.5652466	Yes
MTMR11	828	3.569939137	0.5665121	Yes
RAB32	832	3.561797857	0.5676648	Yes
IL1RN	845	3.552880049	0.5683199	Yes
TCIRG1	847	3.546749592	0.56957686	Yes
ATG16L2	852	3.538807154	0.5706661	Yes
ODF2L	854	3.537391663	0.57191956	Yes
TPD52	857	3.534867764	0.5731172	Yes
FHOD1	859	3.533617496	0.57436925	Yes
SEMA4A	864	3.52808857	0.57545453	Yes
LGALS2	865	3.52244997	0.5767574	Yes
NCAPG2	868	3.518845558	0.57794905	Yes
GBP5	870	3.517119646	0.579195	Yes
EOMES	879	3.507873297	0.58005315	Yes
SLC44A3	883	3.505701065	0.5811851	Yes
PHTF1	886	3.494273663	0.5823677	Yes
CACNA2D4	913	3.465837002	0.5822218	Yes
MATK	920	3.455084085	0.5831703	Yes
RNF165	924	3.452568531	0.5842825	Yes
HIP1	927	3.450010061	0.58544874	Yes
FLJ20245	929	3.448262691	0.58666927	Yes
OSM	930	3.445040941	0.5879435	Yes
TBXAS1	931	3.44433713	0.5892175	Yes

APOBEC3A	935	3.441273928	0.59032553	Yes
SERPINA1	941	3.42944169	0.59131944	Yes
NETO2	949	3.41789937	0.5921992	Yes
TRIM7	965	3.402243853	0.59263384	Yes
CHST13	974	3.394920826	0.59345025	Yes
IRAK2	976	3.390859842	0.5946495	Yes
PTGS1	977	3.388207674	0.5959027	Yes
LOC401233	991	3.364709616	0.59643334	Yes
GTF3C1	1002	3.343645573	0.5971209	Yes
IL6	1013	3.331519842	0.597804	Yes
MKNK1	1015	3.329552412	0.5989806	Yes
ATN1	1023	3.320897818	0.5998245	Yes
HOP	1037	3.307687759	0.600334	Yes
JUN	1050	3.290838718	0.6008922	Yes
AIM2	1061	3.27833128	0.60155565	Yes
SPRY1	1074	3.266071796	0.60210466	Yes
FGL2	1079	3.258044243	0.60309005	Yes
PDE4B	1083	3.249843597	0.60412735	Yes
CCDC46	1089	3.243891716	0.6050526	Yes
ABAT	1095	3.235709906	0.60597485	Yes
IGFBP4	1102	3.232088566	0.6068408	Yes
SNAI3	1103	3.232073069	0.6080363	Yes
SIGLEC7	1107	3.22671032	0.609065	Yes
ALOX5	1121	3.209399223	0.60953814	Yes
GPR171	1127	3.203947067	0.6104486	Yes
IL1B	1134	3.194858789	0.6113008	Yes
PLA2G7	1139	3.189864397	0.612261	Yes
S100A9	1144	3.1816113	0.6132181	Yes
ATP2A2	1146	3.179727793	0.6143393	Yes
FCHO2	1149	3.174367428	0.6154036	Yes
NADK	1176	3.142243624	0.61513805	Yes
MYO1D	1178	3.138985157	0.61624414	Yes
DPY19L1	1193	3.12052083	0.61662954	Yes
CYFIP1	1196	3.116620779	0.61767244	Yes
CACNB1	1197	3.116112947	0.618825	Yes
ANXA2P1	1207	3.108178377	0.6194804	Yes
BLK	1211	3.103300333	0.6204635	Yes
IGSF4	1222	3.094072819	0.62105876	Yes
FAM46C	1225	3.089554787	0.62209165	Yes
PRSS35	1232	3.078603029	0.62290084	Yes
CIAS1	1240	3.072924137	0.62365305	Yes
TMEM62	1242	3.070973158	0.624734	Yes
CD14	1243	3.070876598	0.6258698	Yes
GPR114	1244	3.070453882	0.62700546	Yes
SPIRE1	1247	3.069132328	0.62803084	Yes
IGSF6	1259	3.052056551	0.62855566	Yes
SP140	1261	3.051899672	0.62962955	Yes
ADAM15	1267	3.048643827	0.63048255	Yes
NEK3	1268	3.047788858	0.63160986	Yes
MATN2	1271	3.046103239	0.6326267	Yes
TNFRSF25	1274	3.043996334	0.6336428	Yes
RGS2	1281	3.039242268	0.6344374	Yes
IRF8	1282	3.039004803	0.63556147	Yes

YWHAH	1284	3.038379192	0.63663036	Yes
NFKBIA	1289	3.031543255	0.63753194	Yes
CEBPA	1290	3.030234337	0.63865274	Yes
PPP2R3A	1303	3.017175913	0.63910973	Yes
DDAH2	1313	3.009362936	0.6397286	Yes
ABCD1	1323	2.998993874	0.6403436	Yes
ACSL1	1334	2.981038094	0.64089704	Yes
GDPD5	1335	2.980474472	0.6419994	Yes
HCK	1338	2.978556156	0.6429913	Yes
SH2D2A	1353	2.966213703	0.6433196	Yes
CAPN12	1358	2.964043856	0.6441963	Yes
FPR1	1378	2.943536758	0.64424163	Yes
CD86	1393	2.928996325	0.64455616	Yes
ELOVL4	1411	2.91498661	0.64470077	Yes
PTMS	1423	2.90745759	0.6451721	Yes
HPGD	1442	2.894640207	0.6452543	Yes
IGF2BP2	1449	2.889443636	0.64599353	Yes
FSIP1	1479	2.865753651	0.64546096	Yes
NCF4	1482	2.86461091	0.64641064	Yes
LAT2	1484	2.862391949	0.64741445	Yes
LIM2	1518	2.835563183	0.6466511	Yes
DUSP2	1521	2.834377289	0.64758956	Yes
CENTA2	1551	2.805279732	0.64703465	Yes
LRRN6C	1556	2.801183224	0.64785105	Yes
PLOD3	1558	2.800857306	0.64883214	Yes
NPDC1	1564	2.796108484	0.64959174	Yes
ABCA1	1588	2.779903412	0.6493569	Yes
DOPEY2	1590	2.779615402	0.65033007	Yes
KIF13A	1593	2.778516054	0.651248	Yes
UNC13D	1607	2.766874313	0.65155745	Yes
DBN1	1613	2.762182713	0.65230453	Yes
PPAPDC1B	1630	2.745987654	0.65244156	Yes
BASP1	1637	2.740585566	0.65312576	Yes
TGFA	1655	2.72881937	0.6532015	Yes
CDKN1C	1702	2.688635826	0.65166986	Yes
LARP2	1715	2.681653738	0.65200275	Yes
SNTB2	1729	2.670999527	0.6522768	Yes
OGDH	1741	2.664944172	0.6526584	Yes
HOXA5	1742	2.664867163	0.6536441	Yes
RBP7	1747	2.659271717	0.654408	Yes
PDE5A	1753	2.65438962	0.6551152	Yes
CCL4	1778	2.636820555	0.6547725	Yes
DOK3	1783	2.633845329	0.65552706	Yes
RHBDF2	1789	2.630845308	0.65622556	Yes
SERPINB2	1798	2.628425598	0.6567584	Yes
IER5	1810	2.621505737	0.657124	Yes
CYP27A1	1816	2.619147539	0.65781814	Yes
LOC162073	1823	2.613550663	0.6584554	Yes
AFF3	1839	2.604640245	0.658595	Yes
CTSZ	1841	2.603923559	0.6595032	Yes
LTB4R	1842	2.60384202	0.6604663	Yes
NHS	1847	2.596761942	0.6612071	Yes
COL5A1	1859	2.588991642	0.66156065	Yes

PLEKHF1	1867	2.583128929	0.66213167	Yes
CSF2RB	1902	2.55858016	0.6612109	Yes
UCK2	1908	2.554558277	0.6618812	Yes
LILRA3	1930	2.540462494	0.66166764	Yes
S100A12	1932	2.539981127	0.6625522	Yes
CLIC4	1945	2.53615284	0.66283125	Yes
IL29	1955	2.533492327	0.66327405	Yes
ITPKA	1960	2.531010628	0.66399056	Yes
SULF2	1966	2.527225256	0.66465074	Yes
F3	1979	2.516509056	0.66492254	Yes
ZDHHC1	1982	2.515810728	0.66574323	Yes
ABCC3	1993	2.511808157	0.66612315	Yes
FUCA2	2002	2.506487131	0.6666109	Yes
HMOX1	2014	2.502239466	0.66693234	Yes
PTPRE	2020	2.496199846	0.667581	Yes
SLC45A3	2035	2.484881163	0.66773134	Yes
CXCL2	2039	2.482931852	0.6684849	Yes
LPAL2	2053	2.478730202	0.6686879	Yes
PPAP2C	2064	2.472122431	0.6690531	Yes
P2RX1	2070	2.470788479	0.6696924	Yes
PDK4	2080	2.464746475	0.6701098	Yes
OLFM1	2102	2.454750776	0.66986454	Yes
LAG3	2124	2.446820498	0.66961634	Yes
FRY	2140	2.440843821	0.6696954	Yes
GAS1	2157	2.432703018	0.66971654	Yes
LTBR	2180	2.422415972	0.6694044	Yes
RASSF4	2207	2.409572124	0.6688678	Yes
MGC99813	2210	2.408913612	0.669649	Yes
KCNK7	2211	2.408056974	0.6705397	Yes
FOLR1	2216	2.405284643	0.6712097	Yes
OGFRL1	2217	2.404600382	0.67209905	Yes
ECGF1	2220	2.403534889	0.6728782	Yes
LAMA2	2261	2.383359194	0.67156315	Yes
CARD14	2268	2.379199982	0.67211366	Yes
SLC7A7	2272	2.376197338	0.67282784	Yes
GPBAR1	2289	2.368089676	0.6728251	Yes
FLJ20021	2337	2.345180035	0.67111146	Yes
PDLIM7	2358	2.33707571	0.67087764	Yes
TYRO3	2359	2.336915016	0.67174196	Yes
B3GALT2	2362	2.335890055	0.67249614	Yes
ANXA4	2370	2.332709551	0.6729745	Yes
C5AR1	2374	2.331262827	0.673672	Yes
FLJ39501	2392	2.32219243	0.6735974	Yes
GREM2	2414	2.312208652	0.67329943	Yes
ROR2	2415	2.311079979	0.6741542	Yes
HK3	2445	2.299030781	0.673412	Yes
BMPR1A	2466	2.291373014	0.67316127	Yes
SSH3	2470	2.289829731	0.67384344	Yes
MS4A6A	2490	2.281709671	0.673644	Yes
IRAK3	2509	2.274199724	0.6734967	Yes
GFI1B	2530	2.263063669	0.6732354	Yes
PRR5	2531	2.262978315	0.67407244	Yes
ST3GAL6	2535	2.259574413	0.6747435	Yes

ALDH3B1	2540	2.258307457	0.6753591	Yes
KCNMB1	2547	2.255347252	0.6758638	Yes
GP1BB	2586	2.240118504	0.6746056	Yes
MERTK	2596	2.234256983	0.6749377	Yes
BCL3	2601	2.231661797	0.6755435	Yes
RTN2	2604	2.229003429	0.67625815	Yes
HYPE	2618	2.222064734	0.6763661	Yes
IFI44L	2657	2.20558691	0.67509514	Yes
VLDLR	2661	2.203542471	0.6757454	Yes
CENTD3	2665	2.202069283	0.6763951	Yes
SMAD7	2717	2.182220936	0.67440164	Yes
COL5A3	2721	2.179727793	0.6750431	Yes
FSD1	2733	2.172428846	0.67524254	Yes
GCHFR	2748	2.168635368	0.67527586	Yes
POU2F2	2750	2.167578697	0.6760227	Yes
ETV6	2783	2.154008865	0.6750621	Yes
TNFAIP6	2835	2.135616064	0.67305136	Yes
SOD2	2838	2.133938789	0.6737308	Yes
PACSIN1	2847	2.131647587	0.67407995	Yes
LOC285513	2850	2.129124641	0.6747576	Yes
UST	2857	2.126056433	0.67521447	Yes
ANXA2P3	2858	2.12587595	0.6760008	Yes
CPNE7	2864	2.124094248	0.6765118	Yes
NRG1	2865	2.124079704	0.6772975	Yes
LRRC33	2869	2.121527672	0.6779174	Yes
RBM24	2873	2.119808197	0.6785368	Yes
CD72	2877	2.118317842	0.6791555	Yes
HLA-DRB6	2881	2.114668131	0.6797729	Yes
GFPT2	2891	2.111592054	0.68005973	Yes
ASGR1	2901	2.10874033	0.6803454	Yes

A3.2. Geneset enrichment analysis for DOWN-REGULATED GENES

A3.2.1 Statistics

Dataset	LucyW_E2_plusplus-minus_collapsed
Phenotype	NoPhenotypeAvailable
Upregulated in class	na_neg
GeneSet	DOWN REG RAW P 0.01
Enrichment Score (ES)	-0.5632127
Normalized Enrichment Score (NES)	-3.2237494
Nominal p-value	0.0
FDR q-value	0.0
FWER p-Value	0.0

A3.2.2 Genes contributing to leading edge enrichment score

PROBE	RANK IN GENE LIST	RANK METRIC SCORE	RUNNING ES	CORE ENRICHMENT
PINX1	14012	-1.376793385	-0.5628746	Yes
PLEKHF2	14015	-1.378279328	-0.5626502	Yes
BAG5	14019	-1.380649805	-0.5624822	Yes
RCL1	14025	-1.383131027	-0.56242764	Yes
PTP4A3	14032	-1.386532903	-0.56242925	Yes
CDK4	14033	-1.387801409	-0.56208843	Yes
CCDC34	14040	-1.392524719	-0.56208855	Yes
LOC51035	14048	-1.395613909	-0.56214494	Yes
ZNF417	14050	-1.39686358	-0.56185895	Yes
PFN2	14051	-1.396910667	-0.561516	Yes
GYPC	14065	-1.401070118	-0.5619131	Yes
ZNF365	14078	-1.405950546	-0.5622519	Yes
NDUFA10	14084	-1.40936625	-0.56219095	Yes
TBRG4	14088	-1.410308838	-0.56201565	Yes
LOC150383	14094	-1.414225817	-0.5619534	Yes
DHPS	14100	-1.417417645	-0.5618904	Yes
KTI12	14104	-1.419562936	-0.5617129	Yes
TSPAN32	14111	-1.423526764	-0.5617054	Yes
LOC221143	14112	-1.424204946	-0.5613557	Yes
PDCD8	14114	-1.425332785	-0.56106275	Yes
HMGN2	14118	-1.426622868	-0.56088346	Yes
ATP6V0E2L	14120	-1.427449465	-0.56058997	Yes
DPAGT1	14129	-1.432266593	-0.56069434	Yes
FBXO46	14133	-1.433626294	-0.5605134	Yes
ZIK1	14144	-1.436910391	-0.56073064	Yes

SRGAP3	14145	-1.437208772	-0.5603777	Yes
LOC57228	14146	-1.438207746	-0.56002456	Yes
DIABLO	14158	-1.443092465	-0.5602973	Yes
TP53RK	14161	-1.444393873	-0.5600567	Yes
SCOC	14170	-1.450096011	-0.5601567	Yes
PHKB	14172	-1.452332735	-0.5598571	Yes
MFNG	14175	-1.452892065	-0.55961436	Yes
MRFAP1L1	14190	-1.458590984	-0.5600543	Yes
ZNF345	14192	-1.459527135	-0.55975294	Yes
AHSA1	14198	-1.461051702	-0.55967927	Yes
ECD	14209	-1.466996312	-0.55988914	Yes
SUNC1	14216	-1.470515966	-0.5598701	Yes
NICN1	14220	-1.471313	-0.55967987	Yes
CRSP8	14223	-1.472243786	-0.5594324	Yes
SOCS5	14229	-1.475043774	-0.5593552	Yes
EPHX1	14246	-1.481360078	-0.5599036	Yes
ARRDC3	14252	-1.482216716	-0.5598247	Yes
LOC401431	14272	-1.491667628	-0.5605416	Yes
PDE6B	14287	-1.497688055	-0.560972	Yes
IL21R	14290	-1.499487758	-0.5607178	Yes
LOC144233	14293	-1.50159812	-0.56046313	Yes
SAP18	14294	-1.501652598	-0.5600944	Yes
VCAM1	14295	-1.501756668	-0.55972564	Yes
ZNF80	14301	-1.505572677	-0.559641	Yes
AFF1	14313	-1.51176393	-0.5598969	Yes
ELMO1	14318	-1.514952779	-0.55975294	Yes
ZNF286	14324	-1.517214417	-0.55966544	Yes
CECR1	14333	-1.521388531	-0.55974793	Yes
HERC3	14339	-1.522441149	-0.5596592	Yes
TERF2	14342	-1.523636222	-0.55939907	Yes
GSTM2	14354	-1.528705001	-0.5596508	Yes
TSNAX	14370	-1.535079479	-0.560129	Yes
RKHD3	14372	-1.535192609	-0.5598091	Yes
TOP1	14377	-1.538375497	-0.55965936	Yes
SMARCD1	14381	-1.53964448	-0.55945235	Yes
PHF17	14386	-1.541688085	-0.5593018	Yes
PABPC4	14389	-1.543503165	-0.55903685	Yes
HIRIP3	14392	-1.544794679	-0.55877155	Yes
PTK9	14403	-1.549883246	-0.55896103	Yes
SETD3	14417	-1.553838611	-0.5593206	Yes
CALM3	14418	-1.553850889	-0.5589391	Yes
CLK3	14445	-1.565414548	-0.56003696	Yes
EIF4G2	14477	-1.577217817	-0.561417	Yes
NUDT16L1	14483	-1.578861713	-0.56131434	Yes
TBCE	14490	-1.580650091	-0.56126827	Yes
BTBD1	14501	-1.585144639	-0.5614491	Yes
LBR	14508	-1.589532375	-0.5614009	Yes
RFC2	14520	-1.596970201	-0.56163585	Yes
LGALS3BP	14523	-1.597166181	-0.5613577	Yes
SLC37A3	14528	-1.598798156	-0.56119317	Yes
TMEM69	14531	-1.599527121	-0.5609144	Yes
RBMXL1	14537	-1.603497863	-0.56080574	Yes
FAHD1	14558	-1.615323186	-0.56154925	Yes

OLFM2	14565	-1.617754459	-0.5614941	Yes
ZFP3	14575	-1.623440862	-0.56160855	Yes
VPS16	14576	-1.624048233	-0.56120974	Yes
RPS4Y1	14577	-1.624141693	-0.560811	Yes
CCNT2	14584	-1.626730323	-0.5607536	Yes
SLC16A7	14592	-1.630213499	-0.56075233	Yes
BCL9	14596	-1.631779194	-0.5605227	Yes
PSMB8	14599	-1.632693648	-0.5602358	Yes
FLNB	14601	-1.633112431	-0.5598918	Yes
NAALADL1	14606	-1.636545777	-0.559718	Yes
KIAA1008	14610	-1.639118433	-0.55948657	Yes
HDDC2	14617	-1.641582608	-0.55942553	Yes
CCT6A	14626	-1.643349051	-0.5594781	Yes
LCK	14637	-1.650240302	-0.559643	Yes
CHCHD7	14638	-1.650572181	-0.55923766	Yes
ERBB2IP	14641	-1.652226925	-0.558946	Yes
HIGD2A	14650	-1.657661557	-0.558995	Yes
CSNK1A1	14659	-1.661091328	-0.5590432	Yes
LOC201164	14660	-1.661355972	-0.5586353	Yes
CD8A	14665	-1.664381862	-0.55845463	Yes
COQ7	14667	-1.665259123	-0.5581028	Yes
APPBP2	14694	-1.679821134	-0.5591725	Yes
ANXA6	14719	-1.688379884	-0.5601262	Yes
LETMD1	14729	-1.692663431	-0.56022364	Yes
ZNF96	14735	-1.694968581	-0.5600925	Yes
FAM113B	14750	-1.700191617	-0.56047314	Yes
ZNF581	14755	-1.701848984	-0.5602833	Yes
FLJ40142	14763	-1.7047261	-0.56026375	Yes
PIGK	14764	-1.705058455	-0.5598451	Yes
TCEA3	14766	-1.705305815	-0.55948335	Yes
LOC136306	14770	-1.706228495	-0.55923545	Yes
DENND2D	14779	-1.71101284	-0.5592714	Yes
BET1L	14787	-1.714293957	-0.5592495	Yes
ZNF197	14789	-1.715064526	-0.5588854	Yes
SNX14	14799	-1.720165849	-0.5589761	Yes
TRIM14	14801	-1.722079277	-0.55861026	Yes
UTP14A	14819	-1.727837563	-0.55915517	Yes
PLCG1	14820	-1.727856755	-0.5587309	Yes
CCDC5	14826	-1.729702353	-0.5585912	Yes
WRNIP1	14831	-1.731854558	-0.558394	Yes
FYTTD1	14832	-1.731925607	-0.55796874	Yes
HSPB1	14836	-1.733089209	-0.55771416	Yes
HAPLN3	14842	-1.738034368	-0.5575725	Yes
UBXD7	14860	-1.749559045	-0.558112	Yes
BCKDHB	14862	-1.750189662	-0.55773926	Yes
UBTF	14865	-1.750807047	-0.5574234	Yes
HNRPH2	14876	-1.755219698	-0.55756253	Yes
NECAP2	14877	-1.756373405	-0.55713123	Yes
MRPL21	14878	-1.756385684	-0.55669993	Yes
ATP6V1E2	14886	-1.75978899	-0.5566669	Yes
GLE1L	14907	-1.769664407	-0.55737257	Yes
KIAA0179	14910	-1.771579981	-0.5570516	Yes
KIAA0251	14921	-1.777011395	-0.55718535	Yes

ZC3H3	14928	-1.780201197	-0.5570903	Yes
USP33	14930	-1.781805277	-0.55670977	Yes
UBQLN2	14936	-1.783412457	-0.5565569	Yes
NGRN	14954	-1.790337205	-0.55708647	Yes
CBX1	14963	-1.792211056	-0.55710244	Yes
ZC3H11A	14969	-1.794495702	-0.5569469	Yes
PPIE	14976	-1.799607992	-0.55684704	Yes
TNK1	14979	-1.801972747	-0.55651855	Yes
FAM98B	14980	-1.802275419	-0.55607605	Yes
SMPD1	14984	-1.803245544	-0.5558043	Yes
DET1	14997	-1.807068229	-0.5560447	Yes
PPFIA1	14999	-1.807368994	-0.5556579	Yes
ERGIC3	15001	-1.808039188	-0.55527097	Yes
EFNA1	15004	-1.808799744	-0.5549408	Yes
ZC3H14	15018	-1.81247437	-0.5552369	Yes
ZNF510	15019	-1.812595606	-0.5547918	Yes
RBM4	15021	-1.813609838	-0.5544035	Yes
FLJ12886	15022	-1.813851118	-0.5539581	Yes
EI24	15028	-1.815664768	-0.5537973	Yes
SPA17	15037	-1.818119645	-0.55380696	Yes
SUMF2	15043	-1.820663571	-0.55364496	Yes
THEM4	15044	-1.820774794	-0.55319786	Yes
CCT2	15054	-1.826407313	-0.5532625	Yes
RANBP3	15057	-1.827302933	-0.55292785	Yes
CISH	15072	-1.833747029	-0.5532757	Yes
PPM1K	15078	-1.836920738	-0.5531097	Yes
EXOSC2	15086	-1.840301275	-0.5530569	Yes
THOC3	15091	-1.842225313	-0.55283254	Yes
COPS2	15098	-1.847836375	-0.5527209	Yes
ANAPC13	15103	-1.850537181	-0.5524945	Yes
CCNE1	15112	-1.853289723	-0.55249554	Yes
NSMCE1	15117	-1.854871869	-0.5522681	Yes
HP1BP3	15118	-1.856010318	-0.55181235	Yes
SLC14A1	15121	-1.857381344	-0.55147034	Yes
ITGB1	15123	-1.858434796	-0.551071	Yes
USP4	15130	-1.862716675	-0.55095565	Yes
TCTA	15136	-1.864443898	-0.5507829	Yes
BTF3	15153	-1.873155951	-0.55123514	Yes
TAF6	15156	-1.874668479	-0.55088884	Yes
MRPL49	15160	-1.876070499	-0.55059916	Yes
SMYD4	15175	-1.883203745	-0.5509349	Yes
LMBR1	15177	-1.88363874	-0.55052936	Yes
ZF	15181	-1.884374261	-0.5502377	Yes
HAT1	15192	-1.888054967	-0.55034417	Yes
BAG3	15201	-1.890017629	-0.5503362	Yes
LOC440104	15209	-1.892763615	-0.5502705	Yes
TINP1	15210	-1.893405557	-0.5498056	Yes
CD96	15215	-1.894866586	-0.54956836	Yes
HSZFP36	15223	-1.900190949	-0.5495008	Yes
ZWILCH	15236	-1.905907512	-0.54971695	Yes
ENSA	15260	-1.917538166	-0.5505573	Yes
PML	15272	-1.924317002	-0.55071187	Yes
BTN3A2	15279	-1.926507592	-0.5505809	Yes

ZCWPW1	15289	-1.930638671	-0.5506199	Yes
ACSL6	15295	-1.9314996	-0.5504307	Yes
RTN4	15299	-1.933241367	-0.550127	Yes
SAMHD1	15304	-1.93565619	-0.5498798	Yes
ZNF658	15309	-1.938252926	-0.5496319	Yes
POLM	15318	-1.941246033	-0.5496113	Yes
CDK10	15323	-1.943638206	-0.54936206	Yes
PSAT1	15336	-1.951429248	-0.549567	Yes
KLHDC3	15342	-1.954451799	-0.54937214	Yes
ZNF575	15346	-1.956004024	-0.5490629	Yes
PTPRC	15347	-1.956119299	-0.54858255	Yes
GTF2H5	15361	-1.962664962	-0.5488418	Yes
FAM11A	15362	-1.963647246	-0.5483596	Yes
EIF4B	15377	-1.968314052	-0.5486744	Yes
RING1	15383	-1.970134735	-0.5484757	Yes
EHHADH	15384	-1.970572352	-0.5479918	Yes
STK33	15385	-1.971260309	-0.5475078	Yes
SF3B1	15393	-1.975019813	-0.54742193	Yes
CCS	15397	-1.979548097	-0.54710686	Yes
EEF1B2	15404	-1.980833054	-0.5469625	Yes
THUMPD3	15409	-1.983654141	-0.54670346	Yes
FLJ13197	15423	-1.989651561	-0.54695606	Yes
M6PR	15433	-1.993619919	-0.5469796	Yes
ZC3H12B	15440	-1.996889234	-0.54683137	Yes
FUS	15451	-2.003782511	-0.5469094	Yes
PAIP2	15452	-2.00500989	-0.5464171	Yes
ZNF670	15462	-2.008028984	-0.5464371	Yes
MRPL43	15495	-2.02775383	-0.5477635	Yes
RPS7	15512	-2.032492876	-0.5481766	Yes
ASB8	15514	-2.033994436	-0.54773414	Yes
FXYD2	15535	-2.043868542	-0.54837245	Yes
HERC4	15554	-2.052078962	-0.54889476	Yes
RPL32	15562	-2.055605888	-0.5487891	Yes
MGC52498	15564	-2.055915117	-0.5483413	Yes
PHF10	15573	-2.059857845	-0.54829156	Yes
VPS13C	15575	-2.062059164	-0.5478422	Yes
PPP1R8	15581	-2.064787149	-0.54762024	Yes
EPDR1	15585	-2.065863609	-0.547284	Yes
TRIM35	15588	-2.067858219	-0.5468903	Yes
SUHW2	15592	-2.069076061	-0.54655325	Yes
PYCR2	15597	-2.074803352	-0.54627186	Yes
CTDSP2	15601	-2.075565815	-0.54593325	Yes
MAX	15605	-2.078101397	-0.545594	Yes
NRCAM	15609	-2.080610514	-0.5452541	Yes
ATP5G2	15614	-2.085758209	-0.54497	Yes
COL18A1	15617	-2.086549997	-0.5445717	Yes
FLJ10781	15619	-2.086884975	-0.54411626	Yes
IHPK2	15622	-2.087643147	-0.5437177	Yes
G3BP2	15630	-2.090418339	-0.5436034	Yes
NSFL1C	15636	-2.094153166	-0.5433743	Yes
BUB3	15642	-2.101142168	-0.5431434	Yes
EIF3S5	15646	-2.101556063	-0.5427984	Yes
ZNF570	15647	-2.102170706	-0.5422822	Yes

TPCN1	15650	-2.103955507	-0.5418796	Yes
RNF38	15652	-2.104531288	-0.54141986	Yes
PLEKHK1	15676	-2.113907337	-0.542212	Yes
NOLC1	15680	-2.11472559	-0.5418638	Yes
AEBP1	15685	-2.119179726	-0.54157144	Yes
FAM122A	15686	-2.119413137	-0.54105103	Yes
KRT1	15697	-2.123503923	-0.5410997	Yes
MRPS35	15702	-2.12590766	-0.54080576	Yes
TSPAN3	15710	-2.129855871	-0.54068184	Yes
PPHLN1	15711	-2.130015135	-0.5401588	Yes
AGA	15712	-2.130049944	-0.5396358	Yes
CNIH	15714	-2.130525351	-0.53916967	Yes
TMEM66	15716	-2.130924225	-0.53870344	Yes
ZXDC	15723	-2.134884119	-0.53852123	Yes
PLEKHB1	15728	-2.136962414	-0.5382246	Yes
RAB3GAP1	15731	-2.140906811	-0.5378129	Yes
ALS2CR8	15733	-2.143307447	-0.5373436	Yes
WDR20	15735	-2.143942595	-0.5368742	Yes
RWDD2	15741	-2.145970583	-0.5366323	Yes
SDCCAG10	15748	-2.150349379	-0.53644633	Yes
MRPL11	15750	-2.151255846	-0.53597516	Yes
TCHP	15769	-2.159265518	-0.5364711	Yes
PSMA1	15773	-2.160551548	-0.5361116	Yes
SMARCA1	15797	-2.167287111	-0.5368906	Yes
FRAG1	15815	-2.175833941	-0.53732556	Yes
KLRA1	15821	-2.180035114	-0.5370753	Yes
EPB41L5	15837	-2.182899475	-0.5373944	Yes
TMEM118	15838	-2.183834314	-0.5368582	Yes
LOH11CR2A	15849	-2.1875875	-0.53689116	Yes
HTATIP	15852	-2.189857721	-0.53646743	Yes
LATS1	15859	-2.191539288	-0.5362714	Yes
NSF	15862	-2.192183256	-0.5358471	Yes
PATZ1	15866	-2.195994616	-0.5354789	Yes
MARS2	15867	-2.196150064	-0.53493965	Yes
OR2A7	15872	-2.198145866	-0.534628	Yes
FAM82B	15875	-2.199527264	-0.53420186	Yes
MRPL20	15879	-2.201374769	-0.5338324	Yes
HNRPA3	15882	-2.204182148	-0.5334052	Yes
NRF1	15883	-2.204192638	-0.5328639	Yes
IPO7	15885	-2.204546213	-0.5323796	Yes
ILF3	15894	-2.209257364	-0.5322932	Yes
UBE2D2	15906	-2.216212511	-0.5323761	Yes
LOC93349	15911	-2.222188234	-0.53205854	Yes
SLC24A6	15921	-2.226672888	-0.53202486	Yes
H2AFY2	15936	-2.232379436	-0.53227484	Yes
TYSND1	15944	-2.234712362	-0.5321252	Yes
FAM36A	15947	-2.238030195	-0.53168964	Yes
ROBO3	15955	-2.241711855	-0.53153825	Yes
MRPS18B	15975	-2.254439354	-0.5320679	Yes
SCO1	15976	-2.256280422	-0.53151387	Yes
MCM3	15993	-2.264116287	-0.53187007	Yes
ACACB	15997	-2.265762568	-0.5314847	Yes
JAK1	16001	-2.26809597	-0.53109884	Yes

SMAP1L	16012	-2.272345781	-0.53111094	Yes
SPTLC1	16017	-2.275956631	-0.53078014	Yes
ZNF683	16027	-2.284590483	-0.5307323	Yes
ST8SIA1	16037	-2.288263798	-0.53068346	Yes
LOC653761	16046	-2.291447163	-0.5305769	Yes
PCNA	16050	-2.296456337	-0.53018403	Yes
CYFIP2	16060	-2.302808523	-0.5301317	Yes
SON	16062	-2.305095911	-0.5296227	Yes
NARS2	16064	-2.306498289	-0.52911335	Yes
SNTB1	16065	-2.306764364	-0.5285469	Yes
WDR71	16077	-2.31444931	-0.5286057	Yes
POLDIP2	16084	-2.318771124	-0.52837837	Yes
EIF2S2	16095	-2.327108622	-0.52837706	Yes
KCNMB4	16099	-2.329892635	-0.52797604	Yes
CAMSAP1L1	16100	-2.331256628	-0.5274036	Yes
BCL2L13	16109	-2.333919287	-0.5272866	Yes
GPR174	16114	-2.337167501	-0.5269407	Yes
SCAND2	16116	-2.33806181	-0.52642363	Yes
VAMP1	16130	-2.342856646	-0.52658945	Yes
IPO8	16133	-2.344108582	-0.5261279	Yes
CD200R1	16135	-2.344742298	-0.52560914	Yes
RRAGB	16136	-2.344758034	-0.5250334	Yes
AZIN1	16140	-2.348064899	-0.52462786	Yes
HNRPM	16141	-2.350754738	-0.52405065	Yes
TTC9C	16153	-2.354342699	-0.52409965	Yes
BTRC	16162	-2.361408949	-0.5239759	Yes
ZNF415	16168	-2.363260269	-0.5236807	Yes
GRPEL2	16170	-2.364547491	-0.52315706	Yes
EPHB4	16173	-2.367712021	-0.5226897	Yes
SLC22A17	16179	-2.373064518	-0.52239203	Yes
SLC25A25	16191	-2.378356457	-0.5224351	Yes
SPG21	16198	-2.384012938	-0.5221918	Yes
RGMB	16199	-2.385499001	-0.5216061	Yes
JAK3	16207	-2.393773556	-0.5214174	Yes
OBSCN	16211	-2.395510674	-0.52100015	Yes
TPST2	16215	-2.398752928	-0.5205822	Yes
TMEM123	16246	-2.416113615	-0.5216992	Yes
MAGED2	16250	-2.418960333	-0.5212763	Yes
GCC2	16252	-2.419172049	-0.52073926	Yes
MCM3APAS	16256	-2.421273708	-0.52031577	Yes
IMPDH2	16260	-2.422266245	-0.519892	Yes
EHMT1	16263	-2.424046516	-0.5194108	Yes
KIAA0776	16267	-2.426205635	-0.5189861	Yes
CHES1	16270	-2.426867008	-0.5185042	Yes
APPBP1	16280	-2.434727192	-0.51841944	Yes
KIAA0895	16283	-2.435217857	-0.5179355	Yes
PIK3CD	16286	-2.436314344	-0.5174513	Yes
LZIC	16296	-2.440037966	-0.5173652	Yes
NOLA1	16297	-2.441018105	-0.51676583	Yes
CCDC25	16298	-2.443232059	-0.5161659	Yes
MAP3K7	16302	-2.444549084	-0.5157367	Yes
SALL2	16303	-2.445196152	-0.5151363	Yes
FBL	16306	-2.446521521	-0.51464957	Yes

ALDH5A1	16314	-2.450550079	-0.5144469	Yes
ZNF627	16316	-2.452495337	-0.5139017	Yes
APOLD1	16329	-2.458589792	-0.5139821	Yes
EEF1D	16333	-2.461405277	-0.5135488	Yes
WDR23	16335	-2.463532209	-0.51300085	Yes
CACNA1I	16338	-2.464329243	-0.51250976	Yes
CASP10	16344	-2.469291687	-0.5121885	Yes
RGC32	16346	-2.470240593	-0.51163894	Yes
RAB6IP1	16347	-2.471070766	-0.51103216	Yes
ZNF540	16351	-2.473799944	-0.5105958	Yes
OPN3	16354	-2.474514723	-0.5101022	Yes
KIAA2010	16362	-2.476948261	-0.50989306	Yes
DCHS1	16377	-2.485666513	-0.5100808	Yes
CCNG1	16380	-2.48621583	-0.50958437	Yes
IRAK4	16385	-2.487963676	-0.5092015	Yes
HLA-DOA	16388	-2.492774963	-0.5087034	Yes
USP11	16391	-2.4933815	-0.50820524	Yes
MRPL30	16399	-2.495882273	-0.50799143	Yes
FLJ38969	16402	-2.496865034	-0.50749236	Yes
TCF7	16405	-2.498334169	-0.5069929	Yes
STAT1	16411	-2.500455141	-0.506664	Yes
TRIAD3	16413	-2.501308918	-0.5061068	Yes
TIMM17A	16414	-2.501392841	-0.50549257	Yes
CD248	16417	-2.502493382	-0.5049921	Yes
TOMM20	16420	-2.505070448	-0.50449103	Yes
VPS24	16422	-2.506297112	-0.50393265	Yes
PARC	16425	-2.506936312	-0.5034311	Yes
IGBP1	16429	-2.508826733	-0.5029861	Yes
GPA33	16442	-2.517362833	-0.50305206	Yes
CIAPIN1	16450	-2.522711515	-0.5028317	Yes
BTN2A1	16451	-2.523488522	-0.50221205	Yes
TSC1	16457	-2.525918961	-0.50187683	Yes
PMPCB	16467	-2.533922434	-0.50176775	Yes
KIAA0265	16469	-2.53509903	-0.5012023	Yes
SF1	16470	-2.535906553	-0.5005796	Yes
RAB43	16480	-2.53967762	-0.5004691	Yes
GSTM4	16490	-2.549232244	-0.5003562	Yes
NAPB	16499	-2.552636862	-0.5001855	Yes
COMMD6	16500	-2.553248167	-0.49955854	Yes
FBXL3	16506	-2.560515165	-0.49921486	Yes
NKX3-1	16510	-2.561738729	-0.49875686	Yes
ZFAND6	16515	-2.566741467	-0.49835464	Yes
PHF19	16529	-2.57345438	-0.49846387	Yes
FOXO1A	16535	-2.576445341	-0.49811625	Yes
TCEA1	16544	-2.581263781	-0.4979385	Yes
MLLT11	16547	-2.583541632	-0.49741817	Yes
YME1L1	16551	-2.585278511	-0.49695438	Yes
RIC3	16552	-2.58533287	-0.49631956	Yes
TRIM37	16591	-2.605307102	-0.4978462	Yes
DGCR14	16593	-2.60605979	-0.49726328	Yes
SLC25A14	16595	-2.607068777	-0.49668014	Yes
RASA2	16602	-2.611768484	-0.4963809	Yes
LOC201229	16612	-2.617389202	-0.49625129	Yes

MTMR4	16617	-2.619434357	-0.49583614	Yes
DHX40	16621	-2.620650291	-0.49536365	Yes
HRSP12	16640	-2.632715464	-0.49574336	Yes
SYPL1	16644	-2.63384223	-0.4952677	Yes
BEX1	16647	-2.636529446	-0.49473432	Yes
POLH	16652	-2.63836503	-0.4943145	Yes
POT1	16662	-2.645615816	-0.49417797	Yes
HSD17B8	16663	-2.645712137	-0.4935283	Yes
QRICH1	16664	-2.648901224	-0.4928779	Yes
PRPS2	16668	-2.649813414	-0.49239826	Yes
BNIP3L	16670	-2.650955677	-0.49180433	Yes
LY9	16674	-2.652243853	-0.49132413	Yes
MGC12966	16678	-2.654021502	-0.49084347	Yes
KBTBD4	16690	-2.662951708	-0.49081668	Yes
ITK	16696	-2.665058613	-0.49044734	Yes
ZNF443	16700	-2.666258097	-0.48996368	Yes
RPL28	16712	-2.673154354	-0.48993438	Yes
GNAQ	16716	-2.675030947	-0.48944858	Yes
TAF15	16717	-2.675093174	-0.4887917	Yes
NUDT9	16718	-2.675162077	-0.48813483	Yes
FBXO22	16721	-2.677877903	-0.48759133	Yes
RPIA	16725	-2.679061174	-0.4871045	Yes
CTNNB1	16747	-2.694396496	-0.4876401	Yes
HIP1R	16765	-2.7065413	-0.4879447	Yes
PSCDBP	16766	-2.707053423	-0.48727998	Yes
CCT8	16774	-2.712518215	-0.48701298	Yes
PLCL1	16776	-2.713138103	-0.4864038	Yes
ARID5B	16784	-2.716541767	-0.48613584	Yes
FIGNL1	16788	-2.719686031	-0.48563904	Yes
MRPL52	16791	-2.721550226	-0.4850848	Yes
WSB1	16795	-2.726868153	-0.48458624	Yes
NAP1L1	16801	-2.729221344	-0.48420113	Yes
CBR3	16802	-2.730144978	-0.48353076	Yes
HAX1	16803	-2.730538607	-0.4828603	Yes
UBA52	16816	-2.736039639	-0.48287258	Yes
CCT3	16824	-2.741220713	-0.48259854	Yes
BTN3A1	16825	-2.741788149	-0.4819253	Yes
RBM8A	16841	-2.744817019	-0.48210648	Yes
FLT3LG	16858	-2.757132053	-0.48234162	Yes
CCNB1IP1	16862	-2.758193731	-0.4818354	Yes
ZNF167	16867	-2.761824131	-0.48138526	Yes
SERPINE2	16873	-2.763605595	-0.48099172	Yes
YEATS4	16878	-2.766722918	-0.4805404	Yes
TMEM97	16888	-2.776486874	-0.4803717	Yes
TCP1	16889	-2.776612997	-0.47968993	Yes
FLJ20489	16890	-2.777826786	-0.47900784	Yes
ZNF2	16909	-2.791152239	-0.47934866	Yes
RPUSD4	16915	-2.793150187	-0.47894785	Yes
ST6GAL1	16918	-2.796240568	-0.47837526	Yes
ZNF545	16921	-2.801758766	-0.47780132	Yes
ATP8B2	16922	-2.802498102	-0.4771132	Yes
PPP2R5C	16926	-2.805725813	-0.47659528	Yes
RPL4	16927	-2.806094646	-0.47590625	Yes

LGTN	16933	-2.808656931	-0.47550163	Yes
SPFH2	16939	-2.814086437	-0.4750957	Yes
CDKAL1	16942	-2.817432642	-0.4745179	Yes
TNFRSF7	16952	-2.823604107	-0.47433767	Yes
RPP40	16971	-2.835237026	-0.47466764	Yes
GDAP1	16975	-2.838740349	-0.47414163	Yes
NUDT11	16981	-2.845304966	-0.47372803	Yes
RAN	16984	-2.846986055	-0.47314298	Yes
RPL10A	16989	-2.857411861	-0.4726694	Yes
ALKBH7	17005	-2.87057519	-0.47281966	Yes
CDC42SE2	17006	-2.870816946	-0.47211474	Yes
PSMD11	17010	-2.873592138	-0.47158018	Yes
CRSP9	17013	-2.878991604	-0.47098726	Yes
ACSL3	17022	-2.885257006	-0.47073486	Yes
COX11	17023	-2.885436535	-0.47002637	Yes
LOC653316	17026	-2.888851404	-0.46943104	Yes
OCIAD2	17029	-2.891275644	-0.46883512	Yes
MAP3K7IP2	17030	-2.891762018	-0.46812505	Yes
TRIM5	17031	-2.893726826	-0.4674145	Yes
NAP1L4	17051	-2.903605223	-0.4677847	Yes
USP14	17054	-2.904733896	-0.4671855	Yes
CUL4B	17061	-2.907071352	-0.4668137	Yes
ELA1	17063	-2.908484221	-0.46615657	Yes
SH3PXD2A	17068	-2.911316156	-0.46566972	Yes
TGIF2	17074	-2.917587757	-0.4652384	Yes
PPIL2	17078	-2.921902418	-0.46469194	Yes
LAT	17080	-2.922293186	-0.4640314	Yes
BHLHB9	17089	-2.927262306	-0.4637687	Yes
DDX47	17093	-2.932456017	-0.46321967	Yes
TATDN1	17094	-2.934033394	-0.46249923	Yes
KLC4	17099	-2.937277555	-0.46200603	Yes
DNAJA4	17106	-2.944489002	-0.46162507	Yes
MBNL1	17110	-2.945171356	-0.46107292	Yes
KLRC3	17111	-2.946383476	-0.46034944	Yes
CASP6	17122	-2.954084396	-0.46019417	Yes
ACN9	17126	-2.957278728	-0.45963904	Yes
NPAT	17144	-2.972916126	-0.4598782	Yes
CEP170	17158	-2.981953382	-0.45988715	Yes
HN1	17169	-2.989630222	-0.45972314	Yes
BZW2	17173	-2.991213799	-0.45915967	Yes
ZNF330	17179	-2.997838259	-0.4587086	Yes
NFYA	17203	-3.008401632	-0.45928112	Yes
FKBP1A	17204	-3.009323359	-0.4585422	Yes
SNAP23	17206	-3.011192083	-0.4578598	Yes
LOC203547	17214	-3.0181427	-0.4575178	Yes
TCEAL1	17215	-3.018855572	-0.45677653	Yes
MCM6	17218	-3.020544767	-0.45614886	Yes
ZNF134	17219	-3.021520138	-0.45540693	Yes
CYLD	17225	-3.024285078	-0.45494938	Yes
TBXA2R	17226	-3.024492025	-0.45420673	Yes
SEPN1	17232	-3.029757738	-0.45374784	Yes
UBE2E2	17242	-3.0341537	-0.4535159	Yes
CUGBP1	17250	-3.038972139	-0.45316875	Yes

DAP3	17255	-3.041255713	-0.45265	Yes
AMY2B	17260	-3.044013739	-0.4521306	Yes
GIMAP5	17271	-3.051620007	-0.45195138	Yes
MCM7	17272	-3.052282333	-0.4512019	Yes
PRPS1	17277	-3.057299852	-0.4506792	Yes
DPH2	17281	-3.060023069	-0.45009887	Yes
GLT8D1	17283	-3.060275555	-0.44940445	Yes
CABC1	17293	-3.067659616	-0.44916427	Yes
PPARD	17295	-3.067998886	-0.44846794	Yes
MOCS2	17306	-3.074856281	-0.44828302	Yes
MEIS3P1	17314	-3.080997944	-0.44792557	Yes
VIPR1	17320	-3.086311102	-0.44745278	Yes
TMEM42	17321	-3.087543249	-0.44669464	Yes
ZNF175	17344	-3.102854252	-0.44718695	Yes
ZNF217	17357	-3.110879898	-0.4471072	Yes
MED28	17364	-3.116807222	-0.44668394	Yes
DEPDC7	17372	-3.120666981	-0.44631672	Yes
FAM101B	17379	-3.129985809	-0.44589022	Yes
FLJ20152	17394	-3.149137497	-0.4459151	Yes
SFXN4	17396	-3.150448561	-0.44519854	Yes
LOC338799	17399	-3.152003288	-0.4445386	Yes
FCMD	17402	-3.153572798	-0.44387826	Yes
TOP1MT	17405	-3.156450748	-0.44321722	Yes
MAGEE1	17409	-3.159885406	-0.44261235	Yes
MAPK14	17416	-3.164544344	-0.44217736	Yes
SLC16A10	17437	-3.180217981	-0.44253665	Yes
PECAM1	17444	-3.18618083	-0.44209635	Yes
SLC25A30	17449	-3.192348003	-0.4415405	Yes
PRIM2A	17455	-3.195475101	-0.44104093	Yes
FAM29A	17456	-3.196027756	-0.44025615	Yes
AHCY	17471	-3.208949327	-0.44026634	Yes
ARHGEF5	17475	-3.209972382	-0.43964916	Yes
DUSP22	17480	-3.211668015	-0.43908858	Yes
UBL3	17482	-3.212660551	-0.43835676	Yes
SNPH	17491	-3.217422247	-0.4380228	Yes
YTHDC1	17496	-3.22171545	-0.43745974	Yes
COQ6	17497	-3.222252846	-0.43666855	Yes
NFX1	17500	-3.223721743	-0.435991	Yes
AP1GBP1	17501	-3.223777294	-0.43519938	Yes
ARMC8	17506	-3.226802111	-0.4346351	Yes
DOCK9	17508	-3.22780776	-0.43389952	Yes
PRO1853	17509	-3.228964806	-0.43310666	Yes
BNIP3	17511	-3.229755402	-0.43237063	Yes
ZNF85	17536	-3.242734432	-0.4329426	Yes
DLL1	17539	-3.24483943	-0.43225986	Yes
RASA3	17540	-3.244927406	-0.4314631	Yes
PTCD2	17548	-3.249530554	-0.43106425	Yes
RNMT	17549	-3.250662088	-0.43026605	Yes
AGMAT	17556	-3.260272026	-0.42980757	Yes
VNN2	17560	-3.264240026	-0.42917708	Yes
MGC42367	17561	-3.265124559	-0.42837533	Yes
DNMT3A	17566	-3.271369696	-0.4278001	Yes
ICOS	17574	-3.280454397	-0.42739365	Yes

MBP	17575	-3.280960798	-0.42658803	Yes
TH1L	17583	-3.289204597	-0.42617944	Yes
CRTAM	17586	-3.291432619	-0.42548525	Yes
MRPL35	17588	-3.292532682	-0.4247338	Yes
GART	17589	-3.293054581	-0.4239252	Yes
MLX	17590	-3.295621634	-0.42311597	Yes
ALDH6A1	17594	-3.296476126	-0.42247754	Yes
TFG	17601	-3.30544281	-0.42200798	Yes
CSTF3	17606	-3.313611984	-0.42142236	Yes
MORC2	17609	-3.315079927	-0.42072237	Yes
GIMAP8	17611	-3.317411661	-0.41996482	Yes
PTK7	17618	-3.324686766	-0.4194905	Yes
MGC40499	17619	-3.325305462	-0.418674	Yes
PPAP2A	17624	-3.327934265	-0.41808486	Yes
ANAPC7	17626	-3.328795195	-0.41732448	Yes
CHD3	17634	-3.338394165	-0.41690382	Yes
UBE1C	17636	-3.341652632	-0.41614032	Yes
GIT2	17640	-3.343590975	-0.41549033	Yes
KIAA1715	17642	-3.346798658	-0.41472554	Yes
MGC16169	17645	-3.348352671	-0.41401738	Yes
ZNF586	17647	-3.34889698	-0.4132521	Yes
SSFA2	17649	-3.351225853	-0.4124862	Yes
NSUN5	17658	-3.357267141	-0.41211793	Yes
UBE2G2	17671	-3.370413542	-0.41197443	Yes
PSIP1	17673	-3.370667219	-0.4112038	Yes
DIDO1	17681	-3.380166054	-0.41077286	Yes
KIAA1147	17686	-3.386012316	-0.41016948	Yes
PRIM1	17687	-3.386510372	-0.40933794	Yes
ZNF174	17689	-3.387238503	-0.40856323	Yes
ZNF200	17692	-3.391492605	-0.40784448	Yes
MGC18216	17695	-3.39659524	-0.40712446	Yes
PRRT1	17705	-3.405332804	-0.40680137	Yes
LYK5	17707	-3.407646179	-0.40602165	Yes
LEPROTL1	17711	-3.408693552	-0.4053557	Yes
GJB6	17718	-3.416381598	-0.40485886	Yes
GPRASP2	17730	-3.425684929	-0.40464482	Yes
ATP5L	17733	-3.428204536	-0.40391704	Yes
KRAS	17738	-3.433760405	-0.40330192	Yes
EPB41	17752	-3.443487406	-0.40319753	Yes
HELB	17753	-3.446439266	-0.40235126	Yes
MORC3	17754	-3.447032213	-0.40150484	Yes
GPR55	17766	-3.457211971	-0.40128306	Yes
VSIG1	17771	-3.459734917	-0.40066156	Yes
LOC400965	17780	-3.467569351	-0.40026617	Yes
PCID1	17782	-3.468142986	-0.3994716	Yes
TMEM38B	17786	-3.471172333	-0.3987903	Yes
ZNF671	17788	-3.472848892	-0.39799455	Yes
LDHB	17795	-3.47830534	-0.3974825	Yes
NPAL3	17812	-3.499979496	-0.39753526	Yes
ITGA6	17820	-3.506879568	-0.39707324	Yes
ZNF24	17829	-3.51249814	-0.39666682	Yes
RPE	17831	-3.513379812	-0.39586115	Yes
NDUFC1	17836	-3.519622564	-0.39522493	Yes

FUBP1	17838	-3.523071527	-0.39441687	Yes
COQ5	17841	-3.526884079	-0.39366487	Yes
LRPPRC	17861	-3.550238609	-0.3938763	Yes
OGFOD1	17871	-3.566180229	-0.39351374	Yes
BCL11B	17873	-3.568691015	-0.39269447	Yes
PPT2	17878	-3.576601744	-0.39204428	Yes
TRUB1	17886	-3.583499193	-0.39156342	Yes
TBL1XR1	17888	-3.585448027	-0.39074004	Yes
FLJ38663	17893	-3.58863759	-0.3900869	Yes
NLE1	17894	-3.590707064	-0.38920522	Yes
AKAP7	17898	-3.595631361	-0.38849336	Yes
ZNF655	17899	-3.602879047	-0.38760868	Yes
TMPO	17900	-3.603321791	-0.38672388	Yes
IKBKE	17908	-3.616263151	-0.386235	Yes
LXN	17910	-3.618904114	-0.3854034	Yes
HEXA	17913	-3.621057749	-0.38462827	Yes
GIMAP2	17920	-3.625399828	-0.38408014	Yes
BPGM	17925	-3.628380537	-0.38341722	Yes
DDX17	17933	-3.638405085	-0.3829229	Yes
FXR1	17934	-3.63874507	-0.3820294	Yes
ZNF561	17935	-3.638863564	-0.3811359	Yes
RAI2	17944	-3.64723587	-0.38069642	Yes
STX16	17947	-3.656075239	-0.3799127	Yes
ARRDC2	17948	-3.656721592	-0.3790148	Yes
FAIM3	17951	-3.659270048	-0.3782303	Yes
MGC39900	17961	-3.667777538	-0.37784278	Yes
KCNN4	17962	-3.670164585	-0.3769416	Yes
CDK2	17971	-3.675977945	-0.37649503	Yes
FBLN2	17978	-3.684280396	-0.37593243	Yes
BEX2	17982	-3.687486649	-0.375198	Yes
LIMK2	17985	-3.694277287	-0.3744049	Yes
CCM2	17989	-3.701544046	-0.37366703	Yes
PIAS2	17991	-3.703027964	-0.37281477	Yes
WBP5	18000	-3.711856365	-0.37235942	Yes
ANKZF1	18012	-3.725166798	-0.3720718	Yes
NET1	18021	-3.733565331	-0.37161112	Yes
LOC202134	18023	-3.737661839	-0.37075037	Yes
ZNF101	18025	-3.741217852	-0.36988872	Yes
LIN7C	18027	-3.742907763	-0.3690267	Yes
RAB15	18030	-3.749907494	-0.3682199	Yes
ZHX3	18031	-3.752404451	-0.36729854	Yes
TCF3	18033	-3.753867149	-0.3664338	Yes
GGPS1	18042	-3.763917685	-0.36596566	Yes
KLHL9	18044	-3.766842842	-0.36509773	Yes
PFKM	18047	-3.769749641	-0.3642861	Yes
NPM3	18050	-3.772450447	-0.3634738	Yes
SLC7A6	18055	-3.775233746	-0.36277485	Yes
U2AF2	18061	-3.779232502	-0.36213192	Yes
TMEM14A	18062	-3.782445431	-0.36120316	Yes
UCP2	18064	-3.784501314	-0.36033088	Yes
LSM5	18066	-3.788796663	-0.35945758	Yes
LOC90624	18069	-3.794097424	-0.35863996	Yes
AK5	18071	-3.79729104	-0.35776457	Yes

ACPL2	18078	-3.805333853	-0.35717222	Yes
ZNF512	18079	-3.805377483	-0.35623783	Yes
KIAA0748	18082	-3.815832853	-0.3554149	Yes
PPIL3	18084	-3.819120169	-0.35453412	Yes
HSPD1	18093	-3.835772753	-0.35404834	Yes
PPAPDC2	18098	-3.839939594	-0.3533335	Yes
UBE2H	18102	-3.847482204	-0.35255978	Yes
PPP1R2	18110	-3.863929272	-0.35201007	Yes
MRPS14	18114	-3.874942303	-0.35122964	Yes
PHGDH	18116	-3.877457619	-0.35033455	Yes
FBXO9	18120	-3.883733749	-0.34955195	Yes
RIOK1	18122	-3.885241747	-0.34865493	Yes
MMP28	18123	-3.886880875	-0.34770054	Yes
GIMAP6	18127	-3.890651703	-0.34691623	Yes
ZNF550	18133	-3.899726152	-0.3462437	Yes
GIMAP1	18134	-3.901474237	-0.3452857	Yes
APEX1	18136	-3.904470682	-0.34438398	Yes
SNX5	18140	-3.906056404	-0.3435959	Yes
DPH5	18145	-3.914681435	-0.3428627	Yes
TSGA10	18146	-3.91501379	-0.3419014	Yes
UXT	18150	-3.921949387	-0.3411094	Yes
ATP2C1	18151	-3.922044754	-0.34014633	Yes
CD5	18154	-3.927927256	-0.33929586	Yes
WDR33	18162	-3.935695648	-0.33872855	Yes
ZNF667	18165	-3.941237211	-0.3378748	Yes
WHSC1L1	18166	-3.942240953	-0.3369068	Yes
SRPK2	18171	-3.950554132	-0.3361648	Yes
NIN	18174	-3.954987049	-0.3353077	Yes
SP110	18177	-3.963044882	-0.33444858	Yes
FBXO32	18191	-3.978063107	-0.3342129	Yes
PAICS	18196	-3.995852709	-0.33345976	Yes
CXCR3	18200	-3.998439312	-0.332649	Yes
TIA1	18206	-4.007909775	-0.33194992	Yes
ALS2CR2	18207	-4.008839607	-0.33096558	Yes
CASP2	18211	-4.014579296	-0.3301508	Yes
LOC346887	18215	-4.019270897	-0.32933494	Yes
GRAP	18216	-4.020462036	-0.3283477	Yes
LOC196394	18224	-4.028495312	-0.3277576	Yes
RAD51C	18225	-4.028617859	-0.3267684	Yes
FBXO11	18233	-4.041556358	-0.32617506	Yes
MDN1	18239	-4.048912525	-0.32546592	Yes
CGI-09	18247	-4.058244228	-0.3248685	Yes
BTN3A3	18251	-4.069602966	-0.32404026	Yes
MRPS33	18253	-4.071179867	-0.3230976	Yes
CLEC11A	18254	-4.072202206	-0.3220977	Yes
LYPD3	18258	-4.077339649	-0.32126755	Yes
ITSN2	18259	-4.077403069	-0.32026634	Yes
CCDC57	18261	-4.078286648	-0.31932193	Yes
ZMYM5	18265	-4.0865798	-0.31848952	Yes
HSMPP8	18269	-4.09693861	-0.31765455	Yes
PDE9A	18277	-4.114309311	-0.31704336	Yes
LRRC8C	18280	-4.117504597	-0.31614634	Yes
KIAA1429	18281	-4.118433952	-0.3151351	Yes

YPEL2	18285	-4.128033161	-0.3142925	Yes
SETMAR	18286	-4.128680706	-0.3132787	Yes
ARMCX2	18289	-4.131403446	-0.3123783	Yes
DKFZP434B0335	18300	-4.150736809	-0.31192917	Yes
TSPYL4	18314	-4.171669006	-0.31164595	Yes
USF1	18315	-4.172408104	-0.31062144	Yes
WHDC1L1	18319	-4.178920269	-0.30976635	Yes
TNRC5	18321	-4.184491634	-0.30879587	Yes
SPINK2	18329	-4.194141865	-0.30816507	Yes
NCBP2	18337	-4.204483032	-0.30753174	Yes
LSP1	18338	-4.205947876	-0.30649897	Yes
NSUN5B	18341	-4.209895134	-0.30557927	Yes
MAD2L1	18345	-4.21679163	-0.3047149	Yes
STMN1	18352	-4.227796078	-0.30401883	Yes
MGC3207	18357	-4.231642246	-0.30320778	Yes
CDC14B	18362	-4.238899708	-0.302395	Yes
FKBP5	18367	-4.252856255	-0.30157876	Yes
VRK3	18369	-4.261698723	-0.30058932	Yes
SLC25A23	18372	-4.263041019	-0.29965657	Yes
MTRF1	18374	-4.268042564	-0.29866555	Yes
SUV420H1	18387	-4.29109478	-0.298296	Yes
BTF3L4	18388	-4.291741371	-0.2972422	Yes
TMEM103	18389	-4.293417454	-0.29618797	Yes
CHMP7	18390	-4.297939301	-0.2951326	Yes
FUNDC1	18391	-4.298069	-0.29407725	Yes
SDCCAG8	18395	-4.30669117	-0.29319078	Yes
MDM1	18397	-4.309529305	-0.2921896	Yes
XRN1	18400	-4.318842411	-0.29124314	Yes
TSGA14	18411	-4.348339081	-0.2907455	Yes
NUP50	18415	-4.351694107	-0.289848	Yes
MBD5	18416	-4.353312016	-0.28877905	Yes
LANCL1	18418	-4.35986042	-0.2877655	Yes
SLC2A11	18421	-4.368453979	-0.28680688	Yes
CR2	18422	-4.369679928	-0.2857339	Yes
SIRPG	18429	-4.387885094	-0.28499854	Yes
AXIN2	18430	-4.388235569	-0.28392103	Yes
CDCA7	18438	-4.413024902	-0.2832365	Yes
BEXL1	18439	-4.413538456	-0.28215277	Yes
NSUN5C	18443	-4.420216084	-0.2812384	Yes
PPM1M	18450	-4.433567524	-0.28049183	Yes
UQCRC2	18453	-4.442080498	-0.27951512	Yes
ESD	18455	-4.449281216	-0.2784796	Yes
JRKL	18457	-4.455178261	-0.27744266	Yes
GPR18	18458	-4.462444305	-0.27634692	Yes
ZSWIM1	18467	-4.477629185	-0.27570355	Yes
SBNO1	18468	-4.481348991	-0.27460316	Yes
RDH14	18471	-4.487220764	-0.27361536	Yes
ORMDL3	18473	-4.497743607	-0.27256796	Yes
GCET2	18475	-4.503325939	-0.2715192	Yes
GLS2	18482	-4.522778034	-0.2707507	Yes
GFM2	18492	-4.53971529	-0.27014908	Yes
CNKSR2	18494	-4.540040493	-0.2690913	Yes
FRYL	18496	-4.549173355	-0.26803127	Yes

MYB	18498	-4.554571629	-0.26696992	Yes
KIAA1394	18499	-4.556229591	-0.26585117	Yes
GTF2H2	18500	-4.557996273	-0.26473194	Yes
SUCLG2	18501	-4.55850172	-0.26361263	Yes
RPL37	18502	-4.567221642	-0.26249117	Yes
P2RY10	18503	-4.570112228	-0.261369	Yes
UBE2D3	18508	-4.585819244	-0.260471	Yes
FCGBP	18509	-4.587768078	-0.2593445	Yes
THYN1	18510	-4.590425968	-0.25821733	Yes
GSTM3	18511	-4.594307423	-0.2570892	Yes
TRNT1	18516	-4.598945618	-0.256188	Yes
ZNF439	18520	-4.61626339	-0.2552255	Yes
MPP6	18521	-4.618621349	-0.2540914	Yes
NOD27	18523	-4.620131016	-0.25301397	Yes
RASGRP2	18525	-4.621139526	-0.2519363	Yes
LMO7	18528	-4.624986649	-0.25091466	Yes
HPCAL4	18532	-4.628282547	-0.24994922	Yes
CAND1	18536	-4.641564846	-0.24898054	Yes
ADD3	18543	-4.660127163	-0.2481783	Yes
BCAS4	18549	-4.670325279	-0.24731657	Yes
NCK2	18550	-4.672367096	-0.24616928	Yes
CNOT7	18551	-4.67261982	-0.24502194	Yes
SCML4	18558	-4.685699463	-0.24421345	Yes
NAG6	18562	-4.702867508	-0.2432297	Yes
SPINT2	18575	-4.726006031	-0.24275336	Yes
CDC42	18581	-4.733793736	-0.24187604	Yes
MGC17330	18582	-4.734067917	-0.2407136	Yes
ARMCX4	18583	-4.738472462	-0.23955008	Yes
TAF9	18584	-4.73908329	-0.23838642	Yes
SLC7A3	18591	-4.750224113	-0.23756208	Yes
PRKCB1	18599	-4.765089989	-0.23679109	Yes
PYGB	18602	-4.783475876	-0.23573054	Yes
PRL	18606	-4.801812172	-0.23472251	Yes
FLJ12334	18613	-4.817826271	-0.23388156	Yes
CHI3L2	18615	-4.821043968	-0.23275478	Yes
PRPSAP2	18620	-4.835295677	-0.23179553	Yes
TAF4B	18622	-4.842403889	-0.23066351	Yes
EPHX2	18639	-4.883567333	-0.23037651	Yes
MLXIP	18641	-4.893361092	-0.22923197	Yes
PARP6	18645	-4.912405968	-0.22819677	Yes
RNF138	18654	-4.934339046	-0.22744124	Yes
SH3YL1	18655	-4.935585022	-0.22622932	Yes
PLAG1	18657	-4.941557407	-0.22507295	Yes
MAN2A1	18658	-4.948252201	-0.22385792	Yes
MDM4	18661	-4.956943035	-0.22275479	Yes
LDLRAP1	18663	-4.973134518	-0.22159065	Yes
HNRPDL	18664	-4.975712299	-0.22036889	Yes
KLRK1	18677	-5.031085491	-0.21981764	Yes
HSPH1	18679	-5.031700611	-0.21863914	Yes
LRRC8D	18683	-5.042447567	-0.217572	Yes
GEMIN6	18684	-5.04483223	-0.21633326	Yes
MGC33556	18689	-5.06870079	-0.2153167	Yes
PDE3B	18693	-5.081614971	-0.21423995	Yes

MAGEH1	18696	-5.087090969	-0.21310486	Yes
GSDML	18705	-5.109850407	-0.21230622	Yes
SUSD3	18706	-5.110429287	-0.21105137	Yes
ABLIM1	18712	-5.146125793	-0.21007282	Yes
MINA	18713	-5.148953915	-0.2088085	Yes
ZNF706	18714	-5.154315948	-0.20754288	Yes
NAP1L3	18715	-5.15569973	-0.20627691	Yes
ITGA4	18717	-5.169025898	-0.20506468	Yes
UQCRB	18718	-5.173238754	-0.20379442	Yes
KIAA1729	18721	-5.184669495	-0.20263536	Yes
FASTKD2	18731	-5.229976177	-0.20186424	Yes
RASSF3	18735	-5.242774487	-0.20074792	Yes
ACCN2	18736	-5.256612301	-0.19945718	Yes
PRKCA	18738	-5.264512062	-0.1982215	Yes
LOC144363	18744	-5.282175541	-0.19720954	Yes
XRCC5	18745	-5.285582066	-0.19591168	Yes
ENPP2	18746	-5.287848473	-0.19461326	Yes
DCK	18747	-5.291426659	-0.19331397	Yes
CRYZL1	18754	-5.325658321	-0.19234833	Yes
CLUAP1	18756	-5.335834026	-0.19109514	Yes
TDP1	18758	-5.341606617	-0.18984054	Yes
RPL22	18760	-5.362154007	-0.1885809	Yes
ZNF416	18763	-5.373373508	-0.1873755	Yes
SFI1	18772	-5.413758755	-0.18650225	Yes
PAQR8	18773	-5.416780472	-0.18517217	Yes
BIRC2	18775	-5.417789459	-0.18389887	Yes
SLC25A15	18777	-5.423950672	-0.18262404	Yes
PRKACB	18778	-5.428730965	-0.18129104	Yes
LIMA1	18781	-5.436377525	-0.18007018	Yes
MSH2	18785	-5.446300983	-0.17890388	Yes
CCR7	18789	-5.464542389	-0.17773311	Yes
ATP8A1	18795	-5.489654541	-0.1766702	Yes
ATM	18796	-5.495287418	-0.17532085	Yes
MCCC2	18797	-5.50050211	-0.17397022	Yes
CD55	18798	-5.502316952	-0.17261915	Yes
ACP1	18808	-5.559927464	-0.17176701	Yes
CPA5	18809	-5.569312572	-0.17039949	Yes
MTUS1	18818	-5.60344553	-0.16947965	Yes
LINS1	18819	-5.615604877	-0.16810076	Yes
RBM12	18822	-5.624106884	-0.16683379	Yes
RALA	18824	-5.627717495	-0.16550894	Yes
COL6A3	18829	-5.635437965	-0.16435322	Yes
CD8B	18830	-5.665790558	-0.162962	Yes
LOC283130	18831	-5.672034264	-0.16156925	Yes
UBASH3A	18836	-5.699422359	-0.16039781	Yes
ALS2CR4	18837	-5.702289581	-0.15899764	Yes
LOC391356	18843	-5.73793602	-0.15787375	Yes
MTA3	18846	-5.741965771	-0.15657786	Yes
BACH2	18847	-5.755344868	-0.15516464	Yes
GGTL3	18860	-5.836336613	-0.15441567	Yes
SELL	18866	-5.869499207	-0.15325949	Yes
FBXO38	18868	-5.881027222	-0.15187243	Yes
DGKA	18874	-5.925069332	-0.1507026	Yes

RFC3	18876	-5.933187485	-0.14930274	Yes
KLHL6	18879	-5.943556309	-0.14795732	Yes
LOC641518	18884	-5.973675251	-0.14671855	Yes
LRRC16	18890	-5.997844696	-0.14553085	Yes
ANKRD49	18894	-6.04171133	-0.14421836	Yes
ITPKB	18897	-6.071320534	-0.14284158	Yes
GPC2	18899	-6.084791183	-0.1414045	Yes
ORC5L	18901	-6.08907795	-0.13996635	Yes
RAB30	18902	-6.095242023	-0.13846968	Yes
MAP4K4	18904	-6.10276413	-0.13702819	Yes
MRPL1	18905	-6.113470554	-0.13552704	Yes
SFXN1	18906	-6.114293098	-0.1340257	Yes
HPS4	18908	-6.125074863	-0.13257872	Yes
PCMTD2	18909	-6.141806602	-0.13107061	Yes
VPS8	18912	-6.152574062	-0.1296739	Yes
ZNF682	18914	-6.158275127	-0.12821876	Yes
PCSK5	18916	-6.17317152	-0.12675998	Yes
CMTM7	18917	-6.17820406	-0.12524293	Yes
TGFBR2	18919	-6.181517601	-0.1237821	Yes
ZNF154	18924	-6.222164154	-0.1224823	Yes
WDR4	18929	-6.270862579	-0.12117055	Yes
CACHD1	18932	-6.302461624	-0.11973702	Yes
PTPRK	18933	-6.321682453	-0.11818475	Yes
NGFRAP1	18935	-6.332648277	-0.116686806	Yes
CRLF3	18941	-6.407112598	-0.11539861	Yes
NUCB2	18944	-6.432621956	-0.113933116	Yes
RHOH	18946	-6.438371658	-0.11240921	Yes
ABCC1	18947	-6.470094681	-0.1108205	Yes
ZNF238	18952	-6.519909859	-0.1094476	Yes
SPTBN1	18954	-6.596320629	-0.107884906	Yes
APBA2	18955	-6.613531113	-0.10626098	Yes
ROBO1	18956	-6.625176907	-0.10463419	Yes
NBEA	18958	-6.636442184	-0.10306164	Yes
CLEC2D	18965	-6.680236816	-0.10176339	Yes
SDK2	18966	-6.687561512	-0.10012128	Yes
SEH1L	18967	-6.688095093	-0.09847904	Yes
FTS	18968	-6.695840359	-0.096834905	Yes
FHIT	18971	-6.771793842	-0.09528613	Yes
CSDA	18976	-6.813225269	-0.0938412	Yes
CHD2	18979	-6.871833324	-0.09226787	Yes
TSPYL5	18986	-6.975561142	-0.0908971	Yes
LEF1	18987	-6.980289459	-0.089183114	Yes
HIVEP1	18991	-7.012509823	-0.08763225	Yes
FYB	18995	-7.049576283	-0.08607227	Yes
TACC3	18997	-7.065536022	-0.084394366	Yes
CA6	18999	-7.077093124	-0.08271363	Yes
PSMD6	19000	-7.087213993	-0.08097339	Yes
TNFRSF10D	19005	-7.167728424	-0.07944141	Yes
NPAS2	19007	-7.187989235	-0.077733435	Yes
NARG1L	19013	-7.267116547	-0.076234065	Yes
MAML2	19014	-7.285495281	-0.074445136	Yes
CLN5	19015	-7.287261009	-0.072655775	Yes
BTLA	19016	-7.29296875	-0.07086501	Yes

MPHOSPH9	19019	-7.367672443	-0.06916993	Yes
HSF2	19022	-7.453682899	-0.06745372	Yes
SERINC5	19023	-7.476694107	-0.065617844	Yes
MAN1C1	19029	-7.648103714	-0.064024925	Yes
ZNF307	19031	-7.66795063	-0.062199097	Yes
SLC12A6	19035	-7.721162796	-0.06047422	Yes
RAB33A	19041	-7.824965954	-0.058837876	Yes
PPP1R3E	19044	-7.918353558	-0.05700757	Yes
ALS2CR13	19045	-7.951728344	-0.055055052	Yes
RGS10	19048	-8.002251625	-0.053204145	Yes
MSL3L1	19049	-8.034273148	-0.05123136	Yes
KLHL3	19054	-8.085844994	-0.049473945	Yes
TMEM46	19057	-8.221989632	-0.047569085	Yes
PASK	19059	-8.287055016	-0.04559124	Yes
OGT	19060	-8.313270569	-0.043549944	Yes
PKIA	19061	-8.363794327	-0.041496243	Yes
CDCA7L	19063	-8.491423607	-0.039468214	Yes
MEST	19066	-8.652479172	-0.037457645	Yes
PRMT2	19068	-8.88123703	-0.0353339	Yes
NELL2	19072	-9.041952133	-0.03328471	Yes
GPR155	19073	-9.116639137	-0.03104615	Yes
AMIGO1	19074	-9.26227951	-0.02877183	Yes
SCML1	19075	-9.268380165	-0.026496012	Yes
NOG	19077	-9.314891815	-0.024265783	Yes
NDFIP1	19078	-9.324086189	-0.021976287	Yes
MAL	19080	-9.358784676	-0.01973528	Yes
ARMCX1	19081	-9.482999802	-0.017406764	Yes
REG4	19082	-9.542575836	-0.015063617	Yes
KBTBD6	19083	-9.573023796	-0.012712996	Yes
IL6ST	19084	-9.634144783	-0.010347365	Yes
TBC1D4	19087	-10.16576099	-0.007965218	Yes
LRRN3	19088	-10.51739311	-0.00538271	Yes
ACTN1	19089	-10.54227543	-0.002794091	Yes
DSC1	19092	-12.30721569	1.14E-04	Yes

Appendix 4

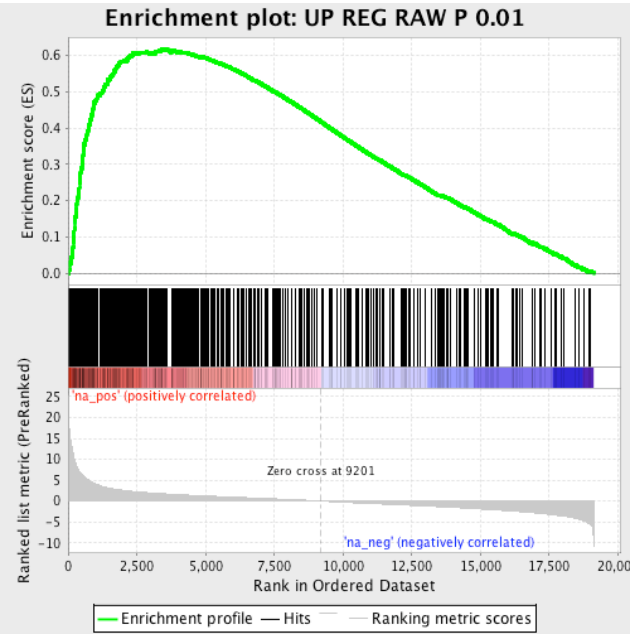
Geneset enrichment analysis comparing CD161+CD8α+ vs CD161-CD8α+ datasets in cord and adult blood.

A4.1 Geneset enrichment analysis for UP-REGULATED GENES

A4.1.1 Statistics

Dataset	LucyW_E2_plus-minus_collapsed
Phenotype	NoPhenotypeAvailable
Upregulated in class	na_pos
GeneSet	UP REG RAW P 0.01
Enrichment Score (ES)	0.6189969
Normalized Enrichment Score (NES)	2.8773324
Nominal p-value	0.0
FDR q-value	0.0
FWER p-Value	0.0

A4.1.2 Enrichment plot



A4.1.3 Genes contributing to leading edge enrichment score

PROBE	RANK IN GENE LIST	RANK METRIC SCORE	RUNNING ES	CORE ENRICHMENT
LILRB1	30	18.07667351	0.010117482	Yes
CTNNA1	66	15.6480751	0.018389387	Yes
KLRB1	68	15.50030708	0.02839629	Yes
ITGAX	97	14.23398495	0.036127307	Yes
PLEK	111	13.70126438	0.044320304	Yes
FAM49A	147	12.56380463	0.05059031	Yes
LYN	159	12.03443718	0.057809126	Yes
FGR	163	11.86683083	0.06534995	Yes
CEBPD	176	11.50942612	0.07217415	Yes
PIK3AP1	184	11.26294231	0.07910761	Yes
PRDM1	185	11.22662163	0.08639446	Yes
PHLDA1	191	11.08384895	0.09331938	Yes
ZFHX1B	207	10.54290581	0.099354684	Yes
C3AR1	214	10.46581459	0.10582461	Yes
CD63	216	10.33135509	0.11247651	Yes
MAP3K8	224	10.01951504	0.11860291	Yes
SUSD1	229	9.965938568	0.12485608	Yes
ANXA2	239	9.636741638	0.13062632	Yes
S100A11	240	9.609298706	0.13686341	Yes
LIMS1	242	9.540575981	0.14300205	Yes
ZAK	246	9.480718613	0.14899413	Yes
TNFRSF1B	247	9.477203369	0.15514548	Yes
FAM43A	283	8.655474663	0.15887871	Yes
LATS2	296	8.486053467	0.16374053	Yes
MYO1F	300	8.416950226	0.16904216	Yes
PTPRE	302	8.39863205	0.17443958	Yes
GAS7	306	8.296169281	0.17966281	Yes
DUSP5	308	8.241480827	0.18495825	Yes
IFIT3	310	8.214314461	0.19023605	Yes
B4GALT5	317	8.171068192	0.19521652	Yes
LOC401233	318	8.147279739	0.20050466	Yes
PTPN12	349	7.753953934	0.20392199	Yes
RHOQ	351	7.727253437	0.20888366	Yes
SLAMF7	366	7.546423435	0.2130279	Yes
ARHGAP18	371	7.492209435	0.21767545	Yes
IL18RAP	377	7.468749046	0.22225392	Yes
STX11	393	7.282696724	0.22617313	Yes
MGC14376	394	7.275776863	0.23089561	Yes
CTSC	407	7.115369797	0.23486777	Yes
PNKD	409	7.104696751	0.23942535	Yes
SRXN1	410	7.099370956	0.24403332	Yes
MAF	411	7.094069958	0.24863786	Yes
GLB1	418	7.038667202	0.25288332	Yes
RAI17	422	7.008750439	0.25727093	Yes
CCL4	438	6.867743492	0.26092082	Yes
SPIRE1	442	6.849815369	0.26520526	Yes
ADAMDEC1	446	6.809903622	0.2694638	Yes
LRRC33	448	6.788215637	0.27381596	Yes
CD58	450	6.770676136	0.27815673	Yes
IL15	458	6.69727993	0.28212678	Yes
TNFSF14	470	6.598083019	0.28581703	Yes

MAFF	487	6.463563919	0.2891507	Yes
CCR6	502	6.344641685	0.29251492	Yes
VCL	503	6.342045307	0.29663134	Yes
SIGLEC9	509	6.302942753	0.30045313	Yes
RCBTB2	511	6.291993141	0.3044832	Yes
SOCS6	517	6.254992962	0.30827388	Yes
CLIC1	528	6.20141983	0.31176051	Yes
KIF1B	529	6.193343639	0.3157804	Yes
LOC653127	536	6.132117271	0.31943747	Yes
MN1	540	6.095628738	0.32323238	Yes
TBK1	543	6.056247234	0.3270556	Yes
EFHD2	552	6.010371208	0.33052596	Yes
PROK2	555	5.985405922	0.33430317	Yes
ADAM8	557	5.96958828	0.338124	Yes
MTSS1	561	5.952979088	0.34182635	Yes
RRBP1	562	5.925059795	0.3456721	Yes
NPC1	568	5.869344234	0.34921247	Yes
ZBTB16	575	5.833602428	0.35267577	Yes
RASSF4	584	5.79822588	0.3560084	Yes
TNF	616	5.643579483	0.35800213	Yes
FLJ20245	617	5.634045601	0.361659	Yes
ANTXR2	620	5.624500751	0.36520198	Yes
ADAM19	621	5.620066166	0.36884978	Yes
CFLAR	660	5.397890568	0.37030706	Yes
EMP1	669	5.355392456	0.3733523	Yes
GBP5	672	5.337254047	0.3767088	Yes
BHLHB2	679	5.299209118	0.37982526	Yes
LGALS1	685	5.277026653	0.38298115	Yes
TICAM1	688	5.268937588	0.38629335	Yes
IQSEC1	716	5.132977486	0.38817105	Yes
CD300A	719	5.129143715	0.39139253	Yes
AHNAK	731	5.053142071	0.39407998	Yes
KLRF1	739	5.031414032	0.39696878	Yes
AYTL2	756	4.956148624	0.39932406	Yes
IL15RA	757	4.953257084	0.40253904	Yes
PSCD3	761	4.937447548	0.40558225	Yes
ANXA4	767	4.901609421	0.40849447	Yes
PTGDR	786	4.814125538	0.41064987	Yes
IFNGR1	789	4.803050995	0.41365966	Yes
RDX	790	4.800262928	0.41677535	Yes
WIPI1	794	4.793786526	0.4197253	Yes
LOC339745	796	4.785474777	0.42277753	Yes
CHST12	827	4.655991554	0.42418408	Yes
ITGAM	834	4.636325836	0.4268703	Yes
SLCO3A1	836	4.631661415	0.42982268	Yes
CES1	840	4.627289772	0.43266457	Yes
GPR56	842	4.618930817	0.4356087	Yes
CEBPA	868	4.505409241	0.43718678	Yes
TPM1	880	4.478034019	0.439501	Yes
DAB2	881	4.477255344	0.442407	Yes
PRF1	885	4.471072197	0.44514748	Yes
DNAJC1	889	4.450855732	0.44787484	Yes
AIM2	896	4.444692135	0.45043665	Yes

FRY	910	4.369570732	0.45257276	Yes
SMAD3	915	4.3606143	0.45518768	Yes
SIPA1L2	930	4.308218002	0.45723012	Yes
PAK6	933	4.287428379	0.45990524	Yes
PLOD3	938	4.281956196	0.46246913	Yes
AGPAT4	939	4.281747818	0.46524826	Yes
RHBDF2	940	4.279283047	0.4680258	Yes
S100A4	944	4.26849556	0.47063482	Yes
PMAIP1	977	4.159807682	0.4716116	Yes
KLRD1	994	4.114377022	0.4734205	Yes
SOX13	999	4.100191593	0.4758664	Yes
MAP3K5	1012	4.075381279	0.4778654	Yes
DNAPTP6	1040	4.014746189	0.4790173	Yes
ABI3	1048	3.99361062	0.48123246	Yes
ACTN4	1052	3.978840351	0.48365346	Yes
GAB3	1054	3.974344254	0.48617923	Yes
SLC15A4	1073	3.913071632	0.48774976	Yes
ADRB2	1082	3.889022827	0.4898432	Yes
OASL	1092	3.867156029	0.4918686	Yes
NEK3	1146	3.73054266	0.49143592	Yes
CCR2	1147	3.727671146	0.49385542	Yes
GOLPH4	1157	3.704975843	0.49577555	Yes
ITGB1	1183	3.643767834	0.49679434	Yes
FLJ20699	1213	3.550427198	0.49753717	Yes
SAP30	1233	3.517030239	0.4987968	Yes
FEZ1	1244	3.500377655	0.50053024	Yes
CHN2	1249	3.496879339	0.5025846	Yes
SLC27A3	1271	3.464265585	0.5037023	Yes
KLF11	1282	3.439421415	0.5053962	Yes
IL12RB2	1283	3.436179399	0.5076265	Yes
ERN1	1306	3.398232222	0.5086475	Yes
SLC1A5	1307	3.39720273	0.5108525	Yes
RHOC	1314	3.380245686	0.5127234	Yes
ANXA2P1	1318	3.373168707	0.51475126	Yes
IGSF4	1333	3.333185434	0.51616085	Yes
CX3CR1	1334	3.332838297	0.5183241	Yes
NCAM1	1338	3.328579903	0.520323	Yes
FHOD1	1360	3.291663647	0.5213286	Yes
FASLG	1398	3.243864536	0.5214417	Yes
ATXN1	1421	3.202971458	0.5223359	Yes
TFEB	1423	3.199354887	0.5243587	Yes
NCR3	1435	3.179026604	0.52582973	Yes
ASCL2	1441	3.170716524	0.52761847	Yes
SETBP1	1442	3.169953346	0.52967596	Yes
EDG8	1446	3.154218197	0.53156173	Yes
CREB3L2	1447	3.152264118	0.5336078	Yes
PDZD4	1491	3.083245277	0.5332934	Yes
GPR68	1503	3.060992002	0.5346879	Yes
PHACTR2	1522	3.039041758	0.53569114	Yes
ELOVL6	1527	3.035920858	0.53744626	Yes
ATP9A	1536	3.025636196	0.5389793	Yes
TCF7L2	1541	3.022995472	0.540726	Yes
PHTF1	1549	3.018165588	0.54230803	Yes

KIAA0427	1565	2.996525764	0.5434452	Yes
TGFA	1572	2.990687609	0.5450633	Yes
KIR2DL5A	1600	2.961051941	0.5455313	Yes
FCGR3B	1629	2.926766634	0.5459231	Yes
ADAM15	1633	2.92509532	0.5476602	Yes
HSPA1A	1634	2.925043344	0.5495587	Yes
CYBRD1	1645	2.905431032	0.55090606	Yes
STOM	1647	2.901721001	0.5527356	Yes
LGR6	1648	2.901227236	0.5546187	Yes
RHOBTB3	1655	2.891118526	0.55617213	Yes
LOC387895	1670	2.868441582	0.55728006	Yes
KIR3DL3	1708	2.830955505	0.5571251	Yes
CD244	1709	2.830202818	0.55896205	Yes
PODXL	1718	2.821060419	0.56036234	Yes
ATP2B4	1725	2.81306076	0.5618651	Yes
YPEL1	1726	2.812599182	0.56369066	Yes
SLC7A5	1737	2.798192739	0.56496835	Yes
PTGDS	1750	2.784201145	0.56612927	Yes
NKG7	1755	2.779314756	0.56771785	Yes
MAPK1	1773	2.758028746	0.56859255	Yes
FAM38A	1775	2.755474329	0.57032716	Yes
KIR2DS5	1786	2.746232986	0.5715712	Yes
PDGFD	1817	2.709479094	0.5717143	Yes
SNX24	1820	2.705267429	0.5733625	Yes
FAM53B	1833	2.692638397	0.574464	Yes
PTMS	1850	2.67511797	0.5753387	Yes
ST3GAL4	1852	2.674262047	0.57702065	Yes
KIAA1539	1863	2.662253618	0.5782102	Yes
TNIP3	1869	2.658329725	0.5796663	Yes
TMEM62	1879	2.650244713	0.58090186	Yes
IQGAP2	1913	2.620070696	0.5808254	Yes
FLJ11292	1915	2.619113684	0.58247155	Yes
GHRHR	1937	2.596276999	0.5830259	Yes
CST7	1971	2.571106195	0.58291763	Yes
PLCB1	1992	2.558177233	0.58350104	Yes
IL18R1	2006	2.544543982	0.58445257	Yes
SLC4A4	2038	2.524054766	0.5844215	Yes
IFI27	2048	2.517263174	0.5855707	Yes
PPP2R2B	2062	2.504804611	0.5864965	Yes
DTNBP1	2113	2.459022999	0.5854	Yes
PPP1R14C	2124	2.448293686	0.58645064	Yes
AUTS2	2126	2.446923256	0.587985	Yes
IL8RB	2136	2.434890747	0.58908075	Yes
HSPA6	2161	2.416177034	0.5893566	Yes
ZDHHC14	2162	2.416016102	0.59092474	Yes
NCR1	2163	2.415674925	0.5924927	Yes
LRIG1	2175	2.406434298	0.5934623	Yes
ERBB2	2191	2.394804239	0.5942089	Yes
ADCY9	2204	2.380465984	0.5951078	Yes
CYP2C19	2208	2.378496885	0.59649	Yes
GZMB	2221	2.371834993	0.5973833	Yes
LOC284757	2257	2.34145546	0.59701836	Yes
LTB4R	2258	2.341050148	0.59853786	Yes

MMP24	2278	2.328256369	0.5990259	Yes
PLEKHG3	2295	2.317821503	0.5996687	Yes
WEE1	2315	2.305245161	0.6001418	Yes
DCBLD1	2329	2.298047066	0.6009333	Yes
FCHO2	2335	2.294792891	0.60215354	Yes
LAMA2	2345	2.290893555	0.60315585	Yes
CENTD3	2346	2.290679455	0.6046427	Yes
ZBP1	2358	2.280720472	0.6055307	Yes
KIR2DL2	2360	2.28018713	0.6069568	Yes
TGFBR3	2362	2.279341459	0.6083824	Yes
TTYH2	2419	2.24703908	0.60682523	Yes
CAPN12	2455	2.227093697	0.606386	Yes
ENPP4	2491	2.208233595	0.60593456	Yes
CXCR6	2498	2.203609705	0.6070418	Yes
PAM	2518	2.195827007	0.60744387	Yes
MXRA7	2565	2.173846245	0.6063777	Yes
ZNF193	2574	2.168704271	0.6073545	Yes
FLJ14213	2602	2.153940678	0.6072986	Yes
ZNF663	2622	2.137885094	0.6076631	Yes
LIMK1	2629	2.130476713	0.6087228	Yes
PHLDB2	2662	2.114080667	0.6083718	Yes
CENPO	2694	2.094015837	0.6080616	Yes
NBEAL2	2724	2.079209089	0.6078495	Yes
JAKMIP2	2761	2.059734821	0.60724777	Yes
LOC89944	2786	2.046463251	0.60728365	Yes
AKR1C3	2806	2.033388853	0.6075803	Yes
SCD5	2819	2.026156664	0.60824925	Yes
SYNGR1	2845	2.011172771	0.60820836	Yes
CYB561	2861	2.004258156	0.6087015	Yes
KIR3DL1	2867	2.00105381	0.6097311	Yes
TLE1	2954	1.950687766	0.6063661	Yes
PLEKHF1	2972	1.944883704	0.606713	Yes
ATP1B1	2991	1.935745358	0.6070001	Yes
PALLD	3059	1.902856946	0.60462725	Yes
VAV3	3068	1.89952302	0.60542935	Yes
GZMH	3108	1.880655885	0.6045499	Yes
GFOD1	3114	1.878587723	0.6054999	Yes
KATNAL1	3123	1.876507521	0.6062871	Yes
SPON2	3154	1.861854196	0.6058801	Yes
IFNG	3165	1.858321667	0.6065478	Yes
RHEBL1	3166	1.857677102	0.6077535	Yes
ACOT4	3175	1.854086995	0.6085262	Yes
MYO6	3189	1.846933484	0.6090249	Yes
CACNB3	3191	1.845817327	0.6101691	Yes
ZFYVE28	3198	1.844288468	0.61104304	Yes
AP4M1	3205	1.842113972	0.6119156	Yes
HOP	3256	1.812075496	0.61039925	Yes
LOC58489	3259	1.811513901	0.61146736	Yes
RASSF1	3293	1.797035098	0.6108567	Yes
CLIC3	3295	1.794607639	0.6119677	Yes
FLJ39501	3300	1.793867707	0.6129166	Yes
FLJ38984	3325	1.786351919	0.6127837	Yes
PDE5A	3357	1.772639513	0.6122649	Yes

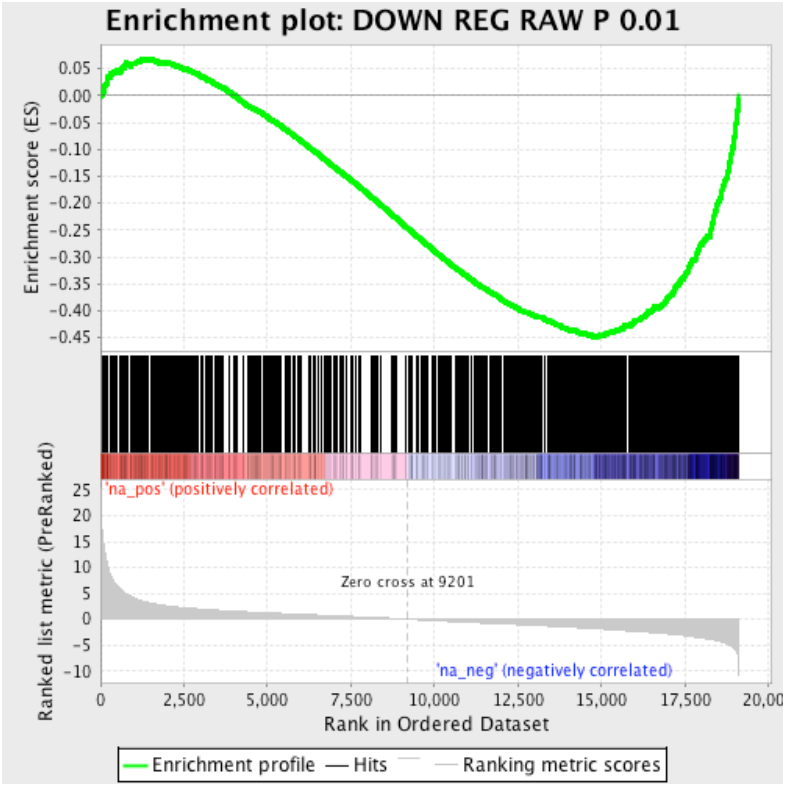
GAS1	3370	1.767202258	0.61276567	Yes
TM6SF1	3377	1.763542295	0.61358726	Yes
ME1	3397	1.757732034	0.613705	Yes
SATB2	3398	1.757664204	0.6148458	Yes
MCOLN2	3416	1.746477723	0.61506397	Yes
BFSP1	3418	1.74557209	0.6161431	Yes
WNT1	3424	1.742581844	0.61700493	Yes
SCRIB	3428	1.742080808	0.6179741	Yes
PTDSR	3431	1.741778731	0.6189969	Yes

A4.2 Geneset enrichment analysis DOWN REGULATED GENES

A4.2.1 Statistics

Dataset	LucyW_E2_plus-minus_collapsed
Phenotype	NoPhenotypeAvailable
Upregulated in class	na_neg
GeneSet	DOWN REG RAW P 0.01
Enrichment Score (ES)	-0.44938713
Normalized Enrichment Score (NES)	-2.5510142
Nominal p-value	0.0
FDR q-value	0.0
FWER p-Value	0.0

A4.2.2 Enrichment plot



A4.2.3 Genes contributing to leading edge enrichment score

PROBE	RANK IN GENE LIST	RANK METRIC SCORE	RUNNING ES	CORE ENRICHMENT
BTBD7	14777	-1.790534616	-0.4487497	Yes
TP53	14780	-1.792187572	-0.44822258	Yes
WDR5	14792	-1.795033336	-0.4481935	Yes
SYPL1	14801	-1.799571753	-0.44799644	Yes
FLJ10661	14817	-1.804416299	-0.44818583	Yes
THNSL1	14831	-1.813650012	-0.44826102	Yes
TSPYL2	14836	-1.815021992	-0.44783667	Yes
NDUFA10	14841	-1.816568255	-0.44741178	Yes
MEIS3P1	14851	-1.820816159	-0.44726261	Yes
TSC22D3	14860	-1.824793458	-0.44705656	Yes
PPIE	14862	-1.825318575	-0.4464622	Yes
ALDOC	14872	-1.832962871	-0.44630873	Yes
NOD27	14891	-1.840419054	-0.44665164	Yes
ACCN2	14907	-1.84850347	-0.44682533	Yes
LOC150383	14929	-1.859119296	-0.44732794	Yes
CRTAM	14936	-1.862508535	-0.44699758	Yes
AHCY	14941	-1.863540769	-0.44655594	Yes
ZSWIM1	14942	-1.863759875	-0.44589245	Yes
FBXO7	14949	-1.870193243	-0.44555935	Yes
SRP54	14952	-1.871543288	-0.445004	Yes
TSPYL5	14976	-1.88049078	-0.44560987	Yes
FLJ20489	14990	-1.888128161	-0.44565856	Yes
ZNF471	14999	-1.893809676	-0.44542795	Yes
RHPN2	15019	-1.902528167	-0.4458042	Yes
SDCCAG8	15036	-1.907290697	-0.44601244	Yes
HEXA	15055	-1.913679957	-0.44632927	Yes
POLR3D	15060	-1.91621232	-0.44586888	Yes
DDX3X	15069	-1.92120719	-0.44562852	Yes
SLC22A17	15085	-1.927817941	-0.445774	Yes
ZNF616	15092	-1.930833578	-0.4454193	Yes
ERGIC3	15098	-1.934092522	-0.445008	Yes
GFM2	15103	-1.935643077	-0.4445407	Yes
DHX40	15112	-1.939548492	-0.44429383	Yes
EI24	15118	-1.9417454	-0.4438798	Yes
SMARCD1	15121	-1.943599463	-0.4432988	Yes
DPP7	15130	-1.946661472	-0.44304937	Yes
WRNIP1	15141	-1.950929403	-0.44290933	Yes
MAP3K7	15142	-1.951097131	-0.44221476	Yes
THRAP5	15151	-1.95604527	-0.441962	Yes
HHLA3	15161	-1.957864285	-0.44176403	Yes
PNPO	15170	-1.964195728	-0.44150838	Yes
TERF2	15174	-1.964717746	-0.44097528	Yes
SOCS5	15197	-1.973413467	-0.44149265	Yes
BTN2A1	15206	-1.976126909	-0.44123274	Yes
ATP6V0E2L	15222	-1.982239723	-0.44135883	Yes
PKNOX1	15226	-1.982965708	-0.44081923	Yes
KIAA1900	15237	-1.988059878	-0.440666	Yes
PYGB	15242	-1.989733338	-0.44017944	Yes
TNPO1	15257	-1.993092299	-0.4402462	Yes
FAM102A	15258	-1.99336946	-0.43953654	Yes

UBXD7	15266	-1.995465755	-0.43921432	Yes
DDB1	15301	-2.004841328	-0.4403859	Yes
ALKBH7	15305	-2.008196354	-0.43983734	Yes
TSGA14	15323	-2.015981674	-0.44006228	Yes
TAF7	15326	-2.017388582	-0.439455	Yes
KNS2	15330	-2.018968344	-0.4389026	Yes
LYPD3	15341	-2.023215055	-0.43873683	Yes
CSNK1A1	15366	-2.032297134	-0.43934414	Yes
GIT2	15369	-2.032708168	-0.43873137	Yes
TRIAD3	15376	-2.036316156	-0.43833914	Yes
RANBP1	15390	-2.041828156	-0.43833312	Yes
ZIK1	15395	-2.04594636	-0.43782654	Yes
FBXO22	15405	-2.049210787	-0.43759608	Yes
CCNC	15411	-2.051208973	-0.4371431	Yes
ESD	15417	-2.055033922	-0.43668875	Yes
MRPS35	15427	-2.057719707	-0.43645525	Yes
ILF3	15435	-2.062685728	-0.43610907	Yes
SFI1	15438	-2.063242197	-0.43548545	Yes
CHI3L2	15448	-2.068255901	-0.4352482	Yes
CUGBP1	15487	-2.089711666	-0.43661138	Yes
LOC317671	15489	-2.090249777	-0.43592268	Yes
HAPLN3	15493	-2.092332125	-0.43534416	Yes
GCC2	15508	-2.099464655	-0.43537307	Yes
MYH10	15510	-2.10075593	-0.43468064	Yes
LSP1	15516	-2.103813648	-0.43420893	Yes
TMEM123	15548	-2.123967648	-0.43517175	Yes
LOC201164	15556	-2.126041412	-0.43480304	Yes
RPL32	15557	-2.127017975	-0.4340458	Yes
ZNF3	15570	-2.133949995	-0.43395153	Yes
CATSPER2	15580	-2.139148235	-0.43368903	Yes
DKFZP434A0131	15582	-2.140661716	-0.4329824	Yes
CCT6A	15608	-2.15634346	-0.433601	Yes
CRSP8	15609	-2.156886816	-0.43283314	Yes
ZNF417	15628	-2.166293383	-0.43306002	Yes
ZBTB41	15632	-2.167534113	-0.43245474	Yes
TLE4	15634	-2.167927742	-0.4317384	Yes
SLC24A6	15639	-2.169856548	-0.43118772	Yes
KIAA0738	15652	-2.174610138	-0.43107894	Yes
KIAA0179	15659	-2.178151608	-0.43063623	Yes
SON	15668	-2.180962801	-0.4303034	Yes
SUMF2	15675	-2.185361624	-0.42985812	Yes
ZNF232	15677	-2.187448502	-0.42913482	Yes
FLJ38969	15688	-2.193764925	-0.42890835	Yes
SERPINE2	15689	-2.194303513	-0.42812714	Yes
MRRF	15690	-2.195327282	-0.4273456	Yes
HMBS	15696	-2.197151661	-0.42684066	Yes
FAM112A	15712	-2.202254295	-0.4268884	Yes
TOP1MT	15718	-2.205319166	-0.42638057	Yes
ZNF135	15722	-2.206510305	-0.4257614	Yes
SIRT4	15724	-2.206689358	-0.42503124	Yes
SLC38A1	15748	-2.21586132	-0.42551777	Yes
EHHADH	15757	-2.220089674	-0.42517102	Yes
MRPL45	15815	-2.252439022	-0.4275298	Yes

DNAJC16	15839	-2.262759924	-0.42799965	Yes
ZC3HAV1	15854	-2.2669034	-0.42796892	Yes
GLIS3	15868	-2.2719872	-0.42788094	Yes
BZW2	15870	-2.273189783	-0.42712712	Yes
AMACR	15873	-2.274431705	-0.42642832	Yes
ASB3	15882	-2.283499241	-0.42605898	Yes
ZNF187	15887	-2.283886194	-0.42546773	Yes
VIPR1	15888	-2.284070492	-0.42465457	Yes
TFG	15901	-2.291226625	-0.4245043	Yes
MARS2	15928	-2.304107904	-0.42512575	Yes
RCL1	15934	-2.306466818	-0.4245819	Yes
ECD	15938	-2.308358908	-0.42392647	Yes
UGP2	15947	-2.310111046	-0.42354766	Yes
KBTBD9	15951	-2.3116467	-0.42289105	Yes
HIVEP1	15953	-2.312146187	-0.42212337	Yes
ANKHD1	15960	-2.31501317	-0.42163193	Yes
PRRT1	15965	-2.320677757	-0.42102754	Yes
TRIM37	15972	-2.322379112	-0.42053348	Yes
APPBP2	15977	-2.323691607	-0.41992804	Yes
GCET2	15987	-2.326318026	-0.4195989	Yes
LOC93349	15988	-2.326659203	-0.4187706	Yes
PDDC1	15999	-2.3307693	-0.41849536	Yes
HNRPA3	16019	-2.338314056	-0.41871646	Yes
UCP2	16022	-2.33974123	-0.4179944	Yes
KLHL6	16029	-2.342994452	-0.417493	Yes
EPB41L5	16030	-2.343253374	-0.4166588	Yes
FAM113B	16042	-2.347733974	-0.41643295	Yes
THOC3	16057	-2.354658842	-0.416371	Yes
INPP5B	16069	-2.360450983	-0.41614062	Yes
NSF	16094	-2.369219065	-0.41662797	Yes
UBA52	16116	-2.38088131	-0.41694483	Yes
PPAP2A	16149	-2.391552925	-0.41786787	Yes
DLL1	16157	-2.395884752	-0.41740307	Yes
AEBP1	16163	-2.399096251	-0.41682625	Yes
TRIM14	16167	-2.400405169	-0.41613802	Yes
RPS6KA3	16170	-2.401334763	-0.41539407	Yes
PRMT1	16181	-2.407456398	-0.41509148	Yes
SEH1L	16191	-2.409909964	-0.4147326	Yes
EIF2S2	16192	-2.410351992	-0.4138745	Yes
NRCAM	16199	-2.413270712	-0.41334808	Yes
AGMAT	16210	-2.418460131	-0.41304162	Yes
MAGED2	16217	-2.422197819	-0.412512	Yes
ZNF654	16219	-2.423001528	-0.41170487	Yes
ARRDC2	16240	-2.433257103	-0.4119476	Yes
CHMP7	16253	-2.440294266	-0.41174427	Yes
ZNF2	16255	-2.440546036	-0.41093087	Yes
EPHB4	16293	-2.461318493	-0.4121063	Yes
CACHD1	16298	-2.46339035	-0.41145113	Yes
BTBD11	16302	-2.464479446	-0.41074014	Yes
CHM	16307	-2.465774536	-0.4100841	Yes
ZNF167	16318	-2.469436884	-0.4097595	Yes
USP33	16320	-2.471259594	-0.40893516	Yes
15E1.2	16322	-2.473051548	-0.4081102	Yes

DPH2	16332	-2.479771376	-0.40772644	Yes
SPINK2	16334	-2.480745316	-0.40689874	Yes
GJB6	16341	-2.483307123	-0.40634736	Yes
GOSR1	16348	-2.485610008	-0.4057952	Yes
ABCF2	16356	-2.490973473	-0.40529653	Yes
WDR23	16365	-2.4950881	-0.40485188	Yes
TCP1	16377	-2.501629114	-0.40457124	Yes
TCF7	16378	-2.502421379	-0.40368038	Yes
LOC201229	16379	-2.502521038	-0.40278947	Yes
ACSM3	16384	-2.503664732	-0.40211996	Yes
PLEKHB1	16396	-2.510937691	-0.401836	Yes
GEM	16403	-2.512471199	-0.40127426	Yes
MAGED1	16431	-2.527219296	-0.40187174	Yes
NGFRAP1	16436	-2.530878305	-0.40119252	Yes
SELL	16443	-2.533520222	-0.4006233	Yes
RFC2	16458	-2.542283535	-0.40049455	Yes
GTF2A1	16489	-2.557725191	-0.4012475	Yes
ZNF586	16495	-2.562473059	-0.4006125	Yes
TSGA10	16497	-2.562538147	-0.3997557	Yes
APEX1	16509	-2.56679821	-0.39945185	Yes
SALL2	16534	-2.577937603	-0.3998649	Yes
ZNF14	16535	-2.578170776	-0.39894706	Yes
CNN3	16543	-2.580425978	-0.39841658	Yes
CLEC11A	16544	-2.580501795	-0.3974979	Yes
EBAG9	16553	-2.586391211	-0.39702076	Yes
NBR1	16560	-2.59110117	-0.396431	Yes
TRIM5	16567	-2.595067978	-0.39583987	Yes
FLJ10781	16569	-2.596576929	-0.39497092	Yes
RPS23	16575	-2.598494768	-0.39432308	Yes
LTB	16577	-2.599733114	-0.39345303	Yes
ZNF96	16582	-2.602434397	-0.39274836	Yes
POLR1E	16585	-2.604748249	-0.39193195	Yes
TNFRSF25	16593	-2.606768608	-0.39139208	Yes
SULT1B1	16624	-2.621916056	-0.39212218	Yes
SUHW2	16666	-2.645864248	-0.39345375	Yes
PINX1	16706	-2.659830332	-0.3946694	Yes
NOSIP	16727	-2.670270681	-0.39482778	Yes
CORO2A	16733	-2.675134659	-0.3941527	Yes
MAPK14	16735	-2.677295446	-0.393255	Yes
ENPP2	16747	-2.680702686	-0.39291063	Yes
EIF4B	16765	-2.691248417	-0.3928952	Yes
MTUS1	16770	-2.693224907	-0.3921582	Yes
CSNK2A1	16778	-2.69851613	-0.39158568	Yes
IKBKE	16791	-2.708170414	-0.39128697	Yes
ALDH5A1	16798	-2.712767839	-0.3906539	Yes
FBLN5	16803	-2.714211464	-0.38990945	Yes
MYB	16821	-2.723768711	-0.38988242	Yes
ZNF32	16827	-2.725784063	-0.38918927	Yes
PFN2	16831	-2.726350307	-0.38838506	Yes
PRR3	16853	-2.742191315	-0.3885733	Yes
HSPC047	16858	-2.748939037	-0.38781646	Yes
CD8A	16860	-2.749726057	-0.38689297	Yes
PPM1K	16881	-2.758934259	-0.3870198	Yes

LRRC8D	16886	-2.760915279	-0.38625872	Yes
PPA1	16891	-2.762337446	-0.38549712	Yes
BTF3L4	16894	-2.765264988	-0.38462356	Yes
SLC12A6	16905	-2.772310495	-0.38419113	Yes
ZNF611	16915	-2.77760458	-0.38370132	Yes
SIRPG	16917	-2.777834177	-0.38276786	Yes
PGK1	16923	-2.780637503	-0.3820552	Yes
RANBP6	16938	-2.790916681	-0.38183793	Yes
RPIA	16945	-2.795064211	-0.38117558	Yes
KIAA2010	16950	-2.801249504	-0.38040012	Yes
MGC39900	16953	-2.802109718	-0.37951347	Yes
TBXA2R	16955	-2.804182529	-0.37857062	Yes
SYNC1	16968	-2.814289331	-0.37823412	Yes
NUFIP1	16973	-2.815339088	-0.37745366	Yes
VAMP1	16983	-2.820931673	-0.37694845	Yes
MGC29671	16987	-2.824920654	-0.37610912	Yes
DIDO1	16991	-2.827464819	-0.37526888	Yes
SEC14L2	17014	-2.843415976	-0.3754765	Yes
DPPA4	17020	-2.846354485	-0.37474045	Yes
RP11-450P7.3	17026	-2.849867582	-0.37400314	Yes
GRAP	17030	-2.853753567	-0.37315354	Yes
DGUOK	17046	-2.865633965	-0.37296513	Yes
POT1	17067	-2.879994631	-0.37304887	Yes
STT3B	17069	-2.881169319	-0.3720786	Yes
ANKZF1	17074	-2.883498669	-0.37127388	Yes
BAG5	17092	-2.892247438	-0.37118688	Yes
BAT1	17097	-2.894520044	-0.37037823	Yes
UBTF	17113	-2.906279087	-0.37017533	Yes
PYCR2	17116	-2.907198906	-0.36925125	Yes
MEOX1	17126	-2.910593987	-0.36871412	Yes
LIMK2	17140	-2.920336723	-0.36839533	Yes
PPAPDC2	17141	-2.921309471	-0.36735535	Yes
FAM98B	17156	-2.931998968	-0.36708784	Yes
CCT3	17158	-2.933351517	-0.366099	Yes
MSI2	17161	-2.934129715	-0.36516535	Yes
MDM1	17163	-2.934398413	-0.36417612	Yes
ABI2	17166	-2.935576677	-0.36324197	Yes
PATZ1	17181	-2.943419456	-0.3629704	Yes
CDC42SE2	17182	-2.943576336	-0.36192247	Yes
LCK	17183	-2.943957806	-0.3608744	Yes
ZNF136	17199	-2.952043533	-0.36065522	Yes
RBM4	17200	-2.95205617	-0.3596043	Yes
EPB41	17204	-2.956608772	-0.35871807	Yes
LDOC1	17206	-2.958472967	-0.3577203	Yes
TNFRSF7	17216	-2.965433598	-0.35716364	Yes
BRWD1	17224	-2.969737291	-0.35649455	Yes
IMPDH2	17228	-2.970879078	-0.35560328	Yes
TACC3	17231	-2.972583055	-0.35465592	Yes
MCCC2	17235	-2.977493048	-0.35376227	Yes
RUVBL1	17242	-2.982442141	-0.3530332	Yes
AMFR	17265	-3.002030611	-0.35318437	Yes
ANAPC7	17273	-3.003993273	-0.3525031	Yes
CUL4B	17274	-3.004820824	-0.35143337	Yes

NOLA1	17306	-3.023965597	-0.35207582	Yes
TCF20	17310	-3.026550531	-0.3511647	Yes
ETS1	17311	-3.028045654	-0.3500867	Yes
SERF1A	17317	-3.035104752	-0.34928343	Yes
TXK	17324	-3.038450718	-0.34853444	Yes
THAP5	17328	-3.043038368	-0.34761745	Yes
CASP6	17332	-3.045876026	-0.34669948	Yes
NGRN	17343	-3.0566926	-0.34616578	Yes
ITSN2	17374	-3.08104372	-0.34673244	Yes
PRKDC	17380	-3.08503294	-0.3459114	Yes
ZMYM2	17386	-3.087781906	-0.34508938	Yes
PHGDH	17387	-3.090477467	-0.34398916	Yes
FXR1	17388	-3.091017246	-0.34288874	Yes
CBR3	17399	-3.097323179	-0.3423406	Yes
CD55	17409	-3.101262569	-0.3417356	Yes
GYPC	17434	-3.116781712	-0.34195682	Yes
NRF1	17436	-3.119257689	-0.3409018	Yes
HSP90AB1	17439	-3.120794058	-0.3399017	Yes
ATP8B2	17465	-3.141157866	-0.3401697	Yes
PPP2R5C	17472	-3.145246506	-0.33938268	Yes
TRIM35	17473	-3.145398378	-0.3382629	Yes
LOC136306	17478	-3.149047375	-0.33736363	Yes
DDX47	17486	-3.153020859	-0.3366293	Yes
TCEA3	17488	-3.155186415	-0.33556148	Yes
RGS10	17495	-3.159438372	-0.3347694	Yes
KLHL8	17500	-3.164053202	-0.3338648	Yes
GPC2	17503	-3.167318821	-0.33284813	Yes
FLJ20152	17519	-3.177661657	-0.33254862	Yes
MYC	17520	-3.177770138	-0.33141732	Yes
ZC3H11A	17528	-3.18321991	-0.33067223	Yes
CD248	17539	-3.192224979	-0.33009028	Yes
ALS2CR8	17542	-3.195753336	-0.3290635	Yes
BCL2	17545	-3.196722746	-0.32803634	Yes
ARTS-1	17567	-3.219602823	-0.3280546	Yes
NUP50	17571	-3.224006891	-0.32707322	Yes
ARMCX1	17589	-3.238248825	-0.32686305	Yes
SLC39A9	17591	-3.238753557	-0.3257655	Yes
CCT2	17597	-3.244074821	-0.32488784	Yes
FOXO1A	17606	-3.251751661	-0.3241738	Yes
NGFRAP1L1	17611	-3.253891945	-0.3232372	Yes
AP1GBP1	17614	-3.256517172	-0.32218876	Yes
PRIM1	17620	-3.25962472	-0.32130557	Yes
PAICS	17623	-3.261019707	-0.32025555	Yes
LIN7C	17624	-3.264019489	-0.31909353	Yes
CDKAL1	17626	-3.265036345	-0.3179866	Yes
ZNF447	17634	-3.270337105	-0.31721053	Yes
CSNK1G1	17640	-3.280331612	-0.31631997	Yes
FCGBP	17642	-3.281652689	-0.31520712	Yes
KIAA0265	17656	-3.290593624	-0.3147565	Yes
TCEAL1	17659	-3.292490959	-0.31369528	Yes
APPBP1	17666	-3.295580387	-0.31285474	Yes
MCM7	17675	-3.30318141	-0.3121224	Yes
RPL10A	17687	-3.311629772	-0.31155342	Yes

NAP1L1	17707	-3.32527256	-0.31142315	Yes
PIM2	17709	-3.326225758	-0.31029445	Yes
CYLD	17713	-3.329531431	-0.30927548	Yes
THRAP3	17717	-3.332759619	-0.30825534	Yes
JAK3	17722	-3.335556507	-0.3072897	Yes
RGMB	17731	-3.339020729	-0.3065446	Yes
NDRG2	17733	-3.3398211	-0.30541104	Yes
SFXN4	17738	-3.343200922	-0.30444264	Yes
SLC16A7	17754	-3.359317303	-0.3040785	Yes
P2RY10	17783	-3.391266108	-0.3044238	Yes
GTF2H2	17819	-3.432568789	-0.30514258	Yes
KIAA1008	17822	-3.435038805	-0.30403057	Yes
LDHB	17824	-3.438504696	-0.3028619	Yes
CDC42	17826	-3.43956089	-0.30169287	Yes
CUGBP2	17836	-3.446222067	-0.30096504	Yes
POLH	17838	-3.449159861	-0.2997926	Yes
ZNF286	17839	-3.449848175	-0.2985644	Yes
ABCC1	17842	-3.450554609	-0.2974469	Yes
IHPK2	17849	-3.456408501	-0.2965491	Yes
PAG1	17860	-3.461748838	-0.29587123	Yes
PDE9A	17861	-3.462118387	-0.2946387	Yes
PARP6	17864	-3.463507891	-0.29351658	Yes
KIAA0748	17872	-3.468173504	-0.29267004	Yes
GNL3	17885	-3.475119352	-0.29209828	Yes
LOC400721	17887	-3.477077007	-0.29091588	Yes
NPAL3	17890	-3.478800535	-0.2897883	Yes
MRPS14	17892	-3.479545355	-0.28860503	Yes
UBASH3A	17897	-3.487702847	-0.2875852	Yes
MAX	17905	-3.493057728	-0.2867298	Yes
SUSD4	17907	-3.493450165	-0.2855416	Yes
RPL7L1	17920	-3.506079912	-0.2849588	Yes
NCBP2	17921	-3.506122112	-0.2837106	Yes
DALRD3	17926	-3.513659	-0.28268152	Yes
COX11	17942	-3.531230688	-0.28225616	Yes
LEPROTL1	17944	-3.533904552	-0.28105354	Yes
ZNF667	17947	-3.535784721	-0.27990568	Yes
ENSA	17959	-3.548561335	-0.27925232	Yes
ARMC8	17962	-3.551999331	-0.2780987	Yes
USP21	17975	-3.565098763	-0.27749494	Yes
UBE2H	17979	-3.566908836	-0.27639145	Yes
ATR	18000	-3.584475517	-0.27622437	Yes
PLCG1	18016	-3.604643583	-0.27577287	Yes
TRUB1	18017	-3.604662657	-0.27448958	Yes
ACTN1	18032	-3.620284557	-0.27397704	Yes
NAP1L4	18034	-3.622850657	-0.27274275	Yes
MORC2	18053	-3.644600391	-0.27244338	Yes
NIN	18056	-3.645911932	-0.27125633	Yes
NLE1	18058	-3.646058559	-0.27001375	Yes
ROBO1	18072	-3.659844398	-0.26943168	Yes
TSPYL4	18084	-3.672849655	-0.2687341	Yes
FASTKD2	18091	-3.686053038	-0.26775455	Yes
BTN3A3	18108	-3.70244813	-0.26732367	Yes
G3BP2	18116	-3.708462954	-0.2663916	Yes

RPL28	18127	-3.713522196	-0.26562408	Yes
LOC643079	18138	-3.723435402	-0.26485303	Yes
STX16	18151	-3.734501839	-0.26418895	Yes
DDX17	18156	-3.739115715	-0.26307958	Yes
ZNF569	18159	-3.741002798	-0.26185867	Yes
SATB1	18171	-3.751007795	-0.26113325	Yes
MIA3	18203	-3.780212879	-0.26150647	Yes
SLC16A10	18236	-3.844234705	-0.26191232	Yes
AK5	18248	-3.864661217	-0.26114646	Yes
EPHX2	18251	-3.870862246	-0.25987932	Yes
MLX	18264	-3.880893707	-0.2591631	Yes
CHCHD7	18269	-3.895808697	-0.257998	Yes
PLAG1	18279	-3.904921293	-0.25710687	Yes
SLC25A15	18280	-3.906523466	-0.25571612	Yes
HNRPM	18281	-3.907496452	-0.25432503	Yes
FBXO11	18282	-3.908181906	-0.2529337	Yes
PIAS2	18283	-3.909582138	-0.25154188	Yes
RAN	18286	-3.915941238	-0.25025868	Yes
ZNF101	18287	-3.916452646	-0.24886441	Yes
MAP2K6	18289	-3.921197653	-0.2475239	Yes
RASGRP2	18291	-3.923035383	-0.24618274	Yes
TBL1XR1	18293	-3.925625324	-0.24484064	Yes
RNF138	18302	-3.942203999	-0.24388081	Yes
MLXIP	18304	-3.943350077	-0.2425324	Yes
NOLC1	18307	-3.943967342	-0.24123923	Yes
CD28	18320	-3.965131044	-0.24049304	Yes
USF1	18324	-3.967184067	-0.23924705	Yes
RNF38	18326	-3.969213724	-0.23788945	Yes
ITGA6	18335	-3.977413893	-0.23691708	Yes
WHSC1L1	18342	-3.982199192	-0.23583211	Yes
TMEM19	18347	-3.987477303	-0.23463434	Yes
MGC18216	18349	-3.987577677	-0.2332702	Yes
ATP8A1	18350	-3.989497423	-0.23184992	Yes
TMEM118	18354	-3.996335268	-0.23059356	Yes
ABLIM1	18357	-4.002175331	-0.22927967	Yes
TAPBP	18366	-4.015095234	-0.22829388	Yes
LASS6	18373	-4.019259453	-0.22719571	Yes
DOCK9	18380	-4.027373314	-0.22609465	Yes
CCR7	18381	-4.028219223	-0.22466059	Yes
TNRC5	18382	-4.028553963	-0.22322641	Yes
LOC90624	18385	-4.03019619	-0.22190253	Yes
FLT3LG	18386	-4.034071922	-0.22046639	Yes
CCT8	18396	-4.043483734	-0.21952595	Yes
SF1	18400	-4.047417641	-0.2182514	Yes
THYN1	18404	-4.055055141	-0.21697414	Yes
DHX9	18405	-4.057168961	-0.21552977	Yes
PTPRK	18414	-4.072121143	-0.21452367	Yes
STXBP1	18421	-4.075593948	-0.21340546	Yes
CDH1	18433	-4.099939823	-0.21255581	Yes
SNRPN	18438	-4.105920315	-0.21131589	Yes
PCSK5	18439	-4.10603857	-0.20985413	Yes
LDLRAP1	18442	-4.107209682	-0.20850284	Yes
CPA5	18447	-4.112291336	-0.20726065	Yes

LY9	18455	-4.117287159	-0.20618303	Yes
GLT8D1	18462	-4.12996006	-0.20504545	Yes
SLC7A6	18463	-4.131024361	-0.20357479	Yes
U2AF2	18468	-4.136182308	-0.20232409	Yes
CR2	18480	-4.158059597	-0.20145376	Yes
SCAND2	18481	-4.158558846	-0.1999733	Yes
MGC40499	18492	-4.177950859	-0.19904043	Yes
CCDC57	18495	-4.184808731	-0.19766152	Yes
GLS2	18499	-4.186719418	-0.19633739	Yes
ARMCX2	18530	-4.241167068	-0.19649103	Yes
CD8B	18533	-4.246183395	-0.19509028	Yes
YTHDC1	18537	-4.251285076	-0.19374315	Yes
GART	18538	-4.252243996	-0.19222933	Yes
CRLF3	18547	-4.277776241	-0.19115002	Yes
BEXL1	18557	-4.301739693	-0.19011764	Yes
LRRC16	18571	-4.329608917	-0.18929715	Yes
MEST	18578	-4.33823967	-0.18808542	Yes
BEX2	18582	-4.350221634	-0.18670307	Yes
NPM3	18583	-4.351269245	-0.185154	Yes
ZNF671	18595	-4.372272491	-0.18420741	Yes
BCAS4	18605	-4.389444351	-0.18314381	Yes
FTS	18609	-4.392208099	-0.18174651	Yes
NOL6	18611	-4.397744179	-0.18023634	Yes
PRKACB	18612	-4.398647308	-0.1786704	Yes
GSTM3	18614	-4.402423382	-0.17715858	Yes
KLC4	18615	-4.403999329	-0.17559072	Yes
MGC17330	18618	-4.407083988	-0.17413269	Yes
SDK2	18622	-4.414856434	-0.17272733	Yes
PSIP1	18628	-4.419899464	-0.17143108	Yes
HNRPL	18636	-4.435902596	-0.17024003	Yes
CDCA7L	18637	-4.437222481	-0.16866037	Yes
LRPPRC	18659	-4.47386694	-0.16823211	Yes
COL6A3	18664	-4.484051704	-0.16685757	Yes
LOC641518	18668	-4.499874592	-0.16542195	Yes
BACH2	18670	-4.501171589	-0.16387497	Yes
CDC14B	18675	-4.507550716	-0.16249205	Yes
CLEC2D	18681	-4.516429424	-0.16116144	Yes
HP1BP3	18691	-4.532500744	-0.1600469	Yes
GPR155	18695	-4.537565231	-0.15859787	Yes
JRKL	18705	-4.559099197	-0.15747386	Yes
PGBD4	18713	-4.585979462	-0.15622939	Yes
LMO7	18732	-4.633470535	-0.15557797	Yes
PAQR8	18746	-4.658502579	-0.15464038	Yes
FHIT	18754	-4.668257713	-0.15336661	Yes
ZNF238	18768	-4.699608803	-0.1524144	Yes
VSIG1	18775	-4.719017982	-0.15106711	Yes
PRKCA	18779	-4.725947857	-0.149551	Yes
KIAA0888	18780	-4.72746563	-0.14786799	Yes
LEF1	18783	-4.748040676	-0.14628857	Yes
CA6	18784	-4.748842239	-0.14459796	Yes
BCL11B	18785	-4.751838684	-0.1429063	Yes
ORMDL3	18793	-4.770420074	-0.14159615	Yes
TAF15	18799	-4.781208992	-0.14017127	Yes

SUSD3	18808	-4.8309412	-0.13889505	Yes
CHD2	18813	-4.849038601	-0.13739057	Yes
PASK	18815	-4.858271122	-0.13571645	Yes
ALDH6A1	18822	-4.879024029	-0.1343122	Yes
SPTBN1	18825	-4.886610508	-0.13268344	Yes
MBNL1	18828	-4.906515121	-0.1310476	Yes
TDP1	18836	-4.925699234	-0.1296822	Yes
DGKA	18839	-4.940194607	-0.12803437	Yes
ACSL6	18840	-4.947421551	-0.12627305	Yes
MDM4	18842	-4.948067188	-0.12456697	Yes
BTLA	18851	-4.97105217	-0.12324086	Yes
STMN1	18857	-4.985451698	-0.12174327	Yes
LRRN3	18863	-4.996200562	-0.12024186	Yes
IL6ST	18864	-5.00290966	-0.1184608	Yes
MGC5139	18865	-5.00297451	-0.11667971	Yes
MSL3L1	18868	-5.014688969	-0.11500537	Yes
WSB1	18874	-5.042555332	-0.113487445	Yes
MMP28	18881	-5.068472385	-0.112015754	Yes
RPL22	18889	-5.096682072	-0.11058947	Yes
CLN5	18896	-5.110071182	-0.10910296	Yes
MINA	18898	-5.113268852	-0.10733806	Yes
MDN1	18899	-5.1165905	-0.10551653	Yes
TMEM18	18923	-5.277231216	-0.10491318	Yes
PDE3B	18924	-5.281275749	-0.10303303	Yes
CASP2	18927	-5.296615124	-0.10125831	Yes
MAL	18928	-5.296821117	-0.09937262	Yes
PPP1R3E	18935	-5.313223362	-0.097813785	Yes
ORC5L	18937	-5.321962833	-0.095974594	Yes
THEM4	18953	-5.391113758	-0.09488709	Yes
HSMPP8	18955	-5.396916389	-0.09302122	Yes
TAF4B	18963	-5.438649178	-0.09147319	Yes
RNF157	18968	-5.463132381	-0.089750096	Yes
MGC33556	18969	-5.474364758	-0.087801196	Yes
TTN	18971	-5.475732803	-0.08590726	Yes
LOC202134	18973	-5.485590935	-0.08400982	Yes
NOG	18974	-5.498509884	-0.08205232	Yes
SFXN1	18977	-5.515925884	-0.080199525	Yes
UMPS	18983	-5.525399208	-0.07850971	Yes
MAN1C1	18984	-5.526921272	-0.0765421	Yes
PRL	18995	-5.616292953	-0.07509719	Yes
PCID1	18997	-5.624927044	-0.073150136	Yes
CLUAP1	18998	-5.625541687	-0.07114742	Yes
ZNF154	19001	-5.651575089	-0.06924634	Yes
ZNF345	19003	-5.666570663	-0.06728446	Yes
MAML2	19004	-5.66922617	-0.06526619	Yes
SH3YL1	19014	-5.744319439	-0.06372024	Yes
TBC1D4	19017	-5.746919632	-0.061785214	Yes
LOC283130	19019	-5.764316082	-0.05978854	Yes
NUCB2	19022	-5.780636311	-0.05784151	Yes
TMEM30B	19028	-5.821726322	-0.056046203	Yes
NUPL1	19031	-5.867659569	-0.05406819	Yes
RPL37	19036	-5.901010036	-0.052189205	Yes
NBEA	19042	-5.960479736	-0.0503445	Yes

TMEM46	19048	-5.997469425	-0.048486628	Yes
NPAS2	19050	-6.004946709	-0.04640429	Yes
ALS2CR13	19055	-6.034940243	-0.044477627	Yes
XRCC5	19064	-6.183551788	-0.042719863	Yes
DPH5	19066	-6.200353146	-0.040567957	Yes
REG4	19069	-6.328730106	-0.038425803	Yes
HOOK1	19071	-6.396897793	-0.03620393	Yes
LINS1	19072	-6.428850651	-0.03391523	Yes
SCML4	19075	-6.519052982	-0.031705316	Yes
SUCLG2	19076	-6.548739433	-0.029373934	Yes
PKIA	19081	-6.682213306	-0.027216839	Yes
NDFIP1	19091	-7.005984783	-0.025221733	Yes
NELL2	19092	-7.024726868	-0.0227209	Yes
AMIGO1	19094	-7.08995533	-0.020252293	Yes
SCML1	19095	-7.151054382	-0.017706485	Yes
ITPKB	19098	-7.515433788	-0.015141857	Yes
FLJ40722	19102	-7.926594257	-0.012486305	Yes
ZNF550	19104	-8.137879372	-0.009644633	Yes
OGFOD1	19106	-8.225205421	-0.006771873	Yes
KLHL3	19110	-8.801589012	-0.003804819	Yes
DSC1	19111	-10.68569756	-6.62E-07	Yes

Appendix 5

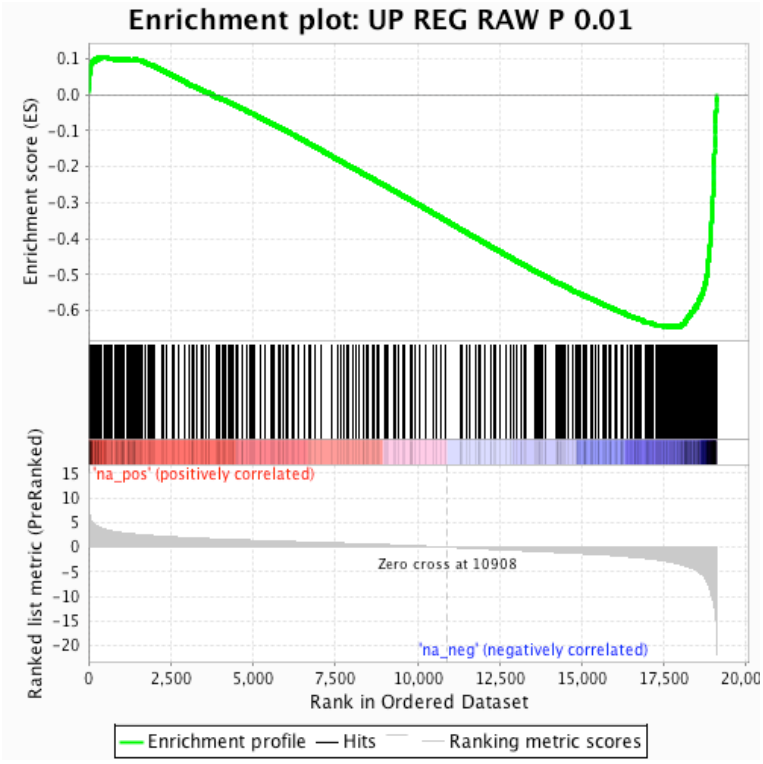
Geneset enrichment analysis comparing CD161++CD8α+ vs CD161+CD8α+ datasets in cord and adult blood

A5.1 Geneset enrichment analysis for UP REGULATED GENES

A5.1.1 Statistics

Dataset	LucyW_E2_plusplus-plus_collapsed
Phenotype	NoPhenotypeAvailable
Upregulated in class	na_neg
GeneSet	UP REG RAW P 0.01
Enrichment Score (ES)	-0.6466313
Normalized Enrichment Score (NES)	-3.104356
Nominal p-value	0.0
FDR q-value	0.0
FWER p-Value	0.0

A5.1.2 Enrichment plot



A5.1.3 Genes contributing to leading edge enrichment score

PROBE	RANK IN GENE LIST	RANK METRIC SCORE	RUNNING ES	CORE ENRICHMENT
CYSLTR1	17682	-2.980244637	-0.6455408	Yes
ST14	17683	-2.980819941	-0.64445	Yes
SEMA4A	17703	-3.012038231	-0.6443735	Yes
UNC93B1	17722	-3.031689167	-0.6442358	Yes
MGC61598	17747	-3.077368021	-0.64440525	Yes
IFNGR2	17758	-3.091122866	-0.64381397	Yes
ARHGAP22	17797	-3.141561985	-0.64471567	Yes
NAPSB	17811	-3.162909508	-0.64426005	Yes
NRG1	17822	-3.17796731	-0.643637	Yes
CLEC1B	17844	-3.209548473	-0.6435962	Yes
FCGR2A	17882	-3.276452065	-0.6443945	Yes
SDSL	17918	-3.325132847	-0.64506716	Yes
NYD-SP21	17924	-3.331879854	-0.64411783	Yes
TBC1D9	17957	-3.391248941	-0.6446043	Yes
TCL1A	17958	-3.395897865	-0.6433617	Yes
CD33	17987	-3.450541019	-0.64361054	Yes
ZNF185	17997	-3.468536139	-0.64282715	Yes
PRAM1	17998	-3.470288754	-0.6415573	Yes
SOCS3	18034	-3.546401501	-0.6421489	Yes
ATP6V0A1	18036	-3.546998501	-0.64090496	Yes
PDK4	18041	-3.558200359	-0.63981885	Yes
STARD5	18043	-3.562708378	-0.6385692	Yes
CENTA2	18055	-3.590668678	-0.6378491	Yes
ZNF467	18068	-3.623155117	-0.63717103	Yes
IRF8	18092	-3.681287527	-0.6370656	Yes
TBXAS1	18114	-3.724266529	-0.63683635	Yes
ECGF1	18116	-3.726671219	-0.6355267	Yes
QPCT	18126	-3.746511936	-0.6346416	Yes
TTYH3	18145	-3.785146236	-0.63422817	Yes
LRRC25	18146	-3.785396338	-0.632843	Yes
CD300C	18148	-3.790403605	-0.63151	Yes
CD4	18154	-3.815515995	-0.63038373	Yes
VENTX	18172	-3.84684062	-0.6298938	Yes
OAS1	18173	-3.846937656	-0.6284861	Yes
AMPD3	18188	-3.88150692	-0.6278215	Yes
SNFT	18192	-3.894684076	-0.6265583	Yes
LST1	18198	-3.903253555	-0.62539995	Yes
NALP12	18199	-3.906058073	-0.6239706	Yes
OLIG1	18203	-3.912174225	-0.62270105	Yes
GPBAR1	18207	-3.940528631	-0.62142104	Yes
JUP	18221	-3.966248035	-0.62067145	Yes
SGK	18229	-3.984982014	-0.6195911	Yes
FCGR1A	18244	-4.019942284	-0.61887586	Yes
CD302	18245	-4.023573875	-0.61740357	Yes
LY86	18268	-4.083564281	-0.6170969	Yes
MERTK	18271	-4.091197014	-0.6157078	Yes
DAPK1	18283	-4.119734764	-0.6147941	Yes
RGS18	18287	-4.124779224	-0.6134467	Yes
TUBB1	18292	-4.134316444	-0.6121498	Yes
SIGLEC10	18298	-4.15049696	-0.61090094	Yes

GNG11	18302	-4.154802799	-0.60954255	Yes
MCTP1	18307	-4.167133331	-0.60823363	Yes
SLC24A4	18310	-4.180666924	-0.6068118	Yes
HK3	18312	-4.186849594	-0.60533375	Yes
FOLR3	18330	-4.21791172	-0.60470796	Yes
MARCO	18343	-4.241781712	-0.6038036	Yes
IRF5	18383	-4.361001492	-0.6043131	Yes
CFD	18386	-4.366476059	-0.60282326	Yes
DSC2	18389	-4.371487617	-0.6013316	Yes
ASGR2	18396	-4.400446415	-0.60004526	Yes
EMR3	18398	-4.403978825	-0.59848773	Yes
S100Z	18401	-4.406832695	-0.59698313	Yes
LRRK2	18412	-4.443892002	-0.59589684	Yes
ENTPD1	18418	-4.463706493	-0.5945334	Yes
MEF2C	18434	-4.498898029	-0.59369683	Yes
SPI1	18442	-4.52882719	-0.59241754	Yes
P2RX1	18447	-4.547949791	-0.59096926	Yes
FLJ11151	18466	-4.639396191	-0.5902433	Yes
KCNMB1	18474	-4.670600891	-0.58891207	Yes
HK2	18503	-4.775239944	-0.58867615	Yes
GPR177	18508	-4.802166939	-0.5871349	Yes
EMR1	18515	-4.83418417	-0.58568984	Yes
PDLIM7	18518	-4.844916821	-0.58402497	Yes
IGF2BP2	18521	-4.86476469	-0.58235276	Yes
ZNF503	18528	-4.939395905	-0.58086926	Yes
LILRA3	18534	-4.958659172	-0.57932466	Yes
TP53I3	18539	-4.98267889	-0.5777173	Yes
CD1C	18548	-5.01564312	-0.57631385	Yes
RTN1	18550	-5.026624203	-0.57452846	Yes
PARVB	18553	-5.045232773	-0.57279027	Yes
ACPP	18560	-5.073408604	-0.5712577	Yes
LRP1	18566	-5.083475113	-0.56966746	Yes
OSM	18582	-5.16102314	-0.5685886	Yes
CLEC4A	18588	-5.195774078	-0.5669573	Yes
GNA15	18597	-5.229933262	-0.5654754	Yes
ST3GAL6	18610	-5.307264328	-0.56418115	Yes
ANKRD50	18620	-5.365860462	-0.5627035	Yes
SLC37A2	18624	-5.378468513	-0.56089735	Yes
IFITM3	18626	-5.384545803	-0.558981	Yes
CTSZ	18644	-5.463957787	-0.5578993	Yes
SORT1	18651	-5.504159927	-0.5562091	Yes
HSPC159	18662	-5.602539539	-0.5546988	Yes
CD300LB	18670	-5.650986195	-0.55300885	Yes
CD83	18685	-5.752508163	-0.55165964	Yes
IBRDC2	18688	-5.774206161	-0.54965466	Yes
CSF3R	18694	-5.798828125	-0.5478027	Yes
ADM	18697	-5.808861732	-0.54578507	Yes
BCL11A	18700	-5.814370155	-0.5437654	Yes
DHRS9	18703	-5.829904556	-0.5417401	Yes
ALDH1A1	18704	-5.831231117	-0.53960633	Yes
CD68	18714	-5.953670979	-0.53791356	Yes
CLIC4	18723	-6.03074646	-0.53613865	Yes
FBP1	18729	-6.098376274	-0.534177	Yes

SIGLEC5	18735	-6.144952297	-0.53219837	Yes
PNKD	18740	-6.178595543	-0.5301534	Yes
CYFIP1	18741	-6.178890705	-0.5278924	Yes
FLJ20701	18742	-6.18939352	-0.5256276	Yes
PLXNB2	18759	-6.399059296	-0.5241497	Yes
SLC2A6	18760	-6.447974205	-0.52179027	Yes
SART2	18772	-6.638041019	-0.5199551	Yes
PTX3	18773	-6.691739559	-0.5175064	Yes
BRI3	18774	-6.697779655	-0.51505554	Yes
SLC43A3	18782	-6.830914974	-0.51293385	Yes
HNMT	18783	-6.835007668	-0.5104328	Yes
CTSH	18784	-6.880676746	-0.507915	Yes
TRIB1	18792	-6.944756508	-0.5057516	Yes
FCER1G	18798	-7.015754223	-0.5034543	Yes
KCTD12	18804	-7.100313187	-0.50112605	Yes
STAB1	18816	-7.189302921	-0.49908915	Yes
RBP7	18820	-7.244400978	-0.4966002	Yes
TLR8	18823	-7.270076275	-0.49404788	Yes
KLF4	18824	-7.276798725	-0.49138516	Yes
CD1D	18825	-7.280004501	-0.48872125	Yes
PYGL	18827	-7.297765732	-0.48610482	Yes
HLA-DMB	18831	-7.362388611	-0.48357272	Yes
SLC31A2	18832	-7.395060539	-0.4808667	Yes
BTK	18835	-7.452842236	-0.4782475	Yes
CARD15	18837	-7.490656376	-0.4755605	Yes
FLJ22662	18838	-7.525721073	-0.47280666	Yes
TMEM51	18842	-7.600640774	-0.4701874	Yes
CAPG	18843	-7.601438046	-0.46740586	Yes
ALDH3B1	18844	-7.619431019	-0.46461773	Yes
GNB4	18845	-7.631735325	-0.46182513	Yes
SLC22A4	18846	-7.643757343	-0.45902812	Yes
PPBP	18862	-7.97193861	-0.4569207	Yes
HMOX1	18864	-8.008213043	-0.45404434	Yes
TNFRSF21	18865	-8.111117363	-0.4510763	Yes
IER3	18866	-8.1170187	-0.4481061	Yes
SYK	18868	-8.131308556	-0.44518468	Yes
CIAS1	18873	-8.238703728	-0.44238588	Yes
CD74	18874	-8.282806396	-0.43935502	Yes
GPX1	18880	-8.461009026	-0.43652886	Yes
G0S2	18884	-8.483659744	-0.43358645	Yes
TNS3	18886	-8.532016754	-0.4305184	Yes
PPIF	18888	-8.545214653	-0.4274455	Yes
RAB32	18889	-8.561198235	-0.42431277	Yes
FAM20C	18894	-8.626433372	-0.42137212	Yes
IL1B	18895	-8.630884171	-0.41821387	Yes
OSCAR	18900	-8.728104591	-0.415236	Yes
VMD2	18903	-8.7576828	-0.41213936	Yes
FCN1	18908	-8.900473595	-0.4090984	Yes
LILRA5	18911	-8.96029377	-0.4059276	Yes
ABCC3	18918	-9.335080147	-0.40283558	Yes
LYZ	18920	-9.393116951	-0.39945242	Yes
PLXDC2	18921	-9.407776833	-0.39600992	Yes
ALOX5	18922	-9.419662476	-0.39256305	Yes

S100A12	18927	-9.557095528	-0.38928184	Yes
RNASE6	18928	-9.611608505	-0.38576475	Yes
IGSF6	18930	-9.633878708	-0.3822935	Yes
HLA-DQB1	18933	-9.695180893	-0.37885377	Yes
SRC	18934	-9.699958801	-0.37530434	Yes
HLA-DRB6	18935	-9.723190308	-0.37174642	Yes
FER1L3	18937	-9.796942711	-0.3682155	Yes
SLC15A3	18939	-9.826304436	-0.36467382	Yes
APOBEC3A	18940	-9.837061882	-0.36107424	Yes
LILRB4	18941	-9.841583252	-0.357473	Yes
CST3	18942	-9.848776817	-0.3538691	Yes
IL8	18943	-9.868003845	-0.3502582	Yes
ALDH2	18945	-9.896321297	-0.34669092	Yes
HLA-DMA	18946	-9.897445679	-0.34306923	Yes
LMO2	18949	-9.943757057	-0.33953854	Yes
MTMR11	18951	-9.957079887	-0.33594903	Yes
HCK	18958	-10.01357174	-0.33260873	Yes
CYP27A1	18959	-10.09517193	-0.3289147	Yes
GALNAC4S-6ST	18960	-10.11350346	-0.32521394	Yes
S100A8	18964	-10.23901939	-0.32162923	Yes
PTGS1	18967	-10.33546543	-0.31795523	Yes
AQP9	18972	-10.41876221	-0.31435868	Yes
S100A9	18975	-10.49983311	-0.31062454	Yes
CSTA	18977	-10.53100395	-0.306825	Yes
NCF4	18978	-10.55988789	-0.3029609	Yes
EMILIN2	18980	-10.58900833	-0.29914016	Yes
SERPINA1	18982	-10.68607044	-0.29528388	Yes
CXCL1	18985	-10.77077198	-0.2914506	Yes
PILRA	18986	-10.78163433	-0.28750536	Yes
CXCL16	18987	-10.8427248	-0.28353778	Yes
TLR4	18988	-10.90078735	-0.27954894	Yes
CSF2RA	18993	-11.03897667	-0.27572545	Yes
MAFB	18994	-11.07913208	-0.27167138	Yes
MGST1	18996	-11.09462738	-0.2676656	Yes
CYBB	18998	-11.18221951	-0.26362777	Yes
IRAK3	19000	-11.21847916	-0.25957668	Yes
AIF1	19001	-11.24455357	-0.25546205	Yes
CXCL2	19002	-11.29689312	-0.25132826	Yes
FCAR	19006	-11.41437912	-0.24731345	Yes
TMEM176B	19007	-11.4217329	-0.24313399	Yes
FCGRT	19009	-11.57099915	-0.2389539	Yes
CD14	19010	-11.58622074	-0.23471425	Yes
LILRA2	19011	-11.59562397	-0.23047116	Yes
MS4A6A	19012	-11.62159729	-0.22621858	Yes
ABCA1	19013	-11.66005611	-0.22195192	Yes
NCF2	19014	-11.70453072	-0.21766898	Yes
KIAA1598	19016	-11.78542805	-0.21341042	Yes
SLC11A1	19017	-11.86246967	-0.20906968	Yes
CCR1	19018	-11.89022064	-0.20471881	Yes
FPR1	19019	-11.94446754	-0.20034806	Yes
PTGS2	19020	-12.0767374	-0.19592893	Yes
CPVL	19021	-12.09502792	-0.19150311	Yes
RASGRP4	19024	-12.28269863	-0.18711656	Yes

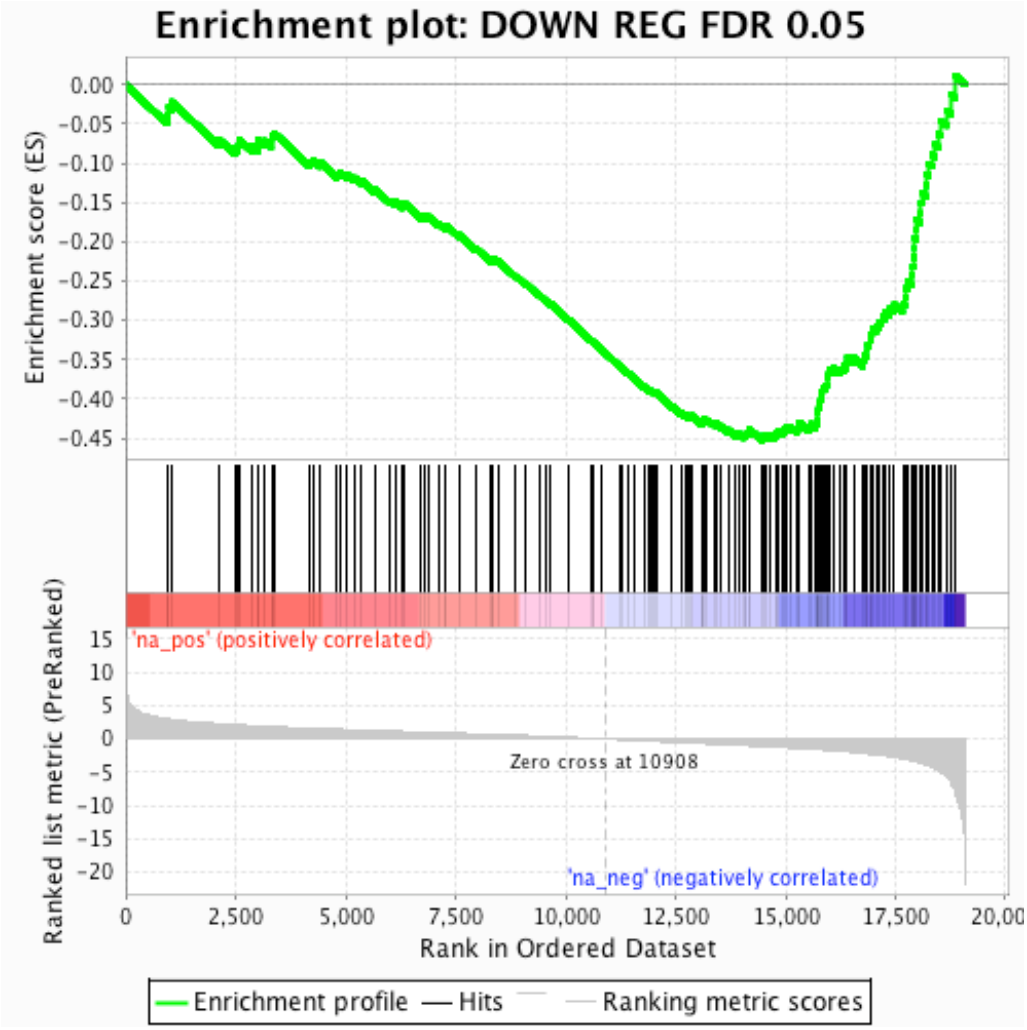
LHFPL2	19026	-12.31144142	-0.18266553	Yes
FLJ20273	19028	-12.34388828	-0.17820261	Yes
C5AR1	19031	-12.397542	-0.17377406	Yes
GRN	19032	-12.42531013	-0.16922738	Yes
ZNF385	19033	-12.42696476	-0.16468008	Yes
HLA-DRA	19034	-12.44805813	-0.16012508	Yes
WARS	19036	-12.52664185	-0.15559529	Yes
BASP1	19039	-12.60323811	-0.15109146	Yes
NPC2	19040	-12.77801704	-0.14641571	Yes
CD300LF	19041	-12.82889366	-0.14172134	Yes
RIN2	19043	-12.84181499	-0.13707623	Yes
FGD2	19044	-12.87588787	-0.13236468	Yes
PLA2G7	19047	-13.08125305	-0.12768592	Yes
CYP1B1	19048	-13.09306717	-0.12289489	Yes
LGALS2	19050	-13.15209961	-0.11813624	Yes
TGFBI	19051	-13.15284729	-0.11332333	Yes
CLEC7A	19052	-13.16984558	-0.108504206	Yes
TNFAIP2	19053	-13.28770924	-0.10364195	Yes
MNDA	19056	-13.48912334	-0.09881395	Yes
PLAUR	19057	-13.56718159	-0.093849435	Yes
EMR2	19058	-13.64319324	-0.0888571	Yes
CD86	19060	-13.66172218	-0.08391196	Yes
CSF1R	19061	-13.68650055	-0.07890378	Yes
RAB31	19064	-13.85207558	-0.073942974	Yes
IFI30	19066	-14.05601501	-0.068853565	Yes
ANPEP	19068	-14.15786266	-0.06372688	Yes
CD163	19069	-14.16409206	-0.058543935	Yes
SULF2	19076	-14.35370636	-0.053615496	Yes
IL1RN	19077	-14.49565601	-0.048311226	Yes
CSPG2	19081	-14.838727	-0.043043364	Yes
IL13RA1	19083	-15.07441616	-0.037581295	Yes
THBS1	19084	-15.63720226	-0.031859312	Yes
CD36	19085	-15.88371849	-0.02604712	Yes
KYNU	19086	-16.13300705	-0.020143708	Yes
SLC7A7	19088	-16.68038177	-0.014093983	Yes
MS4A7	19091	-17.28543091	-0.007876838	Yes
EPB41L3	19093	-21.67412758	2.06E-07	Yes

A5.2 Geneset enrichment analysis for DOWN-REGULATED GENES

A5.2.1 Statistics

Dataset	LucyW_E2_plusplus-plus_collapsed
Phenotype	NoPhenotypeAvailable
Upregulated in class	na_neg
GeneSet	DOWN REG FDR 0.05
Enrichment Score (ES)	-0.45383584
Normalized Enrichment Score (NES)	-1.9278994
Nominal p-value	0.0
FDR q-value	0.0
FWER p-Value	0.0

A4.2.2 Enrichment plot



A5.2.3 Genes contributing to leading edge enrichment score

PROBE	RANK IN GENE LIST	RANK METRIC SCORE	RUNNING ES	CORE ENRICHMENT
SPG3A	14027	-0.987273514	-0.41704115	Yes
ANKRD35	14037	-0.990183651	-0.41595232	Yes
ZNF365	14083	-1.005060792	-0.41676116	Yes
DHCR24	14104	-1.011588693	-0.41622543	Yes
GRK5	14109	-1.014288187	-0.41483158	Yes
GP5	14110	-1.014549255	-0.41322383	Yes
STYK1	14115	-1.016086698	-0.41182712	Yes
CHAF1B	14138	-1.023804903	-0.41137877	Yes
PLAG1	14180	-1.036636233	-0.4119241	Yes
PTPRC	14186	-1.038627505	-0.41054502	Yes
ZNF443	14278	-1.068936467	-0.41370752	Yes
CTSG	14329	-1.089929581	-0.41464868	Yes
KIAA1394	14330	-1.089964271	-0.41292143	Yes
CEPT1	14426	-1.119239569	-0.41621768	Yes
FOXD1	14475	-1.137688637	-0.41697645	Yes
ZNF662	14486	-1.14195621	-0.41570047	Yes
PTTG1	14510	-1.152508378	-0.41510156	Yes
ZNF330	14519	-1.156828046	-0.41369528	Yes
NR3C1	14544	-1.164095879	-0.41313136	Yes
RAB30	14558	-1.167470574	-0.41197506	Yes
ZNF197	14565	-1.170410991	-0.4104405	Yes
FBXL3	14567	-1.170714974	-0.40863866	Yes
SLC1A7	14568	-1.170924187	-0.4067831	Yes
IFT122	14614	-1.185750365	-0.4073056	Yes
KLRC3	14658	-1.201762319	-0.40769598	Yes
EDARADD	14689	-1.213391781	-0.40737414	Yes
SLC14A1	14710	-1.220374465	-0.40650755	Yes
ITGAM	14766	-1.236763954	-0.4074829	Yes
NKX3-1	14783	-1.242409706	-0.40636793	Yes
SYT11	14835	-1.258727789	-0.407095	Yes
SAP30	14873	-1.271496415	-0.40705463	Yes
ERBB2	14946	-1.29663837	-0.40884233	Yes
FCGBP	14974	-1.30611515	-0.40821344	Yes
ZNF415	15013	-1.325191975	-0.4081414	Yes
TPST2	15033	-1.329990864	-0.40704775	Yes
MLLT11	15040	-1.332021475	-0.4052571	Yes
HSPA12A	15049	-1.335555792	-0.4035676	Yes
ST8SIA1	15129	-1.364998102	-0.40562052	Yes
ZNF642	15132	-1.365328074	-0.40356365	Yes
BPGM	15213	-1.393541932	-0.4056247	Yes
CD8B	15270	-1.419607043	-0.40636364	Yes
CRTAM	15294	-1.428924084	-0.40532666	Yes
CCR7	15313	-1.436323047	-0.40401116	Yes
NAG6	15428	-1.477339387	-0.4077539	Yes
DRD3	15480	-1.49328661	-0.40810928	Yes
PCBD1	15494	-1.501008868	-0.4064244	Yes
PARD6G	15512	-1.508192658	-0.40494162	Yes
CCR9	15530	-1.516578436	-0.40344557	Yes
PPIL2	15538	-1.518093586	-0.4014134	Yes
SIGLECP3	15563	-1.529671907	-0.4002702	Yes

SRPK2	15612	-1.549334645	-0.4003766	Yes
NRK	15632	-1.555169344	-0.3989261	Yes
ATR	15697	-1.579776525	-0.39983818	Yes
STXBP6	15712	-1.585073948	-0.39807346	Yes
EPHA1	15723	-1.588377953	-0.39609003	Yes
VSIG9	15724	-1.589025021	-0.3935719	Yes
TSPAN14	15743	-1.598368883	-0.3919996	Yes
MYO5C	15747	-1.600356698	-0.38962364	Yes
MT1H	15748	-1.600465298	-0.3870874	Yes
ZNF658	15761	-1.605103135	-0.3851842	Yes
NAP1L3	15791	-1.615418792	-0.38417193	Yes
DSC1	15806	-1.621518135	-0.38234946	Yes
MGC42367	15810	-1.622530103	-0.37993833	Yes
ENC1	15822	-1.628484607	-0.37794474	Yes
PIAS2	15842	-1.636825323	-0.37636486	Yes
MGC4677	15900	-1.663321257	-0.37677094	Yes
PLEKHK1	15941	-1.681892395	-0.37624037	Yes
IFNG	15942	-1.682265162	-0.3735745	Yes
FXYD2	15962	-1.692588568	-0.37190625	Yes
FCGR3B	15978	-1.700658321	-0.37001172	Yes
SPINK2	16012	-1.71339643	-0.36905766	Yes
GCNT1	16064	-1.740483046	-0.36902127	Yes
CACNA1I	16108	-1.762394309	-0.3685232	Yes
LOC89944	16190	-1.81790185	-0.36996514	Yes
GHRHR	16258	-1.855621576	-0.3706002	Yes
VCAM1	16261	-1.856635571	-0.3677647	Yes
DCAL1	16322	-1.884110689	-0.36798102	Yes
SLC25A25	16352	-1.902002692	-0.3665146	Yes
GGTL3	16394	-1.923432589	-0.36565462	Yes
PPP1R14C	16400	-1.928547859	-0.3628653	Yes
NPTX1	16413	-1.935276866	-0.36043888	Yes
LOC197135	16549	-2.013612747	-0.36445254	Yes
NELL2	16553	-2.017225504	-0.36141595	Yes
KRAS	16624	-2.063146591	-0.3618822	Yes
LOH11CR2A	16652	-2.085472345	-0.3600183	Yes
MAD2L1	16663	-2.09196043	-0.35723686	Yes
POP4	16721	-2.131020069	-0.3569018	Yes
ME3	16763	-2.16360569	-0.3556612	Yes
GCET2	16783	-2.177007914	-0.3532253	Yes
CLN5	16784	-2.177189589	-0.34977514	Yes
CLIC6	16795	-2.185355425	-0.3468457	Yes
TMEM46	16858	-2.224519968	-0.3466293	Yes
CX3CR1	16860	-2.225871086	-0.34315532	Yes
NUDT11	16864	-2.227870941	-0.33978495	Yes
CLEC2D	16869	-2.230736732	-0.33646336	Yes
PTPRK	16896	-2.24956131	-0.33428606	Yes
RHOBTB3	16916	-2.265410662	-0.33171007	Yes
GPA33	16932	-2.276046515	-0.32890373	Yes
FTS	16965	-2.303632021	-0.32696095	Yes
LPL	16990	-2.324455976	-0.32455823	Yes
THEX1	17011	-2.337755203	-0.32192093	Yes
NQO1	17060	-2.375634909	-0.32071793	Yes
MCOLN2	17107	-2.410490036	-0.31935295	Yes

KLRA1	17143	-2.43068409	-0.31736892	Yes
SQLE	17151	-2.436097145	-0.31388202	Yes
LSS	17183	-2.466476679	-0.3116278	Yes
LEF1	17197	-2.48083806	-0.3083902	Yes
GOLPH2	17205	-2.483955622	-0.30482748	Yes
IFI27	17221	-2.506142616	-0.3016565	Yes
CLIPR-59	17255	-2.537126303	-0.29939708	Yes
GPR174	17265	-2.544656038	-0.29584488	Yes
MT1F	17278	-2.555217266	-0.29243606	Yes
WEE1	17286	-2.561820745	-0.28874993	Yes
MMAA	17350	-2.614329338	-0.28796917	Yes
CRSP9	17376	-2.640954971	-0.28511825	Yes
TOX	17377	-2.641610861	-0.2809321	Yes
ENPP4	17441	-2.717610359	-0.2799877	Yes
VIPR2	17470	-2.74545145	-0.27713126	Yes
PRSS23	17475	-2.747807264	-0.27299032	Yes
ZNF682	17566	-2.856084585	-0.27326736	Yes
DCLRE1A	17569	-2.861668587	-0.26883924	Yes
LIMA1	17666	-2.968686581	-0.26925805	Yes
UBL3	17671	-2.972747326	-0.2647606	Yes
MT1E	17717	-3.027485609	-0.26236454	Yes
ARID5B	17725	-3.03833437	-0.25792328	Yes
MTUS1	17777	-3.110199451	-0.2557163	Yes
VAV3	17790	-3.132140398	-0.25139323	Yes
SERINC5	17833	-3.198745489	-0.24856563	Yes
REG4	17848	-3.213845491	-0.24421981	Yes
CD5	17868	-3.248828173	-0.2400854	Yes
CD300A	17879	-3.25994873	-0.23545305	Yes
LOC387895	17883	-3.277635098	-0.23041911	Yes
GPR55	17891	-3.288413763	-0.22558156	Yes
PALLD	17909	-3.311510563	-0.22124107	Yes
SELL	17928	-3.335978985	-0.21691518	Yes
GPR137B	17934	-3.355215073	-0.21186504	Yes
APBA2	17939	-3.364514589	-0.20674677	Yes
TTYH2	17965	-3.415069342	-0.20266913	Yes
PASK	17974	-3.428783417	-0.19766249	Yes
WIPI1	17975	-3.433719635	-0.1922211	Yes
MTSS1	17976	-3.438731432	-0.18677177	Yes
ACCN2	17985	-3.445695877	-0.18173833	Yes
LOC391356	17999	-3.474200964	-0.17692657	Yes
CDCA7	18011	-3.490406752	-0.17198238	Yes
IL28RA	18051	-3.578576565	-0.16839276	Yes
LDLR	18079	-3.64791584	-0.16405286	Yes
ZNF683	18096	-3.687009096	-0.15906397	Yes
MBP	18104	-3.701397419	-0.15357195	Yes
NGFRAP1	18150	-3.801769733	-0.14994885	Yes
SETBP1	18196	-3.901304007	-0.14616801	Yes
ITGB1	18216	-3.956792355	-0.1409117	Yes
P2RY5	18218	-3.961778164	-0.13468686	Yes
HDGFRP3	18249	-4.039843082	-0.12988597	Yes
MAL	18261	-4.061963558	-0.124036044	Yes
RCBTB2	18324	-4.204815865	-0.12068148	Yes
CXCR3	18329	-4.217827797	-0.114210986	Yes

IFIT2	18384	-4.363675594	-0.11017774	Yes
PTPN12	18402	-4.408119202	-0.10409947	Yes
TBC1D4	18406	-4.418840885	-0.09725706	Yes
FLCN	18444	-4.536532879	-0.09204265	Yes
LGALS1	18456	-4.592109203	-0.0853526	Yes
SLC4A7	18461	-4.622473717	-0.07824087	Yes
SOCS6	18475	-4.672082424	-0.07153083	Yes
CTLA4	18517	-4.844704151	-0.06604152	Yes
RAB33A	18535	-4.964289665	-0.05908189	Yes
SUSD1	18636	-5.436046124	-0.05580417	Yes
LRRN3	18655	-5.521193027	-0.048015386	Yes
ZFHX1B	18778	-6.74805212	-0.043832626	Yes
ASPH	18812	-7.141619205	-0.034276474	Yes
PROK2	18858	-7.8698349	-0.024206735	Yes
SAMSN1	18885	-8.517742157	-0.012096278	Yes
LILRB1	19078	-14.60414505	8.00E-04	Yes

Appendix 6

Microarray data comparing up and down regulated genes between CD161++CD8ab and CD161++CD8aa T cells from adult healthy donors.

Gene.Symbol	logFC	adj.P.Val
SYMPK	1.723839334	0.725054322
---	1.468061771	0.775469483
USP13	1.221670648	0.787955408
BCL2L11	1.205229468	0.781756585
---	1.200279979	0.86488192
COQ10B	1.13979628	0.775469483
CHURC1	1.129083583	0.803250364
TRIM59	1.12692482	0.717052686
MCM3APAS	1.122860966	0.717052686
ATP5SL	1.107988682	0.803250364
NRIP2	1.094577939	0.775469483
CYB561	1.085946535	0.717052686
PRUNE	1.02005501	0.775469483
IDH3A	1.006441839	0.717052686
PDXK	1.002481501	0.717052686

Table 1. Comparison of gene expression profiles of CD161++CD8ab and CD161++CD8aa cells. Genes with >1 $\log_2$ fold up-regulation shown.

Gene.Symbol	logFC	adj.P.Val
ZNF343	-1.001846563	0.775469483
MS4A6A	-1.003444047	0.803250364
LOC100288758	-1.005611657	0.775469483
---	-1.019215377	0.717052686
RNASE6	-1.021987342	0.717052686
XCL1 /// XCL2	-1.022824008	0.787955408
SAC3D1	-1.023051505	0.803250364
C1orf43	-1.032510437	0.797821526
LEF1	-1.033104172	0.787955408
ISYNA1	-1.036720129	0.775469483
C1orf61	-1.074996295	0.825064546
---	-1.088574519	0.775469483
HIPK1	-1.089123395	0.872817977
---	-1.091045778	0.787955408
CD8B	-1.093816614	0.717052686
C16orf68	-1.097404699	0.875810756
CD8B	-1.110841774	0.803250364
SDCCAG3	-1.111386167	0.775469483
---	-1.141622745	0.803250364
CTLA4	-1.150416704	0.717052686
---	-1.15617846	0.717052686
LOC100132319	-1.171847858	0.717052686
FGFBP2	-1.179153108	0.787955408
MED14	-1.185415215	0.717052686
TRA@ /// TRD@	-1.186528973	0.799355507
---	-1.193234835	0.803250364
---	-1.19973333	0.717052686

---	-1.20114558	0.803250364
---	-1.222150684	0.787955408
CD8B	-1.27568569	0.775469483
RGL1	-1.287166481	0.814100501
FGR	-1.304511035	0.803250364
S100A12	-1.36824224	0.717052686
---	-1.573989413	0.775469483
DCHS1	-1.597742128	0.717052686
GZMH	-1.68847269	0.717052686

Table 2: Table 1. Comparison of gene expression profiles of CD161++CD8ab and CD161++CD8aa cells. Genes with >1 $\log_2$ fold down regulation shown.